



**The Role and Regulation of Rif1 as an
Anti-Checkpoint Protein in *S.
cerevisiae***

Author: Cameron Michael Robertson

Institute for Cell and Molecular Biosciences

A Thesis Submitted for the
Qualification of Doctor of Philosophy

September 2019



Acknowledgements

I would like to take this opportunity to thank the friends, family, and colleagues that have supported me throughout my PhD, without whom this would not have been possible. Firstly, I would like to thank my supervisor Dr Laura Maringele for the opportunity to take part in this research as part of her lab, and for her continued support, help, and guidance throughout this project. I would like to express my gratitude towards progress review panel members Professor Brian Morgan and Professor David Lydall, for their valuable guidance and comments that have pushed me to improve and develop. I would also like to thank Professor David Lydall for the provision of certain resources including strains and equipment, without which this research would not have been possible.

I would also like to thank all members of the Lydall lab, past and present including Joanna Rodriguez, Eva Holstein, Marta Markiewicz-Potoczny, Vicky Torrance, and Ben Wetherall for their support, advice, and friendship. I would also like to extend this gratitude to other colleagues for both their scientific and social support including Catherine Park, Sara Luzzi, Nicky Hannaway, Emma Corbin, and David Shapira.

Finally, I would like to thank my friends and family for their continued support. My parents for their unwavering confidence, Helen Shaw for her complete support, and my Grandpa without whose influence I may never have entered science. Without these people this would not have been possible. I extend my deepest gratitude to you all.

Abstract

The response to DNA damage is imperative to deciding the future of a cell. Damage needs to be repaired before the cell cycle is allowed to continue, or the cell must be destroyed. We study the role of the budding yeast telomeric protein Rif1 during arrest of the cell cycle, primarily in the temperature sensitive *cdc13-1* strains, which undergoes telomere uncapping and DNA strand resection.

Rap-interacting factor 1 (Rif1) forms a complex with Rap1 and Rif2 to antagonise the action of telomerase at telomeres. Rif1 has since been shown to be conserved across eukaryotes, with roles in a number of processes such as a globally conserved role in regulation of replication timing, and repair pathway choice at mammalian double strand breaks.

We further develop an observed anti-checkpoint role of Rif1 during telomere uncapping, which correlates to a cell cycle arrest dependent phosphorylation of Rif1. In this we have demonstrated the likely phosphorylation sites of Rif1 during cell cycle arrest, as well as the importance of these sites for this anti-checkpoint role. Through substitution of these amino acid residues we have demonstrated that *cdc13-1* strains containing non-phosphorylated Rif1 protein show increased sickness. We have further demonstrated that this phosphorylation is downstream of the activity of the CDK1 equivalent, Cdc28, and also occurs in cell cycle arrest resulting from multiple arresting reagents.

We propose that Rif1 binds to regions of resected DNA and thereby shields ssDNA from recognition by checkpoint proteins, and that this interaction is regulated by the addition of phosphoryl groups at Serine-57 and Serine-110. The potentially conserved nature of this interaction could impact studies on RIF1 in human cells.

Nomenclature

Species-specific nomenclature			
Species	Wild-type Gene	Protein	Mutant Allele
<i>S. cerevisiae</i>	Three letter symbol and Arabic number. Capitalised and italicised. E.g. <i>CDC13</i>	Appropriate symbol and number. First letter capitalised, and non-italic. E.g. Cdc13	Mutant allele indicated by a dash and number. Recessive mutants are lower case and italicised. e.g. <i>cdc13-1</i>
Human	Fully capitalised and italicised, e.g. <i>CDK1</i>	Fully capitalised and non-italic, e.g. CDK1	Changes to nucleotide and amino acids are described as appropriate
Mice	First letter capitalised and fully italicised, e.g. <i>Rif1</i> .	Fully capitalised and non-italic, e.g. RIF1	Mutants are indicated by the addition of mutant symbol in superscript following gene symbol, e.g. <i>Kit^W</i> .

Abbreviations

53BP1 – p53 Binding Protein 1

ALT – Alternate Lengthening of Telomeres

APC – Anaphase Promoting Complex

ARS – Autonomously Replicating Sequence

ASE1 – Anaphase Spindle Elongation 1

ASK1 – Associated with Spindles and Kinetochores 1

ATM – Ataxia Telangiectasia Mutated

ATR – Ataxia Telangiectasia and Rad53-related

BEM2 – Bud Emergence 2

BEM3 – Bud Emergence 3

BFA1 – Byr-Four-Alike 1

BIR1 – Baculoviral IAP Repeat-containing

BRCA1 – Breast Cancer Associated 1

BUB2 – Budding Uninhibited by Benzimidazole

BUR1 – Bypass UAS Requirement 1 (?)

CAK1 – Cdk Activating Kinase

CDC13 – Cell Division Cycle 13

CDC14 – Cell Division Cycle 14

CDC20 – Cell Division Cycle 20

CDC24 – Cell Division Cycle 24

CDC28 – Cell Division Cycle 28, also known as CDK1

CDC42 – Cell Division Cycle 42

CDC45 – Cell Division Cycle 45

CDC5 – Cell Division Cycle 5

CDC6 – Cell Division Cycle 6

CDC7 – Cell Division Cycle 7

CDH1 – CDC20 Homolog 1

CDK – Cyclin Dependent Kinase

CDK1 – Cyclin Dependent Kinase 1, also known as CDC28 in yeast.

CDT1 – Chromosome Licensing and DNA Replication Factor 1

CHK1 – Checkpoint Kinase 1

ChIP – Chromatin Immunoprecipitation

CKB1 – Casein Kinase Beta subunit 1

CKB2 – Casein Kinase Beta subunit 2

CKI – Cyclin-dependent Kinase Inhibitor

CLB1 – Cyclin B 1

CLB2 – Cyclin B 2

CLB3 – Cyclin B 3

CLB4 – Cyclin B 4

CLB5 – Cyclin B 5

CLB6 – Cyclin B 6

CLN1 – Cyclin 1

CLN2 – Cyclin 2

CLN3 – Cyclin 3

CNM67 – Chaotic Nuclear Migration 67

CST – Cdc13-Stn1-Ten1

CTD – C-Terminal Domain

CTK1 – Carboxy-Terminal domain Kinase

DBD – DNA Binding Domain

DDC1 – DNA Damage Checkpoint 1

DDC2 – DNA Damage Checkpoint 2

DDK – Dbf4 Dependent Kinase

DDR – DNA Damage Response

DMSO – Dimethyl sulfoxide

DNA – Deoxyribonucleic Acid

DNA2 – DNA Synthesis Defective

dNTPs – Deoxyribonucleotide Triphosphate

DPB11 – DNA Polymerase B (II) 11

DSB – Double Strand Break

dsDNA – double stranded DNA

DUN1 – DNA-damage Uninducible 1

ESCs – Embryonic Stem Cells

EST1 – Ever Shorter Telomeres 1

EST2 – Ever Shorter Telomeres 2

EST3 – Ever Shorter Telomeres 3

EXO1 – Exonuclease 1

FAR1 – Factor Arrest 1

FEAR – cell division cycle Fourteen Early Anaphase Release

FIN1 – Filaments In between Nuclei 1

FUS3 – Cell Fusion 3

GIN5 – Sld5, Psf1, Psf2, Psf3 (go-ici-ni-san)

GLC7 – Glycogen 7

H2A – Histone 2A

HCM1 – High Copy suppressor of Calmodulin 1

HEAT – Huntingtin, Elongation factor 3, protein phosphatase 2A, TOR1

HML – Mating type cassette left

HMR – Mating type cassette right

HR – Homologous recombination

KAR9 – Karyogamy 9

MCM – Mini-chromosome Mating complex

MEC1 – Mitosis Entry Checkpoint 1

MEC3 – Mitosis Entry Checkpoint 3

MEN – Mitotic Exit Network

MIH1 – Mitotic Inducer Homolog 1

MPS1 – Monopolar Spindle 1

MRE11 – Meiotic Recombination 11

MRN – Mre11 Rad50 Nbs1 complex

MRX – Mre11 Rad50 Xrs2 complex

NHEJ – Non-Homologous End Joining

ORC – Origin Recognition Complex

PCNA – Proliferating Cell Nuclear Antigen

PDS1 – Precocious Dissociation of Sister 1

PGD – Phospho-Gate Domain

PHO85 – Phosphate Metabolism 85

PIKK – Phosphatidylinositol 3-Kinase-related Kinase

POL- α – Polymerase alpha

POL12 – Polymerase 12

PP1 – Protein Phosphatase 1

Pre-RC – pre-Replication Complex

PTC2 – Phosphatase type two C 2

PTC3 – Phosphatase Two C 3

RAD17 – Radiation Sensitive 17

RAD24 – Radiation Sensitive 24

RAD50 – Radiation Sensitive 50

RAD51 – Radiation Sensitive 51

RAD52 – Radiation Sensitive 52

RAD53 – Radiation Sensitive 53

RAD9 – Radiation Sensitive 9

RAP1 – Repressor-Activator site binding Protein

RBM – Rap1 Binding Module

RFA2 – Replication Factor A 2

RFC – Replication Factor C

RIF1 – Rap1 Interacting Factor 1

RIF1-C Δ – *RIF1* mutant containing a deletion of amino acids residues 1351-1916

RIF1-N Δ – *RIF1* mutant containing a deletion of amino acids 2-176

RIF2 – Rap1 Interacting Factor 2

RNA – Ribonucleic Acid

RPA – Replication Protein A

SAC – Spindle Assembly Checkpoint

SAE2 – Sporulation in the Absence of spo Eleven

SGS1 – Slow Growth Suppressor 1

SGS2 – Slow Growth Suppressor 2

SIC1 – Substrate/Subunit Inhibitor of Cycle-dependent protein kinase

SIR2 – Silent Information Regulator 2

SIR3 – Silent Information Regulator 3

SIR4 – Silent Information Regulator 4

SLD2 – Synthetically Lethal with Dpb11-2

SLD3 - Synthetically Lethal with Dpb11-3

SLI15 – Synthetically Lethal with Ipl1 15

SPB – Spindle Pole Body

SPC110 – Spindle Pole Component 110

SPC42 – Spindle Pole Component 42

SRS2 – Suppressor of Rad Six 2

ssDNA – single stranded DNA

SSN3 – Suppressor of Snf1-3

STE11 – Sterile 11

STE18 – Sterile 18

STE4 – Sterile 4

STE5 – Sterile 5

STE7 – Sterile 7

STN1 – Suppressor of CDC13

STU2 – Suppressor of Tubulin

TAS – Telomere Associated Sequence

TEL1 – Telomere maintenance 1
TEN1 – Telomeric pathways with Stn1
TERT – Telomerase Reverse Transcriptase
TLC1 – Telomerase Component 1
TOR – Target of Rapamycin
TPE – Telomere Position Effect
TR - Telomerase RNA component
TRF2 – Telomeric Repeat Binding Factor 2
WHI5 – Whiskey 5
WT – Wild Type
YKU70 – Yeast Ku protein 70
YKU80 – Yeast Ku protein 80

Table of Contents

I: Introduction.....	1
1.1 The architecture of the Telomere	1
1.2 Telomere Replication & Telomere Stability.....	4
1.2.1 Telomerase	4
1.2.2 Telomere Replication.....	5
1.3 Telomere Binding Proteins	7
1.3.1 The CST Complex.....	7
1.3.2 Yku70/80	8
1.3.3 Rap1-Rif1-Rif2 Complex.....	10
1.4 Models of Telomere Damage	14
1.4.1 <i>cdc13-1</i>	14
1.4.2 <i>yku70/80</i> Δ	17
1.4.3 Telomerase negative survivors.....	18
1.4.3.1 Type 1 Survivors	18
1.4.3.2 Type II survivors	19
1.4.3.3 PAL survivors	19
1.5 <i>CDK1</i>	21
1.5.1 <i>CDK1</i> & Mitotic Progression	21
1.5.2 Cdk1-Controlled Processes	27
1.6 The G2/M DNA Damage Checkpoint	31
1.7 The Spindle Checkpoint	34
1.8 Repair Pathway Choice – Non-Homologous End Joining or Homologous Recombination	37
1.9 Down regulating the Checkpoint.....	40
1.9.1 Checkpoint Adaptation	40
1.9.2 Anti-checkpoint Proteins.....	42
1.9.3 The purpose of adaptation & anti-checkpoints.....	42
1.10 The Roles of Rif1 in Eukaryotes	44
1.10.1 Structural Conservation of Rif1	44

1.10.2 Rif1 in Replication Timing	50
1.10.3 Rif1 at DSBs in Mammalian Cells	54
1.10.4 Rif1 as an Anti-checkpoint Protein in Budding Yeast	54
1.11 Aims	58
Chapter II: Materials and Methods	59
2.1 Yeast Strains	59
2.2 Media	59
2.3 Cryogenic Storage of Yeast Strains	62
2.4 Mating and Sporulation	62
2.5 Spot Test	62
2.6 Gene deletion or modification using Longline plasmids	63
2.6.1 Principle of transformation & generation of DNA cassettes	63
2.6.2 High efficiency lithium acetate transformation	64
2.6.2 Hot-Start PCR test of colony transformation	65
2.7 Western Blot	66
2.7.2 Cell Harvest and TCA Protein Extraction or DAPI Staining	66
2.7.3 SDS-PAGE, blotting, and detection	67
2.8 Chromatin Immunoprecipitation	68
2.8.1 Buffers	68
2.8.2 Extraction & Immunoprecipitation	69
2.8.3 qPCR	70
2.9 Targeted Mutagenesis of <i>RIF1</i>	70
2.9.1 Principle of using Gibson Assembly to generate targeted mutations	70
2.9.2 Generation of Plasmid Structure Containing <i>RIF1</i> fragment ...	74
2.9.3 Gibson Assembly to generate mutation	78
2.9.4 Integrating Mutation via Transformation	79
2.9.5 Primers Used to Generate Mutants	80
2.10 Antibodies used in this study	82
Chapter III: Understanding the phosphorylation of Rif1	83
3.1 Rif1 is phosphorylated during telomere damage in <i>cdc13-1</i> cells	83

3.2 Rif1 is Phosphorylated During Nocodazole-Induced Arrest	87
3.3 Investigating phosphorylation of Rif1 in response to other DNA damaging agents	89
3.4 The first 176 residues of Rif1 are essential for Rif1-P and the protective function of Rif1 in <i>cdc13-1</i> cells.	94
3.5 Rif1 residues phosphorylated in <i>cdc13-1</i> cells	103
3.6 Residue S57, S110 are required for Rif1 phosphorylation in nocodazole-induced arrest.....	118
3.7 The same S57, S110 residues of Rif1 are phosphorylated under other stresses	123
3.8 Discussion.....	126
Chapter IV – Investigating the Kinases Leading to Rif1	
Phosphorylation	128
4.1 Checkpoint kinases are upstream of Rif1 phosphorylation	128
4.2 Spindle checkpoint proteins are necessary for Rif1 phosphorylation in nocodazole-induced arrest	133
4.3 Cdc28 (Cdk1) is upstream of Rif1 phosphorylation during <i>cdc13-1</i> dependent DNA damage.....	140
4.4 Discussion.....	147
Chapter V: The phenotypic effects of Rif1 phosphorylation	148
5.1 Investigating the effect of non-phosphorylated Rif1 on the survival of <i>cdc13-1</i> at restrictive temperature	148
5.2 Rif1 phosphorylation mutants do not affect the growth after other cellular stresses	154
5.3 Discussion.....	157
Chapter VI – The molecular effects of Rif1 phosphorylation.....	158
6.1 Rif1 Phosphorylation May Lead to Dissociation from Sites of DNA Damage	158
6.2 Rif1 association in checkpoint-defective <i>cdc13-1</i>	163
6.3 Discussion.....	166
Chapter VII Investigating the Effect of Mimicking Rif1	
Phosphorylation	168

7.1 Investigating the Phosphorylation of Phosphomimetic <i>RIF1</i> Mutations	168
7.2 Examining the growth of phosphomimetic <i>RIF1</i> mutants.....	172
7.3 Discussion.....	174
Chapter VIII: Final Discussion	175
8.1 Rif1 Phosphorylation in <i>cdc13-1</i> cells.....	175
8.2 The location and function of Rif1 phosphorylation	179
8.3 Phosphorylation of Rif1 outside of S57 and S110	183
8.4 Rif1 Phosphorylation Outside of <i>cdc13-1</i>	183
8.5 Rif1 in Budding Yeast and Humans.....	184
Bibliography.....	187

I: Introduction

1.1 The architecture of the Telomere

In eukaryotic cells, the ends of a linear chromosome are protected by specialised structures called telomeres. There are two main documented functions of the telomere:

- 1 To distinguish chromosome ends from double strand breaks (DSBs) and thereby “hide” them from the DNA damage response machinery
- 2 To protect the chromosome from the “end-replication problem”, whereby the canonical DNA replication machinery leads to loss of terminal DNA through successive rounds of replication.

The structure of the telomeres are a complex network of DNA sequence elements, RNA, and proteins.

Telomeric DNA is found across almost all eukaryotic species and consists of short tandem-repeats, however the length of these repeats varies dramatically. Whilst telomere length is dynamic, in budding yeast these repeats are typically ~300bp length and can be described by the consensus sequence C₁₋₃A/TG₁₋₃, the loss of these telomeric repeats leads to high rates of chromosomal loss. The telomeric sequence is further characterised by a widely conserved single-stranded overhang occurring on the G-rich 3' strand, the formation of which is dependent on Cdk1(Cdc28)-regulated resection of the C-strand (Wellinger *et al.*, 1993; Frank *et al.*, 2006; Vodenicharov and Wellinger, 2006). The length of this overhang varies throughout the cell cycle in budding yeast, during a short period in late S/G2 phase it can stretch up to 100nt long (Wellinger *et al.*, 1993). However, through the rest of the cell cycle this overhang is typically between 12 and 15nt in length. The G' overhang is crucial for the recruitment of telomere capping proteins.

Beyond the telomeric repeats, the telomeres of most eukaryotes are also made up of additional subtelomeric repetitive DNA sequences known as TAS (Telomere associated sequences) elements. In budding yeast there are two classes of TAS elements, X' and Y'. Whilst Y' elements are not found at all telomeres, when present they are immediately proximal to the telomeric repeats and are found in up to 4 tandem repeats (C. S. Chan and Tye, 1983). In a given strain, up to half of telomeres may lack Y' elements, the identity of these telomeres will differ between strains (Horowitz *et al.*, 1984; Zakian *et al.*, 1986). These Y' elements occur in one of two sizes; 6.7kb or 5.3kb, which differ by small insertions and

deletions (Louis and Haber, 1992). Alternatively, the X' elements are much shorter, ~475bp, and more heterogeneous, X' elements are present at all yeast telomeres.

These subtelomeric regions contain multiple potential replication origins or ARS (Autonomously Replicating Sequences), which likely contributes to the dynamic and diverging nature of these sequences. Unlike the telomeric repeat sequences, telomeres lacking X' or Y' elements at one end appear to have normal stability through mitosis (Sandell and Zakian, 1993).

In human cells, the telomeric sequence repeat unit is 5'-TTAGGG-3', stretching 5-15kb in length (Samassekou *et al.*, 2010). As with the length of the repeat sequence, the 3' G-overhang is also much larger in these cells than in budding yeast, typically ~200bp in length (Makarov *et al.*, 1997; McElligott and Wellinger, 1997; Wright *et al.*, 1997). This long overhang is related to the much different structure of the mammalian telomere compared to budding yeast. As well as numerous protein structures associated with the telomere, mammalian telomeres also form larger structures referred to as T-loops which are up to 25kb in length. In these structures the chromosome ends are looped back to form a closed structure, this is carried out by strand invasion of the 3' overhang into the double-stranded telomeric DNA and pairing with the C-strand, thereby sequestering DNA ends from the checkpoint proteins (Griffith *et al.*, 1999).

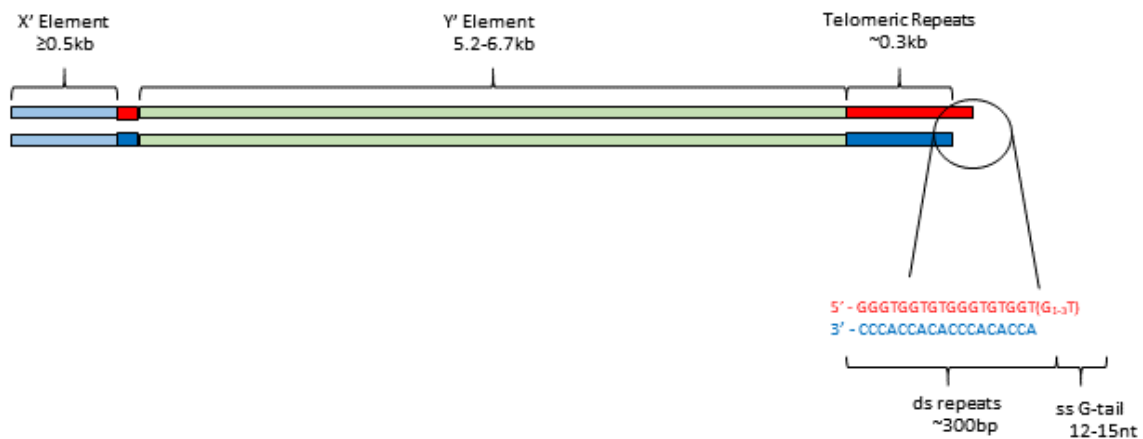


Figure 1.1 The DNA Structure of Budding Yeast Telomeres

The structure of the end of yeast chromosomes. Short (~ 475 bp) X' elements are the most centromeric-adjacent element of the telomere. Y' elements are not found at all telomeres but occur between the X' elements and the telomeric repeats, these are much longer (5.2-6.7kb each) and occur in up to 4 tandem repeats. Finally, at the end of the chromosome there are typically ~ 300 bp of the consensus telomeric repeat sequence C₁₋₃A/TG₁₋₃. Short tracts of telomeric repeats are usually found between the X' and Y' elements. Figure partially adapted from (Wellinger and Zakian, 2012).

1.2 Telomere Replication & Telomere Stability

1.2.1 Telomerase

Telomeres present a unique problem for the DNA replication machinery. In each replication cycle a short region at 5' of the lagging strand will not be replicated, and over multiple cycles this leads to gradual shortening of the chromosome. The telomeric repeats are themselves a partial counter to this problem, delaying shortening into single-gene loci by providing a buffer. However, this alone is not enough as it would only last a finite number of cell cycles. To compensate for this loss the holoenzyme telomerase acts to extend the telomeric repeats as required. In eukaryotes the core telomeric components are the catalytic subunit – telomerase reverse transcriptase (TERT), and the RNA component – telomerase RNA (TR). In telomere extension, TR acts as a template from which TERT synthesises new telomere repeats (Greider and Blackburn, 1987). Telomerase function does however also require additional factors for recruitment to telomeres, and subsequent complex assembly.

In budding yeast, the essential genes for telomerase action are *TLC1*, *EST1*, *EST2*, *EST3*, and *CDC13*. From these *EST2* and *TLC1* encode TERT and TR respectively and are required for enzymatic activity (Singer and Gottschling, 1994; Lingner *et al.*, 1997). The protein structure of Est2 contains similar domains to many other eukaryotic TERTs, including a long basic N-terminal (TEN) domain essential for telomerase activity. This domain supports multiple interactions with Tlc1 and Est3, and cellular levels of Est2 are Tlc1 dependent (Friedman and Cech, 1999; Taggart *et al.*, 2002). Tlc1, the budding yeast TR, is >1000nt in length, however, shorter derivatives are capable of maintaining short but stable telomeres. The RNA structure centres on a pseudoknot domain containing the template sequence that interacts with Est2, the rest of the structure is made up of three duplex arms that scaffold to organise interacting proteins. One of these binds Est1 and is an essential function, another binds Yku80 and is not essential but does bring Tlc1 to the nucleus and recruits Est1 to telomeres in G1 phase (Lemon *et al.*, 2019). The final arm binds the Sm protein ring, an association dispensable for telomerase activity (Singer and Gottschling, 1994; Seto *et al.*, 1999; Zappulla *et al.*, 2005).

Est1 and Cdc13 regulate the recruitment of the holoenzyme. The interaction of Est1-Tlc1 is shown to be essential to recruitment of Est1 and Est2 to telomeres in late S/G2 phase (Chan *et al.*, 2008). Furthermore, the interaction of Cdc13 and Est1 recruits the holoenzyme. In cells expressing a Cdc13-Est2 fusion protein, Est1 is dispensable for telomerase function (Evans and Lundblad, 1999). Suggesting the critical function of Est1 is to mediate the interaction between telomeres and telomerase.

Est3 association as a subunit is Est1-dependent, it is also seen to interact with Est2. However, the precise role played by this protein remains unconfirmed (Tuzon *et al.*, 2011).

1.2.2 Telomere Replication

The replication of the yeast telomeres is one of the last events in the S phase. This is due to the late firing of origins proximal to telomeric sequences, this was later to be determined to be due to the repressive effect of Rif1 on origin firing (discussed in **Section 1.10.2**). Telomere length appears to be particularly sensitive to mutations in the conventional replication proteins, in manner which seems to reflect competition between semiconservative DNA replication and telomere-dependent extension, both occurring in late S-phase. The CST complex is a key regulator of this as both Cdc13 and Stn1 interact with subunits of the DNA polymerase α complex, whilst Cdc13 also interacts with telomerase (Nugent *et al.*, 1996; Qi and Zakian, 2000; Grossi *et al.*, 2004)

Semi-conservative DNA replication begins of origins at replication recognised by the polymerase α -primase complex. As the polymerase can only function 5' to 3', one DNA strand is synthesised continuously (the leading strand) and the other is synthesised in short 5' to 3' sections called Okazaki fragments which are processed to fill any gaps and ligate these fragments together (the lagging strand). At telomeres these correspond to the G strand and the C strand respectively. However, the activity of polymerase requires binding to a short primer sequence within the DNA, in the leading strand this is at the origin and replication then carries through to the chromosome end. However, on the lagging strand Okazaki fragment synthesis requires the binding of the polymerase to multiple primer sequence, inevitably meaning that a short sequence at the telomere end will go unreplicated. This creates what is known as the "end replication problem", whereby semiconservative DNA replication must inevitably lead to progressive shortening of the telomere, a problem faced by mammalian somatic cells. In budding yeast and many other organisms, as well as immortalised cell lines, this problem is solved by the presence of telomerase to lengthen the telomeric repeats. Interestingly however, this is not the only problem created by the replication of telomeres in yeast, and the end processing of both leading and lagging strands are processed separately (Faure *et al.*, 2010). Following leading strand synthesis, the chromosome is left with a blunt end rather than the G-tail required for telomere capping, meaning that the chromosome end will now be recognised as a DSB. Generation of the 3' overhang requires post-replication C-strand degradation, this is mediated by

Mec1/Tel1/Cdk1(also known as Cdc28) recruitment of the MRX complex to resect the 5' DNA strand at the telomere (Faure *et al.*, 2010). This creates an overhang for CST association, which is also a substrate for telomerase binding, which is recruited by the interaction of MRX and Tel1 (Faure *et al.*, 2010). Cdc13 is then able to recruit telomerase for extension of the telomeric repeats, and Cdc13 and Stn1 interact with polymerase subunits to promote C-strand synthesis (Parenteau and Wellinger, 2002). On the lagging strand the G-tail already exists as replication is unable to completely replicate the DNA end via Okazaki fragments. Therefore C-strand degradation is unnecessary, and the CST complex is able to bind.

In budding yeast telomerase recruitment does not occur in every cell cycle, telomerase is shown to only associate with short telomeres during late S-phase, this is not mediated by Cdc13. Tel1 appears instead to preferentially target telomerase recruitment to short telomeres (McGee *et al.*, 2010). Telomere extension is inhibited by a molecular counting method of Rif1 and Rif2, which appear to inhibit Tel1 in a dosage dependent manner (Marcand *et al.*, 1997). When these proteins are depleted then long telomere phenotypes are seen.

In mammalian cells telomerase is active during embryogenesis and in stem cells. Enzyme expression is downregulated in somatic cells ultimately leading to gradual telomere shortening and eventual senescence or apoptosis (Geserick and Blasco, 2006).

1.3 Telomere Binding Proteins

Whilst the DNA structure of the telomere is important for chromosome maintenance, it alone is not sufficient. Telomeres are bound by a diverse array of proteins with versatility to carry out a range of functions; from facilitating end replication to capping the telomeres, a number of these proteins can also be found carrying out a variety of other genomic functions.

1.3.1 The CST Complex

In yeast cells the protection of the telomere ends is largely dependent on the CST complex. This complex is made up of the three proteins Cdc13, Stn1, and Ten1 arranged in a trimeric structure, together these directly bind to the G-tail (Lin and Zakian, 1996; Grandin *et al.*, 1997; Grandin *et al.*, 2001). Interestingly, these subunits have been shown to have similarity to the subunits of the single-stranded binding complex RPA. Much like the CST complex, RPA is made up three subunits however, where the RPA complex binds to all ssDNA the CST complex shows a preference to binding ssDNA in the telomeric repeat. Structural similarities between proteins in these complexes may suggest a common origin, and the development of CST as a telomeric-specific form of RPA (Gao *et al.*, 2007; Gelinias *et al.*, 2009).

As the key telomeric complex, the two main functions of the CST reflect the main functions of the telomere. The complex caps the telomere, to prevent recognition by damage checkpoint proteins, and to recruit telomerase for telomere length maintenance.

The telomere capping function of the CST complex was first demonstrated in cells containing the mutant allele *cdc13-1*. This mutant is temperature sensitive, *cdc13-1* cells at restrictive temperatures accumulate ssDNA in subtelomeric regions which activates a DNA damage response to arrest the cells at G2/M phase (Weinert and Hartwell, 1993; Garvik *et al.*, 1995). Temperature sensitive mutations of *stn1* and *ten1* also showed similar phenotypes to *cdc13-1*, likewise interruption of the interaction between Stn1 and Ten1 was also shown to induce uncapping of the telomere (Grandin *et al.*, 1997; Sun *et al.*, 2009). The capping function of Cdc13 is dependent on the factors Stn1 and Ten1, overexpression of these factors was shown to be able to compensate for the absence of Cdc13 and maintain telomere protection (Petreaca *et al.*, 2006).

The second major function of the CST complex is in replication of the telomere. This has been shown to take place in two manners, the traditionally established pathway was via an

interaction between Cdc13 and the telomerase subunit Est1. The *CDC13* mutant *cdc13-2^{est}* was shown to lead to senescence and telomere shortening, similar to telomerase negative cells (Nugent *et al.*, 1996). A physical interaction between Cdc13 and Est1 in late S-phase was further demonstrated, and shown to be necessary to activate telomerase function at telomeres (Taggart *et al.*, 2002; Bianchi *et al.*, 2004). This interaction is controlled by phosphorylation of Cdc13 by Mec1, Tel1, and Cdk1, these proteins promote the interaction in a cell cycle dependent manner (Tseng *et al.*, 2006; Li *et al.*, 2009). Interestingly, Mec1 also appears to control telomerase recruitment to DSBs via phosphorylation of Cdc13 to instead inhibit its interaction with DNA (Zhang and Durocher, 2010).

The CST complex also appears to play a second role in telomere replication, acting in aid of lagging strand replication at the terminal of the chromosome. Cdc13 has been shown to not only have an interaction with Est1 for recruitment of telomerase, but a further interaction with the DNA pol- α molecule (Qi and Zakian, 2000). Further to this, Stn1 has also been shown to interact with Pol12, the regulatory subunit of polymerase α (Grossi *et al.*, 2004). It has since been shown that this function of the CST complex may be highly conserved in vertebrates and mammals and may function by promoting RNA-priming on the C-strand as well as primase-to-polymerase shift (Miyake *et al.*, 2009; Surovtseva *et al.*, 2009; Chen *et al.*, 2013; Lue *et al.*, 2014).

Initially, the CST complex was thought to be a unique complex in yeast, however it was since shown that an equivalent complex is seen in a range of eukaryotes; from fission yeast, to plants, and to humans. Stn1 and Ten1 are highly conserved, and homologs are found in the human CST complex, in humans the protein CTC1 is seen in place of Cdc13 (Rice and Skordalakes, 2016). This complex however does appear to play a somewhat different role to that seen in budding yeast, whilst it is seen at telomeres it may be disposable due to the role of shelterin, and the ssDNA binding of the complex does not appear to be sequence specific (Miyake *et al.*, 2009). However, current evidence suggests Stn1 and Ten1 function together genome-wide in an RPA-like complex that rescues stalled replication forks independently of Cdc13 (Stewart *et al.*, 2012; Wang *et al.*, 2014).

1.3.2 Yku70/80

The Ku complex was initially discovered in humans and homologs were quickly identified in budding yeast as the genes *HDF1* and *HDF2*, already known to be key for non-homologous end joining (NHEJ) they were also shown to be necessary in the maintenance of telomeres

(Feldmann and Winnacker, 1993). Comprising of a heterodimer complex of 70kDa and 80kDa, referred to as Yku70 and Yku80 respectively, the complex was seen to bind double-stranded DNA ends, both blunt or 3'/5' overhangs, in a manner that is not sequence-dependent (Tuteja and Tuteja, 2000; Fisher and Zakian, 2005). To bind DNA, the Yku70 and Yku80 form a ring-like structure with dsDNA threaded through the central cavity, Yku is then capable of translocation along the duplex to allow the threading of multiple Yku molecules along the DNA.

Deletion of either Yku subunit leads to telomere shortening as first shown by Boulton and Jackson (Boulton and Jackson, 1996). This was later shown to be independent of Tel1 activity, and that these telomeres further showed elongated G-tails throughout the cell cycle (Gravel *et al.*, 1998). This suggested two possible mechanisms; the Yku complex may protect the telomeres from degradation, or it may positively regulate the elongation of telomeres, such as by the recruitment of telomerase. The latter of these was first suggested by studies in *cdc13* alleles which demonstrated a role for Ku in a telomerase dependent hyper-extension of telomeres, when expressed as a fusion protein with Cdc13 (Grandin *et al.*, 2000). Ku was then further demonstrated to interact with *TLC1*, the RNA subunit of the telomerase complex. Through this interaction it then helps to recruit the telomerase catalytic subunit, *EST2*, in G1 (Fisher *et al.*, 2004).

However, it has been further identified that the Ku complex does also play some role in the protection of telomeres from degradation. In WT cells, the G-tails are extended during the S-phase of the cell cycle, corresponding to the phase at which the telomeres are extended. However, it was observed that in Yku-deficient cells, both *yku70Δ* and *yku80Δ*, these G-tails are present at all times (Gravel *et al.*, 1998). This suggests that in these cells, the mechanisms required for degradation of the C-strand are constitutively activated. The long tail phenotype can be partially suppressed by the deletion of *EXO1*, however, without this deletion then at temperatures above 37°C the growth of these cells is arrested (Bertuch and Lundblad, 2004). This is demonstrated to be due to the accumulation of ssDNA in sub-telomeric loci, similar to *cdc13-1* mutants (Maringele and Lydall, 2004b). This suggests that the presence of Yku functions to inhibit the C-strand degradation of the telomere outside of S-phase.

The Yku proteins have also been seen to contribute to the Telomere Positioning Effect (TPE), generated by Rap1. This effect is a mediation of the silencing of telomeric genes carried out by the interaction of Rap1 with the Sir complex (Sir2, Sir3, Sir4) to deacetylate H3 and H4 (Hecht *et al.*, 1995). In the absence of Yku Sir3 and Sir4 both show reduced

localization to the telomeres, an effect overcome by the elongation of the telomeric repeats in *RIF1* or *RIF2* mutants (Tsukamoto *et al.*, 1997; Roy *et al.*, 2004). This suggests that Yku proteins aid in recruitment of the Sir proteins to the telomeres and aid their binding to Rap1 by antagonizing the effect of the competing Rif1 and Rif2 proteins.

1.3.3 Rap1-Rif1-Rif2 Complex

In *S. cerevisiae* the second key complex found at telomeres is made up of Rap1, Rif1, and Rif2, also known as the “shelterin-like” complex.

Rap1 has been established as a general transcription factor at nearly 300 sites in the yeast genome, which equates to ~5% of all genes, and is found at the silencer elements of the silent mating-type loci *HMR* and *HML* (Shore and Nasmyth, 1987; Lieb *et al.*, 2001). However, despite the established ability of Rap1 to bind to multiple genomic sites, its role is best characterised at the telomeres where it directly binds to the double-stranded telomeric repeat sequences (Longtine *et al.*, 1989). In the telomeric repeats it has been shown that Rap1 molecules bind approximately every 15-20bp (Gilson *et al.*, 1993), which means there will may be 15-20 individual complexes in 300bp of telomeric repeats.

The protein Rap1 is comprised of 827 amino acid residues and contains multiple functional domains. The DNA-binding-Doman (DBD) of Rap1 falls within the middle of the protein, residues 361 to 596, which form two helix-turn-helix motifs (König *et al.*, 1996). The C-terminal of the protein is the required for interaction with a number of associated proteins, mutation within this region is shown to lead to elongation of telomeric tracts in *S. cerevisiae* (Wotton and Shore, 1997). The loss of interaction with Rif1 and Rif2 was shown to be responsible for this phenotype, both of which were discovered as interaction partners in two-hybrid assays (Hardy *et al.*, 1992; Wotton and Shore, 1997).

The budding yeast *RIF1* encodes a large 1916 amino acid residue protein and was shown to directly colocalize with Rap1 at telomeres, through an interaction located in the C-terminal domains of both proteins (Mishra and Shore, 1999). Rif1 was also shown to interact with Rap1 through a secondary independent site, albeit with lower affinity. The C-terminal domain of Rif1 was shown to be capable of tetramerization which may act to form a binding interface with Rap1 (Shi *et al.*, 2013).

Rif2 is a much smaller protein, only 395 amino acid residues, which contains two binding sites for the Rap1 protein. This makes it possible for the Rif2 protein to bind two separate

molecules of Rap1 simultaneously. This network of interactions creates a “molecular Velcro” promoting synergistic binding of Rif1 and Rif2 to arrays of telomere-bound Rap1, linking multiple Rap1 molecules together along the length of the telomere (Shi *et al.*, 2013). In this function, Rif1 and Rif2 have both been shown to be necessary for maintenance of the telomeric repeats, in what appears to be a negative feedback loop. Initial studies suggested that the length of telomeres directly correlated to the binding of Rap1, with overexpressed Rap1 leading to shortening of telomeres and the introduction of extra telomeric DNA to samples leading to telomere extension (Conrad *et al.*, 1990). It was proposed that a protein-counting mechanism was responsible for telomere length, with telomere-bound Rap1-termini being inversely proportional to telomere length (Marcand *et al.*, 1997). It became clear that counting of Rap1 was in reality counting of Rap1-bound Rif proteins, particularly when shown that mutations of *RAP1* leading to telomere instability did not need to perturb the DBD of Rap1, only the C-terminal responsible for protein interactions (Kyrion *et al.*, 1992). The mechanism proposed is that bound Rif1 and Rif2 act synergistically to inhibit the association of the Tel1 kinase with the telomere, and thus inhibit the telomerase complex from extending the telomeric repeats. When telomeres are longer, this inhibitory effect is stronger whereas at short telomeres this effect is weak and Tel1 is able to promote telomere extension (Levy and Blackburn, 2004).

Interestingly, Rif1 and Rif2 appear to inhibit telomere extension through independent pathways, shown by the additive effects of deletions of *RIF1* and *RIF2* on telomere length. Recent studies have suggested that Rif1 functions to repress Tel1 recruitment and activation through a known interaction with PP1 (Kedziora *et al.*, 2018). In contrast, Rif2 is proposed to compete with Tel1 for binding to the C-terminus of Xrs2 in the MRX complex, delocalising Tel1 and reducing the association of MRX (Hirano *et al.*, 2009). The ability of Rif2 to exert telomere length regulation is not affected by deletion of *RAD52*, indicating that this function is likely unrelated to the role of Rap1 and Rif2 in inhibiting NHEJ, that is not shared by Rif1 (Marcand *et al.*, 2008; Shi *et al.*, 2013). Perplexingly some studies have since suggested that Rif2 levels may be more important for Tel1 inhibition than Rif1, with Tel1 binding short and wild-type length telomeres equally effectively in the absence of Rif2, and other studies suggesting a short region of Rif2 tethered to Rap1 is sufficient to restore telomere length regulation in even *rif1* Δ cells (McGee *et al.*, 2010; Kaizer *et al.*, 2015). Whilst this may be supported by studies demonstrating the potency of a single Rif2 molecule in restoring WT-phenotype in *rif2* Δ cells, compared to the requirement of multiple Rif1 molecules, this would seemingly be in opposition to the telomere lengths seen in *rif1* Δ and *rif2* Δ cells. In *rif1* Δ cells

telomeric repeats are increased to between 0.5-1kb total in length, whereas in *rif2* Δ cells the repeats are increased to 0.35-0.5kb in total (Hardy *et al.*, 1992; Wotton and Shore, 1997; Levy and Blackburn, 2004).

The Rap1-Rif1-Rif2 complex is also established to play a role in maintaining the TPE through the interaction of Rap1 carboxyl-terminal with the Sir3 and Sir4 subunits of SIR complex, which in turn recruits Sir3 further as well as Sir2 (Moretti *et al.*, 1994; Luo *et al.*, 2002). Rif1 and Rif2 compete with the Sir complex for binding to Rap1 which mediates the TPE.

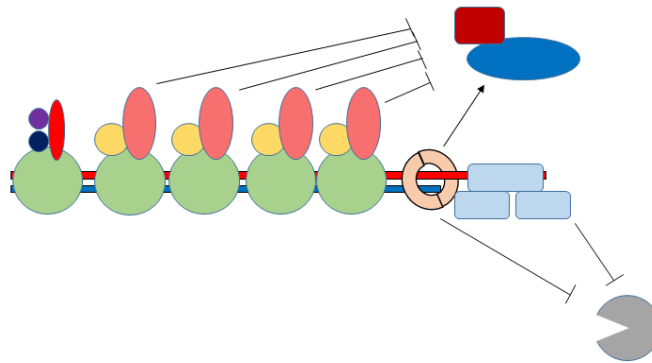
The Rap1-Rif1-Rif2 complex is not found outside of budding yeast. Whilst orthologues of *RAP1* and *RIF1* can be found in fission yeast and in humans, there is currently no known orthologue of *RIF2* in higher eukaryotes.

In *Schizosaccharomyces pombe* both *rap1* (*spRAP1*) and *rif1* (*spRIF1*) encode proteins that are still found at telomeres, however Taz1 instead binds to the telomeric DNA and both *spRap1* and *spRif1* bind Taz1 in turn. *S. pombe* cells defective for *spRAP1* show severe defects in telomere length control, TPE, and telomere clustering to the spindle pole body, whilst *S. pombe* deficient for *rif1* shows defects in telomere length control but shows no effect on telomere silencing (Kano and Ishikawa, 2001).

In humans only hRAP1 is typically found at telomeres, where it binds as part of the shelterin complex through an interaction with the DNA-binding protein TRF2, as it only contains one helix-turn-helix motif and is unable to bind DNA directly (B. Li and de Lange, 2003). Whilst RIF1 is found as part of the damage response in human cells, and as such can be found at aberrant telomeres (a role detailed later in this chapter), it does not bind the telomeres as part of normal telomere homeostasis (Silverman *et al.*, 2004; L. Xu and Blackburn, 2004). Interestingly, reports suggest that RIF1 may be vital for the regulation of telomere length in mice embryonic stem cells, however this role is hypothesised to be through control of chromatin state influencing telomere access rather than a direct binding to the telomere (Dan *et al.*, 2014).

Further to this *RIF1* has been found to be involved with a range of non-telomeric activities, and is conserved across a range of higher eukaryotes (Sreesankar *et al.*, 2012). These further functions will be discussed in-depth later in this chapter, one of which is the focal point of this study.

Long Telomeres



Short Telomeres

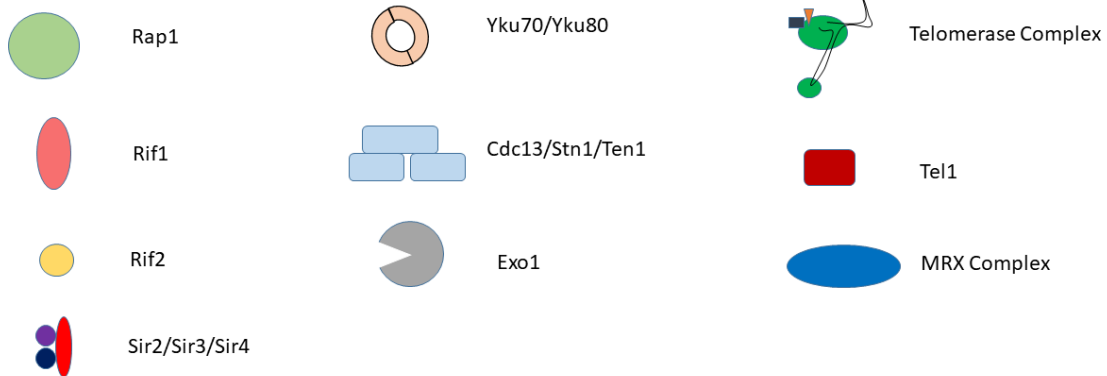
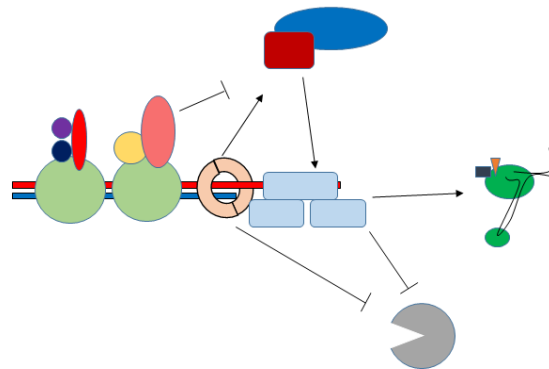


Figure 1.3 Structure of the Telomere and Telomere-Related Complexes

The telomere is bound multiple protein complexes which interact to manage telomere length and protect telomeres from resection. Progressive telomere loss affects the dynamics of the interaction between complexes to promote telomere extension. Information for figure from (Wellinger and Zakian, 2012).

1.4 Models of Telomere Damage

Without the telomere capping complex the chromosomes would closely resemble DSBs. As such mutants defective in telomere capping have been valuable in the elucidation of the DNA damage checkpoint, as well as those factors which also play a role in the telomere cap.

1.4.1 *cdc13-1*

The model system first used to study telomere uncapping is *cdc13-1* (Garvik *et al.*, 1995). In this temperature sensitive mutant, the CST component Cdc13 has a single point mutation (P371S) which leads to dissociation of the capping complex. This mutation has been shown to only affect the capping function and does not influence telomerase recruitment, nor does it affect the binding of Cdc13 to DNA or its association with Stn1 and Ten1 (Nugent *et al.*, 1996; Hughes *et al.*, 2000; Grandin *et al.*, 2001).

Below 26°C, the growth of *cdc13-1* is unimpeded and the cells progress through the cell cycle, this is referred to as permissive temperatures. Above 26°C the temperature sensitive phenotype manifests, this is the restrictive temperature. At restrictive temperatures cells arrest in G2/M phase of the cell cycle, distinguishable by a characteristic dumbbell shape. This occurs due to the failure of the telomere cap in *cdc13-1*, leading to extensive resection of the 5' strand and ssDNA spanning up to 30kb into the chromosome (Garvik *et al.*, 1995; Booth *et al.*, 2001). This resection is the result of exonuclease activity, which interestingly is both up- and down-regulated by the activity of checkpoint proteins. The first identified exonuclease activity at uncapped telomeres was by Exo1, which was found to be essential for extended resection through the sub-telomeric X' elements, and into single-copy genes. However it was also seen to be dispensable for resection of the sub-telomeric Y' repeats, suggesting a second exonuclease was required for the initial resection activity (Zubko *et al.*, 2004). As the MRX complex, Sae2, Sgs1 and Dna2 were all shown to promote resection at DSBs these were likely candidates for this role. However, it was also shown that unlike its activity in promoting resection at DSBs, MRX acts to protect telomeres against resection during telomere uncapping (Foster *et al.*, 2006). Likewise, activity of Sae2, which functions in tandem with the MRX at DSBs, was also shown to improve the viability of *cdc13-1* at restrictive temperatures. Sgs1-Dna2 were later shown to contribute to the exonuclease activity at telomeres, stimulated by the activity of the PCNA-like clamp Ddc1-Mec3-Rad17, known as the 9-1-1 complex (Ngo and Lydall, 2010; Ngo *et al.*, 2014; Ngo and Lydall, 2015).

RPA likely acts as the initial signal for damage in *cdc13-1* cells, binding the ssDNA overhang left vulnerable by the dissociation of the CST. RPA in turn recruits the clamp loader Rad24-Rfc, which loads the 9-1-1 clamp complex onto DNA, and Ddc2-Mec1 which begins the signalling cascade (Piya *et al.*, 2015). Mec1 carries this signal to the transducer kinase Rad9, interestingly Rad9 has been shown to inhibit the formation of ssDNA in *cdc13-1* cells both directly, by inhibiting the action of the Rad24-Rfc clamp loader, and indirectly via activation of Rad53 which inhibits the exonuclease activity of Exo1 (Jia *et al.*, 2004; Zubko *et al.*, 2004; Chappidi *et al.*, 2019).

Rad9 activates two parallel DNA damage checkpoint pathways which regulate arrest in *cdc13-1*. The previously mentioned Rad53, which works partially through Dun1, and Chk1, which acts through Pds1 (Gardner *et al.*, 1999; Blankley and Lydall, 2004). Mitotic exit in budding yeast is controlled by two major pathways; the mitotic exit network (MEN) and the CDC-Fourteen early anaphase release (FEAR) network. Consequently, these two pathways are the targets of the Rad53 pathway and the Chk1 pathway respectively (Liang and Wang, 2007). The action of Rad53-Dun1 is believed to regulate the MEN by the targeted inhibition of Cdc5 polo-like kinase, which normally inhibits the activity of Bfa1 and Bub2, negative regulators of the MEN (Hu *et al.*, 2001; Valerio-Santiago *et al.*, 2013). This pathway is believed to be the more important pathway for inhibition of mitotic progression in *cdc13-1*.

During normal cell cycle progression Cdk1 acts to phosphorylate Pds1 and prevents its degradation, as Cdk1 activity falls Pds1 is degraded (H. Wang *et al.*, 2001; Enserink and Kolodner, 2010). In *cdc13-1* cells with uncapped telomeres Chk1 instead phosphorylates Pds1 and stabilizes it. Phosphorylated Pds1 binds the separin Esp1, which prevents chromosome segregation and arrests the cell cycle (Ciosk *et al.*, 1998). This can only be released by dephosphorylation by the phosphatase, Cdc14 (Shirayama *et al.*, 1999).

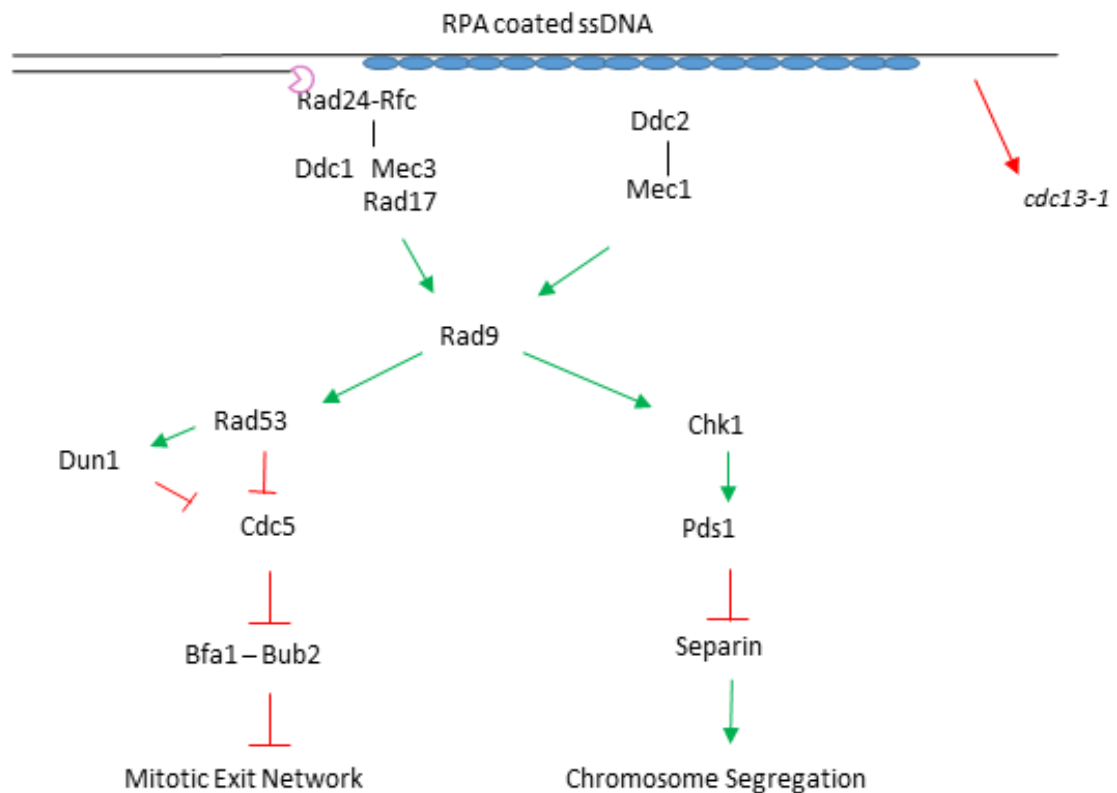


Figure 1.4 Schematic diagram of the checkpoint arrest resulting in *cdc13-1* cells having undergone telomere uncapping.

Diagrammatic representation of the checkpoint pathway in *cdc13-1* cells at restrictive temperature. Green arrows represent activation of the target proteins, red indicates inhibition of a protein or pathway. Information for figure taken from (Enserink and Kolodner, 2010; Harrison and Haber, 2006; Wellinger and Zakian, 2012)

1.4.2 *yku70/80*Δ

The second major model system for studying telomere uncapping in budding yeast is *yku70*Δ cells. Similarly, to *cdc13-1*, deletions of *YKU70* or *YKU80* also lead to temperature induced telomere uncapping, leading to a G2/M checkpoint arrest at restrictive temperatures. This temperature is higher than that of *cdc13-1* cells, with *yku70*Δ and *yku80*Δ mutants failing to form colonies at 37°C and up (Barnes and Rio, 1997). The defect in these cells is known to be telomere specific rather than an effect on the role of Yku in NHEJ, as overexpression of telomerase subunits is capable of partially suppressing this phenotype (Teo and Jackson, 2001). These Yku mutants are also seen to contain short telomeres, decreased telomeric silencing, altered telomere localisation, and critically, ssDNA is seen in the telomeric repeat sequence (Boulton and Jackson, 1998; Laroche *et al.*, 1998; Polotnianska *et al.*, 1998; Mishra and Shore, 1999).

The resection in *yku70*Δ cells has been shown to be Exo1 dependent. However, unlike at DSBs where Exo1 and Mre11 both act in processing to create 3' ssDNA ends, Mre11 instead acts to protect the telomere ends in *yku70*Δ cells. Double mutant *yku70*Δ *mre11*Δ cells actually display increased temperature sensitivity, and accumulate more ssDNA, dependent upon Exo1 activity. It is also noteworthy that in *yku70*Δ cells resection is slower than that seen in *cdc13-1*, and ssDNA reaches sub-telomeres but does not stretch as far as internal loci (Maringele and Lydall, 2002). Interestingly, whilst Mec1 and Rad9 both play important roles in checkpoint arrest in *cdc13-1* and *yku70*Δ, Chk1 is actually essential for the arrest in *yku70*Δ compared to the higher importance of Rad53 in *cdc13-1*. In further contrast to *cdc13-1*, the 9-1-1 complex and Dun1 do not play significant roles in the G2/M arrest of *yku70*Δ cells grown at restrictive temperatures (Maringele and Lydall, 2002). It was also shown that the spindle checkpoint protein Mad2 contributes to the arrest in *yku70*Δ cells, this is contrast to Bub2 which contributes to the arrest of *cdc13-1*. Mad2 is seen to inhibit Cdc20, an essential factor of the Anaphase promoting complex/cyclosome (APC/C) (Hwang *et al.*, 1998).

Unlike *cdc13-1*, the direct molecular mechanism triggering arrest at restrictive temperatures in *yku70*Δ cells was not immediately clear. Instead based on the various phenotypes of *yku70/80*Δ mutants described above, that the trigger may be progressive loss of telomeric repeats. It was shown by Gravel & Wellinger using a temperature-inhibited Yku complex, that the survival of strains after inhibition correlated with the lengths of telomeric repeats and the generation of G' strand overhangs were independent of telomerase activity (Gravel and Wellinger, 2002). It instead suggested that the overhangs induced in S-phase become a

permanent feature of these telomeres. Furthermore, without the known function of Yku to recruit Tlc1 to telomeres, the telomere repeats become shortened (Zappulla *et al.*, 2005). However, other studies have suggested that the role of Yku70/80 in telomere end protection may also be related to creating structures in the telomere to protect against excessive resection. Without Yku70/80 these structures are affected by both the loss of telomeric repeats and the presence of long G-tails, and at high temperatures these structures may be lost (Lopez *et al.*, 2011).

1.4.3 Telomerase negative survivors

Cellular senescence is the term for the gradual decline in proliferation capacity of cells, ultimately leading to permanent growth arrest. This process is usually seen in multi-cellular organisms after a defined number of cell divisions, referred to as the “Hayflick limit”. A number of factors govern the onset of senescence, amongst which is the downregulation of telomerase activity in somatic mammalian cells and the subsequent arrest resulting from progressive loss of telomeric DNA. The immortalisation of cell lines, including in tumorigenesis, requires the reactivation of telomerase to overcome this limit. However, a secondary method of telomere rescue is also seen to be established through homologous recombination. This process and the resulting telomeres are referred to as ALT (Alternate Lengthening of Telomeres) (Henson *et al.*, 2002).

Despite the continual expression of telomerase in single celled eukaryotes, an equivalent to this process can also be seen in budding yeast. This can be seen in telomerase-null strains such as *tlc1Δ*, where a small fraction of cells are seen to survive and form viable colonies (Lundblad and Szostak, 1989). The importance of recombination in this survival was demonstrated by the absence of survivors when telomerase mutations are combined with deletion of key HR genes such as *RAD52* (Lundblad and Blackburn, 1993). These survivors are seen to form into one of two types, dubbed type I and type II survivors. Type I survivors are more common than type II, however due to their unstable nature these are easily converted to type II survivors which grow at a faster rate and rapidly take over liquid cultures (Teng *et al.*, 2000).

1.4.3.1 Type 1 Survivors

In these survivors the majority of cells contain telomeres made up of multiple tandem Y' repeats, whilst the telomeric TG repeats themselves remain short (50-150bp). Type I

survivors are further seen to also contain extrachromosomal circular Y' elements that may serve as substrates for Y' recombination. The generation of type I survivors is dependent upon the activity of *RAD52*, *POL32*, *RAD51*, *RAD54*, *RAD57* and *RAD55* (Chen *et al.*, 2001b; Larrivee and Wellinger, 2006).

1.4.3.2 Type II survivors

Telomeres in type II survivors only show small amplifications of the subtelomeric elements, however they instead have large increases in the TG₁₋₃ telomeric repeats. The telomeres in these survivors are highly heterogenous, ranging from very short repeats to over 12kb in length. These telomeres are not stable and are progressively lost over multiple cell cycles, before short dramatic bursts of lengthening take place. Unlike in type I survivors, the generation of type II survivors requires the MRX complex, *RAD59*, and *SGS1* (Teng and Zakian, 1999; Chen *et al.*, 2001b). Interestingly the formation of Type II survivors can be inhibited by both Rif1 and Rif2 (Teng *et al.*, 2000).

1.4.3.3 PAL survivors

In the absence of either process to generate type I or type II survivors, a percentage of cells are still seen to survive and proliferate. These were first seen in *tlc1Δ rad52Δ exo1Δ* strains, lacking both telomerase activity and capacity for homologous recombination. After an initial period of slow growth, survivors were seen to grow as well as WT cells, and appeared to have become immortalised. After 100 days, most survivors lacked telomeric sequence but maintained chromosomes with abnormal size. These survivors maintained viability by the amplification of large palindromes at chromosome ends, and these abnormal chromosomes contained large numbers of gene duplications and deletions. It was proposed that inverted repeats naturally present in the genome can catalyse palindrome formation, after formation these palindromes amplify essential genes close to the chromosome ends and improve cell viability (Maringele and Lydall, 2004).

The emergence of survivors of all types led to a central question; how do cells overcome the checkpoint barrier to cell cycle progression? It was identified that after telomere loss there is an initial period of growth inhibition reliant on the DNA damage checkpoint proteins, together with Exo1 and Mre11 nucleases. In survivors, the checkpoint pathways become tolerant to the loss of telomeres yet remain responsive to new DNA damage. This study showed that Rif1 and Exo1 were essential for the tolerance of damage, and the extensive

genomic modifications seen in survivors (Xue *et al.*, 2016). This is related to the anti-checkpoint role of Rif1 that is discussed later in this chapter (**section 1.10.3**).

1.5 CDK1

1.5.1 CDK1 & Mitotic Progression

The eukaryotic cell cycle is heavily dependent on cyclin dependent kinases (CDKs). In budding yeast there are six evolutionary conserved CDKs; *CDK1* (also referred to as *CDC28*), *PHO85*, *KIN28*, *SSN3*, *CTK1*, and *BUR1* (Toh-e *et al.*, 1988; Liu and Kipreos, 2000); (Simon *et al.*, 1986; J. M. Lee and Greenleaf, 1991; Yao *et al.*, 2000). *CDK1* (is the only one of these required to drive the cell cycle, although many of the various roles are supported by the non-essential CDKs (Huang *et al.*, 2007). Cdk1 preferentially phosphorylates the consensus sequence S/T-P-x-K/R, however it also phosphorylates a more minimal sequence of S/T-P if required (Nigg, 1993). Throughout the cell cycle Cdk1 interacts with 9 separate cyclins to control kinase activity through the recruitment and selection of target substrates; Cln1-3, and Clb1-6. In the absence of cyclins, CDKs are completely inactive due to the active site being blocked by a T-loop within the protein structure. Phosphorylation of residues within this loop by Cak1 are believed to expose the binding site and increase the number of contacts between Cdk1 and cyclins. There is, however, substantial overlap in these cyclins, as overexpression of either Clb1 or Clb6 would be sufficient to rescue viability of a *clb1Δ clb2Δ clb3Δ clb4Δ clb5Δ clb6Δ* mutant (Schwob and Nasmyth, 1993; Haase and Reed, 1999). The activity of these cyclins, as well as multiple inhibitor kinases and phosphatases, regulates the activity of Cdk1 through the cell cycle. In G1 Cdk1 is inactive due to low cellular concentration of cyclin proteins and the presence of Cyclin dependent Kinase Inhibitors (CKIs). Activity begins to rise in late G1, as cyclin levels rise CKI levels fall. Cdk1 remains highly active until anaphase when cyclins are degraded and CKIs are re-expressed (Mendenhall and Hodge, 1998). This drop in activity is crucial for mitotic exit and the re-set of the cells into G1 of the next cycle.

CLN1, 2, & 3 are all expressed in late G1 to interact with the Cdk1 protein. Cln1 and Cln2 are believed to be required for spindle pole body duplication and initiation of bud morphogenesis, whilst Cln3 is involved in the regulation of transcriptional programs. All three are involved in the transition into S-phase and function redundantly, as only triple mutants of *cln1Δ cln2Δ cln3Δ* fail to progress into S-phase (Tyers *et al.*, 1993; Griffith *et al.*, 1999). After the transition to S-phase they are targeted for destruction by the action of Clb-Cdk complexes (Tyers *et al.*, 1992; Marcand *et al.*, 1997). Clb5 and Clb6 take action next, these are induced during G1, and Clb5 remains stable until anaphase whilst Clb6 is degraded at the G1/S transition. Both appear to be involved in ensuring origins of replication are not re-licensed and fire twice within one cell cycle (Dahmann *et al.*, 1995). Clb3 & 4 are expressed

from S phase until anaphase and are involved in the function of Cdk1 in DNA replication, spindle assembly and the G2/M transition (Richardson *et al.*, 1992). Finally, Clb1 & 2 are expressed during G2-M-phase and degrade at the end of mitosis. These are involved in mitotic events such as spindle elongation and bud morphogenesis (Lew and Reed, 1993).

As previously mentioned, this activity is countered in G1 by the activity of CKIs. Whilst the CKIs Far1 and Sic1 are active, cells are incapable of entering S-phase. These inhibitors bind cyclin-CDK complexes to prevent their interaction with substrates (Chang and Herskowitz, 1990; Mendenhall, 1993; Venta *et al.*, 2012). Interestingly, the only essential function of the Cln-Cdk1 interaction appears to be the degradation of Sic1 (Schneider *et al.*, 1996). The re-expression of Sic1 in late mitosis contributes to mitotic exit and the reset of the cell cycle. There are other proteins also involved in the regulation of CDK activity. To promote the progression through G1, Cks1 acts to increase the activity of Cln-Cdk1 complexes (Reynard *et al.*, 2000). Swe1 phosphatase is present throughout G1 and peaks in late S-phase before degradation by the APC/C. Swe1 acts to dephosphorylate Cdk1 to inhibit activity and delay the cell cycle in response to cytoskeleton stresses (Sia *et al.*, 1998; Keaton and Lew, 2006). Swe1 is in turn countered by the activity of Mih1, which acts to reverse the phosphatase activity and promote entry into mitosis (Russell *et al.*, 1989). Finally, it has been shown that acetylation of Cdk1 on K40 is essential for kinase activity (Choudhary *et al.*, 2009).

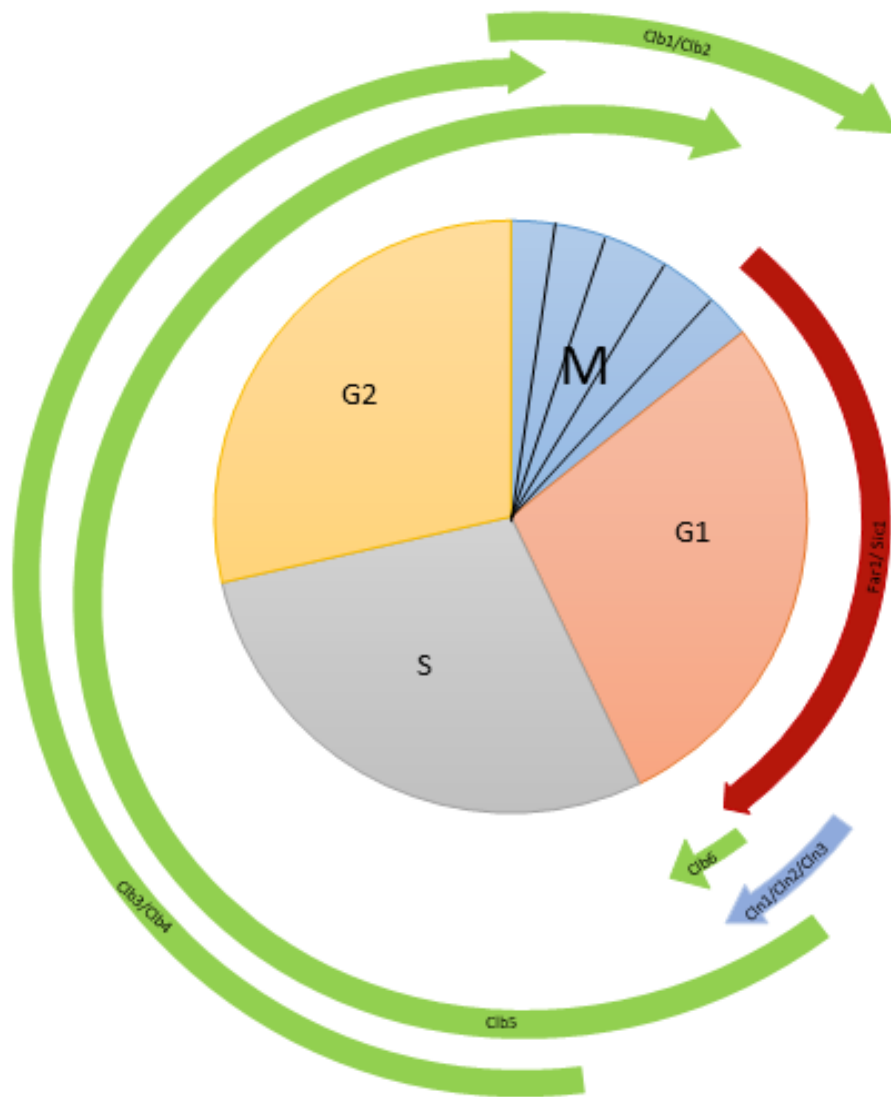


Figure 1.5.1 the activity of Cdk1 & cyclins through the Cell Cycle

The activity of Cdk1 associated cyclins is indicated with green and blue arrows. The location shows the point in the cell cycle at which cyclins are induced and the point at which they are degraded or their interaction with Cdk1 inhibited. The red arrow indicates the activity of Far1 and Sic1, the CKIs, which inhibit the activity of cyclins through G1 phase. Figure assembled using information from Enserink & Kolodner (2010).

1.5.2 Exit from Mitosis

The final exit of cells from mitosis is carried out by a careful balance of the activity of Cdk1 and of Cdc14 phosphatase, via the APC/C. Without Cdc14 activity cells arrest prior to cytokinesis, with long spindles and a divided nucleus (Wood and Hartwell, 1982). The process of mitotic exit is begun by the promotion of the APC/C by the action of Cdk1. The activity of the APC/C rises and falls according its association with the two subunits Cdc20 and Cdh1. As mitosis progresses the APC/C associates highly with Cdc20 (APC/C^{Cdc20}). However, in late mitosis this rebalances and APC/C associates with Cdh1 (APC/C^{Cdh1}), this complex remains active through G1 (Sullivan and Morgan, 2007). Whilst both these two forms of the complex are required for full degradation of Clb2, they do have some differences in substrate specificity, such as APC/C^{Cdc20} targeting of Pds1 and APC/C^{Cdh1} targeting Ase1 (Visintin *et al.*, 1997; Wasch and Cross, 2002). During G1 phase, APC/C^{Cdh1} degrades cyclins to inhibit Cdk1 activity. However, as cells enter into S-phase the interaction between Cdh1 and the APC/C is inhibited by the activity of Cln1, 2-Cdk1 and Clb5-Cdk1 (Crasta *et al.*, 2008). Cdk1 phosphorylates the APC/C components Cdc16, Cdc23, and Cdc27 to promote the binding of the APC/C and Cdc20. This complex targets Pds1 for degradation. Normally Pds1 inhibits activity of Esp1, degradation of Pds1 therefore increases activity of Esp1 and leads to dissolution of chromosome cohesion and the activation of the FEAR network, followed by subsequent activation of the MEN (Shirayama *et al.*, 1999; Rudner and Murray, 2000). During the majority of the cell cycle Cdc14 is sequestered in the nucleolus by Net1, the increased activity of Esp1 leads to decreases in PP2A^{Cdc55} phosphatase activity and thereby increased phosphorylation of Net1, allowing the localisation of Cdc14 to the nucleus (Y. Wang and Ng, 2006). The phosphorylation is targeted by Clb-Cdk1, as well as Clb-Cdk1-activated Cdc5 (Rodriguez-Rodriguez *et al.*, 2016).

As Cdk1 activity drops during anaphase there is potential for Net1 to return to a hypo-phosphorylated state and thereby return Cdc14 to the nucleolus prematurely. To ensure continued Cdc14 activity the MEN pathway is activated through Tem1 which triggers a signalling cascade through Cdc15 and Dbf2-Mob1 (Lee *et al.*, 2001; Mah *et al.*, 2001). The proper timing of MEN activation is maintained by the activity of Bfa1-Bub2, which prevent the activation of MEN prior completion of chromosome separation. Like Net1, Bfa1 phosphorylation is controlled by PP2A^{Cdc55} activity. Therefore, as Esp1 activity increases, the inhibitory phosphorylation of Bfa1 increases by action of Cdc5. Full activation of the MEN pathway also requires Cdc14 mediated dephosphorylation of Cdc15 and Mob1 during FEAR, both of which are targets of Cdk1 (Jaspersen and Morgan, 2000). As mitosis comes

to an end Cdc14 dephosphorylates Cdh1 to permit its re-association with the APC/C complex (Visintin *et al.*, 1998). APC/C^{Cdh1} targets Cdc5 for degradation, downregulating Cdc14 activity by facilitating its return to the cytoplasm (Visintin *et al.*, 2008). The removal of Cdc14 from the nucleus is also controlled by Dbf2-Mob1 mediated phosphorylation of Cdc14 at residues adjacent to its nuclear localisation signal (NLS) (Mohl *et al.*, 2009). Finally, APC/C^{Cdh1} targets the cyclins for degradation, resetting the cell cycle and suppressing Cdk1 activity during G1

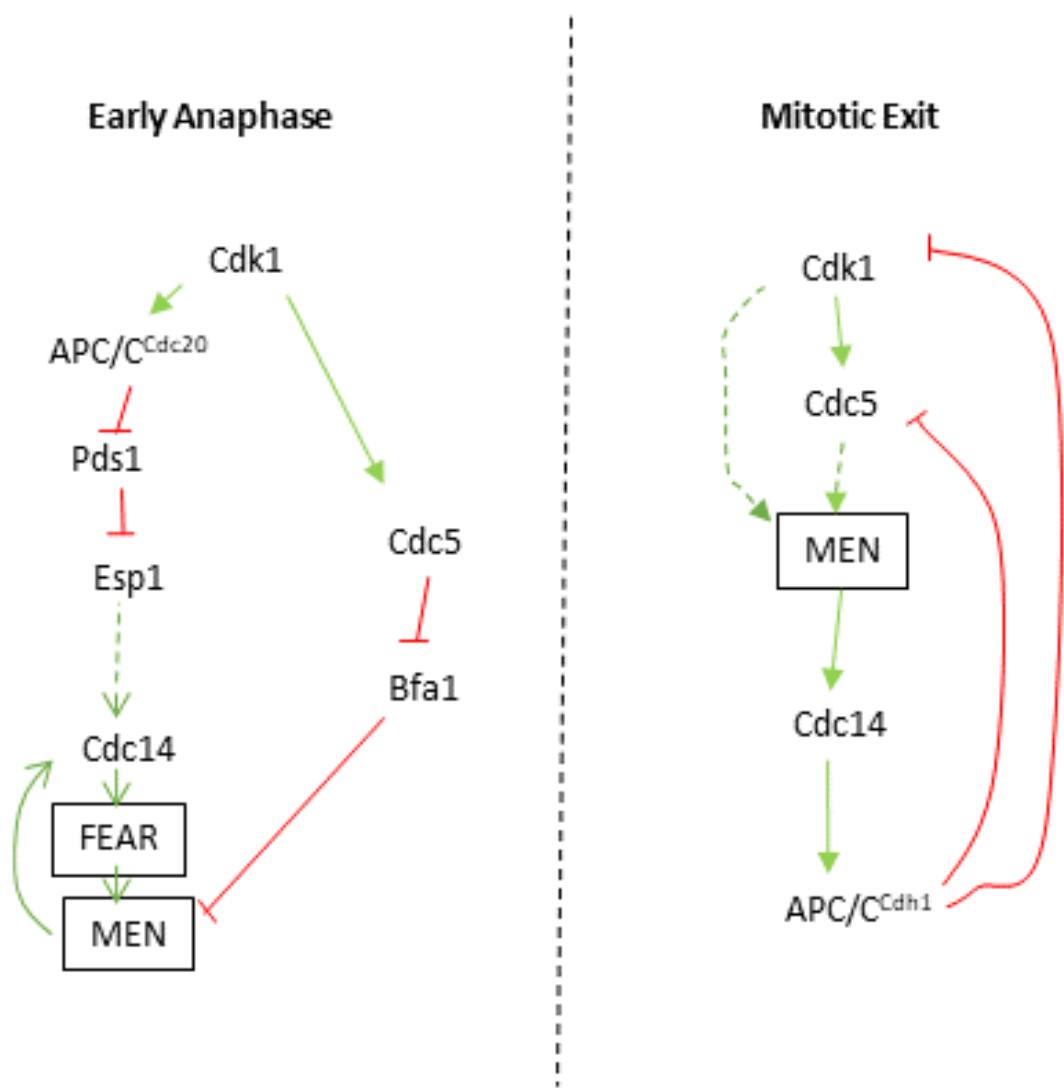


Figure 1.5.2. A schematic diagram of the influence of Cdk1 and Cdc14 in promoting mitotic exit.

Cdk1 promotes the activity of Cdc14 which in turn activates factors and pathways required for mitotic exit. As the cell exits mitosis the factors activate by Cdc14 feedback to inhibit the activity of Cdk1. Information for figure taken from (Enserink and Kolodner, 2010).

1.5.2 Cdk1-Controlled Processes

As a key driver of mitotic progression, it is clear that Cdk1 plays a vital role in a wide range of processes that are targeted by the association of cyclins at appropriate times. These include the arrangement of transcriptional programs, control of cell morphogenesis, restriction of pheromone signalling, control over DNA replication, regulation of chromosome separation, and the maintenance of genome stability.

The proper transcription of genes at the correct time is a key element of maintaining cell cycle progression. In G1 phase, Cln3-Cdk1 control the expression of the G1 cluster, a set of ~200 genes specifically expressed in G1 phase (Spellman *et al.*, 1998). This is mediated by the phosphorylation of Whi5 by Cdk1 and Pho85, repressing the inhibition of SBF transcription complex (Costanzo *et al.*, 2004). Cyclin-Cdk complexes may also target the SBF and MBF directly to shut off transcription of the G1 cluster at the G1/S transition (Geymonat *et al.*, 2004). As the cell transitions into S-phase a new cluster of genes are transcribed, stimulated by Hcm1 activity. The activity and degradation of Hcm1 are both controlled through phosphorylation by Cdk1 (Pramila *et al.*, 2006). From S-phase until the end of nuclear division in mitosis Cdk1 is involved in the increased expression of a group of 35 genes called the CLB2 cluster. This includes genes such as *CDC5*, *CDC20*, and *CLB2* itself. The stimulation of expression of this cluster is mediated by interaction of Clb2-Cdk1, and so Clb2 creates a positive feedback loop in which it stimulates its own synthesis. As mitosis progresses through the final stages before transition into G1 phase, Cdk1 is believed to be involved in the control of four gene clusters; the *PHO* regulon, the *SIC1* cluster, *MCM* cluster, and the *MAT* cluster (Spellman *et al.*, 1998). Of these, Cdk1 and Pho85 only serve to upregulate the activity of the *PHO* regulon. Transcription of the other three gene clusters are downregulated by Cdk1 activity, and so as Cdk1 activity falls towards the end of mitosis transcription of these clusters increases. The *SIC1* and *MAT* cluster include the CKI genes *FAR1* and *SIC1* (Oehlen *et al.*, 1996). The importance of Cdk1 in regulating these is unclear, as it appears there is at least 1 other major factor. Experimental inactivation of Cdk1 showed that around 70% of the genes in these clusters continued to be expressed on schedule (Orlando *et al.*, 2008). This may imply that the function of Cdk1 is to fine-tune coordination of expression and the cell cycle, rather than being the prime determinant.

During bud morphogenesis Cdk1 stimulates the activity of Cdc24. As the cell passes to S-phase Cdk1 promotes removal of inhibition of Bem2/3 and Rfa2, which keep Cdc42 in an inactive state during G1 to prevent bud formation (Nern and Arkowitz, 2000; Sopko *et al.*, 2007). Cdk1 then coordinates membrane growth in the polarized cell by activating the lipase

Tgl4 and inducing expression of genes involved in lipid synthesis, it also coordinates membrane-trafficking dynamics and synthesis of the cell wall (Santos-Rosa *et al.*, 2005). Without Cdk1 vesicles are mistargeted from the growing cell bud, and it has been implicated further in the proper inheritance of cell organelles (McCusker *et al.*, 2012).

The pheromone response pathway is triggered by binding of the mating pheromone to seven transmembrane receptors on the cell surface, stimulating a conformational change in the receptor. This ultimately leads to the activation of the Ste4-Ste18 complex bound to the cell membrane, through a series of effectors this complex recruits Ste5, which serves as an adaptor for Ste11, Ste7, and Fus3 (Herskowitz, 1995; Wu *et al.*, 1995). Through alterations to the transcriptional program, interactions with the actin cytoskeleton, and inhibition of Cln-Cdk1 this pathway arrests the cell in G1, the only phase of the cell cycle in which mating should occur (Yu *et al.*, 2008). Mating outside of G1 would lead to aneuploidy, and therefore must be inhibited, as Cdk1 is inactive during G1 and active elsewhere it is an ideal candidate. Cln/Clb-Cdk1 activity prevents the activation of the response pathway through phosphorylation of a number of core components such as Ste20, Ste5, and Far1 (Gartner *et al.*, 1998; Winters *et al.*, 2005).

DNA replication and its proper timing are crucial for an orderly cell cycle. If replication initiates too early, or late, it can lead to problems in the cell cycle. It is also important to ensure that DNA is replicated only once per cell cycle. Cdk1 has key roles in both of these elements of regulation. The initiation of replication begins with origin licensing, this is when the pre-replication complex (pre-RC) is assembled at origins of replication. The foundation of this complex is the ATP-binding Origin Recognition Complex (ORC), made up of six subunits (Orc1-6). This recruits Cdc6, Cdt1 and the MCM2-7 hexamer complex which functions as an ATP-dependent helicase, finally the GINS is required for initiation of replication (Randell *et al.*, 2006; Z. Chen *et al.*, 2007; Labib and Gambus, 2007). Once the pre-RC is assembled a second transition occurs to the pre-Initiation complex (pre-IC), this requires the recruitment of Cdc45 to the pre-RC dependent upon the action of Clb5/6-Cdk1 (Zou and Stillman, 1998; Zou and Stillman, 2000). Cdk1 and DDK (Dbf4 dependent kinase) act together. DDK phosphorylates the MCM2-7 complex, leading to recruitment of Cdc45 (Sheu and Stillman, 2006). Cdc45 and Dpb11 are required for recruitment and loading of the DNA polymerases alpha and epsilon (Masumoto *et al.*, 2000). Initiation of replication then requires Cdk1 mediated phosphorylation of Sld2 and Sld3, which induces binding to Dbp11 (Zegerman and Diffley, 2007). The complex of Sld2, Sld3, DPb11 and Cdc45 at the origin constitutes a phosphorylation-dependent switch for initiation of replication in G1-S.

After the initiation it is equally important to prevent the re-initiation of an origin of replication. Cdk1 targets the ORC, Cdc6, and the MCM2-7 complex for phosphorylation, leading to the dissociation of Mcm2-7 and Cdc6 from the origin. These proteins cannot reassemble until phosphorylation is removed, and re-replication could only occur if all three were simultaneously uncoupled from regulation (Nguyen *et al.*, 2001).

Cdk1 plays important roles in a number of aspects of proper chromosome segregation and interacts with many protein targets. As described previously, the phosphorylation of Pds1 plays a key role in chromosome cohesion and separation. Further to this, it is seen to influence a range of segregation-related pathways through various protein interactions including; kinetochore attachment (Ask1), spindle pole body (SPB)-spindle attachment (Spc42), SPB duplication and separation (Spc110, Mps1), prevention of SPB re-duplication (unknown), spindle positioning (Kar9, Stu2, Cnm67), and spindle stability and elongation (Sli15, Fin1, Bir1, Ase1) (Enserink and Kolodner, 2010).

Outside of the role of Cdk1 in controlling chromosome segregation and the related pathway timings, Cdk1 also plays a role in genomic stability through interaction with the DNA damage checkpoint response. Direct roles for Cdk1 within the checkpoint response are difficult to separate from indirect roles. As Cdk1 is a controlling factor of many of the cell cycle progression processes, the loss of Cdk1 can lead to checkpoint arrests at various points in the cell cycle. Furthermore, it may be an expected target for any pathway intended to halt the cell cycle. However, it has been shown that inhibitory phosphorylation of Cdk1 is not required for an effective checkpoint arrest as many checkpoint proteins will instead target the processes directly, such as Rad53 targeting the APC/C component Cdc20, or Cdc5. However, Cdk1 has been shown to be directly required for checkpoint arrest in some scenarios. At DSBs Cdk1 is required for the promotion of HR in repair pathway choice and the recruitment of Rad52 to the site (Ira *et al.*, 2004; Barlow and Rothstein, 2009). Cdk1 phosphorylation of Sae2 is required for removal of the MRX complex and end-processing at DSBs, which Cdk1 also promotes through phosphorylation of Exo1 (Tomimatsu *et al.*, 2014). High activity of Cdk1 in G2/M arrest leads to Cdk1 promoting the activity of exonucleases to resect the DNA adjacent to DSBs. Increasing evidence in recent years has suggested that Cdk1-mediated phosphorylation may be required for a full checkpoint arrest at G2/M. A recent study suggested that phosphorylation of Rad9 by Cdk1 was required for activation of the effector kinase Chk1 (Abreu *et al.*, 2013). Cdk1 has also been shown to directly phosphorylate Rad53, although its requirement during checkpoint arrest is uncertain (Diani *et al.*, 2009; Schleker *et al.*, 2010). It appears that Cdk1 may only be required for full Rad53

phosphorylation during arrests occurring due to DNA damaging agents, which occur in G2/M, as opposed to replication-stress based damage occurring during S-phase (Liberi *et al.*, 2000; Enserink *et al.*, 2009).

The wide range of functions of Cdk1 make it incredibly important for the stability of chromosomes and the genome at large. The vast interplay between Cdk1 activity and the activity of various pathways make it relevant to any study of phosphorylation signalling cascades.

1.6 The G2/M DNA Damage Checkpoint

In yeast the primary response to DSBs, and uncapped telomeres, is the G2/M checkpoint. Once damage is detected components of this pathway arrest the cell cycle at the G2/M phase, and activate factors involved in DNA repair. This pathway is largely made up of a series of kinases acting in turn, beginning with sensor proteins binding the damage sites, which recruit sensor kinases. These sensor kinases in turn phosphorylate transducer kinases which carry the signal on to effector kinases, these interact with a range of cellular factors to halt the cell cycle and activate repair.

During the G2/M stage of the cell cycle repair favours homologous recombination due to the presence of replicated DNA to act as a template. In this event, the DSB, or uncapped telomere is resected 5'-3' by exonucleases recruited to the sites of damage. This resection is largely determined by Cdk1 activity, which controls repair pathway choice (Aylon *et al.*, 2004; Ira *et al.*, 2004). The MRX (Mre11-Rad50-Xrs2) helicase complex detects the presence of a DSB and binds, Cdk1 in turn phosphorylates Sae2 which now targets resection to the DNA ends and promotes dissociation of the MRX complex (Huertas *et al.*, 2008). The exonuclease activity of Sae2 is supported by further resection carried out by Exo1, and the helicase activity of Sgs1 (Zhu *et al.*, 2008).

The second signal for damage is the RPA complex which coats the ssDNA exposed after resection. This damage signal is detected by the yeast ATR/ATM phosphatidylinositol 3-kinase (PIKK) equivalents, Mec1 and Tel1. However, Mec1 is the primary sensor kinase in the yeast response to DSBs (Harrison and Haber, 2006). Mec1 and Ddc2 form a heterodimer in which Ddc2 is responsible for the recruitment of Mec1 to sites of damage, and for DNA binding.

The third damage sensor functions independently and is known as the 9-1-1 complex, or the checkpoint clamp and the clamp-loader complexes. The heterotrimeric complex is made up of Rad17, Mec3, and Ddc1 (mammalian homologues Rad9-Hus1-Rad1 which form the PCNA clamp) and is loaded onto the dsDNA by Rad24 acting in complex with the yeast Rfc homologues which bind at the ssDNA-dsDNA junction (Ellison and Stillman, 2003). This clamp complex promotes resection at the DSB and recruits the transducer kinases for Mec1 interaction, thus the co-localisation of these proteins to a DSB is essential for a functional G2/M checkpoint (Emili, 1998; Jia *et al.*, 2004; Majka *et al.*, 2006).

Mec1 phosphorylates the transducer protein Rad9, the recruitment of which further requires H2A phosphorylation and methylation of H3 (Toh *et al.*, 2006). Rad9 in turn targets the

effector kinases Rad53 and Chk1 for recruitment to the damage site where they are phosphorylated. Rad53 and Chk1 start two pathways acting in parallel to arrest the cell cycle and initiate damage repair through shared mechanisms. Rad53 is thought to partially manage this through activation of the kinase Dun1 (Gardner *et al.*, 1999; Sanchez *et al.*, 1999). These pathways include the maintenance of CDK activity, and the inhibition of mitotic exit, through the inhibition of Cdc5 by Rad53 (Cheng *et al.*, 1998).

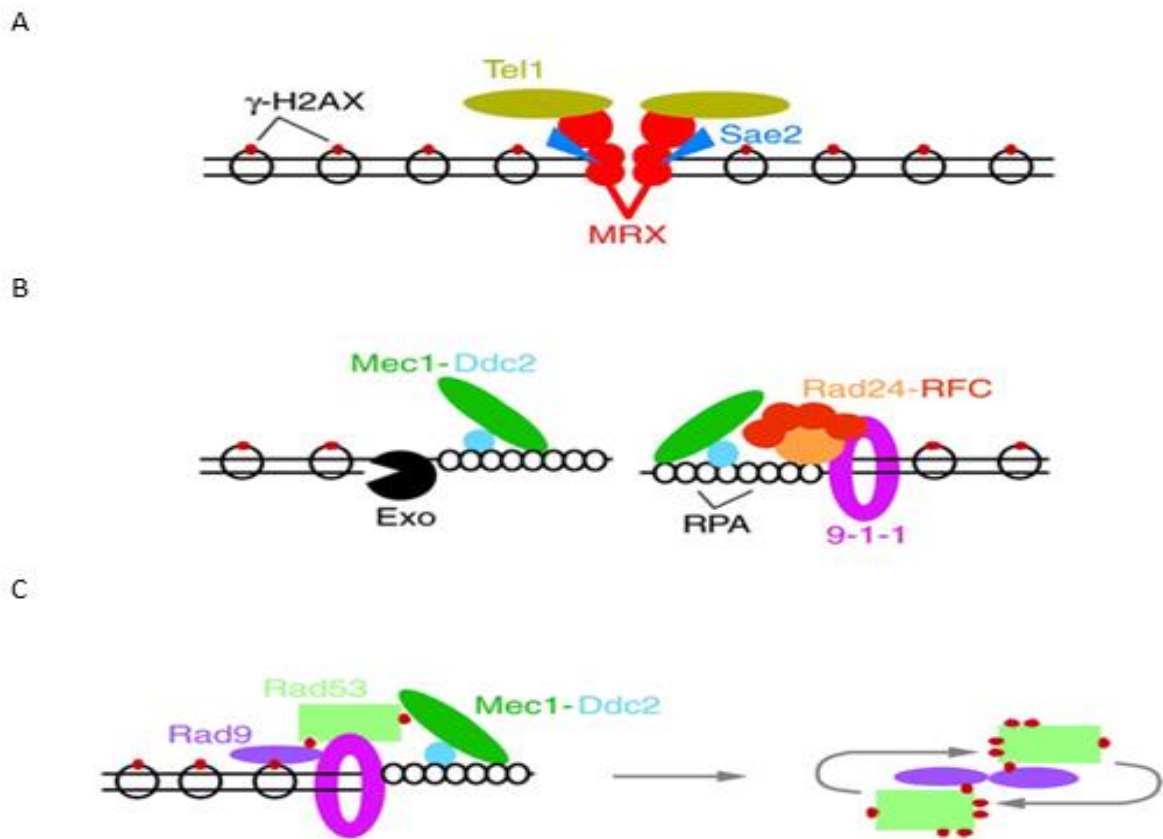


Figure 1.6. The G2/M DNA damage checkpoint in *S. cerevisiae*

(A) DSBs are initially processed by the activity of the MRX complex, Tel1, and Sae2. (B) DNA is resected 5' to 3' by exonuclease activity creating long stretches of ssDNA, which is bound by the RPA complex. RPA bound ssDNA acts to recruit the damage sensor kinases Mec1 (through Ddc2) and the 9-1-1 complex. (C) Once recruited the 9-1-1 complex acts to phosphorylate Rif1 and promote recruitment of the kinase Rad9 and the effector kinase Rad53. Rad53 and Rad9 create an auto-phosphorylation loop and Rad53 interacts with downstream effectors to induce cell cycle arrest and DNA repair. Figure from Harrison & Haber (2006).

1.7 The Spindle Checkpoint

The spindle-assembly checkpoint (SAC) was first identified by screens searching for mutations allowing budding yeast cells to bypass mitotic arrest in the presence of spindle poisons. Identified by these screens were the genes *MAD1*, *MAD2*, *MAD3* (*BUBR1* in humans), and *BUB1*. A further gene was identified, *BUB3*, as an extra-copy suppressor of the mutation *bub1-1* (R. Li and Murray, 1991; Hoyt *et al.*, 1992). These genes are conserved across all eukaryotes and are involved in the SAC, a prometaphase pathway which acts to prevent the separation of sister chromatids (Taylor *et al.*, 2004). The SAC functions to detect potential defects in chromosome separation by monitoring the attachment of spindle-microtubules to the kinetochores, and the tension that is generated by proper spindle attachment to connect the kinetochores and spindle pole bodies.

The SAC acts to target Cdc20, a co-factor of the ubiquitin ligase complex, the APC/C. This creates the formation of the mitotic checkpoint complex (MCC), made up of Mad2, Mad3, Bub3, and Cdc20 (Hwang *et al.*, 1998; Sudakin *et al.*, 2001). Alternatively, the SAC proteins Mad1, Bub1, Mps1 and Aurora-B function to amplify the SAC signal and rate of MCC formation. After exposure to spindle poisons the components of the SAC, including the MCC, concentrate at the kinetochore in prometaphase. However it does not appear that the MCC simply sequesters Cdc20 at the kinetochore, as the MCC is found bound to the APC/C after SAC activation (Sudakin *et al.*, 2001; Morrow *et al.*, 2005). It instead appears that Mad2 facilitates the binding of the components of the MCC, whilst Mad3 reduces the ability of the APC/C to recruit cyclin B1 and securin by interfering with substrate binding (Burton and Solomon, 2007). This inhibits the ubiquitin-ligase activity of the APC/C, and in turn inhibits the ubiquitination of Cyclin-B & Securin, which would usually constitute a signal for their degradation (Peters, 2006). This functions to inhibit mitotic progression in two ways:

- The proteolysis of cyclin B serves to inactivate Cdk1, which promotes mitotic exit. Without ubiquitination of Cyclin B, Cdk1 remains active.
- Securin continues to inhibit the activity of the protease separase. Separase activity is required to cleave the cohesin complex holding sister chromatids together, and thereby activate anaphase.

Through these two actions the SAC prolongs metaphase until all chromosomes have are bi-oriented between the spindle poles. The extinguishing of the SAC signal upon proper kinetochore attachment and tension, appears to be mediated by several factors. Aurora B has been established as a “tension-sensor”, it prevents the premature removal of SAC

proteins from the kinetochore, through the destabilisation of the kinetochore-microtubule attachments. (Gurden *et al.*, 2018). The disassembly of the MCC plays a key role in its removal from the kinetochore, a process mediated by Cdc20 ubiquitination and TRIP13 AAA-ATPase (Uzunova *et al.*, 2012; Eytan *et al.*, 2014).

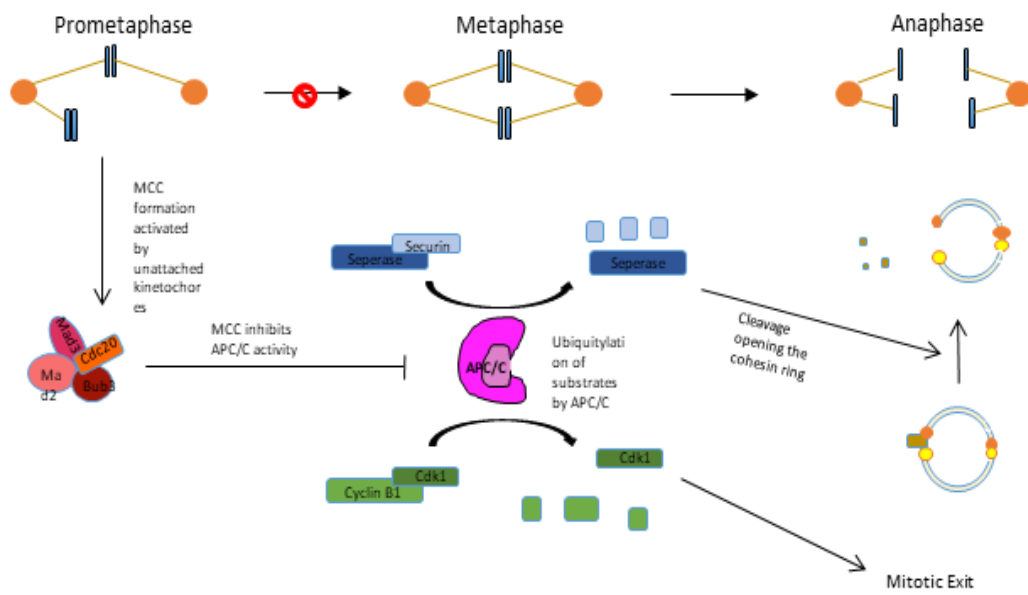


Figure 1.7 the spindle checkpoint prevents separation of chromatids in the presence of unattached kinetochores

Improperly attached spindles are detected in prometaphase, triggering the assembly of the MCC, inhibiting the APC/C/C and preventing cohesin cleavage or mitotic exit. Figure adapted from (Lara-Gonzalez *et al.*, 2012)

1.8 Repair Pathway Choice – Non-Homologous End Joining or Homologous Recombination

The formation of DSBs present severe threats to genomic stability. If broken chromosomes are not repaired this can result in the loss of the damaged chromosome during mitosis. Broken chromosomes can also become fused to other chromosomes, translocating large sections of the genome. Failure of the cells to properly deal with DSBs is a major cause of tumorigenesis. Therefore, two pathways have evolved to efficiently manage DSB repair; non-homologous end joining (NHEJ), and homologous recombination (HR).

HR uses homologous sequence as a template to repair the DSB, this is the primary repair pathway in the G2 phase when the homologous sister chromatid is available after DNA replication. The DNA ends are processed to create resected overhangs that can be used to pair with the template invading strand from the sister chromatid. As this process uses template DNA, the DSB is repaired with high fidelity. NHEJ, however, does not make use of homologous sequence and is the primary repair pathway in G1 phase when a sister chromatid is not available. NHEJ uses a simple end-to-end ligation method to re-join the DNA flanking the DSB, and as such can be far more error prone, and may introduce small deletions and insertions into the sequence. The processing of the DNA ends of the DSB partially dictated pathway choice, with the 5'-3' resection being the major activity guided by Cdk1 (Ira et al, 2004).

Upon a DSB in yeast the Yku70/Yku80 complex binds broken DNA ends, alongside the MRX complex. Typically, a small level of processing takes place to create regions of "microhomology", the yeast DNA ligase complex Dnl4/Lif1 is then recruited to seal the break. NHEJ is estimated to account for 25-50% of DSBs in yeast and mammalian cells (L. Chen *et al.*, 2001a; Clikeman *et al.*, 2001).

HR conversely is initiated with extensive 5'-3' resection at broken ends, initiated by MRX, but further resection is carried out by Exo1 and Sgs1/Dna2, promoted by Cdk1 (Mimitou and Symington, 2008; Zhu *et al.*, 2008). These extensive 3' ssDNA tails are then coated by RPA, which is in turn displaced by Rad51 in a process mediated by Rad52, Rad55, and Rad57. The Rad51 bound filament facilitate the search for suitable regions of homology, both double stranded and single stranded. Srs2 helicase then strips Rad51 from the ssDNA to allow base-pairing of the complementary and invading strands, and the subsequent strand extension by DNA polymerase (Sugawara *et al.*, 2003). Interestingly, whilst this process is more accurate than NHEJ due to the copying of a template sequence, the polymerases

involved in DSB repair are more error-prone than replicative polymerases, and point mutations arise more frequently adjacent to DSB repair sites (Strathern *et al.*, 1995).

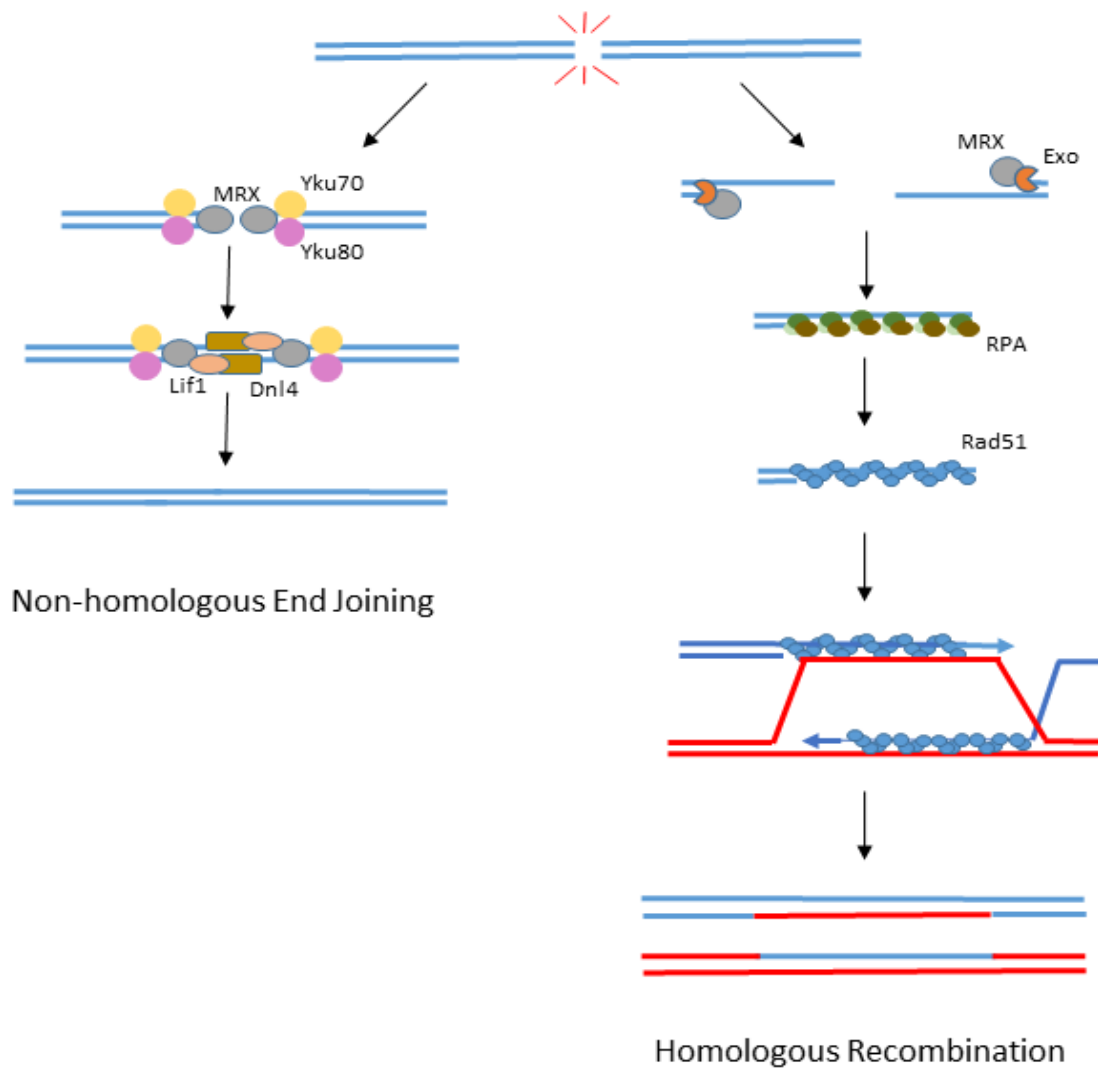


Figure 1.8 Pathways to repair DSBs by NHEJ or HR.

Schematic of the NHEJ and HR pathways to repair DSBs. Low levels of end processing in NHEJ allow Lif1 and Dnl4 to act to religate the DNA ends to repair the chromosome. In HR end-processing is more substantial to create regions of homology to sister chromosomes. These tracts of resected DNA are coated in Rad51 which helps to perform strand invasion, and the sister chromosome is used as a template for strand extension. Figure adapted from (Lans *et al.*, 2012).

1.9 Down regulating the Checkpoint

The DNA checkpoint signal is intended to arrest the cell cycle and allow the time for cells to repair before continuing to proliferate. If the repair process is successful, then the checkpoint signal is extinguished, and the cells re-enter the cell cycle; this process is known as checkpoint recovery. However, if mechanisms exist to turn off the checkpoint signal in the case of repair, are these mechanisms ever co-opted and activated without the necessary repair step taking place?

1.9.1 Checkpoint Adaptation

In the persistence of damage, such as an unrepairable DSB, cells re-enter the cell cycle 12-14h after arrest is initiated. This process is known as checkpoint adaptation and was first observed in budding yeast after the induction of an irreparable DSB near a telomere in wild type cells leading to elimination of the telomere (Sandell and Zakian, 1993). These cells were seen to arrest at G2/M initially, however it was seen that the majority of the cells were able to escape this arrest and resume the cell cycle despite the broken chromosome (Sandell and Zakian, 1993). It was even observed that this chromosome could be normally replicated and segregated for up to 10 cell divisions without triggering subsequent cell cycle arrest. Genes required for adaptation of the checkpoint can therefore be easily screened with this assay, as adaptation-defective mutants will remain arrested in G2/M indefinitely (Toczyski *et al.*, 1997).

A number of genes have been shown to be required for proper checkpoint adaptation. Amongst those first identified were *CDC5*, encoding an essential polo-like kinase which controls activation of the MEN, and *CKB1* and *CKB2*, non-essential sub-units of casein kinase II (Toczyski *et al.*, 1997). The Yku complex was also shown to be required for checkpoint adaptation independently of *CDC5*; *yku70Δ* cells were shown to have significantly increased resection at the unrepairable DSB, however the adaptation-deficient phenotype of these cells was suppressed by the deletion of *MRE11*, which led to reduced resection at these sites (S. E. Lee *et al.*, 1998). The helicase genes *SRS2* and *SAE2* were also found to be required for adaptation. This has been shown to be related to the role of Sae2 in removing the MRX complex from DNA, without Sae2 this complex is not efficiently removed and leads to increased resection (H. Chen *et al.*, 2015). Interestingly, whilst many adaptation-defective mutants are also strongly defective in checkpoint recovery (*srs2Δ*, *ptc2Δ*, *ptc3Δ*, *sae2Δ*) many only show slowed or no impact on checkpoint recovery at all

(*ckb1Δ*, *ckb2Δ*, *yku70Δ*, *cdc5-ad*), this implies that different aspects of checkpoint adaptation may function through independent pathways (Vaze *et al.*, 2002).

It has been shown that during adaptation Ddc2 foci dissociate from damage sites, suggesting Mec1 activation and localisation is a governing factor in adaptation (Melo *et al.*, 2001). This supports that recovery from checkpoint arrest is generally reliant upon the removal of the checkpoint signal, and inactivation of effector kinases such as Rad53 and Chk1. However, it has since been suggested that many of the mechanisms controlling checkpoint adaptation are targeted towards the control of the effector kinases, rather than Mec1 binding. In cells undergoing checkpoint adaptation, loss of phosphorylation of Rad53 and Chk1 can be seen to correlate to adaptation, and in the checkpoint adaptation-defective *yku70Δ* and *cdc5-ad* mutants Rad53 is seen to remain phosphorylated (Pelliccioli and Foiani, 2005; Clerici *et al.*, 2006). It has been further shown that the hyper-phosphorylation of Rad53 in response to DSBs is modulated in order to control the adaptation process. Studies removing the PPC2-like phosphatases *PTC2* and *PTC3* led to defects in adaptation. These were further shown to directly interact with the forkhead-associated domain 1 (FHA1) of Rad53. This interaction was modulated by *CKB1* and *CKB2*, deletions of which are known to be defective for checkpoint adaptation (Leroy *et al.*, 2003; Guillemain *et al.*, 2007). Cdc5 has also been shown to attenuate the phosphorylation of Rad53 during ongoing checkpoint arrest (Vidanes *et al.*, 2010). It has therefore been suggested that Cdc5 may act in the same pathway as casein kinase II and the PPC2-like phosphatases, as inhibition of Cdc5 or Ptc2/3 is capable of completely eliminating adaptation (Toczyski *et al.*, 1997; Leroy *et al.*, 2003; Syljuasen, 2007).

There is a potential alternative hypothesis for the mechanism of adaptation, that is that over time the DNA structure triggering the checkpoint response, and the associated proteins, are modified into a non-signalling structure (Clemenson and Marsolier-Kergoat, 2006). This may be supported by the removal of the Mec1-Ddc2 complex from ssDNA, despite mechanisms in place to remove phosphorylation of Rad53 (Melo *et al.*, 2001). The adaptation-defective phenotype of mutants affecting end processing activity such as *sae2Δ*, *srs2Δ*, and *yku70Δ*. Srs2 was shown to remove Rad51, a signal for homologous recombination, from the DSBs during adaptation (Krejci *et al.*, 2003; Veaute *et al.*, 2003). Sae2 and Srs2 may also be involved in the removal of Mec1-Ddc2 from the ssDNA (Harrison and Haber, 2006). This hypothetical pathway would not be exclusive from the removal of phosphorylation from active Rad53, it would help to explain how cells with persistent damage are able to continue

for up to 10 subsequent divisions without activation of the checkpoint signal, despite rising and falling Cdc5 activity throughout the cell cycle (Schleker *et al.*, 2010).

1.9.2 Anti-checkpoint Proteins

Anti-checkpoint functions were first suggested at telomeres by Michelson *et al.*, (2005) as a mechanism to prevent or reduce the initiation of a checkpoint signal (Michelson *et al.*, 2005). It was previously observed that rapid elongation of telomeres, as well as shortening, was capable of activating the DNA damage checkpoint (Ijma and Greider, 2003; Viscardi *et al.*, 2007). Therefore, it was hypothesised that during the normal cell cycle the telomeres must have systems in place to recognise normal telomere homeostasis and prevent unnecessary delays in the G2/M transition from inappropriate over-activation of the checkpoint, particularly given the involvement of the Mec1 and Tel1 kinases in telomere replication. This study found that tracts of telomeric repeats adjacent to an induced DSB were capable of reducing the resulting checkpoint signals. This attenuated arrest was not the result of reductions in resection, nor successful repair or adaptation. This suggests that these repeats (and the telomeres themselves) act as a repository for factors capable of turning-down the checkpoint response. This is further supported by observations that after the induction of a DSB, resection must occur for several kb before a checkpoint signal is initiated, and that the ssDNA generated in *cdc13-1* is as potent as a DSB. This implies that cells may have a threshold of ssDNA that must be reached before a checkpoint response is initiated, this may imply a role for anti-checkpoint proteins in setting this threshold, predicted to be approximately 10kb of ssDNA (Pellicoli *et al.*, 2001; Vaze *et al.*, 2002; Zubko *et al.*, 2004). A number of studies have implicated Rif1 as playing an anti-checkpoint role in budding yeast, a role which will be discussed in detail later in this chapter (**Chapter 1.10.4**) (Anbalagan *et al.*, 2011; Xue *et al.*, 2011; Mattarocci *et al.*, 2017).

1.9.3 The purpose of adaptation & anti-checkpoints

The question arising from checkpoint adaptation and anti-checkpoint proteins is relatively simple; why would these mechanisms exist and allow cells to proceed with irreparable damage? As previously discussed, many of the mechanisms for adaptation are independent from the checkpoint recovery process, therefore is not as simple as a misregulation of the checkpoint recovery pathways. Adaptation has been shown to promote the mis-segregation of acentric chromosome fragments in up to 95% of divisions, even leading to mis-segregation of centric chromosomes in 45% of divisions (Galgoczy and Toczyski, 2001;

Kaye *et al.*, 2004). This is a source of substantial genomic instability for these cells, so why has it evolved? It has been suggested that it may allow yeast cells the opportunity to repair damage in the following cell cycles, thereby increasing the individual cell's odds of survival. It may also be a mechanism of generating genetic and phenotypic diversity. With this reasoning, it could be seen therefore how this may have been an evolutionary advantage for unicellular organisms such as budding yeast.

Checkpoint adaptation is also been suggested in multicellular organisms. Studies suggested that adaptation is seen in *Xenopus* egg extracts in response to the replication inhibitor aphidicolin through interference with an interaction between claspin and the polo-kinase Plx (Yoo *et al.*, 2004). Further studies have also suggested that human cells may demonstrate checkpoint adaptation in response to genotoxic stresses such as radiation (Syljuasen *et al.*, 2006). The genomic instability this introduces may be a driving factor in cancer development and as such is of greater risk to the organism. It has been suggested that the pathway may exist to drive the cell through the cell cycle until either the damage is sufficiently extensive, or the cell is in the correct phase that apoptosis can be triggered (Lupardus and Cimprich, 2004). The risk introduced by this, and the increased genomic instability, may be a driving factor in many cancers (Kalsbeek and Golsteyn, 2017).

1.10 The Roles of Rif1 in Eukaryotes

1.10.1 Structural Conservation of Rif1

Rif1 was first discovered at the telomeres in budding yeast, as an interacting factor of the telomeric protein Rap1. Here it acts to maintain telomere length as well as play a role in the negative regulation of telomeric silencing, as described earlier in this chapter (Hardy *et al.*, 1992). Since discovery Rif1 has been found to be conserved across a range of higher eukaryotes, as well as being involved with a multitude of pathways both in yeast and other species. As Rif1 contains multiple function-related domains, this subchapter will first detail the conservation of the gene and protein across higher eukaryotes before detailing some of the major functions in which it has been found to play a role.

RIF1 homologs were discovered first in other yeast species such as *Schizosaccharomyces pombe*, where it was found to function alongside Rap1 at the telomeres and also assists in regulation of telomere elongation (Kano and Ishikawa, 2001). This was later expanded to mice, where it was found to be highly expressed in mice ESCs, also associating with telomeres. Eventually a homolog was demonstrated in humans, associated with damaged DNA (Adams and McLaren, 2004; Silverman *et al.*, 2004; Xu and Blackburn, 2004). Phylogenetic analysis conducted by Sreesankar *et al.*, (2012) identified *RIF1* homologues in a total of 92 different species, 54 of these were in fungal species, 18 insects, and 16 were vertebrate species. This analysis suggested that insect and vertebrate *RIF1* were more closely related to each other than they were fungal species. They did not however discover any Rif1 homologues in plant species (Sreesankar *et al.*, 2012). This study identified a number of conserved domains which were later shown to correspond to shared functions of Rif, as well as the identification of specific domains seen in RIF1 for functions related only to vertebrates.

Running from the N-terminal region of the protein in all species through approximately 1000 amino acid residues of the protein are the HEAT repeats. Although there is general poor sequence homology in these repeats, a highly conserved Rif1-specific region of 101-149 residues was identified (Sreesankar *et al.*, 2012). The HEAT repeats are found in a diverse array of proteins and was named for the four in which it was first found (huntingtin, elongation factor 3, PR65/A, TOR). The most common function of these domains is in mediating protein-protein interactions, however, they are seen to be involved in a wide diversity of processes (Andrade and Bork, 1995; Andrade *et al.*, 2001).

The phylogenetic analysis of *RIF1* was the first study to identify the presence of RVxF-SILK domains within the Rif1 protein, highly conserved across species with varying lengths between the two domains (Sreesankar *et al.*, 2012). RVxF-SILK domains are the consensus docking motif required for interaction with phosphatases of the PP1 family, an interaction earlier discovered in mammalian Rif1 by affinity chromatography (Egloff *et al.*, 1995; Moorhead *et al.*, 2008; Hendrickx *et al.*, 2009). Interestingly, this domain appears to have moved within the protein across the course of evolution. In fungal species this domain is found at the N-terminal region in the structure SILK-RVxF, whereas in higher eukaryotes it appears to have moved to the C-terminal region and flipped to the structure RVxF-SILK. This domain has since been confirmed to interact with proteins of the PP1 family to carry out a global role in replication timing, a function which will be discussed in further detail.

The third major conserved domain shown in Rif1 by this study was a DNA-binding domain in the C-terminal region (in all studied species). This domain had been earlier identified in mammalian Rif1 with homology to the alpha-CTD of bacterial polymerases. The DNA-binding capability has only been demonstrated in RIF1, this domain was later identified as being present in all *RIF1* homologues (Xu *et al.*, 2010; Sreesankar *et al.*, 2012; Mattarocci *et al.*, 2016).

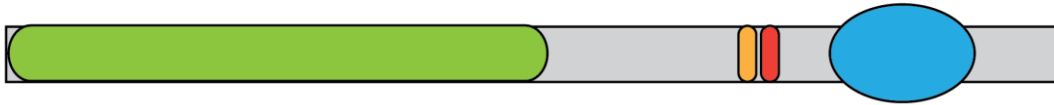
In budding yeast, the interaction of Rif1 with Rap1 has been shown to be via a short alpha-helical peptide motif referred to as the Rap1-binding-module (RBM) that is found close to the C-terminal domain of Rif1. This interaction is further controlled by a lower affinity site created through a tetramer-forming C-terminal domain (Shi *et al.*, 2013).

Interestingly, it appears that the telomeric role of Rif1 may only be seen in fungal species. There is no evidence that Rif1 is found at the telomeres of multi-cellular organisms outside of damage. In mammals, RIF1 has instead been shown to localize to sites of DNA damage, the loss of the protein leads to increased cell sensitivity to ionizing radiation, reduced HR-dependent repair, and defective checkpoint capability (Silverman *et al.*, 2004;

Xu and Blackburn, 2004; Buonomo *et al.*, 2009; Wang *et al.*, 2009). From this RIF1 has been determined in mammalian cells to play a key role in repair pathway choice.

Recent studies suggest that the telomeric functions of Rif1 may actually be an evolutionary divergence from the original function of the protein. Rif1 has been shown to play a highly conserved global role in replication timing, acting to delay the firing of origins of replication, which may be the original protein function. Furthermore, the increased evidence for Rif1 as a checkpoint-interacting factor in yeast as well as mammalian cells suggests this may also be a somewhat conserved role for the protein. It may be that yeast species adopted yeast as a telomeric protein because of this anti-checkpoint function.

Human RIF1



Budding Yeast Rif1

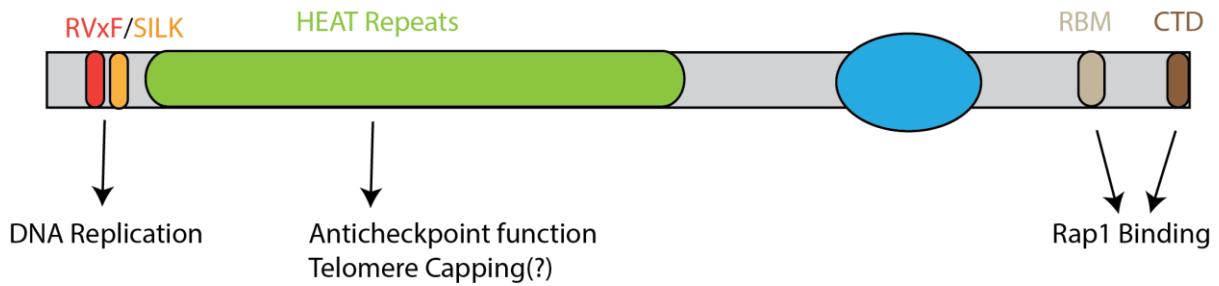


Fig1.10.1 The conservation of Rif1 structural domains in eukaryotes.

Models of Rif1 demonstrating the protein structure in humans and budding yeast. The blue domain represents a sequence with homology to a region found alpha-bacterial polymerases and is shown to be capable of DNA binding in RIF1. Adapted from Mattarocci, et al (2016).

1.10.2 Rif1 in Replication Timing

Thus far the only truly global role of Rif1 is in control of replication timing. In eukaryotes, DNA replication is initiated from specific genomic sites known as origins of replication, these origins begin replication (firing) during S-phase according to a program determined by cell types and developmental stage. If this program is dysregulated then the premature firing of normally late-firing, or dormant origins can lead to activation of the DNA damage response, hypothesised to be likely due to replication fork stalling as a consequence of depletion of dNTPs (Mantiero *et al.*, 2011). This firing process is best understood in budding yeast where origins of replications are well defined, along with a constitutively bound complex termed the Origin Recognition Complex (ORC). Prior to firing the pre-replication complex (pre-RC) is formed at origins by the addition of Mcm2-Mcm7 hexamer, a replicative helicase. This complex then requires activation, critical for activation is the action of two kinase complexes, Cdk1 and DDK (Dbf4-Dependent Kinase). DDK is made up of Cdc7 kinase and the activator subunit Dbf4, whilst Cdk1 is required for the phosphorylation of associating proteins the role of DDK is primarily to phosphorylate the Mcm4 subunit (Sheu and Stillman, 2006). The phosphorylation of Mcm4 leads to recruitment of the key protein factors Cdc45, Sld2/Sld3, and the GINS complex (Heller *et al.*, 2011; Tanaka and Araki, 2011).

The potential role for Rif1 in origin firing was first suggested by the association with telomeres. Despite the presence of numerous potential origins close to telomeres, they are known to replicate late in the S-phase. Whilst this was initially thought to be due to the silencing effect created by histone modifications due to Sir3 and Yku70/Yku80, it was also revealed that mutation of Rif1 lead to earlier telomere replication independent of this pathway (Donaldson, 2005; Lian *et al.*, 2011). Interestingly, despite the most detailed model of origin firing coming from budding yeast, the role of Rif1 in replication timing was seen in *S. pombe* and mammalian cells first. In these species, it was noted that the depletion of Rif1 equivalent led to the loss of replication timing programs (Cornacchia *et al.*, 2012; Hayano *et al.*, 2012; Yamazaki *et al.*, 2012). This affected both early and late firing origins, with early firing origins firing later and late firing origins firing early.

The mechanism by which Rif1 controls replication timing was then further elucidated using the budding yeast model system, where *rif1* Δ mutation was confirmed to partially suppress temperature sensitivity of *cdc7-1* cells (S. Hiraga *et al.*, 2014). These studies determined that an interaction between Rif1 and PP1, in yeast the protein Glc7, via the conserved RVxF-SILK motifs in Rif1 were responsible for controlling this timing. These models proposed that at late replicating origins Rif1 acted to target Glc7 activity towards reversing the DDK-

mediated phosphorylation of Mcm4, thereby delaying origin firing. As S-phase progresses DDK activity becomes higher and Rif1 is itself phosphorylated by DDK to interrupt the association with Glc7. The repressive effect on the origin in question is lifted and replication is initiated (Davé *et al.*, 2014; S. Hiraga *et al.*, 2014; Mattarocci *et al.*, 2014). The conserved PP1-interaction domains found in Rif1 were later confirmed to reflect the conserved interaction, carrying out this role in multiple species (S. I. Hiraga *et al.*, 2017; Sukackaite *et al.*, 2017).

Whilst the mechanism of inhibition was clear, these studies did not answer how Rif1 was targeted to specific origins of replication within the chromosome, outside of subtelomeric origins. However, the ability of Rap1-bound Rif1 to inhibit origins in the subtelomere may indicate an ability to act on multiple origins over distance, it is also noteworthy that deletions of regions of the HEAT repeats within the N-terminal of Rif1 were found partially suppress temperature sensitivity of *cdc7-1*, independent of the presence RVxF-SILK repeats. This suggested a role for protein-protein interactions outside of PP1 in this function. Furthermore, mammalian Rif1 appeared to be capable of controlling chromatin organisation, suggested that sequestration of late firing origins may be a further mechanism of regulation (Cornacchia *et al.*, 2012; Yamazaki *et al.*, 2012).

This origin selection has since been suggested to be partially managed via the presence of G-quadruplexes near late firing origins of replication. G-quadruplexes are secondary DNA structures formed by non-Watson-Crick base pairing between guanine residues and frequently occur in guanine-rich regions of DNA, such as telomeres. Sequences containing G-quadruplexes have been seen to be conserved and are frequently associated with genomic features in budding yeast (Capra *et al.*, 2010). A study by Kanoh *et al.*, (2015) suggested that Rif1 recognises and binds G-quadruplex structures within the chromosome. They hypothesised that the binding of Rif1 to multiple G-quadruplex may reorganize local chromatin structure to exert long-range effects on multiple late-firing origins (Y. Kanoh *et al.*, 2015). Interestingly, it appears that Rif1 may act as a multimer in order to carry out this function. It was previously noted that in budding yeast Rif1 the CTD domain may form a module for tetramerization, this was recently seemingly confirmed in *S. pombe*, alongside the importance of both a high-specificity region of the C-terminal and a lower-specificity region of the HEAT repeats for binding G-quadruplex structures (Shi *et al.*, 2013; Kobayashi *et al.*, 2019). Together these data suggested that Rif1 is capable of binding internal chromosomal regions by means of G-quadruplexes, from this it sequesters multiple late-firing origins to limit the activity of Cdc7. Interestingly, a recent study on the role of Rif1 in

budding yeast suggested that whilst free Rif1 is capable of delaying the firing of origins at chromosome-internal loci, the telomere sequestration acts as a limiting factor and this likely also has the secondary effect of maximising the control of the late-firing telomere-proximal origins (Hafner *et al.*, 2018).

Studies in both yeast and mammalian cells have suggested that the role of Rif1 in replication timing have numerous effects on genomic stability during replication, as well as on the chromatin structure. It has been suggested that in *S. pombe* short internal telomeric repeats may be capable of binding the shelterin complex, of which Rif1 is a component, to control heterochromatin structure and replication timing (Zofall *et al.*, 2016). In budding yeast it has been shown that Rif1-dependent inhibition of rDNA replication plays a critical role in genomic stability by controlling replication fork progression through these difficult regions (Shyian *et al.*, 2016). Interestingly, in mammalian models it has recently been shown that Rif1 has secondary roles in replication outside of blocking initiation. It appears to play critical roles in the stabilisation of newly synthesised DNA, and in slowing the progression of replication forks through difficult to replicate regions (Munden *et al.*, 2018). This role appears to also be dependent on the interaction with PP1, and acts to prevent degradation of synthesised DNA at stalled replication forks (S.I. Hiraga *et al.*, 2018; Garzón *et al.*, 2019).

The global conservation of this role, including the conserved mechanism, would seem to indicate this may be the original function of Rif1 protein. This mechanism appears to make use of many of the structures that have become involved in alternate functions of the protein that have been shown. It would therefore appear that the other roles of the protein may have been retasking based on the usefulness of the structures this original function required.

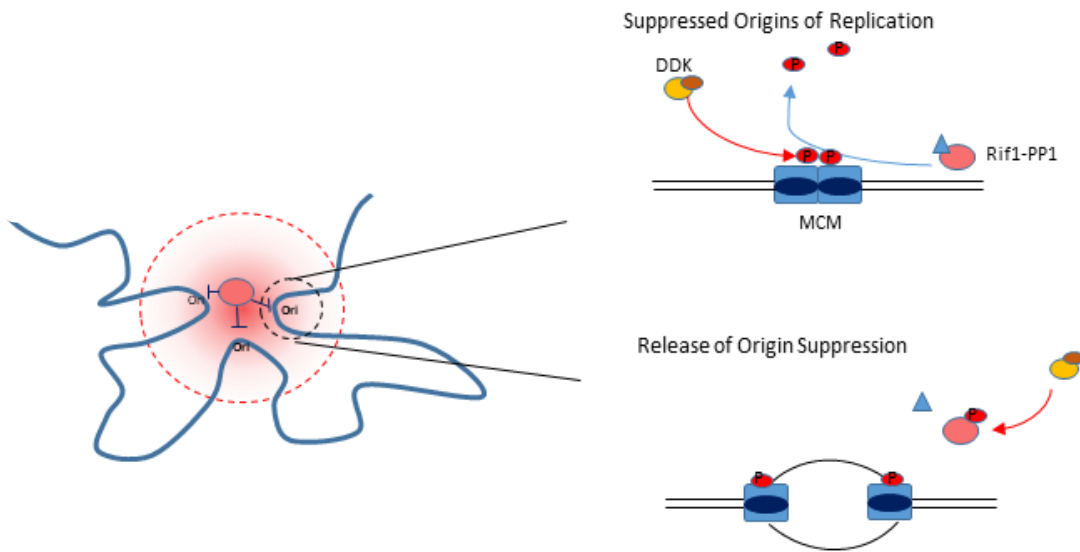


Figure 1.10.2 Rif1 suppresses initiation at origins of replication

A schematic model of Rif1 suppression. Rif1 may alter chromatin structure through interaction with G-quadruplexes located proximal to origins of replication to suppress the firing of multiple origins. At suppressed origins Rif1 & PP1 counter-act DDK-mediated phosphorylation of the pre-RC. Phosphorylation of Rif1 regulates the PP1 interaction. Figure partially adapted from (Davé *et al.*, 2014)

1.10.3 Rif1 at DSBs in Mammalian Cells

Early observations of *RIF1* in mammalian cells quickly observed that RIF1 had no role at the telomeres during the normal cell cycle. It was, however, observed that human RIF1 localized to damaged telomeres, and that after the induction of DSBs RIF1 was seen to co-localise with DDR factors dependent upon ATM and 53BP1 (Silverman *et al.*, 2004). Inhibition of RIF1 activity was noted to lead to defects in the intra-S checkpoint and increased sensitivity to DNA replication stress (L. Xu and Blackburn, 2004; Buonomo *et al.*, 2009).

RIF1 was quickly shown to have a key role in repair pathway choice at DSBs in human cells. It is recruited by a phosphorylated domain of 53BP1, itself dependent on ATM activity, where it is targeted to block resection of the 5' strand (Di Virgilio *et al.*, 2013; Zimmermann *et al.*, 2013). Depletion of RIF1 was further shown to be capable to suppress the resection and RAD51 defect in BRCA1-depleted cells (Escribano-Diaz *et al.*, 2013). This activity acts to promote NHEJ in the G1-phase of the cell cycle. During S-phase it is shown that CDK1 dependent phosphorylation of CtIP causes its association with BRCA1, which act antagonistically to displace the RIF1-53BP1 complex from the DNA ends and promote resection by the MRN complex (Chapman *et al.*, 2013).

Initial reports of the function of Rif1 at yeast DSBs, published by our lab, did not seem to indicate a role (Xue *et al.*, 2011). However, since this time there has been contradictory data published, which may indicate Rif1 is present at budding yeast DSBs. The role Rif1 plays at these sites remains unclear, whilst there has been suggestion that Rif1 cooperates with the MRX complex to promote DNA-end resection, in contrast to its role in mammals, other data has suggested Rif1 may act as a mediating gateway, encasing DNA ends and limiting access of various factors (Martina *et al.*, 2014; Mattarocci *et al.*, 2017). The latter of these roles is hypothesised to be related to the previously described anti-checkpoint function of Rif1 which will be a core element of this study.

1.10.4 Rif1 as an Anti-checkpoint Protein in Budding Yeast

Induction of DSBs adjacent to telomeric repeats first suggested a potential role for Rif1 as an anti-checkpoint protein in budding yeast. These strains showed that both Rif1 and Rif2 were required to aid in the proper capping of short telomeric repeats. Furthermore, they also showed that the two proteins were required to block the accumulation of RPA and Rad24,

and that Rif1 function may have stimulated checkpoint recovery at unprotected ends (Ribeyre and Shore, 2012).

The mechanism behind this, on which the following work is based, was studied in further depth by Xue, *et al.*, (2011). This work used the *cdc13-1* model to establish that during telomere uncapping in these strains, *rif1* Δ mutants exacerbate the temperature sensitivity phenotype of *cdc13-1*, independent of deletion of *rif2* Δ which has no effect on these cells. Interestingly, this phenotype appears to be dosage dependent as overexpression of *RIF1* was shown to lead to decreased temperature sensitivity. Furthermore, a partial *RIF1* mutant containing deletions of the C-terminal was used for its inability to bind the protein Rap1, this mutant does not affect the temperature sensitivity of *cdc13-1* (Xue *et al.*, 2011).

Whilst Rif1 does not appear to affect the resection of *cdc13-1* uncapped telomeres, this study found Rif1 binding to resected regions, including single gene loci. Depletion of *RIF1* also led to increases in recruitment of checkpoint proteins to these resected regions. Further to this, induction of *RIF1* was capable of leading to termination of an ongoing G2/M arrest. Together these data indicate that Rif1 is capable of binding to regions of ssDNA, and out-competing the recruitment of checkpoint proteins to damaged regions. This was hypothesised to functionally shield from a checkpoint response and act as a molecular band-aid to damaged DNA (Xue *et al.*, 2011).

A recent study, published after the onset of this project, determined the crystal structure of regions of the Rif1 protein and their ability to bind DNA in the absence of complexed proteins such as Rap1. The Rif1 protein is formed of a "HOOK and SHAFT" like structure, assembling *in vitro* as Rif1 head-to-tail dimers around short tracts of DNA containing ss/dsDNA junctions. The HOOK region of Rif1 contained two insertion loops on the concave face and was shown to be highly conserved across all orthologs. These loops create a region of positive charge within the hook for DNA backbone contact. The SHAFT region of the dimer-mate was proposed to then act as a lid and close over this interaction, encasing the DNA. This study showed that mutations of the HOOK region decreased the Rif1 association to telomeric repeats flanking an inducible DSB, and an increased delay in recovery from G2/M arrest. Furthermore, it was also demonstrated that this mutation also decreased NHEJ efficiency of cells. These mutants matched closely to the behaviour of *rif1* Δ mutants in *cdc13-1* cells, increasing the sickness of cells and lowering the restrictive temperatures, without effecting the length of the telomeric repeats. Together this further supports the role of Rif1 in protecting vulnerable telomeres from a checkpoint response, as well as suggest this role may be related to a promotion of NHEJ at DSBs (Mattarocci *et al.*, 2017).

However, the particular molecular mechanisms behind this process remain unclear. The potential impact this role could have on genomic instability if left unchecked is clear. Overexpression of *RIF1*, or misregulation of function, may allow cells to continue propagating with significant levels of damage. This is particularly important if this role is determined to be conserved into mammalian cells. Preliminary data produced by the Maringele lab has suggested potential phosphorylation events within Rif1 occur during telomere uncapping in *cdc13-1* (Maringele, unpublished), my study focused around the investigation of these events as a regulatory function for Rif1 in inhibiting checkpoint response.

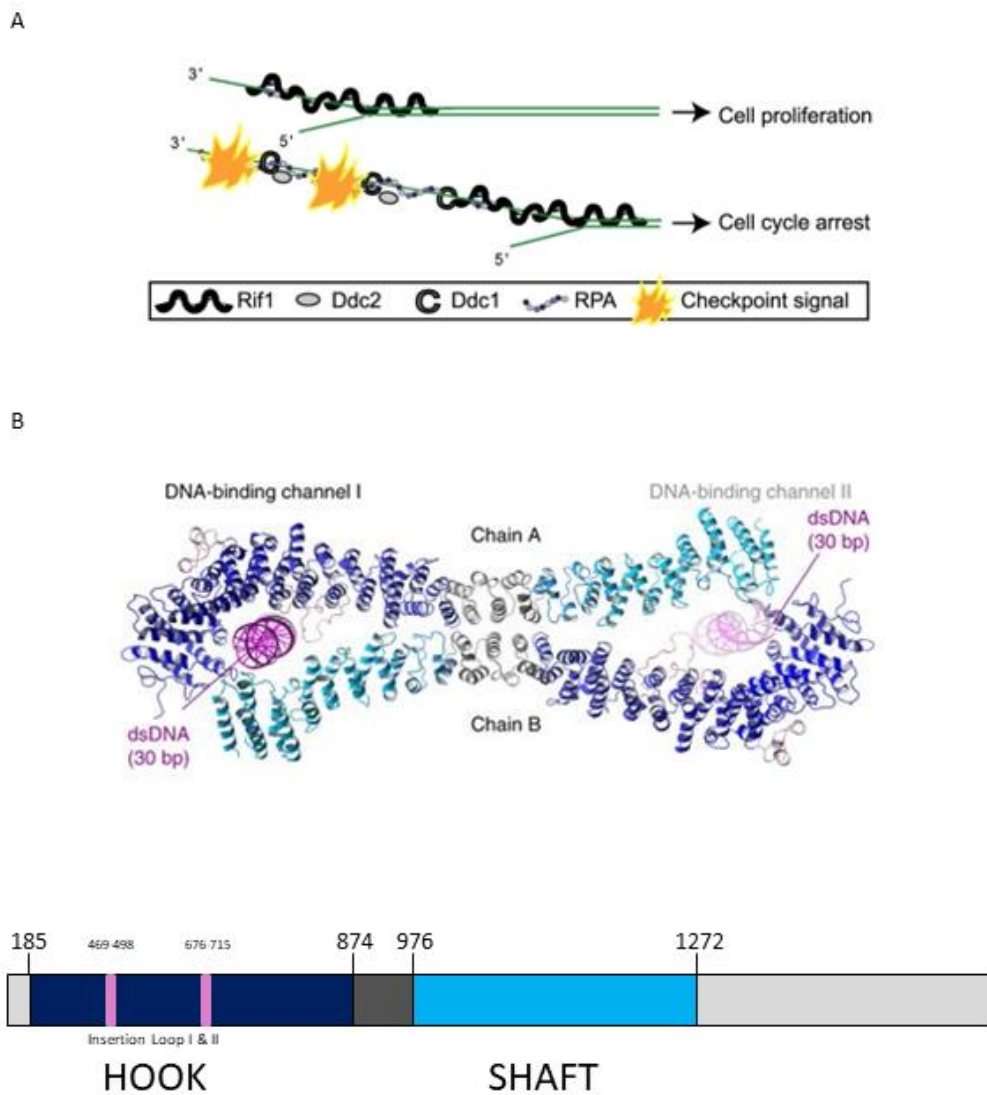


Figure 1.10.3 Rif1 binds to damaged DNA to shield from recognition by checkpoint proteins

(A) Schematic model from Xue et al. (2011) proposing the binding of Rif1 to regions of ssDNA after telomere uncapping to suppress the DDR. (B) Crystal structure of Rif1-NTD and Rif1 dimer, showing the HOOK and SHAFT structure to create DNA-binding channels, and a schematic model of Rif1 protein showing the amino acid residues comprising the HOOK and SHAFT domains. Figure adapted from Mattarocci et al (2017).

1.11 Aims

The aim of my study is to further investigate the anti-checkpoint role of *RIF1* that was described by Xue et al. (Xue *et al.*, 2011). My core aim is to better understand the manner in which Rif1 carries out this role in *Saccharomyces cerevisiae*, focusing primarily on the regulation of activity. The initial examination of this activity was in the telomere-cap defective mutant *cdc13-1* and this will be the primary model studied in this project. I am to determine both the regulatory mechanism of Rif1 anti-checkpoint function, suggested to be phosphorylation, and the impact this mechanism has upon protein structure and function. Furthermore, I would like to determine whether the anti-checkpoint function observed is exclusive to telomere uncapping in *cdc13-1*, or whether it may have wider ranging effects at DSBs breaks or in other forms of genomic instability such as impediments to chromosome segregation. The following questions will be of specific interest to address in this study:

- Is Rif1 phosphorylated in response to telomere uncapping in *cdc13-1* cells?
- Which alternate stress conditions may lead to Rif1 phosphorylation?
- Where does phosphorylation occur within Rif1 structure?
- Which kinases lie upstream of Rif1 phosphorylation?
- What are the molecular and cellular effects of Rif1 phosphorylation on the protein structure and function?

Chapter II: Materials and Methods

2.1 Yeast Strains

Yeast strains used were all of the W303 *RAD5+* background, which contains the following mutations: *ade2-1 trp1-1 can1-100 leu2-3, 112 his3-11,15 ura3 GAL+ psi+ ss1l-d2*. Strains used are listed in **Table 2.1.1**

2.2 Media

1. YEPD

For 1L YEPD medium: 10g yeast extract, 20g Bacto Peptone were mixed in ~950mL of sterile mQ water, for solid medium: 20g bacto agar was added to the mixture. The mixture was autoclaved and cooled to 60°C before supplemented with 50mL sterile 40% (w/v) dextrose and 15mL sterile 0.5% adenine.

2. Complete minimum medium

For 1L solid medium: 1.7g of yeast nitrogen base, 5g of ammonium sulphate, 20g of bacto agar, and 1.3g of amino acid powder minus the appropriate amino acid (e.g. –*leu* represents a plate containing all amino acids except leucine), were mixed with ~950mL mQ water. The mix was autoclaved and cooled to 60°C before supplemented with 5mL sterile 40% (w/v) dextrose and 15mL sterile 0.5% (w/v) adenine.

3. Antibiotic selective medium

400µg/mL of G418 or 100µg/mL Natamycin were added to the cooled YEPD medium mix to make G418 or Natamycin containing agar plates.

4. Sporulation Media

For 1L liquid media 10g of Potassium acetate, 1.25g of yeast extract, and 1g of glucose were mixed in 1L of water. The mixture was autoclaved and allowed to cool.

5. SOC Media

For 1L liquid media 20g of tryptone, 5g of yeast extract, 0.5g of NaCl, and KCl to a final concentration of 2.5mM, were mixed in 950mL of water. The mixture was autoclaved at 121°C and glucose added to a final concentration of 20mM.

Strain	Genotype	Source
LMY59	<i>MATalpha RIF1::MYC::kanMX6</i>	Laura Maringele
LMY79	<i>MATalpha cdc13-1 RIF1-13MYC::G418</i>	Laura Maringele
LMY81	<i>MATalpha cdc13-1 rad9::NATMX RIF1-13MYC::G418</i>	Laura Maringele
LMY83	<i>MATalpha cdc13-1 mec1::TRP1 sml1::HIS3 RIF1-13MYC::G418</i>	Laura Maringele
LMY152	<i>MATalpha cdc13-1 dun1::HIS3 RIF1-13MYC::G418</i>	Laura Maringele
LMY348	<i>MATa cdc13- rif1::G418</i>	Laura Maringele
LMY373	<i>MATa RIF1-CΔ-13MYC::kanMX6</i>	Laura Maringele
LMY510	<i>MATa cdc13-1 RIF1-CΔ-13MYC::kanMX6</i>	Laura Maringele
LMY810	<i>MATalpha cdc13-1 rad53::HIS3 sml1::URA3 RIF1-CΔ-13MYC::G418</i>	Laura Maringele
LMY814	<i>MATalpha cdc13-1 chk1::HIS3 RIF1-CΔ-13MYC::G418</i>	Laura Maringele
LMY819	<i>MATalpha cdc13-1 dun1::HIS3 RIF1-CΔ-13MYC::G418</i>	Laura Maringele
LMY821	<i>MATalpha cdc13-1 mec1::TRP1 sml1::HIS3 RIF1-CΔ-13MYC::G418</i>	Laura Maringele
LMY832	<i>MATalpha cdc13-1 rad9::NATMX RIF1-CΔ-13MYC::G418</i>	Laura Maringele
LMY856	<i>MATa bub13::HIS3 RIF1-CΔ-13MYC::G418</i>	This study
LMY857	<i>MATa mad3::HIS3 RIF1-CΔ-13MYC::G418</i>	This study
LMY858	<i>MATa cdc13-1 bub1::HIS3 RIF1-CΔ-13MYC::G418</i>	This study
LMY859	<i>MATa cdc13-1 mad3::HIS3 RIF1-CΔ-13MYC::G418</i>	This study
LMY912	<i>MATa cdc13-1 HIS3-RIF1-S45C-S57C-S110C-S183C-Y183F-CΔ-13MYC::G418</i>	This study
LMY917	<i>MATa cdc13-1 bar1::HIS6 RIF1-CΔ-13MYC::G418 cdc28-as1::LEU2</i>	This study
LMY943	<i>MATalpha cdc13-1 HIS3::RIF1-S181C-Y183F-CΔ-13MYC::G418</i>	This study
LMY944	<i>MATa cdc13-1 HIS3::RIF1-S181C-Y183F-CΔ-13MYC::G418</i>	This study
LMY962	<i>MATa cdc13-1 HIS3::RIF1-S181C-Y183F-13MYC:G418</i>	This study
LMY963	<i>MATalpha cdc13-1 HIS3::RIF1-S181C-Y183F-13MYC:G418</i>	This study
LMY970	<i>MATa cdc13-1 HIS3::RIF1-S45C-S57C-S110C-S183C-Y183F-13MYC::G418</i>	This study
LMY971	<i>MATalpha cdc13-1 HIS3::RIF1-S45C-S57C-S110C-S183C-Y183F-13MYC::G418</i>	This study
LMY974	<i>MATalpha cdc13-1 HIS3::RIF1-S45C-S57C-S110C-13MYC::G418</i>	This study
LMY975	<i>MATa cdc13-1 HIS3::RIF1-S45C-S57C-S110C-13MYC::G418</i>	This study
LMY1012	<i>MATa cdc13-1 HIS3::RIF1-S45C-S57C-CΔ-13MYC::G418</i>	This study
LMY1023	<i>MATa cdc13-1 HIS3::RIF1-S45C-CΔ-13MYC</i>	This study
LMY1060	<i>MATalpha cdc13-1 HIS3::RIF1-CΔ-13MYC::G418</i>	This study
LMY1061	<i>MATalpha cdc13-1 HIS3::RIF1-CΔ-13MYC::G418</i>	This study
LMY1062	<i>MATa cdc13-1 HIS3::RIF1-CΔ-13MYC::G418</i>	This study
LMY1070	<i>MATa cdc13-1 HIS3::RIF1-S57E-S110E-CΔ-13MYC::G418</i>	This study
LMY1071	<i>MATalpha cdc13-1 HIS3::RIF1-S57E-S110E-CΔ-13MYC::G418</i>	This study
LMY1078	<i>MATa cdc13-1 HIS3::RIF1-S57E-CΔ-13MYC::G418</i>	This study
LMY1079	<i>MATalpha cdc13-1 HIS3::RIF1-S57E-CΔ-13MYC::G418</i>	This study
LMY1088	<i>MATa cdc13-1 HIS3::RIF1-13MYC::G418</i>	This study
LMY1089	<i>MATalpha HIS3::RIF1-13MYC::G418</i>	This study
LMY1090	<i>MATalpha cdc13-1 HIS3::RIF1-13MYC::G418 rad9::LEU2</i>	This study
LMY1091	<i>MATalpha cdc13-1 HIS3::RIF1-13MYC::G418 rad9::LEU2</i>	This study
LMY1095	<i>MATalpha cdc13-1 HIS3::RIF1-S57A-13MYC::G418</i>	This study
LMY1096	<i>MATa cdc13-1 HIS3::RIF1-S57A-13MYC::G418</i>	This study
LMY1097	<i>MATalpha cdc13-1 HIS3::RIF1-S57A-13MYC::G418</i>	This study
LMY1098	<i>MATa cdc13-1 HIS3::RIF1-S57A-13MYC::G418 rad9::LEU2</i>	This study
LMY1099	<i>MATa cdc13-1 HIS3::RIF1-S57A-13MYC::G418 rad9::LEU2</i>	This study
LMY1104	<i>MATalpha cdc13-1 HIS3::RIF1-S57A-S110A-13MYC::G418</i>	This study
LMY1105	<i>MATa cdc13-1 HIS3::RIF1-S57A-S110A-13MYC::G418</i>	This study
LMY1106	<i>MATalpha cdc13-1 HIS3::RIF1-S57A-S110A-13MYC::G418</i>	This study
LMY1107	<i>MATalpha cdc13-1 HIS3::RIF1-S57A-S110A-13MYC::G418</i>	This study

LMY1108	<i>MATalpha cdc13-1 HIS3::RIF1-S57A-S110A-13MYC::G418 rad9::LEU2</i>	This study
LMY1109	<i>MATalpha cdc13-1 HIS3::RIF1-S57A-S110A-13MYC::G418 rad9::LEU2</i>	This study
LMY1110	<i>MATa cdc13-1 HIS3::RIF1-S57A-S110A-13MYC::G418 rad9::LEU2</i>	This study
LMY1126	<i>MATa cdc13-1 HIS3::RIF1-S110A-13MYC::G418</i>	This study
LMY1127	<i>MATalpha cdc13-1 HIS3::RIF1-S110A-13MYC::G418</i>	This study
LMY1130	<i>MATa cdc13-1 HIS3::RIF1-S110A-13MYC::G418 rad9::LEU2</i>	This study
LMY1131	<i>MATalpha cdc13-1 HIS3::RIF1-S110A-13MYC::G418 rad9::LEU2</i>	This study
LMY1142	<i>MATa cdc13-1 HIS3::RIF1-S57E-13MYC::G418</i>	This study
LMY1143	<i>MATa cdc13-1 HIS3::RIF1-S57E-13MYC::G418</i>	This study
LMY1144	<i>MATalpha cdc13-1 HIS3::RIF1-S57E-13MYC::G418</i>	This study
LMY1151	<i>MATalpha cdc13-1 HIS3::RIF1-S57E-S110E-13MYC::G418</i>	This study
LMY1152	<i>MATalpha cdc13-1 HIS3::RIF1-S57E-S110E-13MYC::G418</i>	This study
LMY1159	<i>MATalpha cdc13-1 HIS3::RIF1-S110A-CΔ-13MYC::G418</i>	This study
LMY1160	<i>MATalpha cdc13-1 HIS3::RIF1-S110A-CΔ-13MYC::G418</i>	This study
LMY1162	<i>MATa cdc13-1 HIS3::RIF1-S110A-CΔ-13MYC::G418</i>	This study
LMY1163	<i>MATa cdc13-1 HIS3::RIF1-S110A-CΔ-13MYC::G418 rad9::LEU2</i>	This study
LMY1164	<i>MATalpha cdc13-1 HIS3::RIF1-S110A-CΔ-13MYC::G418 rad9::LEU2</i>	This study
LMY1170	<i>MATa cdc13-1 HIS3::RIF1-S57A-CΔ-13MYC::G418</i>	This study
LMY1171	<i>MATalpha cdc13-1 HIS3::RIF1-S57A-CΔ-13MYC::G418</i>	This study
LMY1172	<i>MATalpha cdc13-1 HIS3::RIF1-S57A-CΔ-13MYC::G418</i>	This study
LMY1173	<i>MATa cdc13-1 HIS3::RIF1-S57A-CΔ-13MYC::G418 rad9::LEU2</i>	This study
LMY1174	<i>MATalpha cdc13-1 HIS3::RIF1-S57A-CΔ-13MYC::G418 rad9::LEU2</i>	This study
LMY1175	<i>MATalpha cdc13-1 HIS3::RIF1-S57A-CΔ-13MYC::G418 rad9::LEU2</i>	This study
LMY1180	<i>MATalpha cdc13-1 HIS3::RIF1- S110E-13MYC::G418</i>	This study
LMY1181	<i>MATa cdc13-1 HIS3::RIF1- S110E-13MYC::G418</i>	This study
DLY9823	<i>MATalpha cdc13-1 rif1Δ2-176-13MYC::HIS3MX6</i>	David Lydall

Table 2.1.1 Yeast strains used in this study

2.3 Cryogenic Storage of Yeast Strains

For long term storage yeast strains were frozen at -80°C in 15% glycerol in cryotube vials. Strains were removed from storage using a sterile toothpick to gently streak frozen samples across YEPD plates and then were incubated at appropriate temperatures.

2.4 Mating and Sporulation

Haploid yeast cells with opposite mating types were mated on YEPD plates by mixing cells of each type together. After o/n incubation at 21°C cells were transferred to selective plates for screening. Cells were subjected to two rounds of selection, the first selective to a marker specific to one parent, and the second selective to a marker specific to the other. Diploid cells should contain markers from both parents. Diploids were then placed in 2mL of sporulation media and sporulation of diploid cells occurred at 23°C on a rotating wheel for 2-3 days. When the culture contained 70% sporulated cells, as examined by phase contrast microscopy, the sporulation culture was spun down and washed twice with sterile water at 1500rpm for 3min. 0.5ml Zymolyase-20T (1mg/mL) solution and $10\mu\text{L}$ of β -mercaptoethanol were added to cultures and incubated overnight at 30°C to lyse diploid cells and the sac around tetrads. The following day the culture was incubated on ice for 15min with 5mL of 1.5% NP-40, it was then sonicated 3x for 30s at centrifuged at 300rpm (in a tabletop centrifuge) for 10 minutes. Cells were resuspended in 1mL 1.5% NP-40 and the sonication and centrifugation repeated as described above. Cultures were diluted at approximately 1000 spores/mL and $100\mu\text{L}$ plated on a fresh YEPD plates for 2-3 days. Colonies were selected and replica plated on selective media plates to determine the genotype of spores.

2.5 Spot Tests

Yeast cells were grown O/N in 1mL YEPD liquid media to saturation, in the morning cultures were diluted 1:10 in fresh YEPD and grown until the cell concentration reached $2 \times 10^7/\text{ml}$, as measured via haemocytometer. $200\mu\text{L}$ of culture was placed into the first column of a 96-well plate and then 5-fold serial dilutions were carried out via multi-channel pipette until there were six columns of cultures. Meanwhile a frog pincer was sterilised in 100% ethanol and flamed, then allowed to cool on the bench for several minutes before transferring diluted samples to YEPD or selective plates. Transfer of samples was done by lowering the frog pincer on to the surface of the plate, gently touching the plate for 1 sec, and then quickly

lifting away. Plates were dried and incubated at the appropriate temperature for several days before imaging.

2.6 Gene deletion or modification using Longtine plasmids

2.6.1 Principle of transformation & generation of DNA cassettes

Gene deletions and modifications, such as tagging, were performed via *in vivo* substitution of the wild type gene with a PCR fragment amplified from a plasmid. This reaction incorporates the PCR fragment via homologous recombination, and as such the PCR fragment is required to contain 40bp sequences at both 5' and 3' which are homologous to the sequence flanking the target gene. For a gene deletion the fragment is comprised of a selective marker such as Kanamycin or HIS3, allowing selection of transformed cells.

For example, the plasmid pFA6a-His3MX6 used in this study contains a gene for the production of histidine. The forward primer was designed to anneal the first 20bp of the *His3* gene, but also contained a 40bp sequence homologous to upstream of the target gene of interest. The reverse primer then anneals to the last 20bp of the *His3* gene and contained 40bp homology to the target gene. Homologous recombination results in this PCR product's integration into the genome in the place of the target gene, and the deletion of the target gene.

Modifying a gene such as with the addition of a tag uses the same principle as above. For example, when tagging *RIF1* with *MYC::kanMX6* for forward primer anneals immediately upstream of the *RIF1* stop codon, and the reverse primer anneals shortly downstream. The *MYC::kanMX6* is therefore integrated and following transcription and translation the Rif1 protein will contain a Myc-tag at the C-terminal.

To amplify the cassettes containing selective markers from plasmids, PCR reactions were set up in the following manner:

- 39µl ddH₂O
- 5µL 10x ExTaq Buffer – Takara Bio Inc.
- 5µL dNTPs (2.5mM) – Takara Bio Inc.
- 2µL pFA6a-His3MX6 (for example) plasmid (1.5ng/µl stock)
- 1µl primer mix (4µL dH₂O + 1µl forward primer (200µM stock) + 1µl reverse primer (200µM stock))
- 0.5µl Ex-Taq Polymerase (250 Units) – Takara Bio Inc.

The PCR reactions were carried out as follows

1. 94°C 4min
2. 35x cycles
 - a. 95°C 30sec
 - b. 55°C 1min
 - c. 72°C 1.5min

After the reaction was completed, 4µL PCR product was checked on a 1% agarose gel for the correct size. The remaining PCR product was used for the transformation.

2.6.2 High efficiency lithium acetate transformation

Yeast cells were inoculated in 5ml YEPD liquid medium and grown overnight on a roller at 21°C. The overnight culture was counted using a haemocytometer and was diluted to a cell density of 5×10^6 cells/ml in 50ml of YEPD medium. The culture was then incubated at 21°C with shaking for 4-7h until cell density reached 2×10^7 cells/ml. Cells were then harvested in a sterile 50ml tube at 3000g for 3min and resuspended in 25ml sterile water and centrifuged again as before. Cells were then resuspended in 1ml 1xLiAc (freshly diluted in TE) and transferred to a 1.5ml Eppendorf tube. Cells were pelleted at 14000rpm for 15sec and the LiAc removed by aspiration. Pellets were resuspended in 400µl 1xLiAc to give a total volume of 500µl and kept on ice. For each transformation reaction 50µl of cell suspension was pelleted at 14000rpm for 15sec, and the LiAc removed by aspiration. The ingredients of the transformation mix were added in the following order:

- 240µL 50%(w/v) PEG 4000
- 36µL 10x LiAc (1M)
- 50µl 2mg/mL salmon sperm DNA (boiled for 5min and chilled in ice)
- 50µL purified PCR product (diluted 1:5 in dH₂O)

The mixture was vortexed vigorously and incubated for 30min at 23°C. It was then transferred to a 42°C water bath for a 20min heat shock (reduced to 5-10min for temperature-sensitive strains). Cells were pelleted at 6000rpm for 15sec and the transformation mix removed by aspiration, the cells were then resuspended in 200µl sterile water by gentle pipetting. Cells were plated out on selective media for 2-4 days until colonies

were selected for testing, those cells with markers containing antibiotic resistance were first allowed to grow for 24hrs on YEPD plates before replica plating to a selective plate.

Colonies grown were streaked on fresh plates and verified for gene deletion or modification using a hot-start PCR method.

2.6.2 Hot-Start PCR test of colony transformation

To determine the presence of the wild type gene or gene deletion/modification in cells, a hot-start PCR was performed on freshly grown cells. A forward primer was designed to bind upstream of the target site (P1), and two reverse primers were designed; one to bind within the WT gene (P2), and one to bind within the gene deletion cassette (P3), both designed to produce fragments of different length in use with P1. Therefore P1 & P2 will produce a PCR fragment within the WT gene of a known length, and P1 & P3 would produce a PCR fragment of a different length in transformed cells. The presence of the WT or deleted/mutated gene could therefore be easily distinguished.

Hot-start PCR master-mix for each reaction was set up as follows:

- 15µl dH₂O
- 2.5µl Hot Start Taq Buffer – Qiagen
- 2.5µl dNTPs (2.5mM) – Takara Bio Inc
- 0.25MgCl₂ (25mM stock) – Qiagen
- 0.5µl primer mix (4µl dH₂O + 1µl P1 primer (200µM stock) + 1µl P2/3 (200µl stock))
- 0.25µl Hot Start Taq Polymerase (Units) – Qiagen
- 1µl fresh yeast cells diluted in dH₂O (Small cluster of cells collected using a toothpick and diluted in 10µl dH₂O)

The PCR reactions were carried out as follows:

1. 94°C 15 min
2. 35x cycles
 - a. 94°C 30sec
 - b. 56°C 20sec
 - c. 72°C 30sec.

Upon completion 8µl of PCR product was checked on a 1% agarose gel.

2.7 Western Blot

2.7.1 Buffers

TBS stock was produced using Sigma-Aldrich Tris-Buffered Saline tablets, 2 tablets were added to 1L of mQ water and left to dissolve overnight, for TBST 1ml of Tween 20 was added to this. Running and transfer buffers were bought from BioRad and diluted to 1x concentration before use, when transferring large proteins, such as Rif1, the running buffer was supplemented with 5ml 100% ethanol. Resolving and stacking buffers used in the production of polyacrylamide gels was also purchased from BioRad.

2.7.2 Cell Harvest and TCA Protein Extraction or DAPI Staining

Cells were inoculated in 50ml of YEPD and grown overnight at 20°C in an incubator with a shaker at 170rpm, if nocodazole is going to be added as part of the time-course DMSO is also added to 1%. In the morning cells were counted using a haemocytometer and diluted to 1×10^7 cells/ml in 50ml of YEPD, 20ml samples were taken for “time 0” samples and 30ml of YEPD was added to the flask cultures. Cell concentration was established by haemocytometer. The cultures were put at the appropriate temperature, and nocodazole added to 1% from 100x stock if required. 20ml samples were taken at 2-hour intervals.

For DAPI staining, 500µL of cell culture was spun at 13000rpm in a benchtop centrifuge for 10sec. The pelleted cells were then resuspended in 500µL of 70% ethanol and refrigerated. Cells were washed twice with 500µL of water, using 8s of centrifugation in a benchtop centrifuge to pellet cells. They were then resuspended in 500µL DAPI mix (0.2µg/mL dissolved in water). The solution was sonicated at an amplitude of 5microns for 3sec. 8µL was then placed on a glass slide and covered with a coverslip and examined with fluorescence microscopy. Cells were classified into the five following categories, at least 100 cells were counted from each sample.


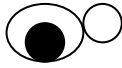
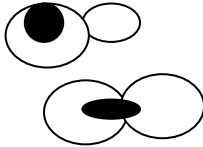
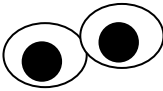
				
1	2	3	4	5
No bud, single cell, single nucleus	Bud <50% diameter of mother cell. Single nucleus	Bud >50% diameter of mother cell. Single nucleus	Two buds, two nuclei	None of the other types.

Table 2.7.2 Classification categories of cells stained with DAPI

20ml samples taken for TCA extraction were spun at 3000rpm for 2min and resuspended in 1ml cold 10% (w/v) TCA. Each sample was split in half, with 550 μ l into each 1.5ml screw-cap tube and spun at 13000rpm for 10sec. The pelleted cells were stored at -80°C prior to protein extraction.

Cells were resuspended in 250 μ l 10% (w/v) TCA, they were then ribolysed with 250 μ l glass beads using the following program three times with 5min gaps between: 6500(rpm) – 3x10sec - 005

400 μ l 10%TCA was added and vigorously vortexed. The liquid was then transferred to a fresh 1.5ml Eppendorf tube by pipette and centrifuged at 13000rpm for 10min at room temperature. Liquid was poured off and the tubes spun again for 5sec, remaining liquid was removed via aspiration. 170 μ l of fresh modified Laemmli buffer was added, made by the following recipe:

- 2.4ml 2xLB (BioRad)
- 1.2ml 10% (w/v) SDS
- 0.4ml 100% glycerol
- 0.4ml β -mercaptoethanol

Pellet was resuspended in buffer using a tip to mix, followed by vortexing until homogenous. 30 μ l of 1M Tris base pH8.6 was added and vortexed again, if the solution was not blue a further 30 μ l 1M Tris base pH8.6 was added. Samples were boiled at 98°C for 5min and spun for 10min at 3000rpm. Protein supernatant was transferred to a fresh tube and stored in the fridge for up to 2 weeks, or aliquoted and stored at -20°C for longer storage.

2.7.3 SDS-PAGE, blotting, and detection

Protein samples were heated to 62°C, vortexed for 3sec and then spun at 3000rpm for 1min. These samples were then loaded into cast 7.5% polyacrylamide gels, using 6 μ of sample per well. Electrophoresis was carried out at 110V constant; 2.5hrs for Rif1-C Δ -Myc, 3.5hrs for Rif1-Myc, and 90mins for Rad53. For large proteins (\geq 150kDa) a nitrocellulose membrane was used, for proteins smaller than this a PVDF membrane was used instead. Prior to the SDS-PAGE finishing the PVDF membrane was soaked in methanol for 30sec prior to soaking in transfer buffer, whereas the nitrocellulose membrane (BioRad) was soaked only in the transfer buffer. Transfer of proteins from polyacrylamide gel to membrane was carried out using the BioRad turbo transfer machine and the in-built programs based

on MW of proteins, for Rif1 the transfer time was extended to 20min rather than 10min. After transfer membranes were blocked with 5% milk (Marvel Fat Free dried milk powder) for 20min before being moved to 15ml 1% milk with the recommended dilution of the primary antibody. Membranes were incubated at room temperature in antibody containing milk on a rocker for 45min when studying Rif1, or 100min when studying Rad53. After incubation the membrane was blocked again in 5% milk for 20min with shaking before 3x5min washes with TBST. The membrane was then incubated in 15ml 1% milk again, this time containing the recommended dilution of the secondary antibody, for 30min before a final 3x5min washes in TBST.

The membrane was then allowed to drip dry and placed on a clean surface (wiped with 100% ethanol) and 1ml mix of 500 μ l of each BioRad chemiluminescent substrates was pipetted on top. The membrane was left for 5min and then placed in a clean transparent sleeve for imaging. Imaging was performed using a FujiFilm LAS-4000 imaging system.

2.8 Chromatin Immunoprecipitation

2.8.1 Buffers

FA lysis buffer was prepared and kept refrigerated before use. The buffer was prepared in a total volume of 250ml as follows; 12.5ml 1M HEPES pH7.5, 7.5ml 5M NaCl, 0.5ml 0.5M EDTA pH8.0, 2.5ml 10% sodium deoxycholate, 2.5ml Triton X-100, and ddH₂O up to 250ml. Solutions used to prepare the FA lysis buffer were autoclaved before mixing and immediately prior to use of a buffer aliquot EDTA-free Complete mini Roche protease inhibitor tablets were added, 1 tablet in 10ml of FA lysis buffer, and mixed until dissolved, 10%SDS was then added to a final concentration of 0.1%.

PBS was prepared using Sigma Aldrich PBS tablets, at the recommended concentration of 100mM NaCl as well as smaller volumes prepared at 200mM NaCl which were used to prepare other buffers. PBS-ChIP elution buffer was prepared in 50ml aliquots using 45ml of 200mM NaCl and 5ml 10% SDS, if SDS had begun to precipitate then the buffer was heated before use to dissolve.

ChIP Elution Buffer (CEB) was prepared and stored at room temperature in 50mL volumes. This is made up of 2xPBS (45mL) and 10% SDS to a final concentration of 1% (5mL).

2.8.2 Extraction & Immunoprecipitation

Yeast cells were grown overnight in liquid YEPD media to a final concentration of 2×10^7 cells/mL. 30mL was collected from T0 samples directly, cultures were then diluted 1:1 with fresh YEPD media before incubation. 1mL of 36.5% formaldehyde was added to the 30mL (final concentration 1%) collected sample for protein cross-linking, Samples were incubated at 24°C for 15 minutes with gentle shaking. 4.5mL of 2.5M glycine was added to stop cross-linking and cells were incubated for a further 5 minutes at 24°C with gentle shaking. Cells were then harvested in a benchtop centrifuge spun at 3500rpm for 2 minutes at 4°C, they were then washed twice with cold TBS and spun as before each time. After final wash the cell pellet was resuspended in 1mL PBS in a 2mL Sarstedt tube and spun for 1min in a micro-centrifuge at 11000rpm. The supernatant was aspirated, and cell pellets were stored at -80°C prior to extraction.

Prior to removal of cells from freezer 1 tablet of protease inhibitor (cOmplete Mini- Roche Diagnostics) was added dissolved in 10mL FA lysis buffer (50mM HEPES pH7.5, 150mM NaCl, 1mM EDTA pH8.0, 0.1% sodium deoxycholate (v/v), 1% Triton-X(v/v), 0.1% SDS), this buffer is referred to as FA-PI. Cells were incubated in 600µL of FA-PI for 20 minutes and resuspended, these were spun at 13000rpm for 8sec and resuspended in 600µL of FA-PI. 0.5mL of glass beads were added and samples were ribolysed 3x on a program of 6500(rpm) – 3x10sec - 005, cells were incubated on ice for 5 minutes between cycles. After ribolysing the bottom of the tube was punctured using a sterilised hot needle and the tubes were placed inside a 1.5mL Eppendorf with the lid removed. These two tubes were placed together inside a 15mL falcon tube and spun at 3500rpm in a benchtop centrifuge for 2mins. 300µL of 0.1% Triton-PBS was added on top of the glass beads, and the tubes were spun again at 3500rpm for 2 minutes. The 1.5mL tube with collected sample was spun at 10000rpm for 2minutes at 4°C. The supernatant was discarded and 1mL 0.1% Triton-PBS was added to the cell pellets, which were gently resuspended using a pipette tip.

The resuspended samples were sonicated using a Bioruptor with 4x30sec cycles, and then spun down for 15min at 10000rpm. The supernatant was then transferred to a fresh tube. 400µL was removed per sample for immunoprecipitation (IP) and 40µL was removed for Input DNA (IN), excess sample was stored at -80°C. 100µL of antibody mastermix (2µg antibody per sample, 100µL PBS per sample) was added to each IP sample, these were mixed for on a wheel for 30mins at 4°C. Samples were then added on top of 40µL Protein-G beads (washed with 500µL 0.1% Triton-PBS), beads were held in place using a magnetic rack. Samples were rotated overnight at 4°C.

The following day the protein beads were transferred to fresh tubes and washed with 1mL cold 1% triton-PBS buffer for three minutes with rotation. Supernatant was discarded using a magnetic rack to hold beads in place. This wash was repeated two further times, before a further three washes were carried out using 0.1% Triton-PBS buffer. After the final wash 100µL of Proteinase K-CEB mix were added (10µL Prot K: 100µL CEB) to the beads. Samples were incubated at 45°C for 1 hr and then transferred to 70°C for a further hour. Prior to removal of samples from incubation 10µL 3M sodium acetate was mixed with 600µL of Qiagen PB buffer (per sample), 580µL was added to a Qiagen column corresponding to each sample. After incubation IP samples were placed on a magnetic rack and liquid was removed and added to columns on top of PB buffer mix. Samples were purified according to the protocol for Qiagen Spin Column purification.

2.8.3 qPCR

qPCR mastermixes were set up in multiples of twelve reactions, with each sample analysed in triplicate blocks. Mastermixes were made up as follows per 12 samples with final concentration indicated: 32µL ExTaq PCR buffer (1x), 24µL dNTPs (200µM), 3.2µL reverse primer (300nM), 3.2µL forward primer (300nM), 3.2µL Taqman probe (200nM), 1.5µL ExTaq polymerase (0.025 U/µL), and 124µL ddH₂O. For each reaction 15µL of mastermix was added to 10µL of sample DNA to make a final reaction volume of 25µL. PCR conditions were as follows:

1. 95°C 5 min
2. 40x cycles
 - a. 95°C 15sec
 - b. 63°C 1min

DNA quantity was determined using DNA standards of 0ng, 0.1ng, 1ng, and 10ng to generate a standard curve of DNA quantity, which was used to determine DNA quantity in experimental samples. All samples were run alongside the corresponding input sample.

2.9 Targeted Mutagenesis of *RIF1*

2.9.1 Principle of using Gibson Assembly to generate targeted mutations

To generate targeted mutations in the *RIF1* gene I adopted a system using Gibson Assembly to substitute single amino acids at multiple sites of interest. This system amplified fragments

of *RIF1* using mismatched primers which were assembled into a single structure within a longtine plasmid which could then be used to transform yeast cells. This procedure utilised several previously detailed protocols, such as LiAc transformation of yeast, which will be referred back to when relevant. An overview of the system can be seen in **Figure 2.1**.

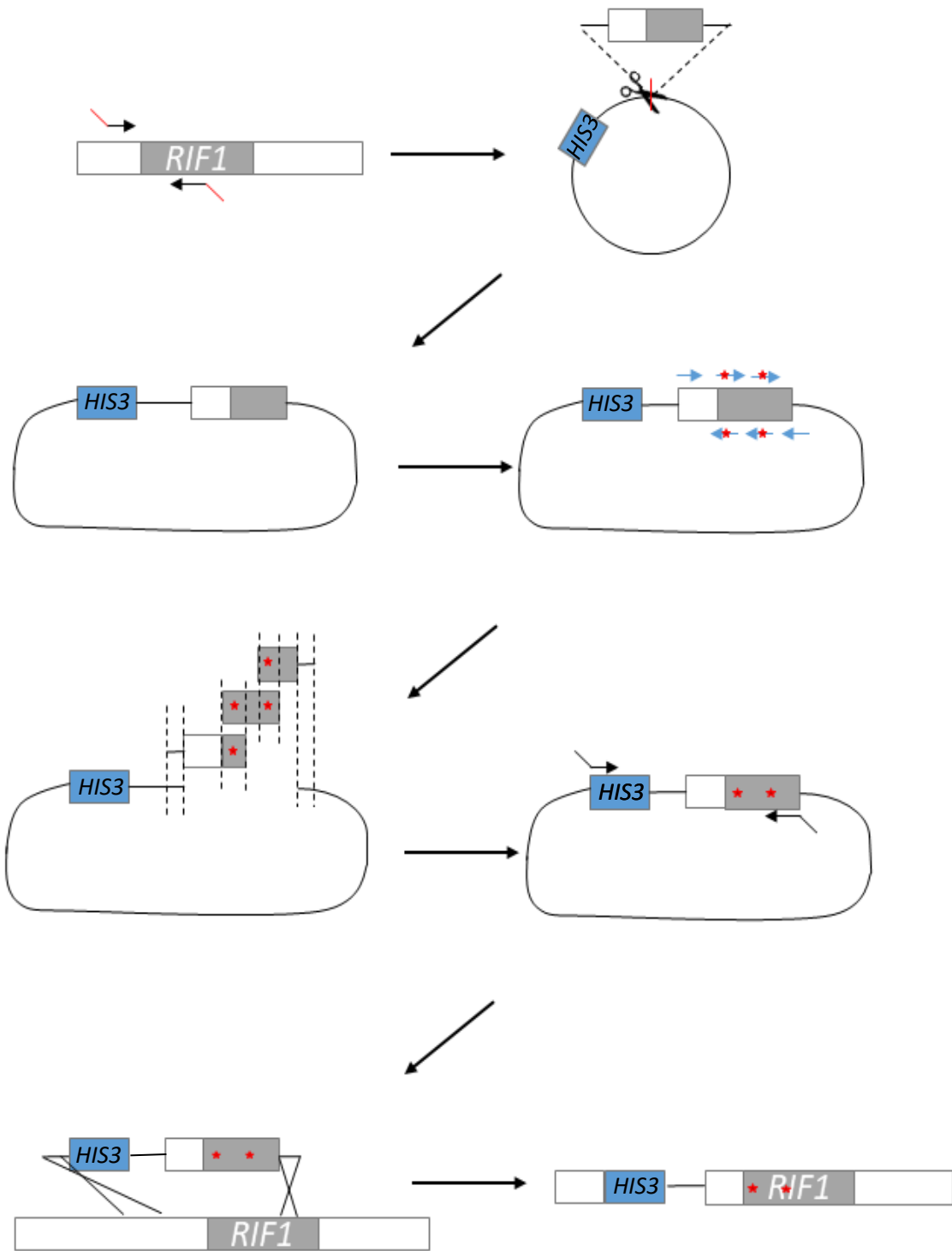


Figure 2.9: An overview of the process of integrating targeted mutations into the genome using Gibson assembly.

Gene fragment of interest (grey) and its upstream region (white) were amplified from the genome using primers with 40bp tails homologous to region adjacent to a cut site on the target plasmid (black arrows with red tails). Gibson assembly method was used to integrate cassette into the plasmid downstream of a HIS3 marker (blue). From this plasmid construct, overlapping fragments were amplified using mismatched primers to generate base substitutions (red stars indicate mismatch and substitution), these fragments were then reassembled into a complete plasmid using Gibson assembly methodology. From the resulting plasmid a cassette was then amplified using primers with tails homologous to the original site from which the fragment was amplified (black arrows with black tails). The cassette contains a marker gene as well as the original inserted fragment (now with mutations) and was transformed into the yeast genome at the native site of the target gene.

2.9.2 Generation of Plasmid Structure Containing *RIF1* fragment

Genomic DNA was first extracted from a strain containing a WT *RIF1*. For this 1.5ml of YEPD culture was inoculated O/N at 21°C. Cultures were spun at 13000RPM for 30sec and the supernatant removed by aspiration. 250µl of fresh sferoplasting solution was added to each pellet. Fresh sferoplasting solution for four samples is made up of 1ml 0.1M EDTA pH7.5, 0.001g Zymolyase and 1µ β-mercaptoethanol. Samples were vortexed until homogenous and incubated at 37°C for 1hr. 50µl miniprep mix was added (for 100µl; 37.5µl 0.5M EDTA pH8.5, 37.5µl 1M Tris base, and 25µl 10% SDS) and samples mixed by inversion. They were then incubated at 65°C for 30min, before the addition of 63µl of 5M KAc, mixing by inversion, and a further 30min incubation on ice. Samples were then spun at 13000rpm and the supernatants poured into fresh tubes containing 720µl 100% ethanol to precipitate DNA. Samples were inverted to mix, and the tubes spun for 5min at 14000rpm before the ethanol was poured off. 130µl of TE containing 1mg/ml RNase A was added to the pellets and incubated at 37°C for 35min, after which the DNA was precipitated using 130µl of isopropanol and mixing by inversion before being again spun at 14000rpm for 5min. The isopropanol was also poured off and 100µl of 70% ethanol was used to wash the pellet, with another 5min spin. Ethanol was removed by aspiration and the pellets were left to air dry. They were then resuspended in TE.

This DNA was used to amplify a section of *RIF1* from the genome as well as its upstream region, using plasmids that would add 40bp tails to the fragment. The reaction was set up as follows:

- 39µl ddH₂O
- 5µL 10x ExTaq Buffer – Takara Bio Inc.
- 5µL dNTPs (2.5mM) – Takara Bio Inc.
- 2µL pFA6a-His3MX6 (for example) plasmid (1.5ng/µl stock)
- 1µl primer mix (4µL dH₂O + 1µl forward primer (200µM stock) + 1µl reverse primer (200µM stock))
- 0.5µl Ex-Taq Polymerase (250 Units) – Takara Bio Inc.

The PCR reactions were carried out as follows

3. 94°C 4min
4. 35x cycles
 - a. 95°C 30sec
 - b. 55°C 1min
 - c. 72°C 1.5min

The tails to these primers had homology to the sequences flanking a restriction site in the plasmid to which this fragment would be inserted, in this case the flanking sequence was the bps surrounding the EcoR1 cut site in pFA6a-His3MX6, seen in **Figure 2.2**.

pFA6a-His3MX6 was cut at this site for several hours to ensure complete digestion and then treated with a phosphatase to prevent religation.

The plasmid pFA6a-His3MX6 and the amplified Rif1 fragment were then added to a premade mix of the relevant enzymes to carry out Gibson assembly. The DNA fragments were added in volumes calculated to approximate equimolarity. These mixes were created as follows (per reaction):

- 4µl 5x Isothermal Buffer
- 0.008µl T5 Exonuclease
- 0.25µl Phusion DNA polymerase
- 2µl Taq DNA ligase
- 8.75µl mQ Water

The 5x Isothermal Buffer was compiled as follows:

- 3ml 1M Tris-HCl
- 150µl 2M MgCl₂
- 60µl 100mM dGTP
- 60µl 100mM dATP
- 60µl 100mM dCTP
- 60µl 100mM dTTP
- 300µL 1M DTT
- 1.5µl PEG-8000
- 300µl 100mM NAD

This reaction was carried out at 50°C for 1hr, after which 5µl of the reaction was used to transform NEB® 5-alpha Competent *E. coli* (Subcloning Efficiency). To transform 5µl from the reaction was mixed with 50µl of *E. coli* cells and incubated on ice for 30min. The cells were then subjected to a 30sec heat-shock at 42°C before being returned to ice for 30min. 850µl of SOC medium was added to the cells and they were incubated at 36°C for 1hr to encourage growth and expression of the ampicillin resistance gene, before they were plated on LB+amp plates and left O/N at 37°C.

Plasmids were extracted using the Monarch® Plasmid Miniprep Kit produced by New England Biolabs as directed. The plasmid was then checked on a 1% agarose gel and by restriction digest. Those plasmids which were larger and were not digested by EcoR1 could be seen to contain the fragment of *RIF1*, as the EcoR1 consensus sequence is disrupted by the integration of the *RIF1* fragment. This was sequenced to ensure there were no unintended mutations during the integration of the fragment.

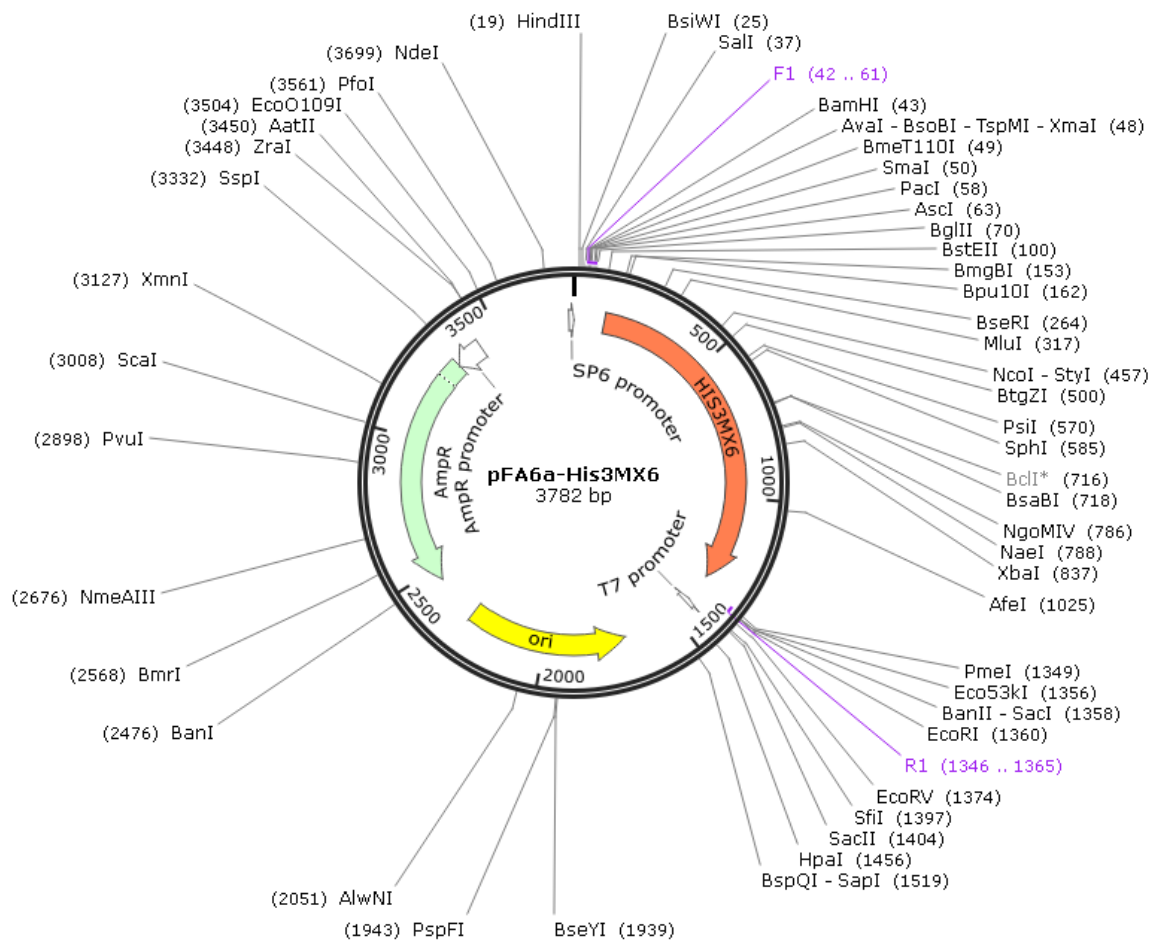


Figure 2.3: Plasmid Map of pFA6a-His3MX6

pFA6a-HisMX6 was used as the plasmid vector to generate mutations in *RIF1* due to several factors; a variety of digestion sites suitable for use, the proximity of the EcoRI site downstream of the marker gene, and the marker itself would not be a duplicate of any markers currently present in the strain to be transformed or strains it would likely be crossed with after transformation.

2.9.3 Gibson Assembly to generate mutation

To generate fragments containing targeted *RIF1* mutations overlapping primers were designed. Each fragment would overlap at each end with the 'adjacent' fragment, and the mutated sites would be present within these fragments as can be seen in **Figure 2.1**. To amplify these fragments the following PCR reactions were used:

- 39µl ddH₂O
- 5µL 10x ExTaq Buffer – Takara Bio Inc.
- 5µL dNTPs (2.5mM) – Takara Bio Inc.
- 2µL pFA6a-His3MX6-RIF1-aa1-aa250 plasmid (1.5ng/µl stock)
- 1µl primer mix (4µL dH₂O + 1µl forward primer (200µM stock) + 1µl reverse primer (200µM stock))
- 0.5µl Ex-Taq Polymerase (250 Units) – Takara Bio Inc.

The PCR reactions were carried out as follows

1. 94°C 4min
2. 35x cycles
 - a. 95°C 30sec
 - b. X°C* 1min
 - c. 72°C 30sec

*X varies by the primer pairing used. As primers were long to create large regions of homology between fragments this temperature was typically 66-70°C.

After amplification these fragments were gel purified on a 1.5% agarose gel and using a Monarch® DNA Gel Extraction Kit produced by New England Biolabs.

The fragments were mixed with pFA6a-His3MX6, digested with EcoR1 and then treated with a phosphatase to prevent re-ligation, and mixed into the Gibson Assembly reaction mix as previously detailed above. This reaction was carried out for 1hr at 50°C and 5µl was used to transform *E.coli* as was detailed above. The plasmids were then extracted and examined, larger plasmids were expected to be those which had reconstructed and integrated the fragments of *RIF1*. As such, the *RIF1* fragment was amplified, confirming its presence, and this fragment was sent for sequencing to confirm the presence of the targeted mutations and that there were no off-site mutations from the assembly process.

2.9.4 Integrating Mutation via Transformation

To integrate these mutations into the yeast genome, I used these plasmids in much the same way as transformation is usually carried out via longtine plasmid. The transformation cassettes were amplified by PCR from the plasmid and contained a *HIS3* marker as well as the *RIF1* containing the upstream region of the gene. This cassette was transformed into the genome at the *RIF1* locus using high efficiency LiAc transformation, as described above. Due to the cassette's large region of homology with the genome, each potential transformant was sequenced to ensure the presence of the mutated sites within the *RIF1* gene.

2.9.5 Primers Used to Generate Mutants

Primer Number	Sequence	Purpose
N863	TAACGCCGCCATCCAGTTTAAACG AGCTCGAACTTTGTTATATAAGTA TACGTAC	Forward Primer to amplify <i>RIF1</i> from genome. Includes 40bp tail adjacent to EcoR1 cut-site on pFA6a-His3MX6
N865	ACTAGTGGATCTGATATCATCGAT GAATTGGTTAGAATGGGTATAATA TTATTAAGG	Reverse Primer to amplify <i>RIF1</i> fragment from genome. Includes 40bp tail adjacent to EcoR1 cut-site on pFA6a-His3MX6
N850	AAAACAACTTGCCACCTCCATGT CCACAAGCTC	Forward primer integrating <i>RIF1-S45C</i> mismatch
N866	TATGAGCTTGTGGACATGGAGGT GCCAAGTTAGTTTCATCCAC	Reverse primer integrating <i>RIF1-S45C</i> mismatch
N870	CGAAAGCTAGCGTCTCAAGTGAT TGCGAGAATAAACAATTTG	Forward primer integrating <i>RIF1-S57C</i> mismatch
N853	CTCTTTGGCGTTGGGCATAGATC GCTTTGTATATG	Reverse primer integrating <i>RIF1-S57C</i> mismatch
N857	TACCCTTGTTCCTTAAAAGGGCA TGTGAAAATATTACCGTTG	Forward primer integrating <i>RIF1-S110C</i> mismatch
N855	GCTACACTTTTTGTAACCGGGCAT ACATTATCACTATTAGAGGC	Reverse primer integrating <i>RIF1-S110C</i> mismatch
N868	TACACAACGGTAATTTTTACAT GCCCTTTAAGGAAACAAGG	Forward primer integrating <i>RIF1-S181C</i> mismatch
N869	TACCCTTGTTCCTTAAAAGGGCA TGTGAAAATATTACCGTTG	Reverse primer integrating <i>RIF1-S181C</i> mismatch
N868	TACACAACGGTAATTTTTACAT GCCCTTTAAGGAAACAAGG	Forward primer integrating <i>RIF1-Y183F</i> mismatch
N869	TACCCTTGTTCCTTAAAAGGGCA TGTGAAAATATTACCGTTG	Reverse primer integrating <i>RIF1-Y183F</i> mismatch
N901	ATATACAAAGCGATCTAGCTCCAA CGCCAAAGAGG	Forward primer integrating <i>RIF1-S57A</i> mismatch
N902	CTCTTTGGCGTTGGAGCTAGATC GCTTTGTATATG	Reverse primer integrating <i>RIF1-S57A</i> mismatch
N903	CTCTAATAGTGATAATGTAGCTCC GGTTACAAAAAGTGTAGC	Forward primer integrating <i>RIF1-S110A</i> mismatch
N904	GCTACACTTTTTGTAACCGGAGCT ACATTATCACTATTAGAGGC	Reverse primer integrating <i>RIF1-S110A</i> mismatch
N890	ATATACAAAGCGATCTAGAACCAA CGCCAAAGAGG	Forward primer integrating <i>RIF1-S57E</i> mismatch
N891	CTCTTTGGCGTTGGTTCTAGATCG CTTTGTATATG	Reverse primer integrating <i>RIF1-S57E</i> mismatch
N886	CTCTAATAGTGATAATGTAGAACC GGTTACAAAAAGTGTAG	Forward primer integrating <i>RIF1-S110E</i> mismatch
N887	GCTACACTTTTTGTAACCGTTCT ACATTATCACTATTAGAGGC	Reverse primer integrating <i>RIF1-S110E</i> mismatch
N871	TCTGTAGGGGTATCGCTGAGGTT AATATGAAGTACACATGTACGCTG CAGGTCGACGGATC	Forward primer to generate cassette for integration of <i>HIS3-RIF1-S*</i> mutant structure into genome. Contains tail with homology to upstream of <i>RIF1</i>

N855	GCTACACTTTTTGTAACCGGGCAT ACATTATCACTATTAGAGGC	Reverse primer to generate cassette for integration of <i>HIS3-RIF1-S45/57/110C</i> mutant structure into genome. Contains tail with homology to <i>RIF1</i>
N853	CTCTTTGGCGTTGGGCATAGATC GCTTTGTATATG	Reverse primer to generate cassette for integration of <i>HIS3-RIF1-S45/57C</i> mutant structure into genome. Contains tail with homology to <i>RIF1</i>
N866	TATGAGCTTGTGGACATGGAGGT GGCAAGTTAGTTTTCATCCAC	Reverse primer to generate cassette for integration of <i>HIS3-RIF1-S45C</i> mutant structure into genome. Contains tail with homology to <i>RIF1</i>
N873	GAATATTGAATTTCTGATCAACCT CGTTAACATTTTTAGTGGTTAGAA TGGGTATAATATTATTAAGG	Reverse primer to generate cassette for integration of <i>HIS3-RIF1-S57/110A/E</i> mutant structure into genome. Contains tail with homology to <i>RIF1</i>

Table 2.9.5 Primers used in to generate point mutations in *RIF1* via Gibson assembly

2.10 Antibodies used in this study

Primary Antibody	Origin	Cat. No.	Company
Monoclonal anti-Myc	Mouse	Sc-40	Santa Cruz
Polyclonal anti-Rad53	Rabbit	ab104232	Abcam

Secondary Antibody	Origin	Cat. No.	Company
anti-mouse (HRP)	Rabbit	ab97046	Abcam
anti-rabbit (HRP)	Goat	ab205718	Abcam

Table 2.10 Antibodies used in this study

Chapter III: Understanding the phosphorylation of Rif1

3.1 Rif1 is phosphorylated during telomere damage in *cdc13-1* cells

Data from Xue et al, (2011) established a model in which Rif1 activity created a threshold of tolerance to DNA damage after telomere resection by acting as a molecular band-aid to short tracts of ssDNA. Thus, Rif1 hides low levels of damage from recognition by checkpoint proteins, thereby functioning as an anti-checkpoint and allowing continued cellular proliferation. Extensive damage will stretch beyond the capability of Rif1 to shield from recognition, subsequently triggering checkpoint pathways and leading to cell cycle arrest. This function of Rif1 was discovered in *cdc13-1* cells, and later shown in the context of a DSB in yeast (Mattarocci *et al.*, 2017).

In this study I have been interested in determining how the anti-checkpoint function of *RIF1* is regulated in telomere damage and other types of DNA damage. Unpublished data from our lab suggested that Rif1 protein may become phosphorylated during telomere damage. Therefore, I investigated this post-translational modification as a potential mechanism by which the Rif1 activity may be regulated.

I first investigated the Rif1 protein using SDS-PAGE and Western Blotting. Cell cultures of temperature sensitive *cdc13-1* and *CDC13* control strains, both with *RIF1-MYC*, were inoculated overnight at 20°C. The first samples (T0) were taken directly from overnight cultures, which were then incubated at 36°C for 6 hours and samples taken every 2 hours.

Across the six-hour time-course in a *CDC13* strain there was no shift in the migration of Rif1 protein during electrophoresis, and across this time there was no accumulation of cells in the G2/M periods of the cell cycle. In contrast, in *cdc13-1* cells there was a distinct shift in the migration of Rif1. This shift began in the samples taken after 2 hours, where the protein appears to be split between a position equivalent to the T0 sample and a second slower migrating form at the same position as was seen in samples taken from T4 and T6 (**Figure 3.1A**). The appearance of the slower migrating form in these samples correlates to a high percentage of cells ($\geq 90\%$) arresting in the G2/M phase of the cell cycle. The slower migrating protein form may indicate size or charge changes in the protein structure, such as may result from post-translational modifications.

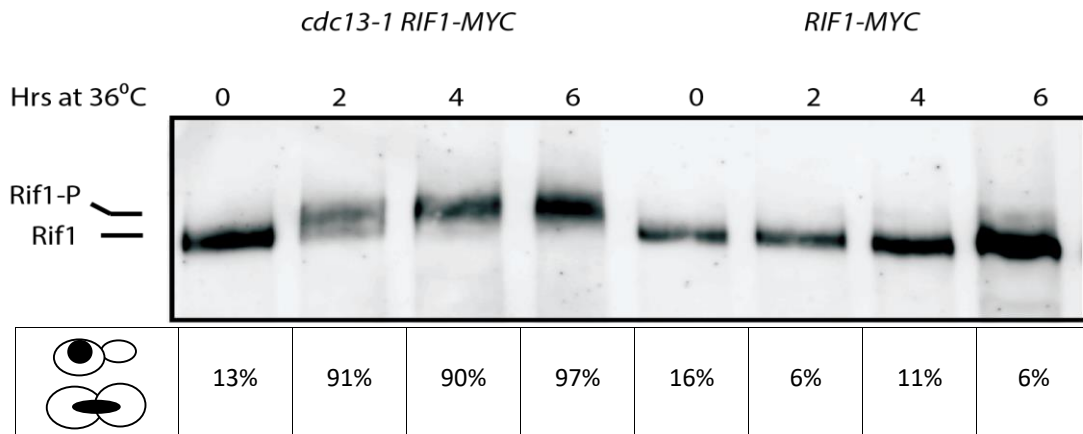
As previous published data has indicated that the Rif1 C-terminal domain is not necessary for any function in protecting resected telomeres, I investigated whether this protein shift of Rif1 would also be seen in *cdc13-1 RIF1-CA-MYC* strains (Xue *et al.*, 2011). Samples were

collected as in the previous experiment. Interestingly, in these cells a second slower migrating form of Rif1 protein was seen after two hours and was maintained across the time-course (**Figure 3.1B**).

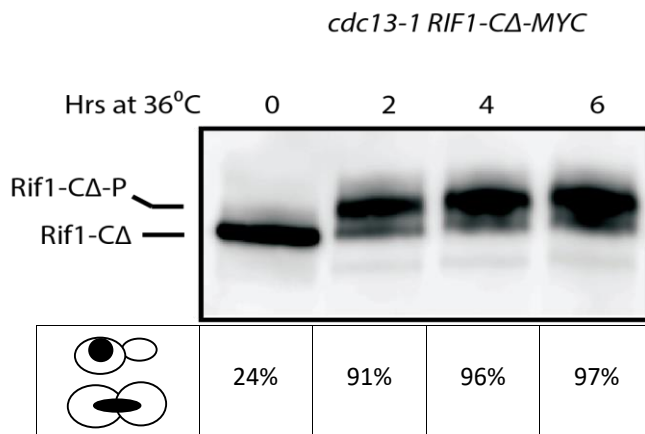
A shift in the migration of a protein is frequently caused by a post-translational modification, such as ubiquitination or phosphorylation, which lead to size or electrostatic changes within the protein structure. Unpublished data from the lab suggested that the shift occurring here in Rif1 migration was due to phosphorylation. To verify this, protein samples from *cdc13-1* cells incubated at 36°C for 4 hours (T4) were treated with alkaline phosphatase to remove any phosphoryl groups from proteins. These treated samples were compared with a mock-treated sample, as well as a sample from the overnight culture grown at 20°C prior to incubation at 36°C (T0). The checkpoint protein Rad53, which is known to be phosphorylated during telomere damage, was also compared to verify the enzyme activity of alkaline phosphatase. The Rad53 control showed a single protein form prior to telomere damage in T0 sample, after 4 hours at 36°C in untreated samples there were slower migrating forms that are the phosphorylated Rad53 protein. However, upon treatment with alkaline phosphatase this returned to a single faster migrating protein form equivalent to the T0 sample, indicating that phosphoryl groups had been removed from the protein. Interestingly, the same is seen in the Rif1 protein analysed here. At T0 there was a faster migrating protein form prior to incubation, however, in the T4 untreated sample there was also a slower migrating protein form. Upon treatment with alkaline phosphatase this slower migrating form disappeared. This indicates that the slower migration of Rif1 was caused by phosphorylation of the protein (**Figure 3.1C**).

The data shown here suggests that during telomere damage Rif1 protein becomes phosphorylated, this phosphorylation is not dependent on the C-terminal domain of the protein. This raises the question of the function of the phosphorylation event, and what impact it has upon Rif1.

A



B



C

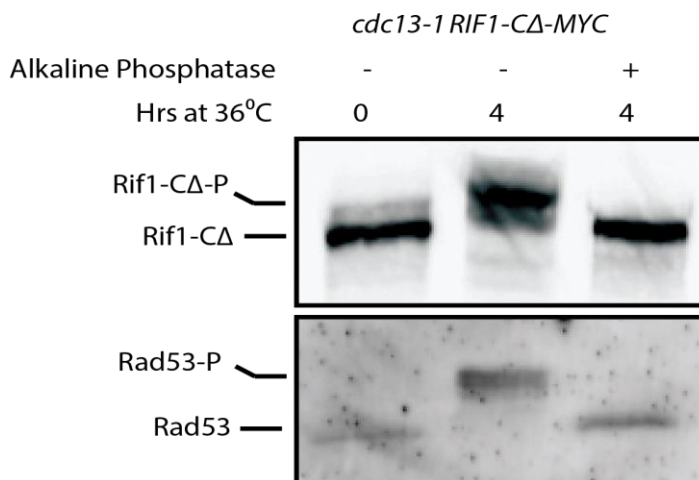


Figure 3.1. Rif1 is phosphorylated during telomere resection in *cdc13-1* cells.

(A) Western blot of Rif1 protein. Cells were grown overnight at 20°C to low cell concentration at T0 (1×10^7 cells/mL), they were then shifted to 36°C for 6 hours. Yeast strains LMY79 (*cdc13-1 RIF1-MYC*) and LMY59 (*CDC13 RIF1-MYC*) were used. Cell samples were also taken for DAPI treatment and cell cycle scoring with fluorescence microscopy. (B) Western blot showing Rif1 containing a deletion of the C-terminal (amino acid residue 1451-1916) in *cdc13-1*, yeast strain LMY510, cells shifted to 36°C after overnight growth at 21°C. Cell samples were taken for DAPI treatment and cell cycle scoring by fluorescence microscopy. (C) Western blot of protein samples showing Rif1 taken prior to, or 4hrs after, shifting *cdc13-1* to 36°C. 4hr samples were split and were treated with alkaline phosphatase or mock treatment (DMSO). Overnight cultures were used to ensure low cell concentrations (1×10^7 cells/mL) at T0. Cultures were then diluted 1:1 with fresh YPD before incubation at 36°C.

3.2 Rif1 is Phosphorylated During Nocodazole-Induced Arrest

In studying the regulation of Rif1 activity, unpublished data from our lab suggested that the telomere damage in *cdc13-1* cells may not be the only condition in which Rif1 protein is phosphorylated. I further investigated the factors that lead to Rif1 phosphorylation.

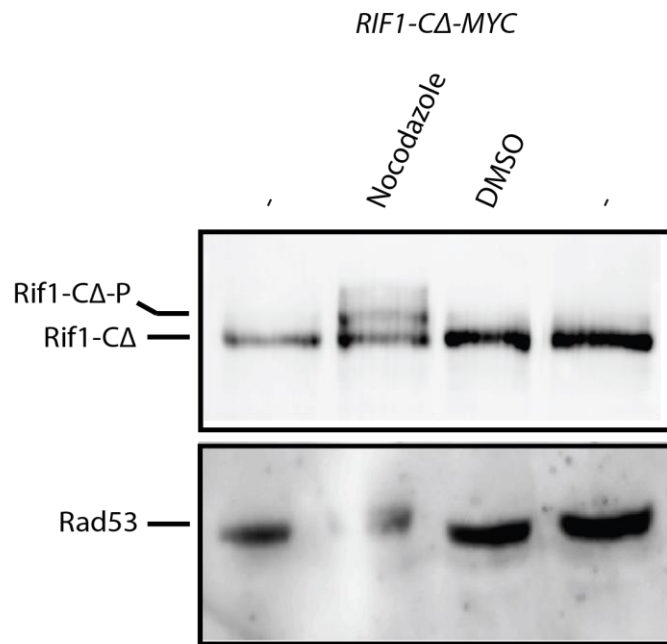
I first investigated the effects of the spindle poison nocodazole, and the resulting cell cycle arrest on Rif1 protein. Nocodazole is a reagent that prevents the polymerisation of the spindle fibres through binding to tubulin, and as such chromosomes do not separate properly during mitosis (Verdoodt *et al.*, 1999). Errors during spindle formation and chromosome separation activate the spindle checkpoint pathway, arresting the cell cycle.

I began by verifying a phosphorylation of Rif1 in *CDC13* cells, when treated with nocodazole. An overnight inoculation of the genotype *CDC13 RIF1-MYC* was grown at 20°C. A starting sample was taken from this culture (T0) before it was split in three. Culture one received treatment with nocodazole, culture two received a mock treatment of DMSO, and culture three received neither treatment. These cultures were then incubated for 4hrs at 30°C.

Results showed a single clear form of Rif1 protein at T0. However, after 4 hours treatment in nocodazole a slower migrating form of Rif1 appeared. This form was not seen in mock-treated cells, nor in cells left untreated. Interestingly, when examining Rad53 in these samples there was also a small migration shift of protein in samples treated with nocodazole. This may be related to a previously seen phosphorylation of Rad53 by Cdk1 in metaphase, independent of its role in the DNA damage checkpoint (Diani *et al.*, 2009). This was also not seen in mock-treated or untreated samples (**Figure 3.2A**).

I then performed a time-course to study how phosphorylation changes over time in cells containing *RIF1* and cells containing the mutation *RIF1-CΔ*. As such, cell cultures of each were grown overnight. Samples were taken from the overnight culture and cultures were treated with nocodazole for 6 hours at 30°C. The control *RIF1* strain showed phosphorylation emerging at T4 and T6, although the protein size appears to have made this phosphorylation difficult to visualise. However, the truncated Rif1 protein found in *RIF1-CΔ* cells is strongly phosphorylated by T4 and T6 (**Figure 3.2B**). These results indicate that this phosphorylation event occurs with similar dynamics to the phosphorylation in *cdc13-1*, and does not require the C-terminal region.

A



B

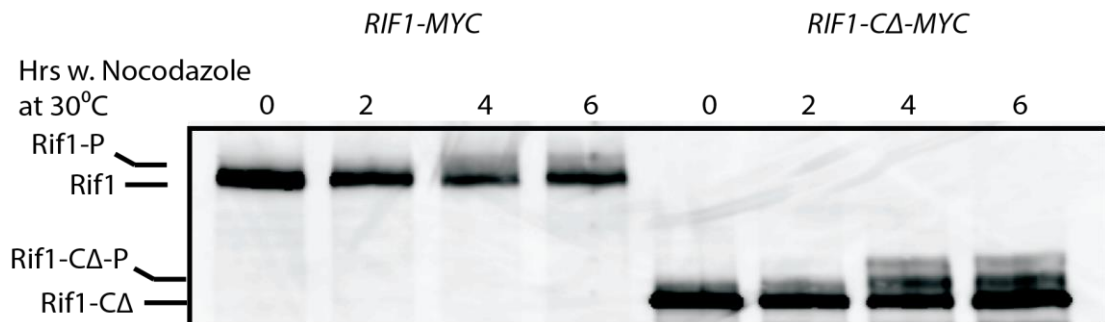


Figure 3.2 Rif1 is phosphorylated in Nocodazole induced arrest

Western blot using protein samples from overnight cultures grown at 20°C to a concentration of 1×10^7 cells/mL, cultures were diluted 1:1 with fresh YPD. (A) *CDC13 RIF1-Δ* cultures were incubated for 4 hours at 30°C in the presence of nocodazole, mock treatment of DMSO, or no treatment. Membrane probed for Rif1 or Rad53. (B) *CDC13 RIF1* and *CDC13 RIF1-Δ* cultures were incubated for 4 hours at 30°C in the presence of nocodazole (15μg/mL).

3.3 Investigating phosphorylation of Rif1 in response to other DNA damaging agents

I have shown that Rif1 is phosphorylated as a result of both telomere damage in *cdc13-1* cells and by treatment with the spindle poison nocodazole. I therefore wanted to answer what other factors might cause the phosphorylation of Rif1 in response to damage.

In order to study this cultures of the strain *CDC13 RIF1-CΔ-MYC* were treated with one of the following reagents:

- Phleomycin (50µg/mL) – Binds and cleaves DNA to create DSBs
- Hydroxyurea (100mM) – Stalls replication forks through inhibition of the production of deoxyribonucleotides
- Methyl-methane sulfonate (MMS) (0.05% w/v) – Stalls replication forks, ultimately leading to replication fork collapse and creation of DSBs
- UV Radiation (30J/m²) – Induces pyrimidine dimers which can be converted to DSBs during replication

Cells were treated with reagents and incubated at 23°C for 3hrs, except for those cultures treated with nocodazole which received 4 hours treatment. Cells treated with UV were resuspended in a low volume of PBS for treatment, they were then resuspended in YPD for 3hrs alongside the other cultures. For this experiment a strain of *cdc13-1*, or a treatment with nocodazole (15µg/mL) were used as controls to show a known phosphorylation of Rif1.

As expected, the control *cdc13-1* showed phosphorylation of both Rif1 and Rad53 after 4 hours at 36°C, as well as an accumulation of cells in the G2/M transition. The results for the reagents are varied and interesting. In nocodazole, there was phosphorylation of Rif1 but only a very slight shift in Rad53 migration, suggesting a very low level of phosphorylation of Rad53. In HU and MMS at this temperature there was no phosphorylation of Rif1 after treatment with either reagent, however, strong phosphorylation of Rad53 was seen in both conditions. In contrast, in both phleomycin and UV damage there was noticeable phosphorylation of Rif1. However, both these conditions resulted in moderate phosphorylation of Rad53. The protein was clearly not as strongly phosphorylated as in *cdc13-1* controls or in HU treatment, but it was more heavily phosphorylated than in nocodazole treatment (**Figure 3.3A**).

To further investigate this finding, I repeated the experiment shown in **Figure 3.3A**, instead incubating samples with reagent at 30°C rather than 23°C. Cells were treated with the same concentrations of reagents and were treated for the same time window as previously. A

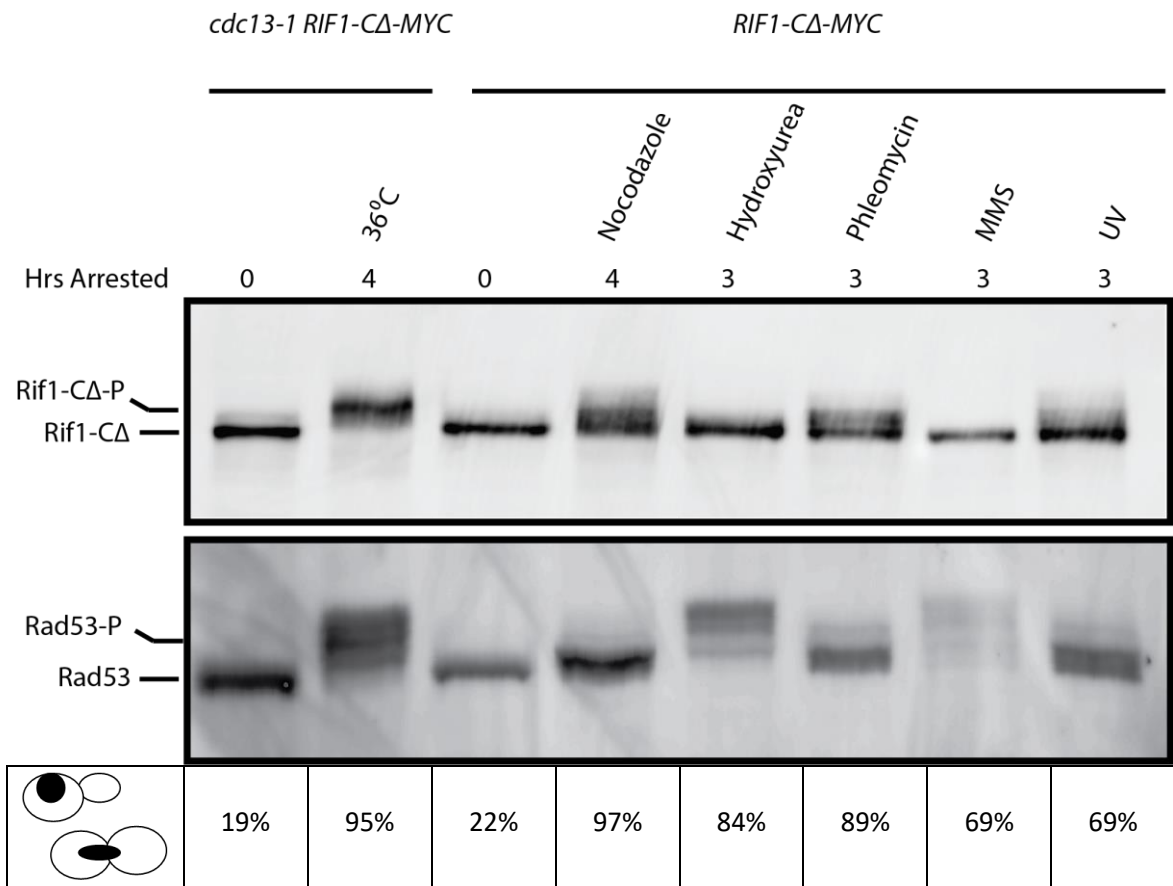
cdc13-1 strain or nocodazole treatment were again used as controls for known phosphorylation of Rif1.

In this experiment, phosphorylation of Rif1 was seen after incubation in media containing nocodazole or phleomycin, as well as after UV radiation, as was seen previously. However, phosphorylation of Rif1 was also seen after incubation with HU, which was not seen at 23°C. In these samples there was strong phosphorylation of Rad53 after treatment with phleomycin, and more moderate phosphorylation of Rad53 after treatment with HU or dosage with UV radiation. However, treatment of cells with MMS did not result in phosphorylation of Rif1 or, unexpectedly, Rad53 (**Figure 3.3B**).

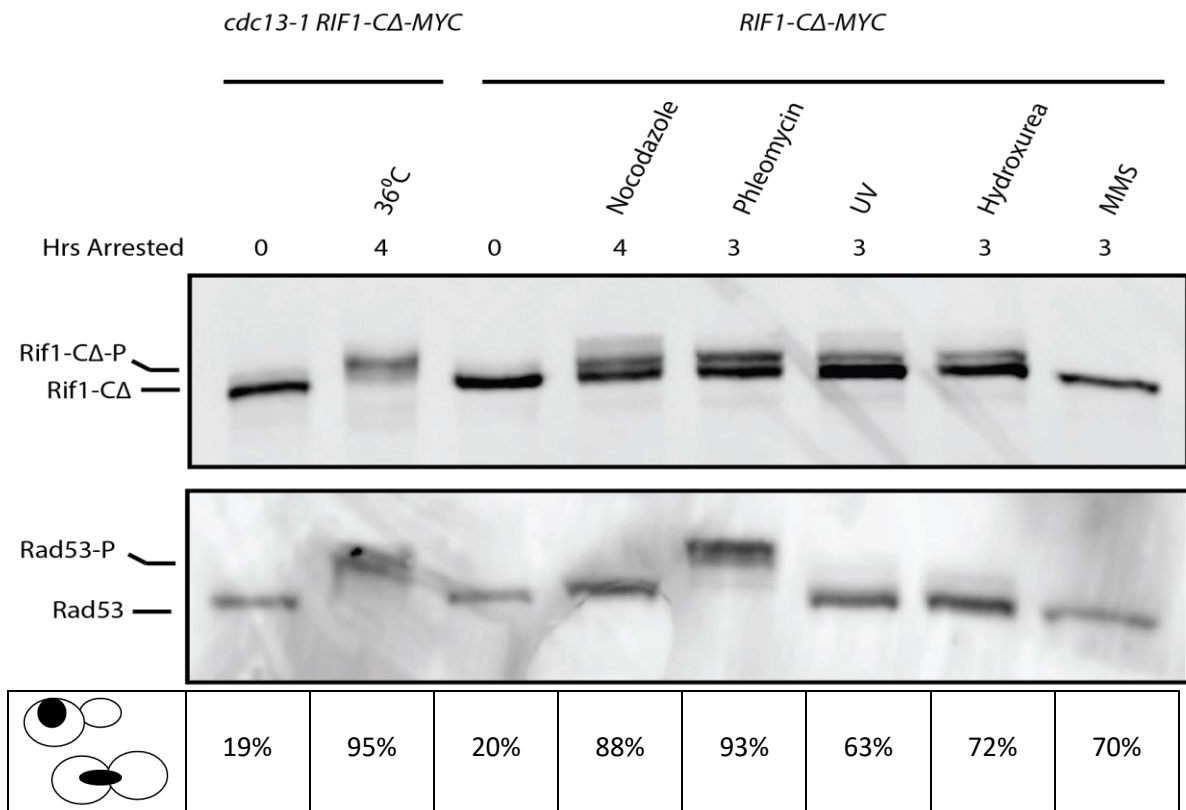
To verify the results further, the experiment for HU and MMS was repeated at 30°C. Interestingly, using fresh MMS the phosphorylation of Rad53 was returned, however Rif1 remained non-phosphorylated. In comparison these results appeared to show a divergence in Rif1 reaction to HU-induced arrest that was seemingly created by the incubation at higher temperature during treatment. Upon incubation at 30°C with HU, Rif1 protein did not appear to become phosphorylated. However, in these cells Rad53 was not phosphorylated (**Figure 3.3C**).

From this data I concluded that spindle damage and telomere damage are not the only conditions that lead to phosphorylation of the protein Rif1. UV radiation and phleomycin exposure are also capable of leading to the phosphorylation of Rif1, however, treatment of cells with MMS does not appear to lead to phosphorylation of Rif1. Our results seem to imply that HU may also lead to phosphorylation of Rif1 but only under certain temperature conditions.

A



B



C

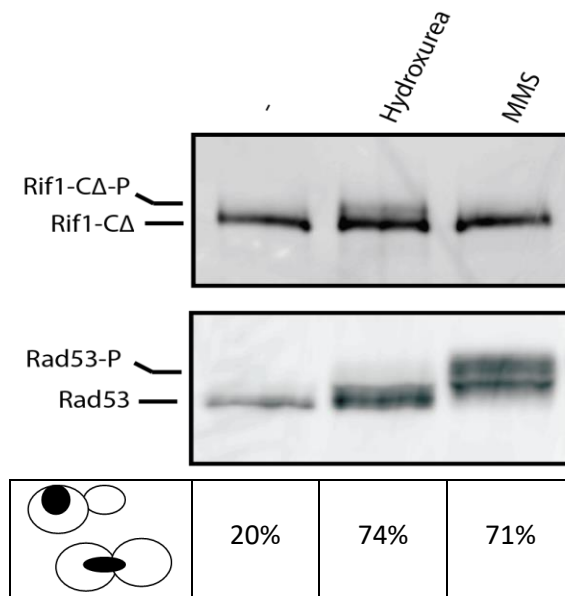


Figure 3.3. Rif1 is phosphorylated in response to a range of genotoxic stressing reagents

Western blots of yeast strains *cdc13-1 RIF1-CΔ-MYC* and *CDC13 RIF1-CΔ-MYC*. Cell cultures were grown overnight at 20 °C to 1×10^7 cells/mL at T0. Cells containing the allele *cdc13-1* were then shifted to 36 °C. *CDC13* cell cultures were split and treated with Nocodazole (15µg/mL), phleomycin (50µg/mL), hydroxyurea (100mM), or MMS (0.05%). Those cells treated with UV radiation were exposed to a dosage of 30J/m² ultraviolet radiation and then grown YPD liquid medium for 3hrs. After addition of reagents, or exposure to UV radiation, cell cultures were incubated at either 23 °C (**A**) or 30 °C (**B**). *cdc13-1* cells and those cells exposed to nocodazole were harvested after 4hrs, cells undergoing all other treatments were collected after 3hrs. (**C**) *CDC13 RIF1-CΔ-MYC* cell culture was grown O/N and split (as in **A** & **B**). Cells were then treated with Hydroxyurea (100mM) or MMS (0.05%) and shifted to 30 °C. Cell samples were taken for DAPI treatment and cell cycle scoring by fluorescence microscopy, percentage of cells with large budded cells (G2/M) or small budded cells (S) is displayed for all samples.

3.4 The first 176 residues of Rif1 are essential for Rif1-P and the protective function of Rif1 in *cdc13-1* cells.

These results showed the phosphorylation of Rif1 protein in *cdc13-1* cells at restrictive temperatures, as well as cells exposed to other genotoxic stresses. This phosphorylation event does not appear to occur within the C-terminus region of the protein, nor does deletion of this C-terminus region affect the sickness of *cdc13-1* (Xue *et al.*, 2011). In order to demonstrate the role of this phosphorylation event, I aimed to locate the residues responsible for the modification.

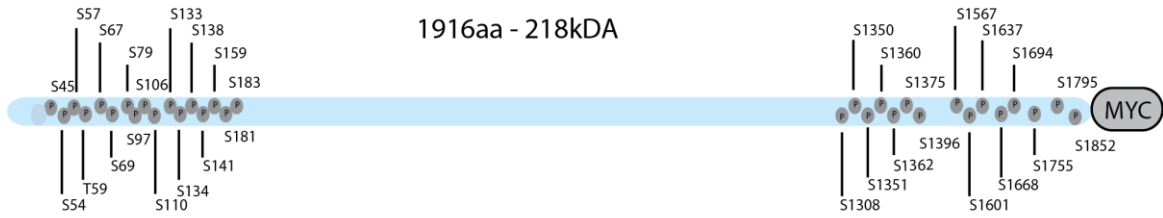
To first determine if the phosphorylation did occur within the N-terminal domain, experiments were conducted utilising a mutant *RIF1* gene which encoded a tagged protein with a full C-terminus region and a smaller deleted region close to the N-terminus. This deletion no longer encoded amino acid residues 1-176 of the Rif1 protein and as such this mutant is referred to here as *rif1-N Δ -MYC* (**Figure 3.4.1A**).

The growth of this mutant was tested via serial dilution. The mutant was grown alongside strains with the genotypes *cdc13-1 RIF1*, *cdc13-1 RIF1-MYC*, *cdc13-1 rif1 Δ* , and then finally the mutant of interest *cdc13-1 rif1-N Δ -MYC*. Both *cdc13-1* strains with full-length Rif1 protein can be seen to have grown normally at 23°C, and once placed at 26°C began to show signs of sickness but retained moderate growth, by 30°C neither strain grew. In comparison *rif1 Δ* cells, which also grew adequately at 23°C, showed severe sickness at 26°C, and no longer grew at 30°C. The mutant *rif1-N Δ* cells showed an intermediate pattern of growth, neither growing as well *cdc13-1 RIF1* cells, nor as poorly as *cdc13-1 rif1 Δ* cells (**Figure 3.4.1B**). Perhaps indicating a partial loss of protein function resulting from the mutation.

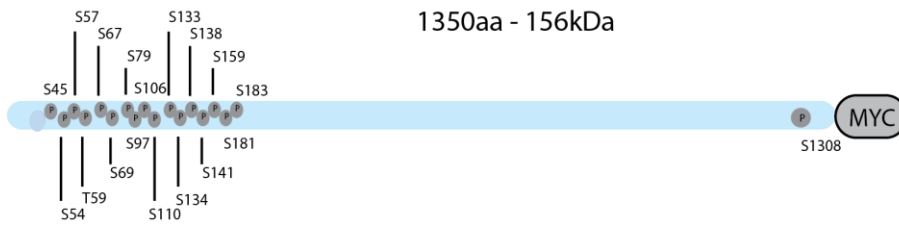
However, it is known that this region also contains the RVxF-SILK domains responsible for the binding of Rif1 and the PP1 protein; Glc7, in order to regulate the timing of replication at late firing origins of replication. Previous studies have, however, determined that the mutation of these sites alone is not sufficient to affect the growth of *cdc13-1* cells (Matarrocci *et al.*, 2017).

A

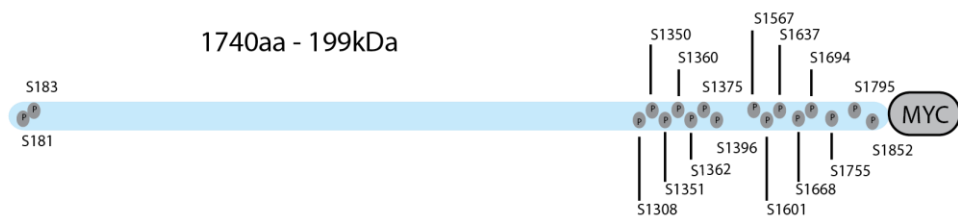
Rif1-MYC



Rif1- Δ C-MYC



Rif1-N Δ -MYC



B

cdc13-1

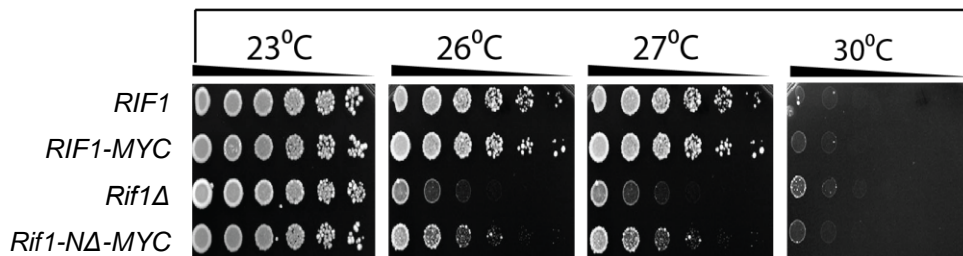


Figure 3.4.1 The Rif1 N-terminal-proximal region increases the viability of *cdc13-1*.

(A) Structural models of the Rif1 proteins containing large deletions of terminus-adjacent regions of Rif1. Previously identified sites of potential phosphorylation are indicated (grey circles). Sites were identified in several large scale studies identifying multiple proteins (Albuquerque *et al.*, 2008; Holt *et al.*, 2009; Swaney *et al.*, 2013) **(B)** Serial dilutions of *cdc13-1 RIF1* variants on YEPD medium at a selection of temperatures. Cells were spotted and incubated at the indicated temperature for 2-3 days before being photographed.

As the mutant *rif1-NΔ* strains increase the temperature sensitivity of *cdc13-1*, I wanted to investigate whether this increased sensitivity may be linked to changes in phosphorylation of Rif1. For this experiment overnight cultures grown at 20°C were shifted to 36°C for 6 hours, with samples taken at 2-hour intervals. For this comparison a *cdc13-1 RIF1-MYC* and a *cdc13-1 rif1-NΔ-MYC* strain were used. As expected from previous experiments the control strain with the complete *RIF1* gene showed phosphorylation of the Rif1 protein after two hours of incubation of cells at 36°C. This phosphorylation was maintained throughout the experiment. Rad53 showed a similar pattern of phosphorylation across this time-course, becoming phosphorylated by two hours, with even stronger phosphorylation at T4 and T6. Interestingly, when I examined samples from the *rif1-NΔ* mutants there was no phosphorylation of the truncated Rif1 protein at any point in the time course. However, Rad53 phosphorylation appeared to be largely unaffected. The protein became phosphorylated at T2, as in the control, and by T4 and T6 had become more phosphorylated again. These mutant cells arrested similarly to the control strain, with a high proportion of cells arresting in the G2/M phase of the cell cycle (**Figure 3.4.2**).

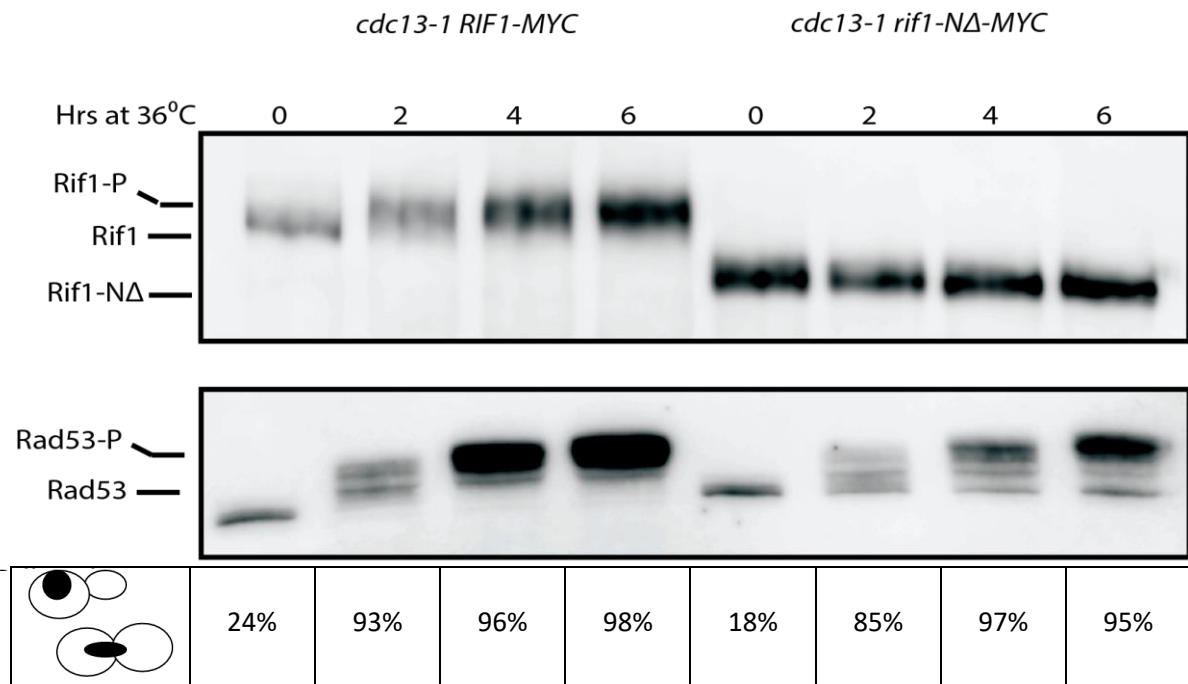


Figure 3.4.2 The Rif1 N-terminal Region is required for Rif1-Chromatin Binding

Western blot of Rif1 and Rad53 in *cdc13-1 RIF1-MYC* (LMY79) and *cdc13-1 rif1-Δ2-176-MYC* (DLY9823). Cells were grown overnight at 20°C (to 1×10^7 cells/mL) and shifted to 36°C for 6 hours, with samples taken every 2 hours. Samples were separated on 7.5% SDS-PAGE gels. Cell samples were also prepared for DAPI treatment and analysed with fluorescence microscopy to score the stage of the cell cycle. Percentage of cells with large buds shown.

As the N-terminal truncated Rif1 protein was not phosphorylated during telomere damage, I then used this strain to further examine the association of Rif1 with the chromosome and how it is affected by phosphorylation. For this, I used ChIP to study the association of Rif1 and the chromosome at three distinct loci:

- *Y'600* - Loci located only 600bp from the telomere. A positive control at T0 as fragments would likely contain telomere-bound Rif1 as part of the Rap1-Rif1-Rif2 complex. Furthermore, multiple Y' elements at multiple chromosomes will mean these loci are present many times in each cell.
- *YER188W* – A single gene locus located approximately 8kb from the telomere of chromosome V
- *PAC2* – A centromeric locus 300kb from the telomere. This locus acted as a negative control of chromosome V.

For this cell cultures of *cdc13-1 RIF1-MYC* or *cdc13-1 rif1-Δ2-176-MYC* were grown overnight at 20°C and then incubated at 36°C for 6 hours, with samples taken every 2 hours. Protein-DNA interactions were fixed by treatment of the cells with formaldehyde at 24°C.

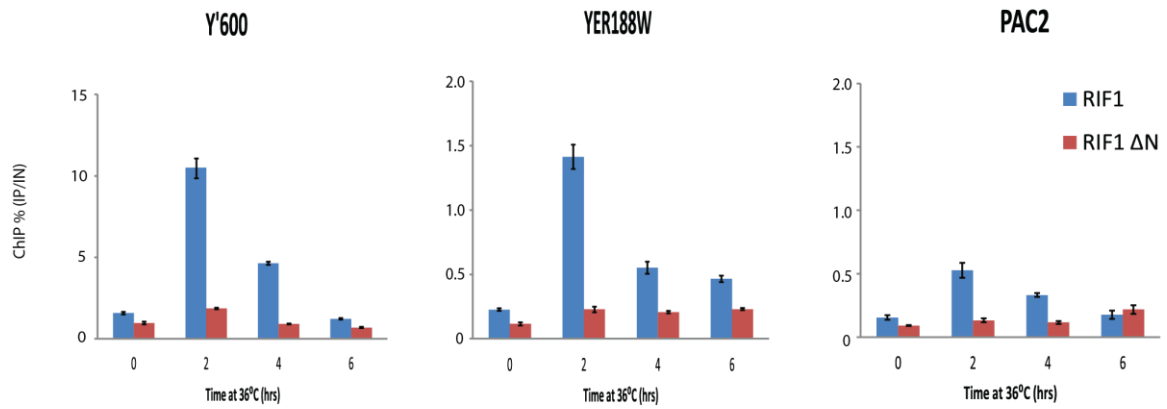
In the control strain in this experiment, *cdc13-1 RIF1-MYC*, at *Y'600* the Rif1 association began at a moderate level, which increased after 2 hours to a peak level. This interaction then declined again after 4 hours and fell even further by T6. A similar pattern is also seen at *YER188W*, but at lower levels of association. At *PAC2* there was a very low association of Rif1 with the chromosome at all time-points.

In contrast, the association of the truncated Rif1 protein with the chromosome was noticeably different. At both *Y'600* and *YER188W* the association of this altered protein was much less than that of the full-length protein at all time-points. When the *PAC2* locus was examined Rif1 association with this locus appears to be relatively similar between the control strain and the truncated Rif1. Multiple experimental repeats are shown, demonstrating that while signal strength varies between experiments, this pattern of association is consistent and repeatable (**Figure 4.3.3A-C**).

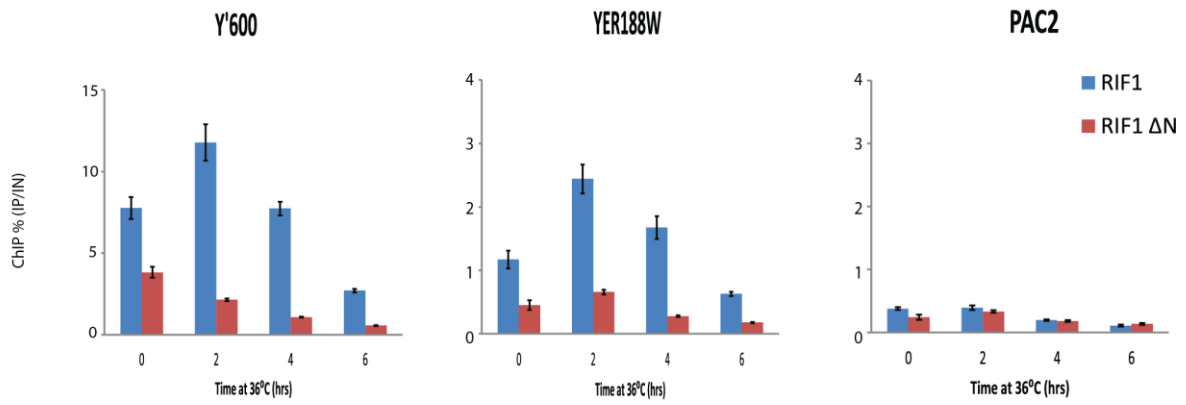
These results together indicate that the mutation of this region of the Rif1 protein has substantial impacts upon the growth of *cdc13-1* cells. Furthermore, this region appears to house the phosphorylation event that occurs during telomere damage, and without the region the Rif1 protein cannot effectively associate with the chromosome at sites of damage.

However, it is unclear if this is due partially to the loss of phosphorylation, or entirely due to the importance of this region in associating with DNA.

A



B



C

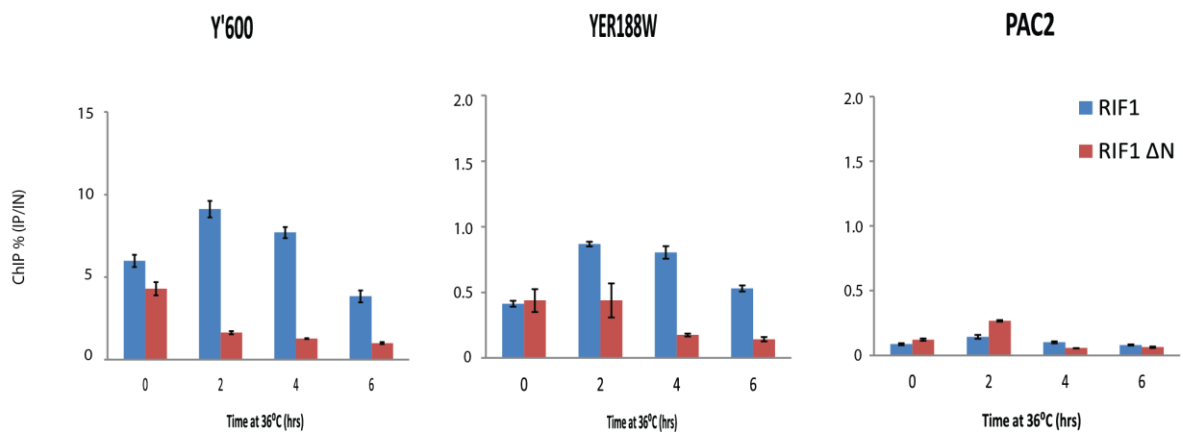


Figure 3.4.3 The Rif1 N-terminal Region is required for Rif1-Chromatin Binding

(A, B, C) Experimental repeats of ChIP of Rif1 from *cdc13-1 RIF1-MYC* (LMY79) and *cdc13-1 rif1-NΔ-MYC* (DLY9823) cells grown overnight at 20°C (2×10^7 cells/mL at T0) and shifted to incubation at 36°C, with samples collected at 2hr intervals. Error bars show standard deviation between three technical replicates.

3.5 Rif1 residues phosphorylated in *cdc13-1* cells

The deletion of the N-terminal domain clearly demonstrated the importance of this region for proper function of Rif1 in *cdc13-1* cells. The knowledge that the phosphorylation site may lie within this region made searching for this site easier. As such, I attempted to find the location of the phosphorylation sites within the Rif1 N-terminal region, with the aim of removing Rif1 phosphorylation without larger structural changes to the protein.

To carry out this experiment the first stage was to ascertain which amino acid residues were the most likely target sites for phosphorylation, and therefore should be targeted for mutation. For this, multiple phosphorylation prediction software available online were used to analyse the protein sequence, as well as data existing from previous published datasets available through SGD. A model of Rif1 protein structure shows the potential phosphorylation sites present in the *RIF1-CA-MYC* mutants (**Figure 3.5.1A**). A subset of these sites were chosen based on predictive software (KinasePhos, etc.), data gathered concurrently regarding likely candidate kinases (discussed later), and recent publications (J. Wang *et al.*, 2018). This suggested the sites S45, S57, S110, S125, S138, and S181 as the most likely residues to be phosphorylated.

The residues S125 and S138 fall between the RVxF-SILK domains, which have previously been established to be crucial for the role of Rif1 in controlling replication timing. The interaction of Rif1 and PP1 has been shown to be controlled via phosphorylation of the Rif1 protein, and as such these sites may be involved in this role (Mattarocci *et al.*, 2017). However, it has been previously demonstrated that interruption of the RVxF-SILK domains does not affect the sickness of *cdc13-1* cells, I elected to discount these sites at this stage of the experiment.

Whilst S181 is outside of the N-terminal region deleted in the previously shown data, other studies have recently indicated a potential phosphorylation of this site in telomere damage resulting from the deletion of the protein Yku70 (Wang *et al.*, 2018). Further to this, this site resembles very closely the “ideal” binding sequence of a CDK protein which is S/T-P-x-K/R (Nigg, 1993). As such I therefore included S181 and Y183 for mutation in this study. These two residues were mutated alongside residues S45, S57, and S110.

To perform mutagenesis Gibson Assembly of plasmids was used to introduce targeted site-specific substitutions. A portion of the *RIF1* gene and its upstream region was cloned onto a plasmid vector, adjacent of a *HIS3* marker gene. Primers with targeted mismatches were used to clone fragments of this gene/plasmid hybrid. These fragments were then

reassembled and sequenced to ensure the mutated sites were included. These gene fragments were then transformed back into the yeast genome, alongside the upstream *HIS3* marker sequence, these cassettes contained tails homologous to the target region located at the *RIF1* locus (**Figure 3.5.1B**). In the following experiments a control strain is used which has had the *HIS3* marker inserted into the genome upstream of *RIF1*, however, the *RIF1* gene sequence has not been changed. As such any differences seen between *RIF1* mutants and this strain cannot be accounted for by any expression differences that may be generated by alterations to the upstream region of *RIF1*. All mutations were confirmed by sequencing before crossing into a range of backgrounds for study.

The initial mutations made immediately grouped into two types, mutants containing substitutions at all 5 intended sites, and those which contained substitutions only at residues S45, S57, and S110.

A

Rif1-C Δ -MYC



B



Figure 3.5.1. The mutation of 5 Serine Residues within Rif1 Protein

(A) A schematic representation of previously identified potential sites of phosphorylation within Rif1-C Δ that may be targeted by kinase activity. Those mutated indicated in red. (B) A schematic representation of the transformed Rif1 gene locus, mutations marked in red and a *HIS3* marker is located 514bp upstream of the TSS.

These strains were investigated to study the differences created by residue substitutions in Rif1. For the following experiments cell cultures were grown overnight at 20°C, and T0 samples were taken directly from these cultures. These cultures were then incubated at 36°C, with samples taken after 2, 4, and 6 hours.

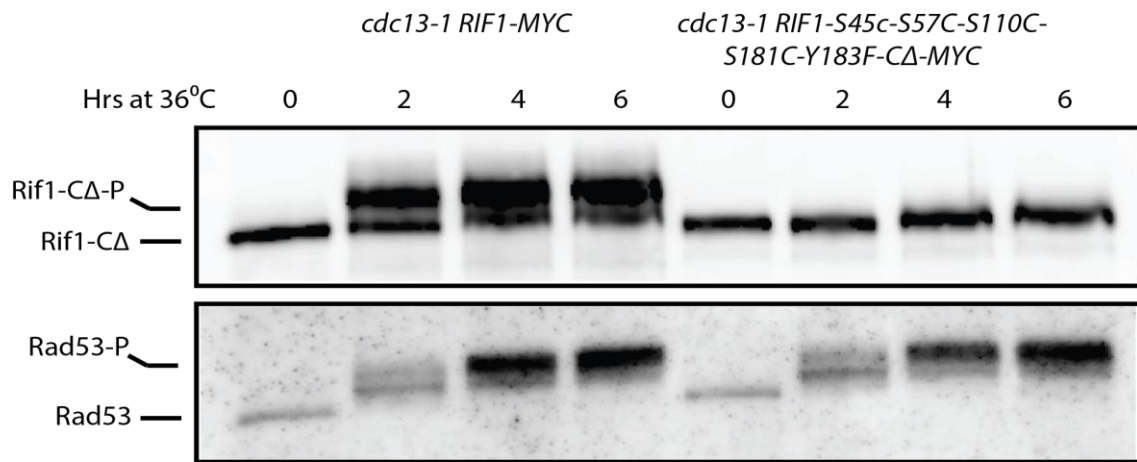
The first of these experiments shows a *cdc13-1 RIF1-CΔ-MYC* control strain against a strain containing substitutions at all 5 sites in *RIF1*. As expected, both Rif1 and Rad53 in the control strain became phosphorylated after 2 hours at high temperature, this phosphorylation increased after 4 hours and was maintained after 6 hours. However, the mutant *RIF1* cells showed no phosphorylation of the Rif1 protein after incubation at 36°C at any time-point studied. This contrasts with the phosphorylation of Rad53 which closely resembled the control (**Figure 3.5.2A**).

Interestingly, when the phosphorylation of Rif1 was examined in a strain with only three sites substituted a similar phenotype was seen. In this experiment Rif1 showed no phosphorylation at any time-point after incubation in 36°C, despite the accumulation of phosphorylated Rif1 in the control strain. However, the phosphorylation of Rad53 was very similar between both strains (**Figure 3.5.2B**).

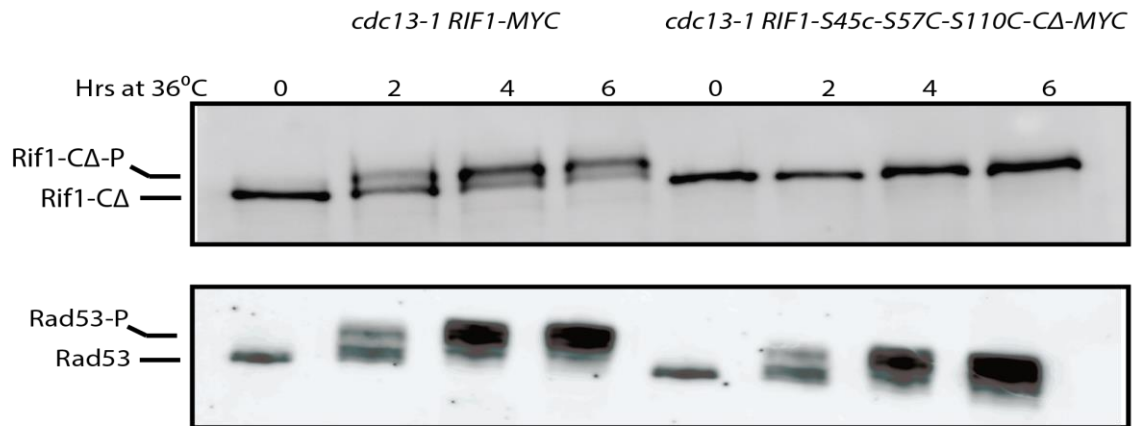
I also generated strains containing substitutions of S181 and Y183, due to suggestions of phosphorylation at S181 in previous studies. When comparing Rif1 in these, the behaviour of the protein was similar to the control. After incubation at 36°C Rif1 became phosphorylated in *RIF1-S181C-Y183F* and this phosphorylation is maintained throughout the 6-hour time-course (**Figure 3.5.2C**).

These results strongly indicate that I successfully located residues key to the phosphorylation of Rif1 during telomere damage, as well as ruling out a residue previously seen phosphorylated in Yku70 damage. These results point to the importance of S45, S57, and S110 for phosphorylation of the protein, and as such would be worthy of further study to even more specifically locate the phosphorylation events.

A



B



C

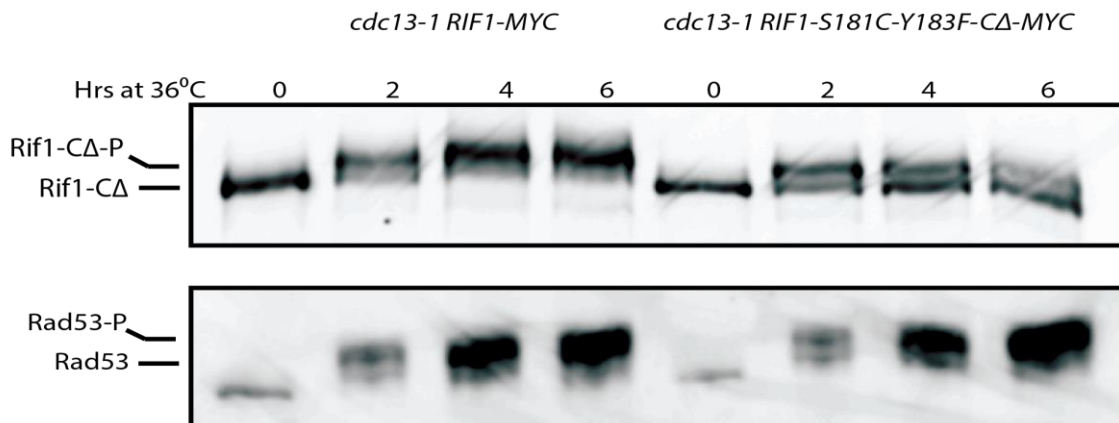


Figure 3.5.2 Substitution of S45, S57, and S110 eliminates phosphorylation of Rif1 during telomere damage.

Western blots from cells grown overnight at 20°C (T0) and shifted to a temperature of 36°C for 6hrs, with samples taken every 2hrs. Proteins separated in a 7% SDS-PAGE gel and probed for Rif1 or Rad53. Samples compared in a control strain of *cdc13-1 RIF1-CΔ-MYC* and (A) *cdc13-1 RIF1-S45C-S57C-S110C-S181C-Y183F-MYC*, (B) *cdc13-1 RIF1-S45C-S57C-S110C- MYC*, or (C) *cdc13-1 RIF1- S181C-Y183F-MYC*.

The previous experiments showed that the phosphorylation of Rif1 occurs within three residues in the N-terminal domain during telomere uncapping; S45, S57, and S110. To determine which of these sites were responsible new *RIF1* mutants were generated using the existing plasmid constructs containing the fragment of mutated *RIF1*. Shorter DNA cassettes for transformation of strains were generated to progressively exclude the sites that were closer to the 3' of gene fragment. This meant that from a plasmid containing a *RIF1* fragment containing substitutions at S45, S57, and S110 I generated cassettes which could produce the following combination of mutations:

- *RIF1-S45C-S57C-S110C*
- *RIF1-S45C-S57C*
- *RIF1-S45C*

This process was sufficient to determine which sites, when mutated, may affect the phosphorylation of Rif1. Although all combinations of mutation could not be achieved by this methodology, it allowed me to determine if any of these sites were not required for phosphorylation.

In the following experiment cell cultures of *cdc13-1* strains containing mutations of the potential phosphorylated residues in Rif1 were grown overnight at 20°C alongside a control *cdc13-1* culture.

As expected, the control samples in this experiment showed a clear shift in Rif1 migration upon incubation at 36°C, corresponding to the phosphorylation event that occurs. Furthermore, as would be expected clear phosphorylation of the Rad53 protein was seen at this temperature. As suggested by previous data, there was no change in protein migration of Rif1 in samples from the strain containing the *RIF1-S45C-S57C-S110C-CΔ* mutations. Substitution of these sites led to a complete loss of phosphorylation. However, the phosphorylation of Rad53 was completely unaffected when compared to that of the control strain.

Interestingly, the substitutions of residue S45 and S57 offer the most information. The mutant containing substitutions at both residues, *RIF1-S45C-S57C-CΔ* showed a clear change in protein migration of Rif1. This change indicated that the protein was less phosphorylated after the mutation of these two sites. However, it is notable that there did appear to be some phosphorylation of Rif1 remaining in these samples. Again, Rad53 was normally phosphorylated. Finally, a mutation of only residue S45 resulted in the least change

in the protein migration of Rif1. In these samples both Rif1 and Rad53 appeared to be phosphorylated equivalent to that of the control samples (**Figure 3.5.3**).

This data strongly suggests that residue S45 is not the site of phosphorylation during telomere damage. Substitution of this site appears to have little to no effect on the phosphorylation of Rif1. In contrast, this data strongly points to both S57 and S110 as sites of phosphorylation in Rif1 protein. Substitutions at either of these sites appears to reduce the overall phosphorylation of the protein. Furthermore, substitution of residue S57 appears to have a larger effect on the shift in Rif1 protein migration than substitution of S110 alone. This may suggest S57 as the primary site of phosphorylation in Rif1.

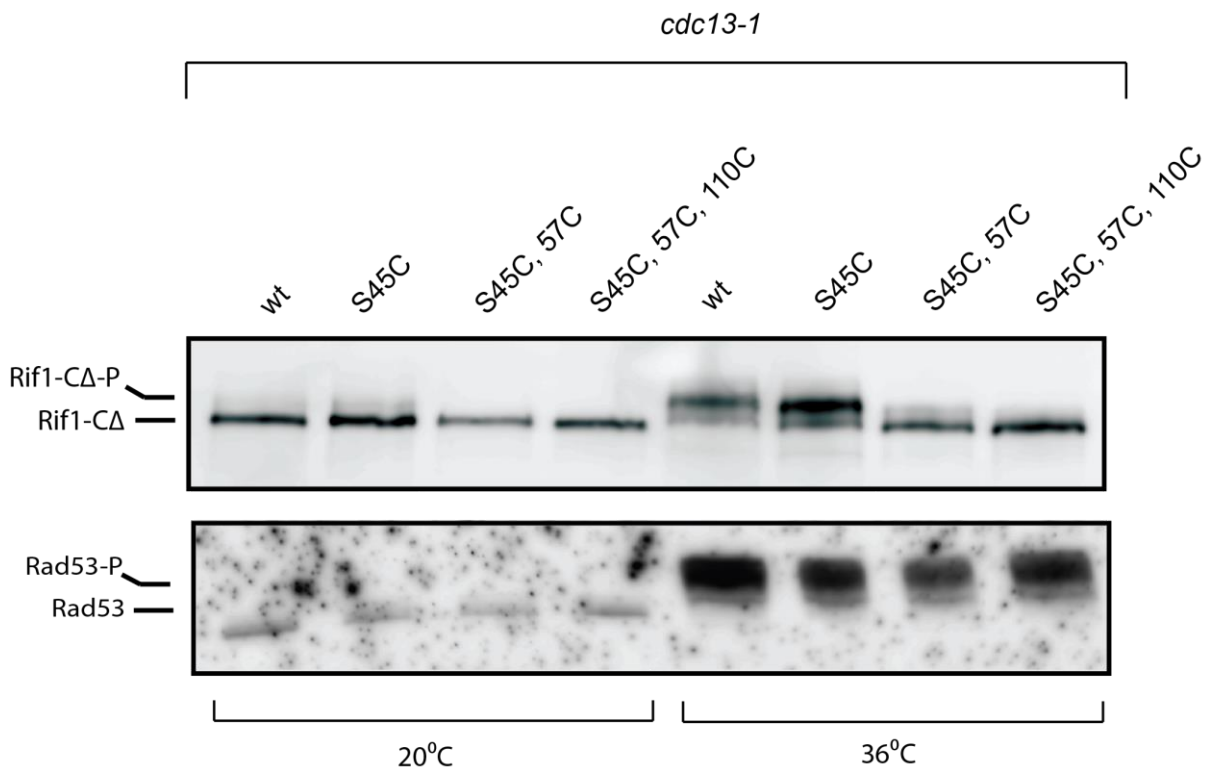


Figure 3.5.3 Rif1 Phosphorylation is Split between Amino Acid Residue S57 and S110.

Western blot using protein samples from cells grown overnight at 20°C to low cell concentration (1×10^7 cells/mL) before being incubated at 36°C for 4 hours comparing *cdc13-1* cells containing *RIF1-Δ-MYC*, *RIF1-S45C-Δ-MYC*, *RIF1-S45C-S57C-Δ-MYC*, and *RIF1-S45C-S57C-S110C-Δ-MYC* probed for Myc-tagged Rif1 and for Rad53.

The data shown in this chapter has used mutants with substitutions of cysteine in place of serine. This is not standard and may have inadvertently introduced larger structural changes into the Rif1 protein than necessary, such as disulphide bridges. From the data gathered I also required the generation of fresh mutants in order to generate strains containing isolated substitutions of S57 and S110 independent from one another, as well as any other mutations. Therefore, these mutants were generated using the same methodology as described previously in this chapter, however, alanine residues were instead substituted in place of serine residues.

Three mutants were generated containing isolated substitutions of S57 and S110, and a mutant containing a substitution of both. These mutants are:

- *RIF1-S57A*
- *RIF1-S110A*
- *RIF1-S57A-S110A*

cdc13-1 strains containing the mutations listed above were cultured overnight at 20°C, T0 samples were taken directly from these and the cultures were then incubated for 36°C for 4 hours. Cell samples were also taken for analysis and cell scoring by fluorescent microscopy. These mutants were compared to samples from a control *cdc13-1 RIF1-CΔ* strain.

As in previous experiments, the Rif1 protein from the control strain became phosphorylated after 4 hours at 36°C. In these cells there was also phosphorylation of Rad53 at high temperatures, and these phosphorylation events correlated to an accumulation of cells in the G2/M phase of the cell cycle. In contrast, Rif1 phosphorylation was greatly reduced in mutants containing a single substitution of amino acid residue S57. At 36°C, whilst there was shift of the Rif1 protein migration, this phosphorylated form was much less visible and most of the protein was non-phosphorylated. However, Rad53 phosphorylation and accumulation of cells in G2/M remained unaffected by this mutation (**Figure 3.5.4A**).

Interestingly, in the *RIF1-S110A-CΔ* mutant the data shows that Rif1 phosphorylation was higher than that of strains with the substitution of S57 alone. It is however notable that the phosphorylation of Rif1 did not appear as substantial as in samples taken from the control strain. In *RIF1-S110A-CΔ* mutants there appeared to be a higher proportion of non-phosphorylated Rif1 after 4 hours at 36°C than in the control. Again, Rad53 phosphorylation and the arrest of cells at the G2/M phase of the cell cycle did not appear to be affected by this mutation (**Figure 3.5.4A**).

Further to this, when both sites were substituted simultaneously there was complete loss of phosphorylation of the Rif1 protein. In this strain, 4 hours at 36°C did not result in any change in the migration of Rif1. Despite Rad53 phosphorylation, and the proportion of cells arrested at G2/M closely matching that of the control strain (**Figure 3.5.4A**).

This experiment would appear to support previous findings. The data clearly demonstrates a loss of Rif1 phosphorylation after the substitution of residue S57 and S110. Furthermore, the data suggests that both sites may work together for Rif1 phosphorylation but does not necessarily suggest equal function. Phosphorylation at S57 appears to be responsible for most of the migratory shift in the Rif1 protein.

To further verify these results these strains were studied more closely across a time-course of exposure to high temperature, to ensure that phosphorylation was not simply occurring earlier or later than studied. Cell cultures of each mutant were grown overnight at 20°C alongside control strains (*cdc13-1 RIF1-CΔ*) and were then shifted to 36°C for 6 hours, with samples taken at 2-hour intervals.

The control strain behaved as expected in the three following experiments. At T0 there was a single clear protein band of both Rif1 and Rad53. After 2 hours at 36°C the migration patterns have shifted and there was a clear band of phosphorylated Rif1 and multiple bands of phosphorylated Rad53. This phosphorylation remains throughout T4 and T6. During this time a high proportion of cells accumulated and arrested in G2/M phase of the cell cycle.

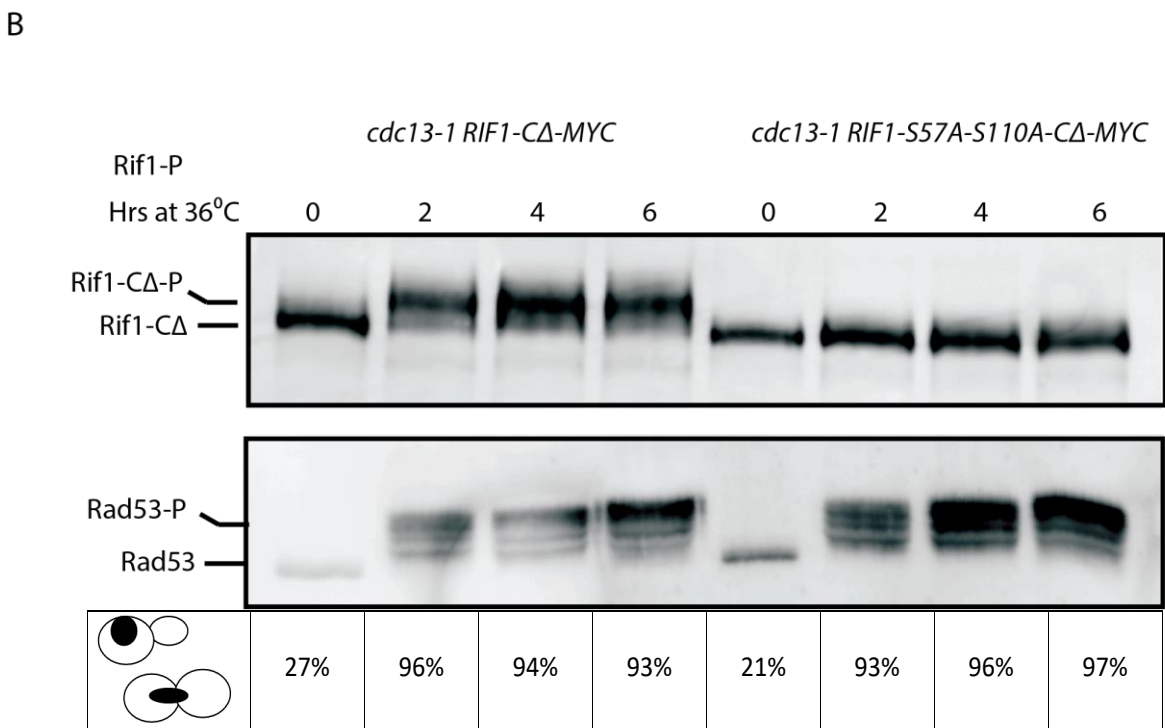
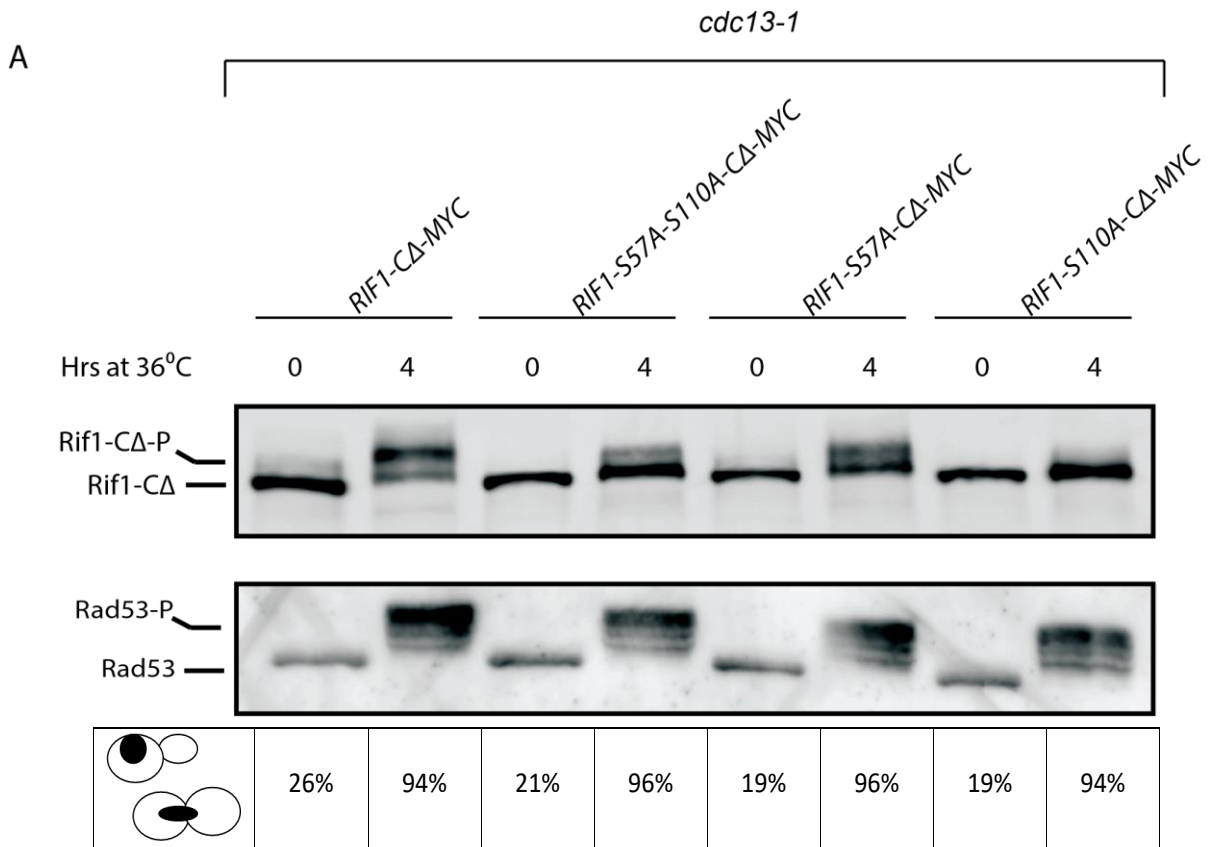
When examining samples from a strain containing the mutation *RIF1-S57A-S110A-CΔ* there was no migratory shift in the Rif1 protein in any sample across the 6 hours. The Rif1 protein did not appear to become phosphorylated despite incubation at 36°C. However, Rad53 phosphorylation occurred similarly to in the control, appearing at T2 and growing stronger by T6. These cells also accumulated and arrested at G2/M at the same rate as the control strain (**Figure 3.5.4B**).

Samples from the mutant *RIF1-S57A-CΔ* show that the phosphorylation of Rif1 is greatly reduced. Whilst there was a small level of Rif1 phosphorylation at T2, it was difficult to distinguish. Whilst this phosphorylated protein did become more visible at T4, the vast majority of Rif1 protein was non-phosphorylated at all timepoints in these cells and was vastly reduced compared to Rif1 in samples taken from the control strain. This was despite

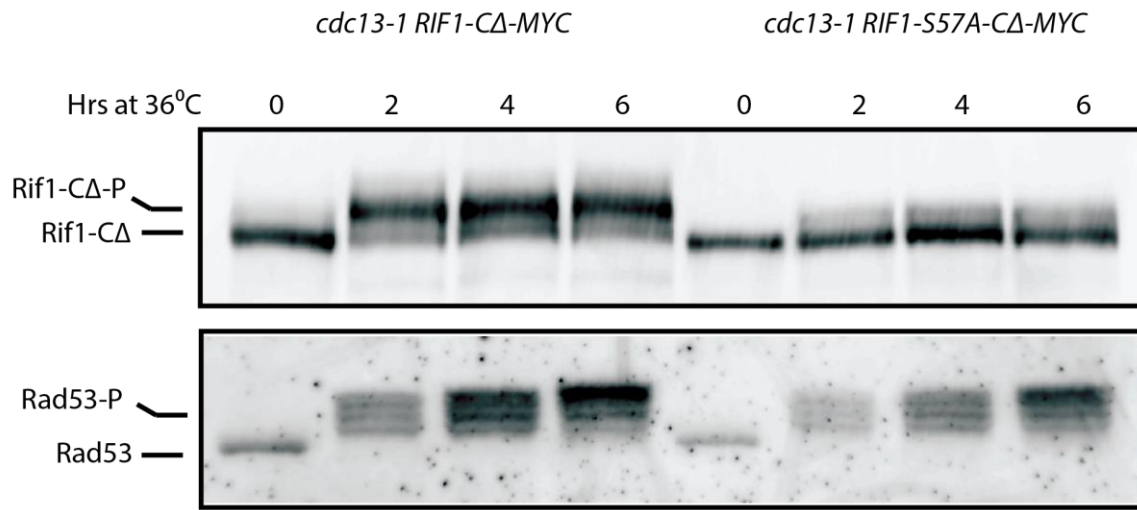
similar Rad53 phosphorylation and accumulation of cells in G2/M as was seen in the control strain (**Figure 3.5.4C**).

In contrast, the Rif1 protein samples taken from *RIF1-S110A-CΔ* were the most phosphorylated of a non-control strain. In these samples, phosphorylated forms of Rif1 were seen after 2, 4, and 6 hours. It is however noteworthy that the migration of these forms was not slowed as much after incubation at 36°C as protein samples from the control strain, suggesting these proteins may have had less phosphoryl groups added. Furthermore, the proportion of non-phosphorylated Rif1 protein, as compared to phosphorylated Rif1, was higher in these samples than was seen in the control strain. In these strains however the phosphorylation of Rad53, and the accumulation of cells in G2/M are similar to that of the control (**Figure 3.5.4D**).

These results together strongly indicate that the phosphorylation of Rif1 may be located at two amino acid residues of the N-terminal region of the Rif1 protein. Furthermore, this data supports that the amino acid residue S57 is the most important residue for phosphorylation of Rif1, and removal of this dramatically reduces Rif1 phosphorylation, compared to the small reduction of phosphorylation after the substitution of residue S110.



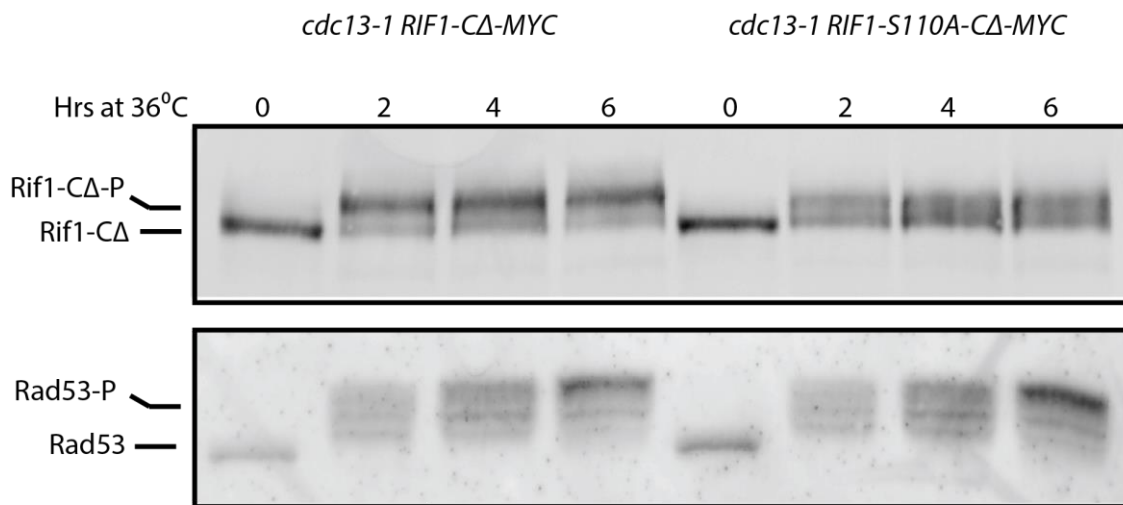
C



C

	27%	96%	94%	93%	19%	95%	96%	95%
--	-----	-----	-----	-----	-----	-----	-----	-----

D



C_t

	27%	96%	94%	93%	19%	93%	92%	94%
--	-----	-----	-----	-----	-----	-----	-----	-----

Figure 3.5.4 Substitution of residue Serine-57 and Serine-110 in Rif1 completely eliminates phosphorylation during telomere damage.

(A) Western blot analysis of Rif1 and Rad53 protein taken from cells incubated overnight at 20°C (1×10^7 cells/mL at T0) and shifted incubation temperature to 36°C for 4 hrs. Cell samples were also taken for DAPI treatment and cell cycle scoring via fluorescence microscopy. (B, C, D) Western blot analysis of Rif1 and Rad53 protein taken from cells incubated overnight at 20°C (T0) and shifted incubation temperature to 36°C for 6 hrs, with cells harvested at 2 hr intervals. Cell samples were also taken for DAPI treatment and analysis and cell cycle scoring via fluorescence microscopy. Strains used here are; *cdc13-1 RIF1-CΔ-MYC* (A, B, C, D), *cdc13-1 RIF1-S57A-S110A-MYC* (A, B), *cdc13-1 RIF1-S57A-MYC* (A, C), and *cdc13-1 RIF1-S110A-MYC* (A, D).

3.6 Residue S57, S110 are required for Rif1 phosphorylation in nocodazole-induced arrest

Prior data shown in this study has indicated that Rif1 phosphorylation is not unique to telomere damage and may also be caused by other genotoxic stresses. I investigated whether the two residues important for phosphorylation of Rif1 in *cdc13-1* cells, could also be important during any of these other conditions. I began with a closer examination of strains with substitutions of the key residues, S57 & S110, and the impact on Rif1 phosphorylation in response to the spindle-poison nocodazole.

CDC13 strains containing the mutation *RIF1-CΔ*, & substitutions of residues S57 and S110 with alanine, were inoculated overnight at 20°C. T0 samples were taken directly from these cultures in the morning, and nocodazole was added (final concentration- 15µg/mL). These treated cultures were then incubated for 4hrs at 30°C. In this experiment a *CDC13 RIF1-CΔ* genotype acted as the control.

In this experiment the control treatment with nocodazole did result in Rif1 phosphorylation as expected. In these samples there was a small shift in Rad53 migration, which may have indicated low levels of phosphorylation. These cells also arrested strongly at the G2/M transition (**Figure 3.7.2A**).

In contrast, this was clearly not the case in those strains containing substitution of both S57 and S110. In this strain, samples taken after a 4-hour nocodazole treatment clearly showed no shift in Rif1 migration, indicating the protein was not phosphorylated. However, similar levels of arrest were seen in these cells as in the controls, and the small shift in Rad53 migration was also seen (**Figure 3.7.2A**).

Further to this, the results for samples taken from *RIF1-S57A-CΔ* mutants are strikingly like those of the double mutants. Again, there appeared to be no phosphorylation of Rif1, whilst Rad53 phosphorylation and arrest of cells at G2/M was were unaffected by this mutation (**Figure 3.7.2A**).

Finally, those strains containing substitutions of residue S110, also appeared to have low phosphorylation of Rif1. As well as phosphorylation of Rad53, and cell arrest at G2/M, that was again unaffected by this mutation (**Figure 3.6A**).

This experiment suggested that the Rif1 residues phosphorylated in nocodazole are the same as those required during telomere damage, it did perhaps suggest equal importance

of S57 and S110 in nocodazole. To ensure the dynamics of phosphorylation did not lead to earlier, or later, phosphorylation, these strains were examined more closely across a time-course.

CDC13 RIF1-C Δ -MYC control strains were grown overnight at 20°C, alongside cultures containing the relevant *RIF1* mutant. The cultures were then incubated for 6 hours at 30°C in the presence of nocodazole, samples were taken at 2-hour intervals.

In the control strain used in this experiment Rif1 began to become phosphorylated after 2 hours treatment with nocodazole, this further increased after 4 hours of treatment. In these samples a small change in migration of Rad53 is clear. After 2 hours treatment there was a very high accumulation of cells in the G2/M phase of the cell cycle, where they are arrested for the duration of the experiment (**Figure 3.6B.C.D**)

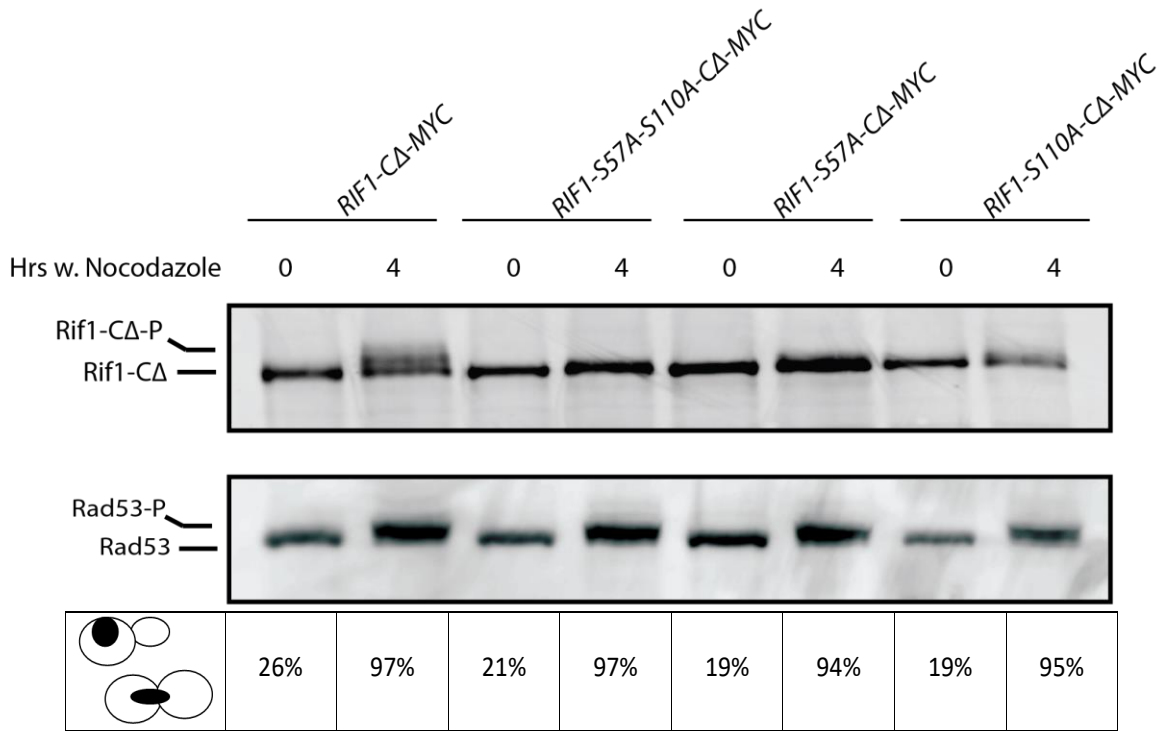
In the double mutant *RIF1-S57A-S110A-C Δ* , a complete loss of phosphorylation of Rif1 was seen at all time-points during the incubation with nocodazole. However, Rad53 phosphorylation and the number of cells arrest in G2/M was similar to the control strain (**Figure 3.6B**).

Interestingly, in the genotype *RIF1-S57A-C Δ -MYC* a shift in protein migration of Rif1 was seen after 4 hours incubation with nocodazole. This was later than in the control strain, and at very low levels which did not increase any further by T6. It appears that while phosphorylation did occur in this mutant it was much less than in the control. Once more however, Rad53 phosphorylation and the arrest of cells in G2/M was unchanged from the control strain (**Figure 3.6C**).

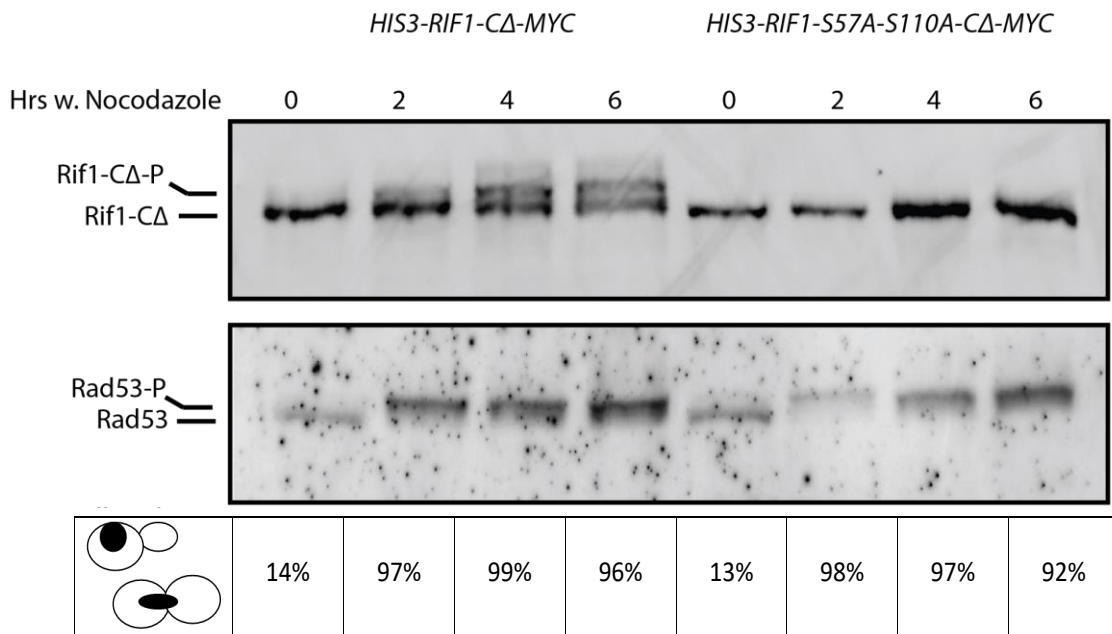
Finally, in the genotype *RIF1-110A-C Δ -MYC* there is again a shift in the migration of Rif1 protein. This occurred after 4 hours, and again at very low levels in comparison to the control. The shift, and levels of protein shifted, did not appear to change between 4 hours of exposure to nocodazole, and 6 hours. Again, the Rad53 phosphorylation of these cells was similar to that of the control strain, and the proportion of cells arrested in G2/M was also very similar (**Figure 3.6D**).

This data strongly indicates that these residues within the protein Rif1 are required for the phosphorylation of Rif1 in nocodazole. Interestingly, it appears that in nocodazole-induced arrest these residues may have equal importance for the phosphorylation of the protein.

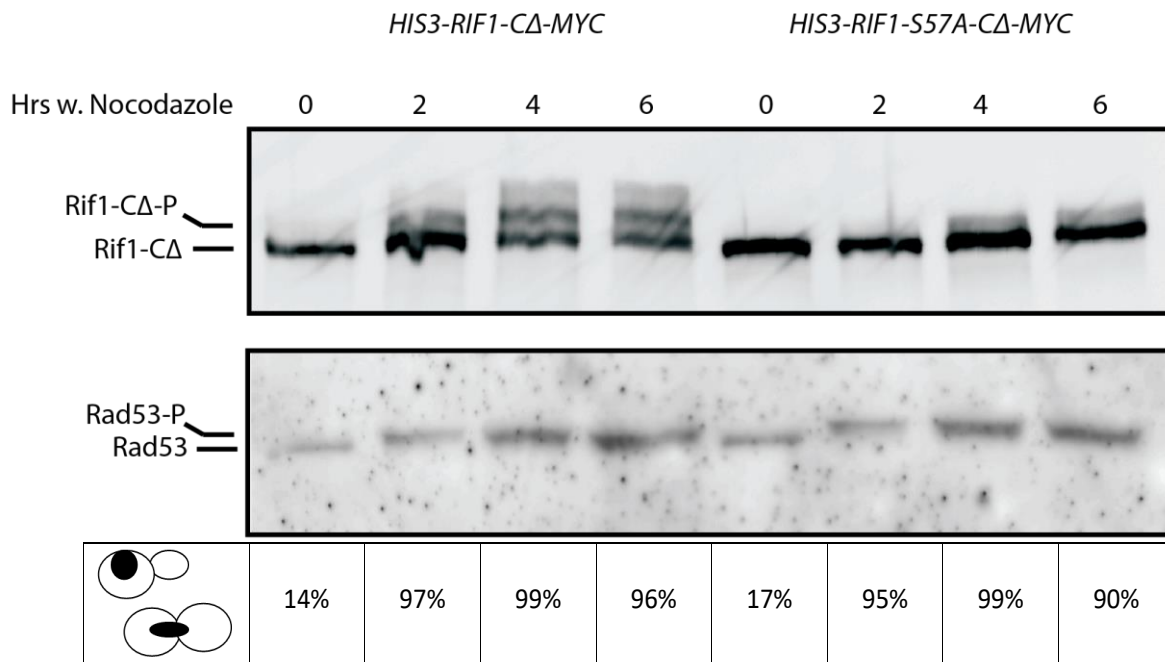
A



B



C



D

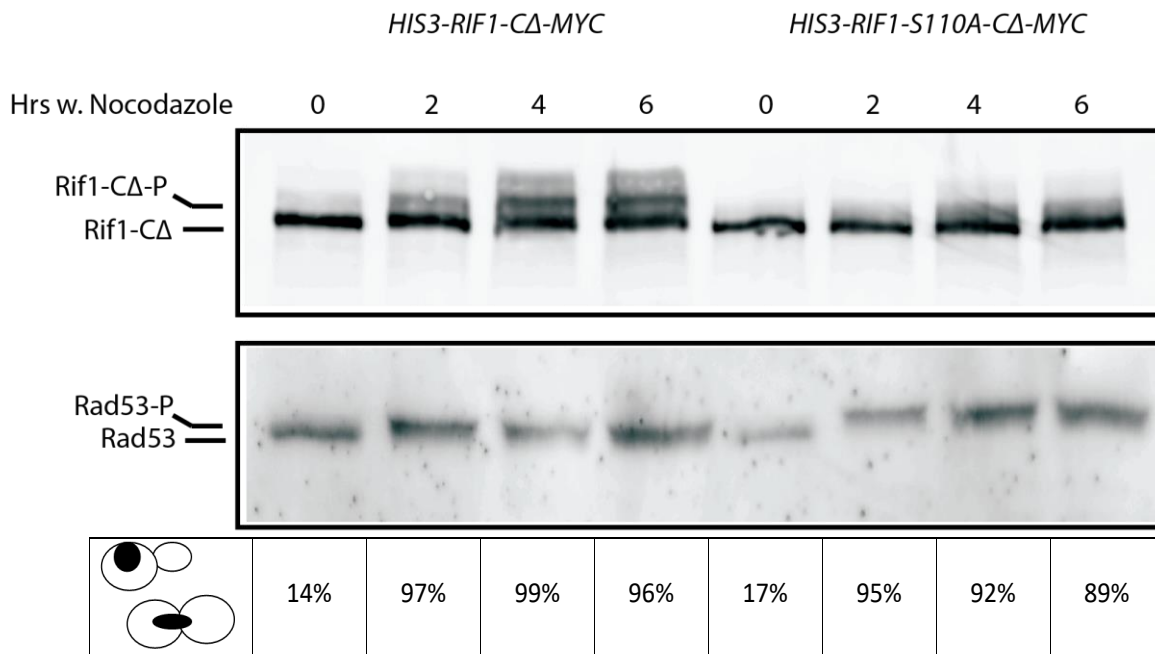


Figure 3.6 Substitution of residue Serine-57 and Serine-110 in Rif1 completely eliminates phosphorylation during spindle damage

(A) Western blot analysis of Rif1 and Rad53 protein taken from cells incubated overnight at 20°C (1×10^7 cells/mL at T0) which were then treated with nocodazole (15µg/mL) and incubated at 30°C for 4 hrs. Cell samples were also taken for DAPI treatment and analysis and cell cycle scoring via fluorescence microscopy. (B, C, D) Western blot analysis of Rif1 and Rad53 protein taken from cells incubated overnight at 20°C (1×10^7 cells/mL at T0) which were then treated with nocodazole (15µg/mL) and shifted to 30°C for 6 hrs, with cells harvested at 2 hr intervals. Cell samples were also taken for DAPI treatment and analysis and cell cycle scoring via fluorescence microscopy. Strains used here are; *RIF1-CΔ-MYC* (A, B, C, D), *RIF1-S57A-S110A-MYC* (A, B), *RIF1-S57A-MYC* (A, C), and *RIF1-S110A-MYC* (A, D).

3.7 The same S57, S110 residues of Rif1 are phosphorylated under other stresses

My data showed that the phosphorylation of Rif1 occurring during both telomere damage and spindle damage, was eliminated by the substitution of two amino acid residues; S57 and S110. Further to this our previous data has shown that Rif1 phosphorylation can also result during cell cycle arrest stemming from exposure to a range of genotoxic stresses, including; phleomycin, UV radiation, and hydroxyurea. From this the question raised was whether the phosphorylation event in Rif1 seen in exposure to these reagents, are all located within S57 and S110? To examine this, strains of the genotype *RIF1-S57A-S110A-CΔ-MYC* were to be exposed to these reagents and the cellular response studied.

Overnight inoculations of the double mutant *RIF1-S57A-S110A-CΔ-MYC* genotype, as well as the control strain of *RIF1-CΔ-MYC*, were grown up at 20°C. The control strain was then treated with nocodazole (15µg/mL) and incubated at 30°C for 4 hours. In contrast, the strain containing mutations of *RIF1* was split and underwent treatment with one of the 5 stresses; Nocodazole (15µg/mL), phleomycin (50µg/mL), UV radiation (30J/m²), Hydroxyurea (100mM), or MMS (0.05% w/v). These strains were then incubated at 30°C for 3 hours. For UV radiation treatment, cells were spun down and re-suspended briefly in PBS. They were then treated with radiation. After treatment they were re-suspended in YPD and incubated alongside other cultures for 3 hours.

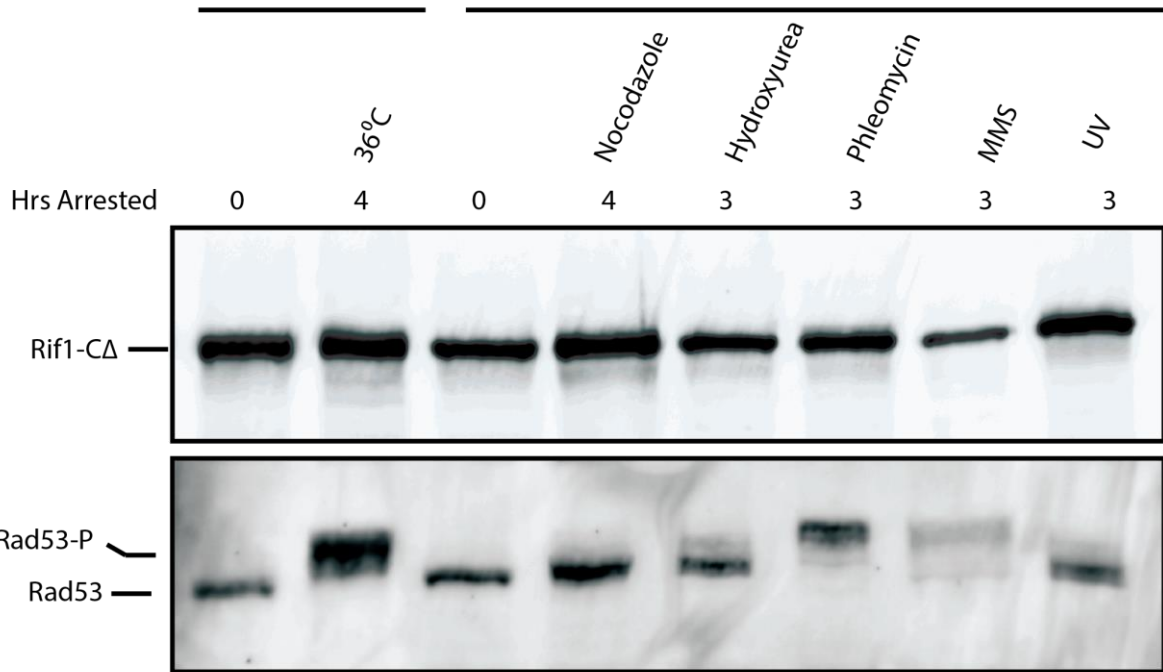
In the control samples of this experiment treatment with nocodazole led to phosphorylation of the Rif1 protein. Further to this there was a small shift in the migration of Rad53, indicating low levels of phosphorylation. These cells arrested during G2/M at a very high proportion after treatment.

In contrast, the phosphorylation of Rif1 was dramatically reduced by the mutation of residue S57 and S110. In these mutants there was no phosphorylation seen after any treatment, this was in opposition to results shown in previous experiments (**Figure 3.3**). Despite this, phosphorylation of Rad53 did not appear to be affected by the lack of phosphorylation in Rif1, nor does it appear to have affected the arrest of cells at G2/M, or S-phase after treatment with hydroxyurea (**Figure 3.7**).

This data supports previous data and suggests that the phosphorylation of Rif1 occurs entirely within the amino acid residues S57 and S110, regardless of the cause of cell cycle arrest that led to Rif1 phosphorylation.

cdc13-1 RIF1-S57A-S110AΔ-MYC

RIF1-S57A-S110A-Δ-MYC



	13%	97%	25%	96%	85%	96%	50%	68%
--	-----	-----	-----	-----	-----	-----	-----	-----

Figure 3.7 Substitution of serine-57 and serine-110 in Rif1 eliminates phosphorylation of Rif1 during cell cycle arrest resulting from a range of damaging reagents

Western blot analysis of Rif1 and Rad53 separated on 7% SDS-PAGE gels. Samples were gathered from cells grown overnight at 20°C (1×10^7 cells/mL at T0) before treatment with nocodazole (15µg/mL), phleomycin (50µg/mL), UV radiation (30J/m²), hydroxyurea (100mM), or MMS (0.05%). Cells were then incubated for 3-4 hrs before cell samples were harvested. Cells were also harvested for DAPI treatment and cell cycle scoring using fluorescence microscopy. A positive control of phosphorylation was used with *RIF1-CΔ-MYC* cells treated with nocodazole. All other samples were of the genotype *RIF1-S57A-S110A-CΔ-MYC*. Cells treated with UV were first resuspended in a low volume (~5mL) of PBS, treated using a stratalinker-3000, and then resuspended in fresh YPD before incubation at 30°C.

3.8 Discussion

In this chapter I confirmed the phosphorylation of Rif1 during telomere damage, and that this phosphorylation event may lie downstream of the activity of checkpoint kinases. Furthermore, I showed that this phosphorylation event is still seen after the deletion of the C-terminal domain of *RIF1*, a region previously shown not to influence the viability of *cdc13-1* cells at restrictive temperatures. This led to the closer study of the N-terminus of Rif1 in which I found that a small region, consisting of the first 176 residues of the protein, were crucial for the majority of Rif1 binding to the chromosome. My studies further indicated that the presence of this region improved the viability of *cdc13-1* cells at restrictive temperatures. Previous studies have suggested there are a number of potential phosphorylation sites within the Rif1, which are largely clustered within the N-terminal region and the C-terminal region (**Figure 3.9.1**). Together this data strongly indicated therefore that the phosphorylation sites relevant for this study were located in the N-terminal.

The locations of two key residues within Rif1 were determined, I found that residue S57 and S110 of the Rif1 protein appear to share the phosphorylation of Rif1. Of these, I also saw that S57 appears to be the more important residue of the two, as a single substitution of this residue saw a larger portion of Rif1 remain non-phosphorylated than in a single substitution of S110. It is interesting to note that these residues were not indicated as highly phosphorylated during a mass spectrometry study identifying phosphorylation during telomere uncapping in *yku70Δ* cells, nor was this region studied during the X-ray crystallography of Rif1 structure (Matarocci *et al.*, 2017; J. Wang *et al.*, 2018).

It was earlier acknowledged that many of the first mutations made in these cells substituted cysteine residues in place of serine. This is unusual, and the more standardly used residue to eliminate phosphorylated serine is alanine. This is due to the possibility of cysteine residues generating disulphide bridges between residues, the introduction of further cysteine residues into the proteins structure could therefore introduce new bridges and alter the tertiary structure of the protein. In later experiments these residues were instead substituted with alanine.

The question remaining from this data is what effect the loss of phosphorylation may have at a cellular level. If phosphorylation is a regulatory mechanism, as hypothesised, then this may act to positively or negatively regulate function. The *rif1-NΔ* serial dilutions and ChIP data shown, may suggest that loss of phosphorylation will lead to increased growth defects in *cdc13-1* cells and lower association with the chromosome. However, this mutant is

missing a key region of the protein with many globally conserved functions. It may be that the deletion of this phenotype has much more severe, or indeed contradictory phenotypes, to mutating the sites of phosphorylation alone.

Further to this, the results presented suggest that a number of different reagents can ultimately lead to the phosphorylation of Rif1, suggesting roles for Rif1 outside of telomere damage. Interestingly, this phosphorylation is not exclusive to cell cycle arrest resulting from direct DNA damage, as Rif1 also appears to be phosphorylated by treatment of cells with the spindle poison nocodazole.

An interesting question from this data is the role of Rif1 in these other forms of damage. The model proposed in Xue et al (2011) could feasibly be applicable to several of these conditions. For example, phleomycin and UV damage both lead to DSBs in the DNA of the chromosome. For the repair of these in the G2/M stage of the cell cycle homologous recombination will be favoured, using the duplicate chromosome as a template for high-fidelity repairs. It is possible that Rif1 activity in down regulating the checkpoint responses may play a role here, alternatively Rif1 may be rapidly phosphorylated in these scenarios to ensure that any free non-telomere bound Rif1 cannot interfere with the repair pathway. However, in the arrest resulting from nocodazole the role of Rif1 is more difficult to explain. This arrests from the spindle checkpoint pathway recognising the improper formation of spindle microtubules and does not require DNA damage for activation. The role of Rif1 in this, and the need for its phosphorylation, would not be explained by our existing model. This would be an interesting avenue of investigation for any future experiments, for instance it may be useful to determine if Rif1 association is enriched at kinetochores after treatment with nocodazole.

Chapter IV – Investigating the Kinases Leading to Rif1 Phosphorylation

4.1 Checkpoint kinases are upstream of Rif1 phosphorylation

Previously published data (Xue *et al.*, 2011) has demonstrated an anti-checkpoint role for the Rif1 protein during telomere damage. Further to this, I have demonstrated that during telomere damage and other conditions such as spindle damage, Rif1 becomes phosphorylated. To help determine the function of phosphorylation, I aimed to establish the kinase, or kinases, that may be upstream of this phosphorylation. Unpublished data (Maringele, unpublished) suggested that checkpoint kinases may play a role in the modification of Rif1 in *cdc13-1*. To investigate the roles of the checkpoint pathway in the phosphorylation of Rif1 the genes *RAD9*, *MEC1*, *RAD53*, *DUN1*, and *CHK1* were deleted from *cdc13-1* backgrounds to study the effect on Rif1 phosphorylation.

In the G2/M checkpoint arrest occurring from telomere uncapping in *cdc13-1* cells, the sensor kinase Mec1 is recruited to ssDNA. This in turn recruits and activates the transducer kinase Rad9, which activates separate pathways to arrest the cell cycle via the effector kinases Rad53 and Chk1. Dun1 is downstream of Rad53 activity. Therefore, deletion of *MEC1* and *RAD9* will eliminate activation of the effector kinases required for arrest. In *cdc13-1*, activation of Rad53 is seen to be more important for the arrest of the cell cycle than the activity of Chk1 (Sanchez *et al.*, 1999).

To confirm the role of DNA damage checkpoint proteins, or cell cycle arrest, in Rif1 phosphorylation logarithmic phase cultures of checkpoint-proficient and checkpoint-defective *cdc13-1 RIF1-CΔ-MYC* strains were shifted to the restrictive temperature of 36°C and samples collected every two hours. These samples were analysed for Rif1 and Rad53 phosphorylation by Western Blot. In the *cdc13-1 RIF1-CΔ-MYC* control, Rif1 protein became slightly phosphorylated after 2 hours (T2) incubation at 36°C, and by 4 hours (T4) there was a clear slower migrating protein form, indicating phosphorylation. This was maintained through to the samples taken after 6 hours. A similar pattern of phosphorylation in Rad53 protein was also seen in these strains, with phosphorylation occurring after 2 hours and peaking at T4 and T6 (**Figure 4.1 A-E**).

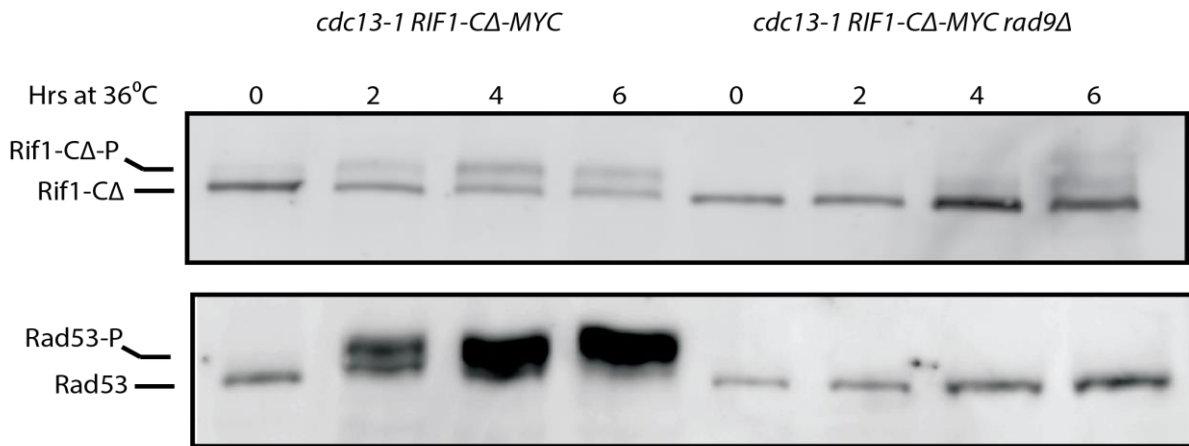
In *cdc13-1 rad9Δ* the phosphorylation of both Rif1 and Rad53 was lost at all time-points (**Figure 4.1A**). Moreover, this same pattern was seen in *cdc13-1 mec1Δ sml1Δ* for both Rif1 and Rad53 (**Figure 4.1.B**) and was seen for Rif1 in *cdc13-1 rad53Δ sml1Δ* cells, although as would be expected there was no protein signal for Rad53 in these samples (**Figure 4.1C**).

Interestingly, in *cdc13-1 dun1Δ* there appeared to be a low level of phosphorylation of Rif1 protein. At after 2, 4, and 6 hours there appears to be a low signal corresponding to the phosphorylated form of Rif1. However, compared to the control strain in this experiment there appeared to be a larger quotient of the non-phosphorylated form of the protein present in these samples. Furthermore, Rad53 phosphorylation is seen to be strong in this genotype (**Figure 4.1D**).

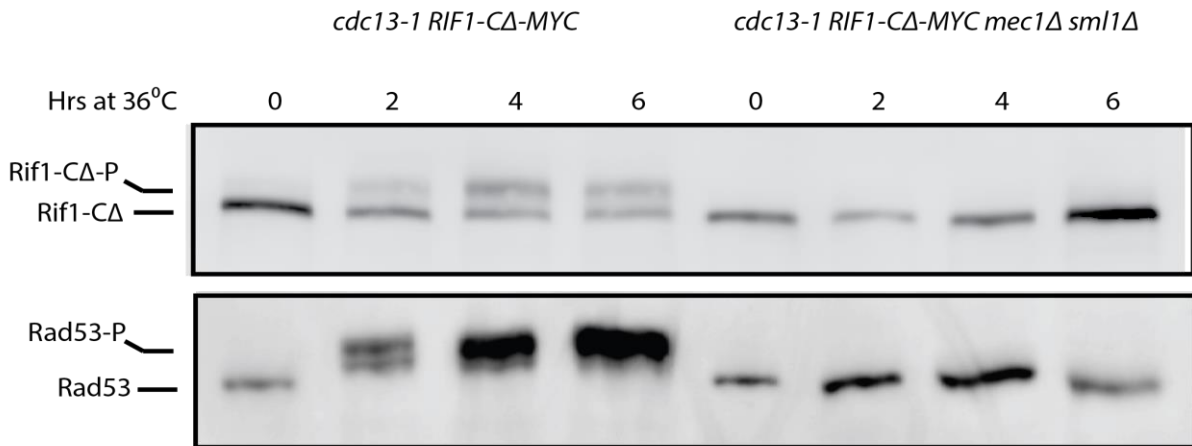
In contrast to this, in *cdc13-1 chk1Δ* Rif1 phosphorylation was strong and appeared to be full and similar to the control samples. In this strain Rad53 protein was seen to be fully phosphorylated (**Figure 4.1E**).

The results of these experiments suggest that the activity of Chk1 has little role in Rif1 phosphorylation, and that Dun1 may be partially involved but not essential. However, these results may suggest that Rad9, Mec1, and Rad53 are necessary for the phosphorylation of Rif1 during telomere damage. However, as Chk1 and Dun1 are not crucial for arrest in *cdc13-1* cells, it may also be that the resulting arrest is the most important factor in Rif1 phosphorylation.

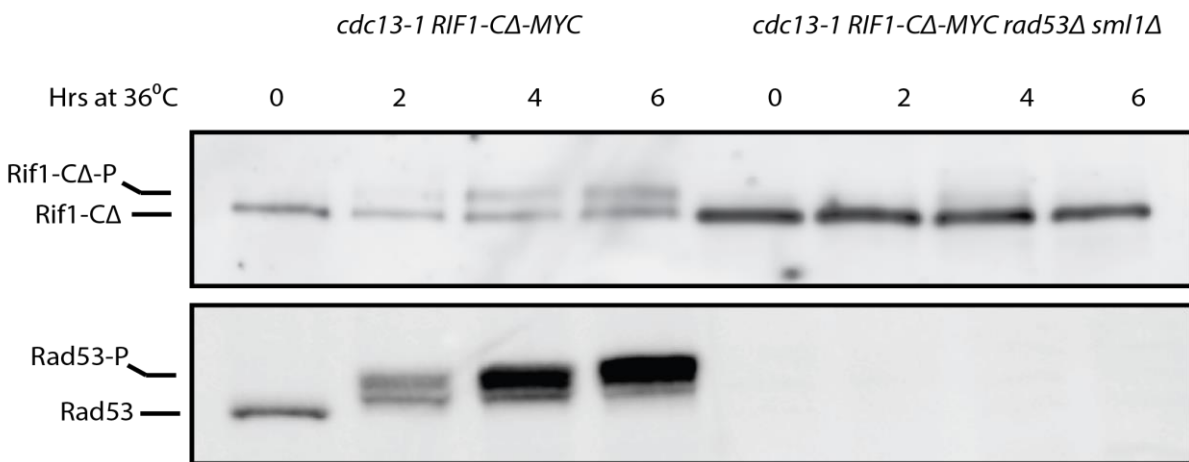
A



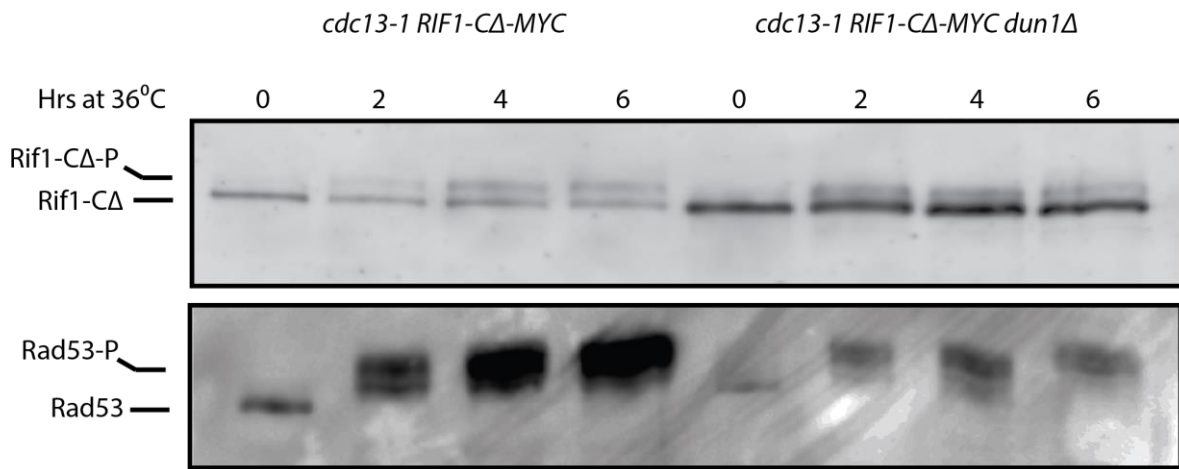
B



C



D



E

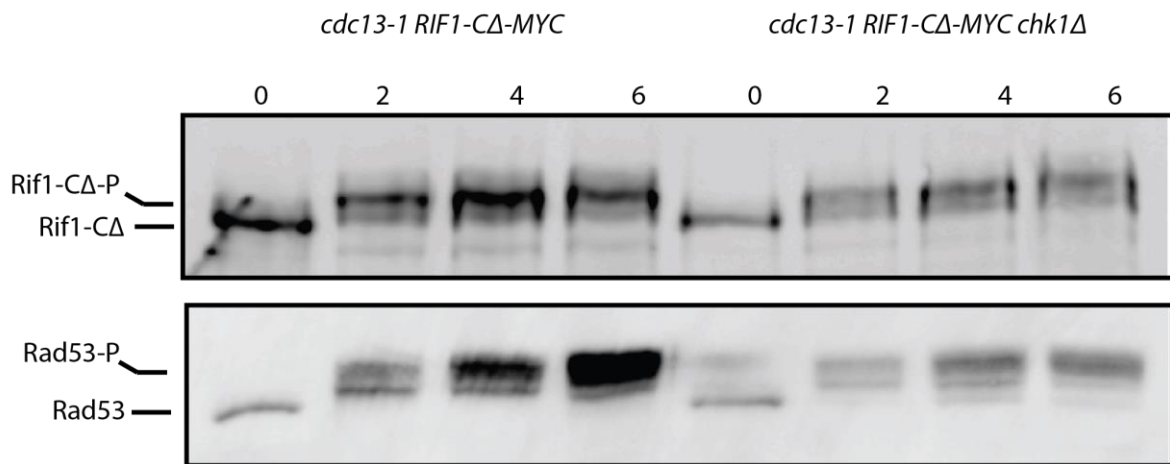


Figure 4.1.1 Rif1 Phosphorylation is eliminated by Removal of DNA damage checkpoint proteins

Western blot showing Rif1 phosphorylation in *cdc13-1* cells after growth overnight at 20°C to low cell concentration (T0 – 1×10^7 cells/mL) and shifted to 36°C for 6hrs, as compared to *cdc13-1* cells also containing deletions of the DNA damage checkpoint; *mec1Δ* (A) *rad9Δ* (B), *rad53Δ* (C), *dun1Δ* (D), or *chk1Δ* (E). After each cell harvest strains containing deletions of the checkpoint pathway were diluted 1:1 with fresh YPD pre-warmed to 36°C.

4.2 Spindle checkpoint proteins are necessary for Rif1 phosphorylation in nocodazole-induced arrest

In studying the regulation of Rif1 activity, previous data shown in **Chapter 3** demonstrated that the telomere damage in *cdc13-1* is not the only condition in which Rif1 protein is phosphorylated. As I had previously seen that Rif1 was phosphorylated during nocodazole-induced arrest, I instead investigated whether components of the SAC were upstream of the phosphorylation.

My results this far had suggested Rad53 as a core kinase upstream of Rif1 phosphorylation in *cdc13-1*, and that deletion of *RAD9*, *MEC1*, or *RAD53*, could all eliminate the phosphorylation of Rif1. I therefore studied the effect of nocodazole treatment on cells in which the DDR had been compromised. To do this, cell cultures experiments were repeated as before in **Chapter 4.1** but with the addition of nocodazole (15µg/mL) dissolved in DMSO as cultures were shifted to 36°C. Overnight cultures were supplemented with DMSO to a final volume of 1%, to control for the addition of the DMSO containing nocodazole at T0. Nocodazole treatment arrests the cell cycle in the checkpoint-defective cells rather than allowing continued proliferation during the time-course.

In the control strain low levels of phosphorylation occurred after two hours. By 4 hours this became more distinct and was at a similar level after 6 hours. Over this time, an accumulation of cells in the G2/M transition of the cell cycle was seen. Interestingly, a similar pattern in *cdc13-1 mec1Δ sml1Δ* cells was also seen. The slower migrating phosphorylated Rif1 became visible after 2 hours, but grew stronger through after 4 and 6 hours, cell scoring also showed that these cells are also accumulated in G2/M (**Figure 4.2.1A**).

I carried out the same experiment using a strain of the genotype *cdc13-1 rad9Δ*, again alongside a *cdc13-1* control, which behaved as expected. The *rad9Δ* mutant also showed strong phosphorylation of Rif1 after 4 hours, which was maintained after 6 hours. In both these strains an accumulation of cells in the G2/M transition was seen, indicating an arrest due to the action of nocodazole (**Figure 4.2.1B**).

These results indicated that these cells arrest in nocodazole and Rif1 becomes phosphorylated, despite the absence of a functional DNA checkpoint.

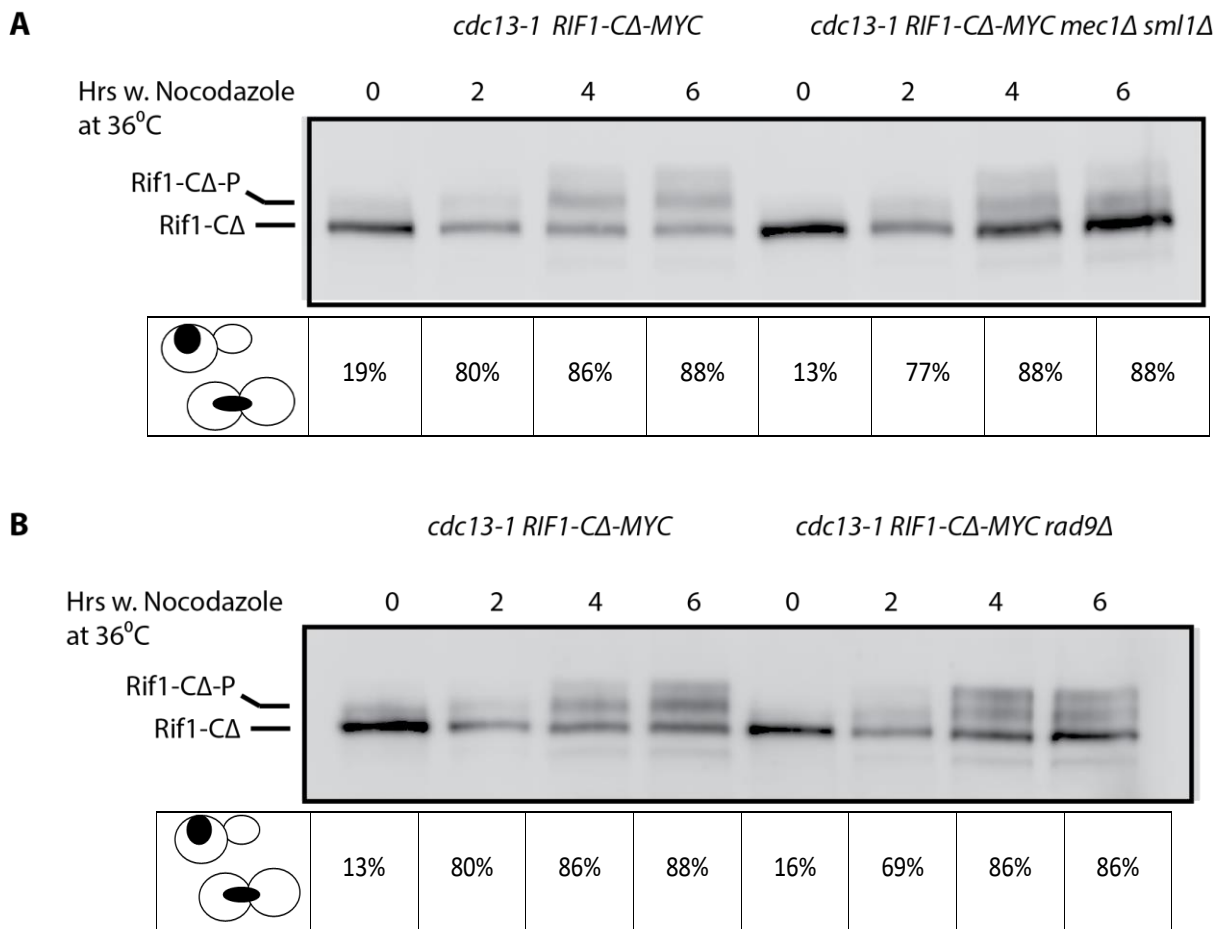


Figure 4.2.1 Rif1 is phosphorylated by Nocodazole induced arrest, independent of DNA damage checkpoint pathways.

Western blot using protein samples from overnight cultures grown at 20°C to a concentration of 1×10^7 cells/mL, cultures were diluted 1:1 with fresh YPD. **(A)** Samples taken from *cdc13-1* and *cdc13-1 mec1Δ sml1Δ* strains grown O/N and shifted to 36°C in the presence of nocodazole (15µg/mL), with membranes probed for Rif1-MYC. **(B)** Samples taken from *cdc13-1* and *cdc13-1 rad9Δ* strains shifted to 36°C in the presence of nocodazole, with membranes probed for Rif1-MYC. Cell samples were taken at each timepoint and treated with DAPI to assess stage in cell cycle via fluorescent microscopy. The percentage of cells in G2/M (the expected point of arrest) is displayed below the corresponding protein sample.

The phosphorylation of Rif1 in the presence of nocodazole, despite the deletions within the DNA damage checkpoint pathway, indicated that the kinase directly upstream of Rif1 phosphorylation was not Rad53. During mitosis, the proper splitting of genetic material between daughter cells is regulated in part by the spindle checkpoint pathway, which ensures proper spindle formation and attachment to chromosomes before mitosis is allowed to progress. As nocodazole is a spindle poison I therefore investigated if the spindle checkpoint may be responsible for the phosphorylation of Rif1.

In this experiment I used cells containing deletions in genes encoding core proteins from the SAC pathway. T0 samples were taken directly from overnight cultures grown at 20°C, cells were then treated with nocodazole and incubated at 30°C for 6 hours, with samples taken every two hours. Cell samples were also taken for cell cycle scoring. The control strain used in this experiment was a *CDC13 RIF1-CΔ-MYC* genotype.

During the 6 hours in nocodazole the control became phosphorylated after 2 hours. An increasing proportion of Rif1 became phosphorylated after 4 & 6 hours. In these samples very low levels of Rad53 phosphorylation began to occur after 2 hours, however this did not increase further. Over this time-course there was an accumulation of cells in the G2/M phase of the cell cycle, as would be expected during a nocodazole-induced arrest of cell cycle progression.

In contrast, a strain containing the mutation *bub1Δ* did not show phosphorylation of Rif1 at any time-point studied. Furthermore, in these cells a lower proportion accumulated in the G2/M transition. This is due to *BUB1* encoding a major protein in the spindle checkpoint, which is inactivated in these mutants. Although it is noticeable there was still a high fraction of cells accumulating in G2/M (65% after 4 hours). When observing Rad53 in these samples there does not appear to be any phosphorylation after 2 hours, unlike the low level in the control (**Figure 4.2.2A**).

The loss of phosphorylation is also seen in cells containing the mutation *mad3Δ*. A strain missing another core member of the SAC pathway. It was seen that in these cells there was no phosphorylation of Rif1 at any time-point after treatment with nocodazole. Neither was there any phosphorylation of the Rad53 protein after the addition of nocodazole to the culture. This is in contrast to the slight change in protein migration seen for Rad53 in the control strain after 2 hours. It is noticeable however, that in *mad3Δ* cells there was still high accumulation of cells in the G2/M phase of the cell cycle (**Figure 4.2.2B**).

The data from these two experiments indicates that the spindle checkpoint pathway is required for Rif1 phosphorylation in cells treated with nocodazole. The low phosphorylation of Rad53 may also suggest that the Rif1 phosphorylation seen here was largely independent from the DNA damage checkpoint pathway.

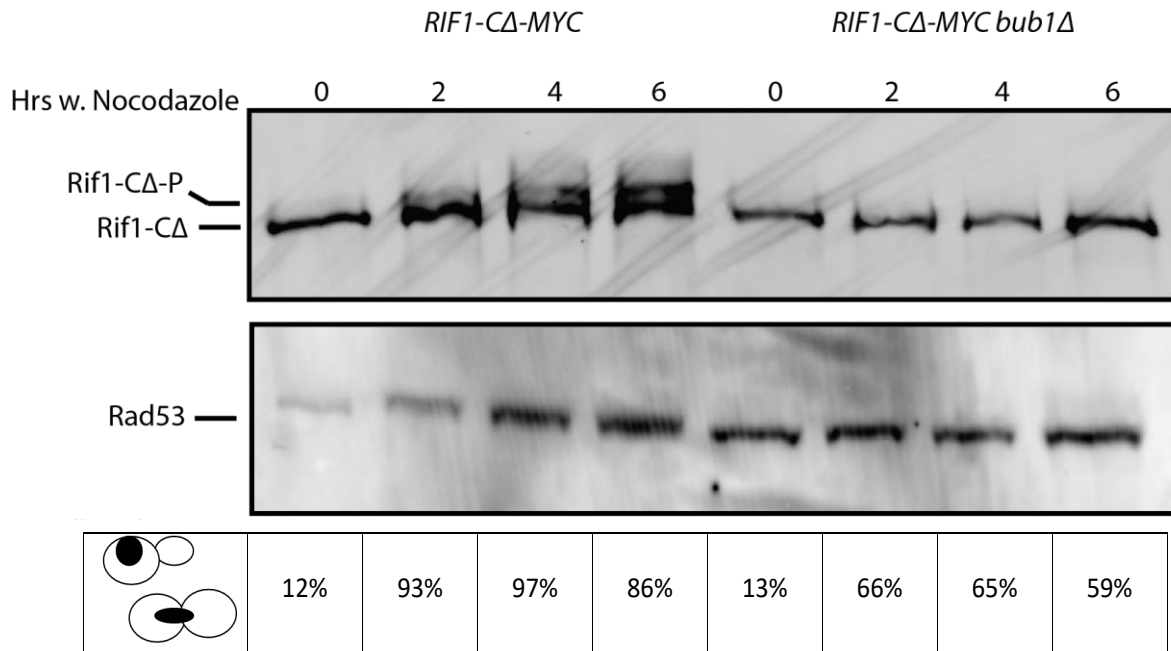
To further investigate the presence of independent pathways leading to the phosphorylation of Rif1, I examined the response spindle checkpoint-deficient mutants after the introduction of the *cdc13-1* allele. The control strain of these experiments were the *CDC13 RIF1-CΔ-MYC bub1Δ* OR *mad3Δ* strains studied in the previous experiment. Strains were again treated with nocodazole and shifted to 30°C.

It can be clearly seen that the *CDC13 RIF1-CΔ-MYC bub1Δ* control behaved as expected, with neither Rif1 nor Rad53 becoming phosphorylated across a six-hour time-course. Interestingly, when this mutation is coupled with the allele *cdc13-1* strong phosphorylation of Rif1 was seen after 2 hours, which was also seen in samples taken after both 4, and 6 hours. This was the same when examining the protein Rad53 in these samples. It is also noteworthy that these cells arrested strongly in G2/M (**Figure 4.2.2C**).

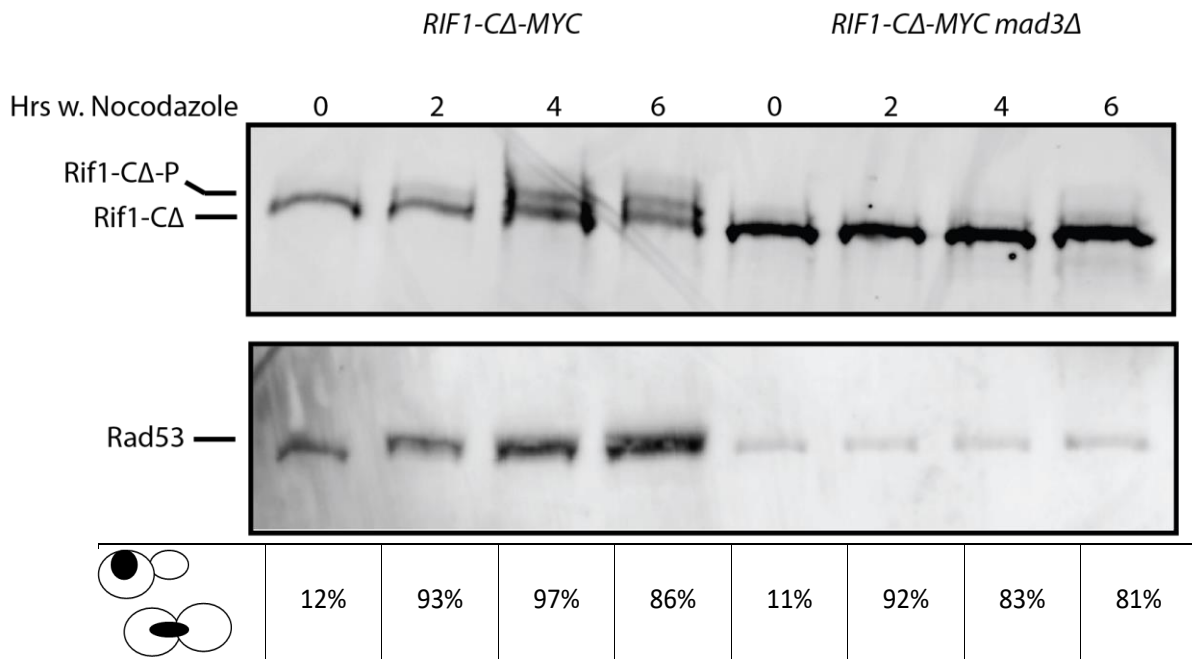
Further to this, a similar result can be seen in *cdc13-1 RIF1-CΔ-MYC mad3Δ* cells. In the control strain neither nocodazole treatment nor incubation at high temperature led to the phosphorylation of Rif1 or Rad53 protein. However, in those strains also containing the allele *cdc13-1* both Rif1 and Rad53 were rapidly phosphorylated, with a strong band of phosphorylated protein becoming visible after 2 hours. These cells were also highly arrested at the G2/M phase (**Figure 4.2.2D**).

These results would both strongly suggest that the SAC is required for Rif1 phosphorylation in nocodazole-induced arrest, much like how the DNA damage checkpoint pathway is required for Rif1 phosphorylation in *cdc13-1* cells. This indicates the key factor for Rif1 phosphorylation may be the arrest of the cell cycle in G2/M phase, suggesting that a kinase involved in the G2/M arrest/progression may be responsible for Rif1 phosphorylation.

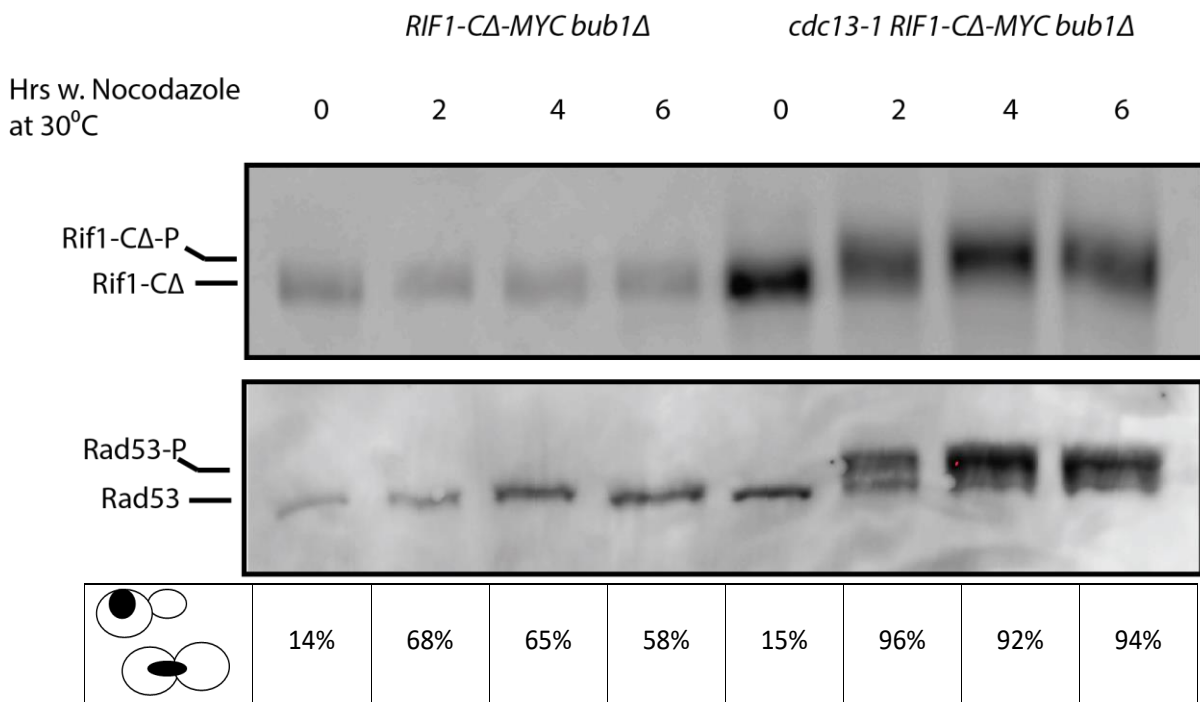
A



B



C



D

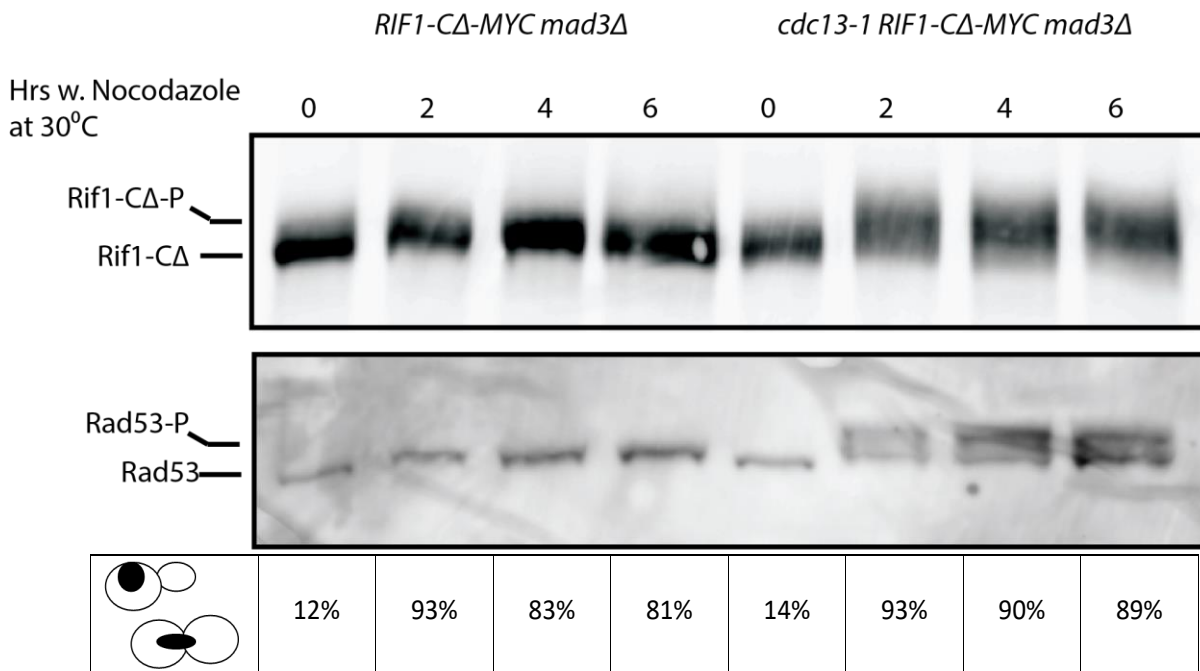


Figure 4.2.2 Rif1 Phosphorylation Is the Result of Independent Activation of the DNA Damage Checkpoint or the Spindle Assembly Checkpoint.

Western blot using protein samples from cultures grown overnight at 20°C to a concentration of 1×10^7 cells/mL. T0 samples were taken directly from these overnight cultures, which were diluted 1:1 with fresh YPD before treatment. Cells were shifted to 30°C with the addition of Nocodazole (15µg/mL), using strains *bub1Δ* (A), *mad3Δ* (B), *cdc13-1 bub1Δ* (C) and *cdc13-1 mad3Δ* (D) targeting the proteins Rif-CΔ and Rad53. Cell samples were also taken for DAPI treatment, and cell scoring by fluorescence microscopy.

4.3 Cdc28 (Cdk1) is upstream of Rif1 phosphorylation during *cdc13-1* dependent DNA damage.

Data in **Chapter 3** showed that the phosphorylation of Rif1 can be induced by numerous genotoxic stresses upon the cell. Furthermore, results shown in this chapter suggested the separate pathways were required for Rif1 phosphorylation. This implied one of two scenarios. The first of these was that the phosphorylation events seen in arrest resulting from various stresses were separate events, controlled by different kinases in each pathway. The second explanation was that there may be a single kinase controlling Rif1 phosphorylation that is highly active during G2/M.

In *S. cerevisiae* there are 5 major CDKs, of these Cdk1, in yeast the protein also referred to as Cdc28, is the core CDK for regulation and progression of the cell cycle. Cdk1 has previously been observed to phosphorylate Rif1 during DNA replication, and is known to be a key kinase in driving progression through G2/M (Davé *et al.*, 2014; S. Hiraga *et al.*, 2014). As such, I questioned whether Rif1 may be one of these factors that is phosphorylated in an extended G2/M arrest by the activity of Cdc28. Upon examination of Rif1 there are 11 sites which could function as the minimum core “SP” target site for Cdc28 activity, of which 8 have been identified as likely phosphorylated residues by previous studies, and there are 6 sites which could function as the core (TP) target site, only one of which has been previously by previous studies (**Figure 4.3.2A**)(Nigg, 1993; L. J. Holt *et al.*, 2009; D. L. Swaney *et al.*, 2013). Furthermore, the phosphorylated sites identified in the previous chapter would meet the criteria for the minimum sequence required for recognition by Cdc28.

In the following experiments I utilised the mutant allele *cdc28-as1*. This allele encodes a protein with an enlarged ATP-binding pocket which allows it to bind the non-hydrolysable ATP-analogue 1-NM-PP1. Treatment of cells with 1-NM-PP1 rapidly and specifically down-regulates the activity of Cdc28, with only a small reduction in Cdc28 activity in the absence of the inhibitor (Bishop *et al.*, 2000).

A culture of *cdc13-1 cdc28-as1 RIF1-C1-MYC* was grown at 20°C overnight to T0. This culture was then split, and one of the two cultures was then treated with addition of the Cdc28-as1 inhibitor, and both cultures were incubated for 6 hours at 36°C with samples taken every 2 hours. The control in this experiment was therefore the culture that remained untreated.

Without the inhibitor treatment Rif1 underwent phosphorylation, as would be expected of a *cdc13-1* strain. This phosphorylation could not be seen after 2 hours, but had become clearly

visible in samples taken after 4 hours. When examining Rad53 protein in these strains a similar pattern was seen; at 2 hours there was very little visible phosphorylation of Rad53, however, after 4 and 6 hours the protein was clearly phosphorylated. The treated samples in this experiment, however, differed greatly. After treatment with the inhibitory molecule Rif1 phosphorylation was greatly reduced. After 2 or 4 hours there was no phosphorylation of Rif1, however, after 6 hours there appeared to be some low levels of phosphorylated Rif1. At 4 hours, when Rad53 phosphorylation has become strong in the control, the treated cells show much lower phosphorylation of Rad53. This trend continues after 6 hours, whilst Rad53 phosphorylation has become stronger in these strains after 6 hours, it does not reach the level of phosphorylation seen in control strains samples taken at 4 hours.

From these results it appears that Cdc28 is indeed required for phosphorylation of Rif1. Interestingly, it is known that the activity of Cdc28 is required for control of Exo1 and Sae2 resection to promote HR pathway choice during DNA repair in S/G2, studies have also demonstrated a role in the DDR (Huertas *et al.*, 2008; Tomimatsu *et al.*, 2014).

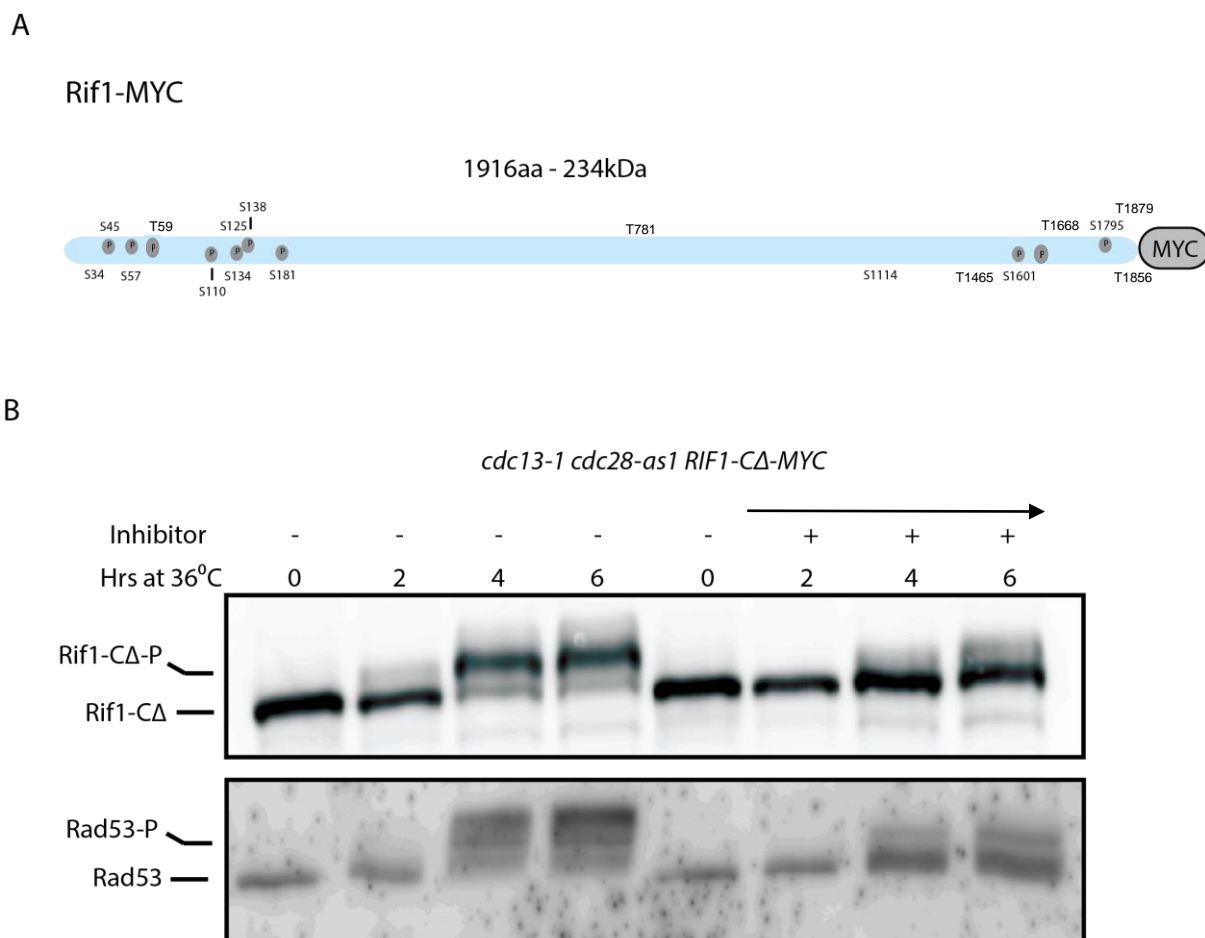


Figure 4.3.1 Rif1 is Likely to be a Target of the Yeast Cdk1 Protein, Cdc28

(A) A schematic of the Rif1 protein showing the location of all “S/T-P” residue sequences that constitute the minimum required target recognition sequence for Cdc28 kinase. Circular icons indicate those sites which have been identified as potential sites of phosphorylation by previous studies. (B) Western blot indicating the phosphorylation of Rif1 & Rad53. Samples were taken from a single overnight culture grown at 20°C to 1x10⁷ cells/mL. T0 samples were taken and this culture was split in two and the NM-1-PP1 (500mM) inhibitor was added to one of these, mock treatment of 0.5% (v/v) DMSO. The cultures were shifted to 36°C for 6hours, with samples taken at 2-hour intervals.

In previous experiments in *cdc13-1* cells I have shown that Rad53 may have been upstream of Rif1, or at least that the cell cycle arrest downstream of Rad53 was required. As such the small increase in Rif1 phosphorylation after 6 hours, shown in **Figure 4.3.1B**, may be the result of a delayed phosphorylation of Rad53 and activation of the checkpoint pathway due to the inhibitor molecule losing efficacy. The experiment was redesigned to allow the DNA damage checkpoint in *cdc13-1* to activate and arrest the cell cycle prior to inhibition of Cdc28.

For this experiment, an overnight culture of *cdc13-1 cdc28-as1 RIF1-CA-MYC* was grown and was then split in two and T0 samples were taken. These two cultures were then incubated at 36°C for 6 hours, with samples taken every 2 hours. However, in these experiments the inhibitor was only added to one of these two cultures after the induction of the G2/M arrest, at either 2, or 4 hours post temperature shift. The control culture was left untreated.

In the control cultures for this experiment phosphorylation of Rif1 was strong after two hours at 36°C. After four hours there was even less of the non-phosphorylated form of Rif1 present in these samples. At all time-points from 2 hours onwards, strong phosphorylation of Rad53 was seen. When assessing these cells by cell scoring, there was a substantial accumulation of cells in G2/M phase

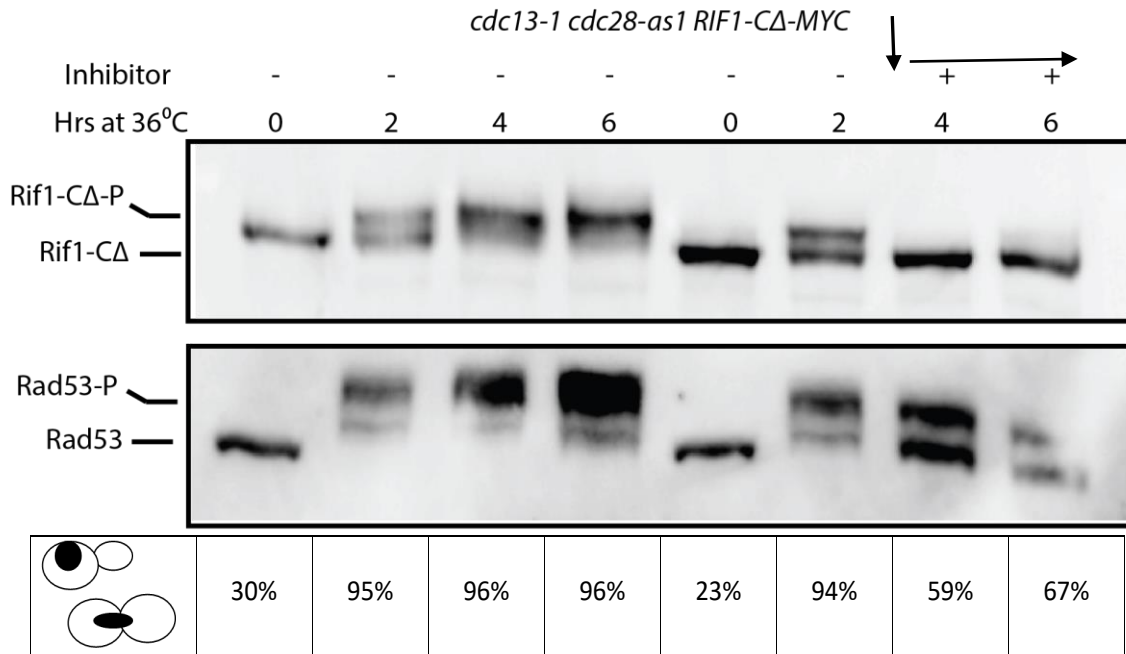
When examining the samples from cells treated with inhibitor there was also phosphorylation of Rif1 after 2 hours. However, after the inhibitor molecule is added to the culture, there was a complete loss of Rif1 phosphorylation. In samples where the inhibitor was added at 2 hours, the samples taken after 4 and 6 hours did not contain the phosphorylated form of Rif1. Furthermore, pattern of phosphorylation of Rad53 was very similar the control, seen at all time-points after incubation at 36°C. However, after the inhibition of Cdc28 the proportion of cells in the G2/M transition dropped at T4, although it did begin to climb again at T6 and at both time-points there was still a disproportionate number of cells in the G2/M stage than would have been expected in non-synchronised freely dividing cells (**Figure 4.3.2A**).

The samples taken from a culture where the inhibitor was added after 4 hours showed similar results. After 2 and 4 hours Rif1 and Rad53 became phosphorylated, similar to the controls. However, after the addition of the inhibitor at 5 hours the band of phosphorylated Rif1 completely disappeared, leaving only a single faster migrating band. When examining Rad53 in this strain it appeared unaffected by the addition of the inhibitor and remained

phosphorylated. Interestingly, in this experiment there was only a small drop in the proportion of cells arrested in G2/M between T4 and T6, when Cdc28 inhibitor was added to the culture (**Figure 4.3.2B**).

The data here provides clear evidence that Cdc28 is upstream of Rif1 phosphorylation. This may suggest that the role of the DNA damage and spindle assembly checkpoint pathways, in relation to Rif1 phosphorylation, were to arrest the cell cycle in G2/M. This in turn induces higher levels of Cdc28 activity, which phosphorylates Rif1. Interestingly, it can be seen that the inhibition of Cdc28 led to the disappearance of existing phosphorylated Rif1. The rapid disappearance of the phosphorylated form of Rif1 may suggest this is a dynamic event which requires Cdc28 activity in order to be maintained. This would further suggest the existence of a phosphatase counteracting Cdc28 activity and dephosphorylating Rif1.

A



B

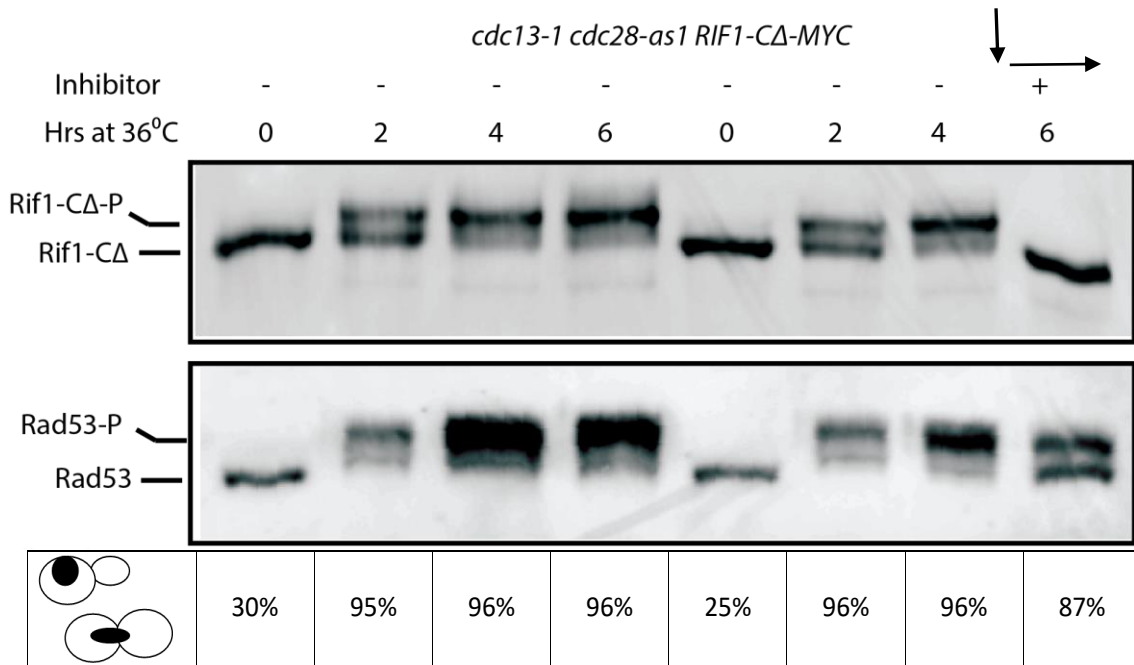


Figure 4.3.2 Rif1 Phosphorylation is Rapidly Lost after the Inhibition of Cdc28

Western blots showing Rif1 & Rad53 from yeast strains with the mutant alleles *cdc13-1* and *cdc28-as1*. Samples for each were taken from single overnight cultures grown at 20°C to 1×10^7 cells/mL, which were split in two and shifted to 36°C. NM-1-PP1 inhibitor (500mM final conc.) was added to one of the two resulting cultures either after 2hrs (**A**) or after 4hrs (**B**). Cells were harvested every two hours; samples were also taken for DAPI treatment and cell cycle scoring via fluorescence microscopy.

4.4 Discussion

In this chapter I aimed to determine the factors that lead to the phosphorylation of Rif1; this included both the pathways leading to it, and the kinase, or kinases, which may directly interact with Rif1. This aspect of my study began with the examination of Rif1 phosphorylation in *cdc13-1* cells undergoing telomere capping.

The primary conclusion from the data in this chapter is the importance of G2/M arrest in the phosphorylation of Rif1. In *cdc13-1* cells with defective DNA damage checkpoint pathways, the phosphorylation of Rif1 is lost. However, arrest of cells with nocodazole also led to a phosphorylation of Rif1. This suggested that Rif1 phosphorylation may not be a direct result of the pathways activated, but an outcome of G2/M arrest, which was lost due to the defects in arrest in checkpoint-defective mutants.

The high activity of Cdk1 in G2/M and its importance in mitotic progression, as well as the known interaction between Cdk1 and Rif1 in replication and a number of potential Cdk1 consensus sites in Rif1, led to the consideration of Cdc28 as the kinase directly upstream of Rif1 phosphorylation. The inhibition of this kinase in the presence of DNA damage, and ongoing G2/M arrest, demonstrated that it appears to be responsible for the phosphorylation of Rif1. It is also of interest to note that Cdk1 phosphorylation of Exo1 and Sae2 has previously been seen to control the resection of DSBs in yeast, to control repair pathway choice in S/G2. Rif1 and Cdk1 have both been seen to be involved with repair pathway choice in mammalian cells (Aylon *et al.*, 2004; Silverman *et al.*, 2004; Huertas *et al.*, 2008; Tomimatsu *et al.*, 2014).

Furthermore, the loss of this kinase also leads to the loss of the phosphorylation of Rif1, suggesting a counteracting phosphatase. This may indicate that Rif1 phosphorylation is carefully mediated during G2/M arrest, and the identification of this phosphatase may be an interesting avenue for future study. One candidate may be Cdc14, a phosphatase with an important role in mitotic progression and previously identified interactions with Rif1 (Breitkreutz *et al.*, 2010; MacGilvray *et al.*, 2018).

Chapter V: The phenotypic effects of Rif1 phosphorylation

5.1 Investigating the effect of non-phosphorylated Rif1 on the survival of *cdc13-1* at restrictive temperature

Previously published data led to the conclusion that Rif1 protein acted as a molecular shield, covering ssDNA and protecting it from recognition by DNA damage proteins (Xue et al 2011). This can be seen in the growth of *cdc13-1* at restrictive temperatures. *cdc13-1 rif1* Δ strains show reduced viability, whereas strains with overexpression of *RIF1* show improved viability. My study hypothesised that phosphorylation of Rif1 may be a key control mechanism regulating activity, to properly balance an anti-checkpoint function with the need for extensive damage to be repaired. With the data shown so far, the question remained to be answered; how does the mutation of S57 and S110 affect the growth phenotype of *cdc13-1* cells, and therefore the role of Rif1 as an anti-checkpoint protein?

This experiment used serial dilutions of yeast cultures to compare the growth of *cdc13-1* strains at a range of temperatures. Whilst the primary question was the effect of phosphorylation on Rif1 function, it was also necessary to determine whether the introduction of the *HIS3* marker interfered with Rif1 function. This marker was introduced during mutagenesis and lies upstream of the Rif1 gene, as such it may affect the promoter and expression of *RIF1* (**Figure 5.1.1A**). In this experiment strains containing the *HIS3* marker were compared to the growth of a WT strain as well as multiple *cdc13-1* variants including; *rif1* Δ , *RIF1*, *RIF1-MYC*, and *RIF1-C Δ -MYC*. WT grew at all temperatures as expected, whereas the *cdc13-1* strains including *RIF1*, *RIF1-MYC*, or *RIF1-C Δ -MYC* all began to show reduced growth at 26°C, with sickness increased further at 27°C. By 30°C these strains showed no growth. In contrast, *cdc13-1 rif1* Δ strains already show no growth at 26°C. The strains containing the *HIS3* marker (indicated as *) grew similarly to one another and did show a small difference to Rif1 under its own promoter, however, they also showed better growth compared to *rif1* Δ . This indicates that Rif1 is largely functional in these strains, and sufficiently expressed (**Figure 5.1.1A**). This experiment verified that the introduction of the marker in our mutants may introduce an increase in temperature sensitivity which should be accounted for when studying the growth of these strains and the effect of the mutation within *RIF1*.

Another serial dilution was then carried out to study the effect of amino acid substitutions with Rif1 on the growth of *cdc13-1*. For this the **RIF1* cells were used as a control to ensure

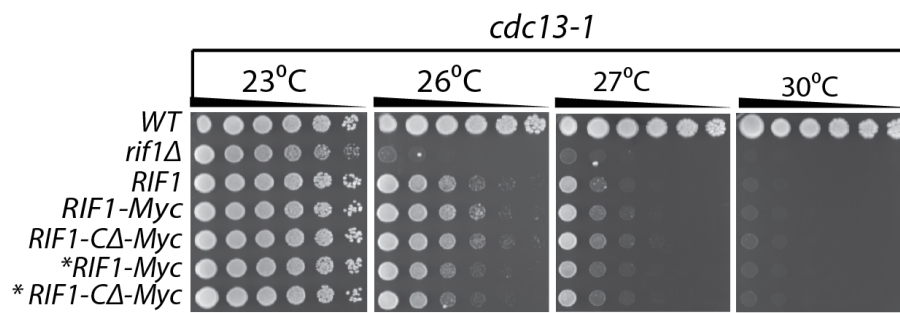
any differences were due to the substitution alone, and not effect on expression. Mutations were studied both in strains with the full length *RIF1* genotype, and the *RIF1-C Δ* variant.

RIF1-C Δ* cells began to see reduced growth at 26°C, and grew poorly at 27°C. By 30°C no growth was seen, as expected. The growth seen in all mutant strains is somewhat improved over the control strains. In the double mutant, **RIF1-C Δ -S57A-S110A*, improved growth was seen at both 26°C, and 27°C. In these mutants, growth was largely unaffected by temperature at 26°C and these cells appeared to grow moderately at 27°C. Interestingly, strains containing a substitution of only S57 displayed similar growth to those the double mutants, however at 27°C it appeared the S57 substituted cells may have been slightly more temperature sensitive. In contrast, those strains with a substitution of S110A did see improved growth over the control strain, however not to the extent of the double mutants or even substitution of only S57. At both 26°C and 27°C the temperature sensitivity of **RIF1-C Δ -S110A* was seen to cause intermediate growth between the control strains and the **RIF1-C Δ -S57A*, or **RIF1-C Δ -S57A-S110A*, mutants. This pattern is also true for cells containing mutations in the full length *RIF1* gene (Figure 5.1.1B**).

A



B



C

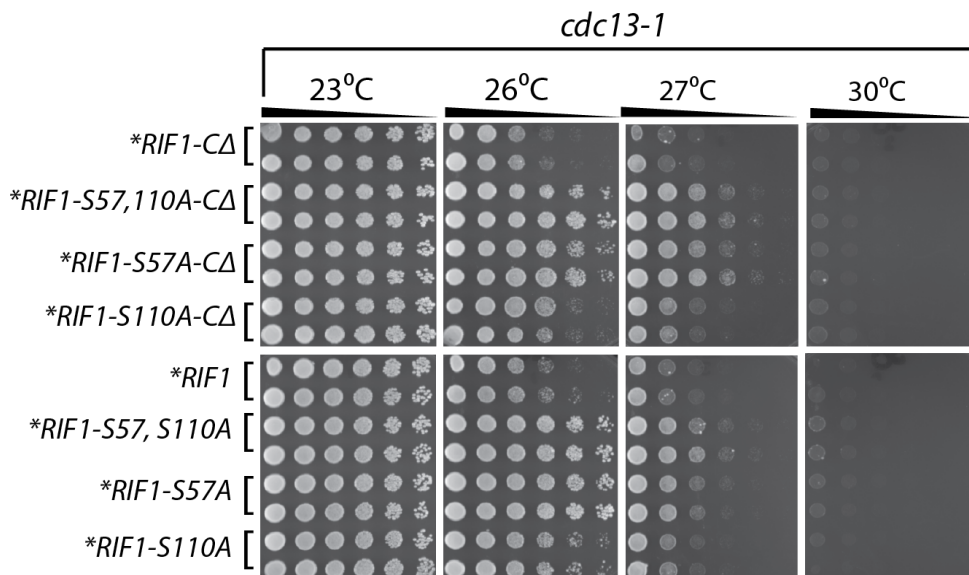


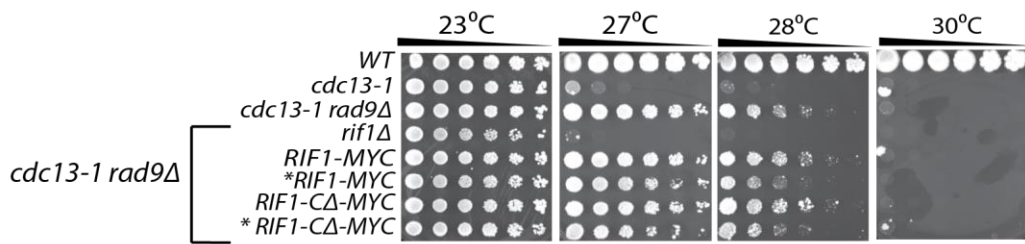
Figure 5.1.1 Substitution of Serine-57 and Serine-110 in Rif1 reduces the sickness of *cdc13-1* cells.

(A) Schematic diagram of *RIF1-S57A-S110A* with mutated sites indicated in red, and the *HIS3* marker upstream of *RIF1* TSS. (B-C) Serial dilutions of cells across YPD plates, and then incubated at indicated temperatures for 3 days before being photographed. (B) Comparison of strains containing the *HIS3* marker upstream of Rif1, indicated by *, against studied Rif1 variants in *cdc13-1* cells. (C) Comparison of *cdc13-1* strains containing *RIF1* with mutations to generate substitutions at S57/S110 against the control strain of strain containing the *HIS3* marker, indicated by *, but no substitutions within *RIF1*.

These mutations were then combined with a *rad9* Δ mutation, in order to answer whether these mutations would have any effect on growth in a strain in which Rif1 is not phosphorylated during telomere damage. I verified the effect of the *HIS3* marker when also coupled with a *rad9* Δ mutation. From this we can see that in those strains containing **RIF1 rad9* Δ or **RIF1-C* Δ *rad9* Δ the growth phenotype is much like that seen in *RAD9+*. These strains displayed a slightly increased temperature sensitivity compared to their equivalents without the marker (**Figure 5.1.2A**). The decreased temperature sensitivity of *cdc13-1 rad9* Δ cells is a known effect (Weinert and Hartwell, 1993)

Mutants containing double substitutions of S57 and S110 within the Rif1 protein were combined with the *rad9* Δ mutation. The control strains acted as expected, showing sickness at 27°C and by 28°C showed considerable reduction in growth. The mutants in this experiment had no effect on growth at any temperature, regardless of which amino acids were substituted (**Figure 5.1.2B**). This suggests that the improvement of growth observed in non-phosphorylated mutants was dependent on the activity of Rad9, perhaps as G2/M arrest is required for Rif1 to become phosphorylated.

A



B

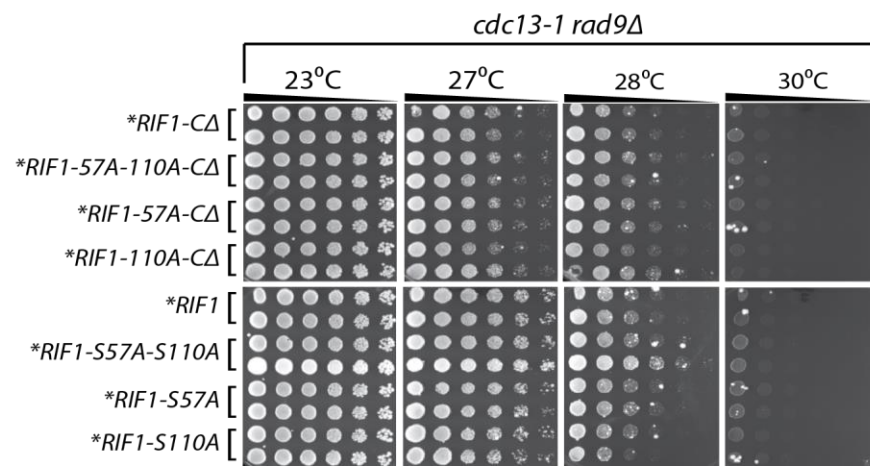


Figure 5.1.2. Substitution of Serine-57 and Serine-110 in Rif1 does not affect the sickness of *cdc13-1 rad9Δ* cells

Serial dilutions of cells across YPD plates, and then incubated at indicated temperatures for 3 days before being photographed. **(A)** Comparison of strains containing the *HIS3* marker upstream of Rif1, indicated by *, against studied Rif1 variants in *cdc13-1 rad9Δ* cells. **(B)** Comparison of *cdc13-1 rad9Δ* strains containing *RIF1* with mutations to generate substitutions at S57/S110, *HIS3* marker indicated by *.

5.2 Rif1 phosphorylation mutants do not affect the growth after other cellular stresses

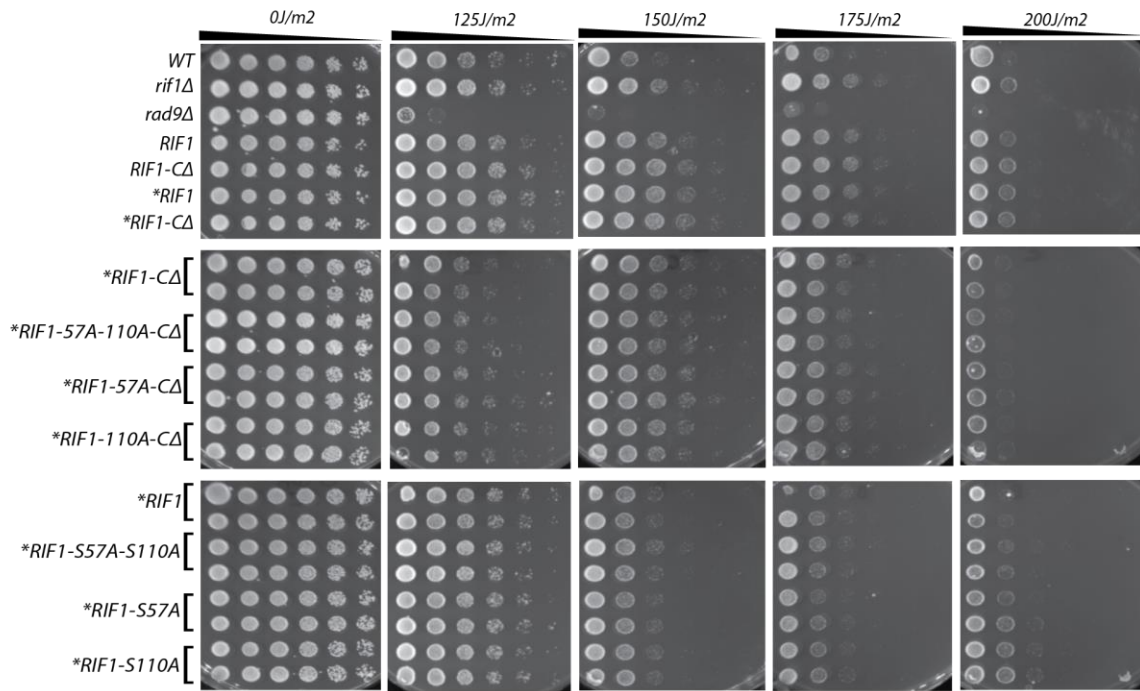
Finally, I aimed to determine if the improved growth created by substitution of residues S57 and S110 in Rif1 during telomere damage could also be seen during other damage types, in which I have shown Rif1 to be phosphorylated. To carry this out, serial dilutions were carried out first on plates exposed to UV radiation at a range of doses, and then on plates containing hydroxyurea at a range of concentrations.

As in previous experiments (**Chapter 5.1**), the first plate shown is a control designed to assess the impact of the *HIS3* marker on the growth of these cells, and the impact of losing Rif1 function entirely, when cells are treated with UV radiation. In these plates it was seen that after a dosage of 125J/m², cells began to see reductions in growth. This steadily worsened at each interval examined until dosages of 200J/m², after which growth was extremely poor. In this experiment *rad9Δ* mutations sensitize the cells to exposure to UV radiation, in contrast the addition of the *HIS3* marker did not appear to affect the growth of cells (Al-Moghrabi *et al.*, 2001). At all radiation doses these strains appeared to grow similarly to their equivalents that did not contain the upstream marker. Similarly, *rif1Δ* did not appear to affect the growth of cells. Further to this, mutants containing substitutions within *RIF1* did not appear to grow differently in comparison to the controls without substitutions. These results suggest that not only does this mutation of Rif1 not affect the cell's response to UV radiation, it may suggest that despite the presence of Rif1 phosphorylation the protein function may not have a role in the response to UV radiation (**Figure 5.2A**).

The effect of HU on cells with different *RIF1* mutations was then tested using serial dilutions on plates on containing HU at 0mM, 100mM, 200mM, or 250mM. On the control plate WT cells saw very little impact on growth from the lowest HU concentration (100mM), however 200mM and 250mM began to increase sickness and led to reduced growth. The control *rad52Δ* strains saw no growth at 100mM or above as expected (Lee *et al.*, 2003), *rif1Δ* cells grew very similarly to the WT. Interestingly, it appears that the *HIS3* marker led to a small reduction in growth on these plates, as they appeared to grow slightly worse than their equivalents at 200mM and 250mM doses of HU (**Figure 5.2B**).

However, when the growth of cells containing substitutions of the S57 and S110 was examined it was seen that these mutations do not appear to impact the growth. These cells grew identically to the control strains on each plate. This again suggests that the removal of Rif1 phosphorylation does not appear to affect the growth of these strains when grown in the presence of HU.

A



B

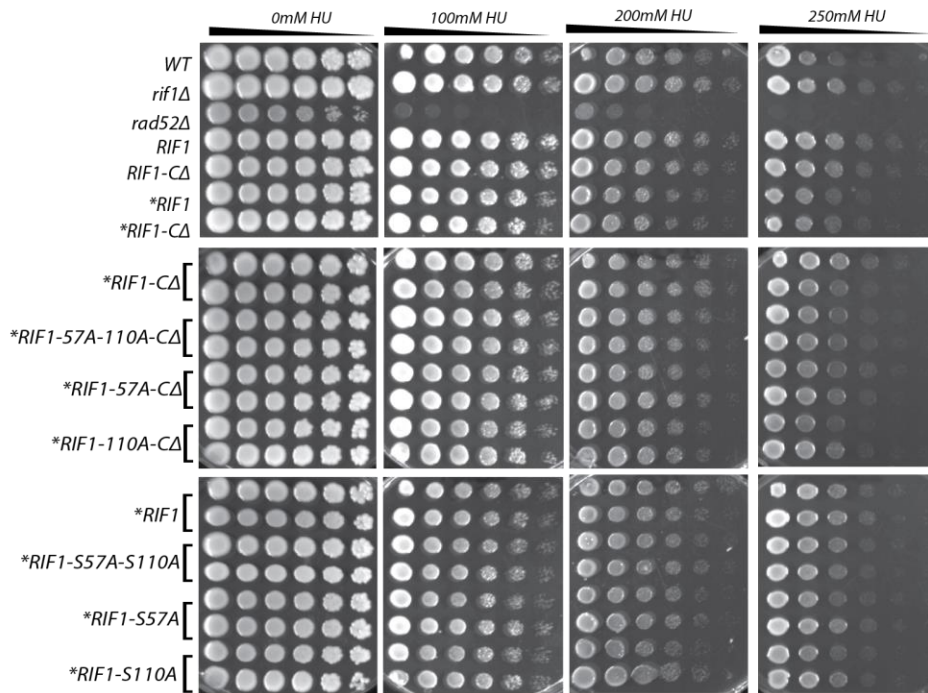


Figure 5.2 Substitutions of Rif1 serine-57 and serine-110 do not affect the sickness of cells exposed to hydroxyurea or UV radiation.

Serial dilutions of cells across YPD plates to compare strains containing the *HIS3* marker upstream of Rif1, indicated by *, against studied Rif1 variants, and of strains containing *RIF1* with mutations to generate substitutions at S57/S110 against the control strain of strain containing the *HIS3* marker but no substitutions within *RIF1*. (A) Cells were first exposed to the indicated dosage of UV radiation and then grown for two days at 23°C before being photographed. (B) Cells were grown on YPD agar plates containing the stated concentration of hydroxyurea added to the mix, cells were grown for 3 days at 23°C before being photographed.

5.3 Discussion

The results from this chapter demonstrated the importance of phosphorylation in the growth phenotype of *cdc13-1* cells. Strains expressing Rif1-S57A-S110 showed improved growth over a strain in which Rif1 contains no substitutions. This suggests that the improved growth phenotype may be due to loss of Rif1 phosphorylation. Interestingly, a single mutant containing the mutation *RIF1-S57A* showed similar growth to double mutants whereas single mutants containing only the mutation *rif1-S110A* do not display as strong an improvement in growth at high temperature. This corresponds to the levels of phosphorylation seen in these strains in **Chapter 3**. In these experiments the double mutant and *RIF1-S57A* showed near complete loss of phosphorylation, whilst *RIF1-S110A* had only a moderate decrease in phosphorylation in comparison. Furthermore, results showed that these improvements in growth are dependent upon the action of Rad9 to implement an arrest of the cell cycle at G2/M phase.

Interestingly, these improvements in growth seem to be specific to *cdc13-1* as they were not seen in *CDC13+* cells exposed to HU or UV radiation, despite the DNA damage and Rif1 phosphorylation induced in these strains.

Chapter VI – The molecular effects of Rif1 phosphorylation

6.1 Rif1 Phosphorylation May Lead to Dissociation from Sites of DNA Damage

Previously published data from our lab showed that Rif1 binds damaged DNA resulting from telomere uncapping and shields it from recognition by DDR proteins (Xue *et al.*, 2011). As such, I investigated the effect of Rif1 phosphorylation upon Rif1 association with the chromosome during telomere damage.

Across the course of this study I generated mutations of *RIF1* which are incapable of phosphorylation, without compromising the DNA damage checkpoint pathways or causing large disruptions of Rif1 protein structure. These strains were ideal to test the effect of Rif1 phosphorylation on association ssDNA during telomere resection.

To study the effect of Rif1 phosphorylation on the protein's association with the chromosome I used chromatin immunoprecipitation. The association of Rif1 with the chromosome was studied at four genomic loci:

- *Y'600* - A locus located only 600bp from the telomere. A positive control at T0 as fragments would likely contain telomere bound Rif1 as part of the Rap1-Rif1-Rif2 complex
- *YER188W* – A single gene locus located approximately 8kb from the telomere to which ssDNA is known to reach during telomere damage.
- *YER186C* – Single gene locus located approximately 15kb from telomere.
- *PAC2* – A centromeric locus 300kb from the telomere. This loci as a negative control which resected DNA will not stretch to during telomere damage.

For this experiment, a control strain of *cdc13-1 RIF1-MYC* was grown overnight alongside a second culture of the strain *cdc13-1 RIF1-S57A-S110A-MYC* at 20°C. These samples were then incubated for 4hours at 36°C, with samples taken at 2-hour intervals. Shown here are multiple repeats of this experiment, using multiple strains of the *RIF1-S57A-S110A* mutant.

At *YER188W* the association of Rif1 in controls began at low levels in one of the *cdc13-1 RIF1-S57A-S110A-MYC* strains studied. This saw a large increase in association after 2 hours, rising by several-fold in both repeats for this strain. This then declined after 4 hours,

to approximately the level of association seen at the start of the experiment. This was true for all loci studied, with a general overall decrease in association corresponding to distance of the locus from the telomere. This pattern was seen in both experimental repeats using this strain (**Figure 6.1A-B**).

The strain containing the Rif1-S57A-S110A protein form contained differences in both the level and pattern of protein association with the chromosome. At *YER188W* the protein association began at similar levels to the control. However, it noticeably increased more than the Rif1 protein association in controls after 2 hours at 36°C. Peak association at the 2-hour time-point was approximately a third higher in both experimental repeats of this mutant strain. After 4 hours there was a markedly slower decline, with chromatin association levels intermediate to those seen at the beginning of the experiment and after 2 hours. This pattern was seen at both *Y'600* and *YER186C* in both experimental repeats. Association with the *PAC2* locus was low at all time-points (**Figure 6.1A-B**).

This experiment was then repeated with a separate strain also containing the mutation *RIF1-S57A-S110A* to verify this association pattern was not unique to the strain used. The experiment was carried out as performed previously.

In this experiment, the control strain again behaved as expected. At *YER188W* Rif1 was associated at low levels at the beginning of the time course, this was followed by a several-fold increase in association after two hours of incubation at 36°C. This then declined again after 4 hours. This pattern was seen at all loci studied, however only at *Y'600* did this association decline to levels equivalent to those seen at the beginning of the time-course. At *Y'600* the peak after the first 2 hours was also proportionally lower than other loci, with a less than 2-fold increase in this 2-hour window. This pattern was seen in both experiment repeats using this strain (**Figure 6.1C-D**)

At *YER188W* the strain expressing Rif1-S57A-S110A showed a similar chromatin association at the beginning of the experiment. There was then a large increase in Rif1 association after 2 hours of incubation at high temperature. In these experiments the association increased by over 5-fold, and Rif1 was approximately twice as highly associated at peak as in control strains. Interestingly, in these strains the decline after 4 hours still occurred but was much lower than previously seen, chromatin association remaining several fold higher than seen in controls. This pattern held across most loci, however it can also be noted that *PAC2* association of Rif1-S57A-S110A was higher than the control in the first

repeat, and in one repeat the association of Rif1-S57A-S110A at *YER186C* did not decline in samples taken after 4 hours incubation at high temperature (**Figure 6.1C-D**).

The final repeat of this experiment also included a comparison of the chromatin association of a control Rif1-C Δ and Rif1-S57A-S110A-C Δ . In this experiment Rif1-C Δ control shows the expected pattern of association at *YER188W*, peaking after two hours of high temperature incubation and then declining. This was also seen at *YER186C*, however, at *Y'600* association of this protein is lower at all time-points (**Figure 6.1D**).

Similarly, to full length Rif1 protein, the substitutions S57A and S110A again led to increases in the association of Rif1 with chromatin. At *YER188W*, association was similar to the control at the start of the time-course, however after 2 hours there was a greater increase and association was approximately 2-fold higher. It then declined again in the following two-hour interval but at a lower rate, with chromatin association much higher than in the controls. This pattern was also true at the *YER186C* locus, and at *PAC2* association was low. Interestingly, whilst the starting association at *Y'600* was as low as in the controls there was an increase in association after 2 hours that was not seen in the controls (**Figure 6.1D**).

Despite variation in signal strength between experiments, this data clearly showed an increase in Rif1 association with chromatin after the substitution of amino acid residues S57 and S110. This occurs in both the full-length protein and the variant containing a deletion of the C-terminal region. This strongly supports the hypothesis that phosphorylation of Rif1 acts as a negative control on association of the protein with tracts of ssDNA during telomere damage.

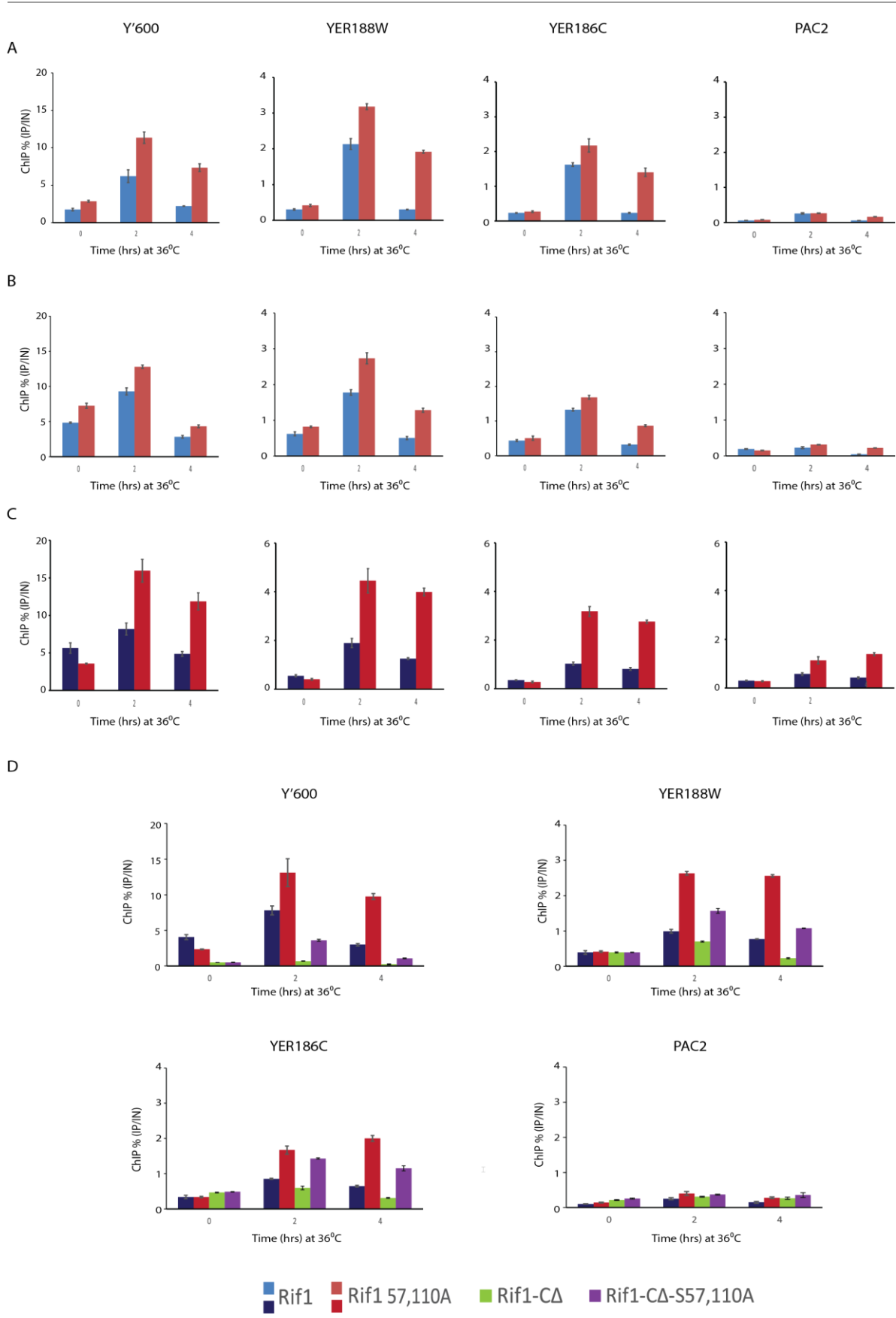


Figure 6.1 ChIP of Rif1 in mutants containing substitutions of serine-57 and serine-110 show higher association with the chromosome.

ChIP of Rif1 from samples grown overnight at 20°C (T0) to logarithmic growth phase (2×10^7 cells/mL). Cultures were then shifted to 36°C with samples taken after 2 and 4hrs. Each represents separate repeats of each experiment and error bars show standard deviation from 3 qPCR measurements in each experiment. **(A, B)** *cdc13-1 RIF1-MYC* compared to the mutant strain *cdc13-1 RIF1-S57A-S110A-MYC*. The experiment was also repeated using a different mutant strain of the same genotype **(C)** *cdc13-1 RIF1-S57A-S110A-MYC* and again also using strains with deletions of the Rif1 C-terminal region; *cdc13-1 RIF1-CΔ-MYC* (LMY510) and *cdc13-1 RIF1-S57A-S110A-CΔ-MYC* (LMY1042) **(D)**. ChIP was studied across four loci; *Y'600* (800bp from telomere), *YER188W* (8kb from telomere), *YER186C* (15kb from telomere), and *PAC2* (300kb from telomere). Error bars show standard deviation from triplicate measurements taken from each sample by qPCR.

6.2 Rif1 association in checkpoint-defective *cdc13-1*

To further verify that the phosphorylation of Rif1 led to its removal from sites of damage, I also examined the chromatin association of Rif1 in checkpoint defective *cdc13-1* cells in which I have shown that Rif1 does not become phosphorylated. These ChIP experiments were carried out as in **Chapter 6.1**, but only examined at the loci *Y'600*, *YER188W*, and *PAC2*. Each experiment compared checkpoint-defective strains to a *cdc13-1 RIF1-MYC* control.

At *YER188W* in both experiments the controls behaved as expected from previous experiments. There was a sharp rise in association during the first two hours, with association of Rif1 and chromatin peaking at the 2-hour timepoint. After this point there was a decline in association. In the first experiment shown this decline was rapid, with less association seen after 4 hours than at the beginning of the experiment, whilst in the other this decline is slower. This pattern was also seen at *Y'600*, and association with *PAC2* remained comparatively low (**Figure 6.2A-B**)

mec1 Δ mutation led to a noticeable change in this pattern of association with the chromatin. Rather than a sharp increase in Rif1 association in the first two hours of incubation, there was only a small increase at *YER188W*. However, this association steadily increased across the entire time-course rather than declining after 2 hours. After 4 hours the association of Rif1 was much higher in this mutant than in the control. A similar pattern was seen at *Y'600*, however there was also a small decline in association during the first two hours of the experiment after which association rises. *PAC2* association was low at all time-points (**Figure 6.2A**).

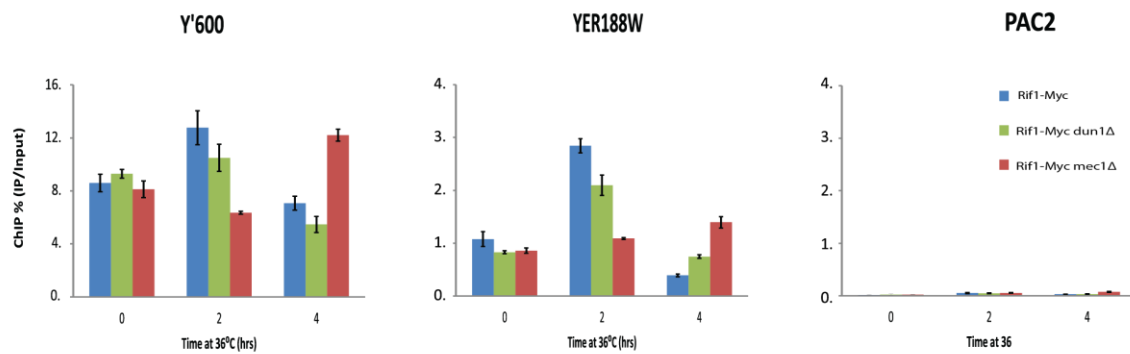
Interestingly, the mutation *dun1* Δ largely did not affect the pattern of Rif1 at any loci. At *YER188W* Rif1 association began at a lower level in this strain and did not peak as highly after 2 hours. However, after 4 hours the association of Rif1 was slightly higher in *dun1* Δ than in controls. In contrast, at *Y'600* the association of Rif1 started similar to controls and was then lower in *dun1* Δ cells after both 2 and 4 hours. This mutation did not affect Rif1 association with the *PAC2* locus (**Figure 6.2A**).

The mutation *rad9* Δ also led to substantial changes to the pattern of Rif1 association with the chromatin. At *YER188W* there was little change to Rif1 association in the first two hours of incubation at high temperature, there was then a ~2-fold increase after 4 hours to similar levels seen in the control after 2 hours. The pattern at *Y'600* was similar, however there was a small decline in the first two hours of the experiment. The association in this mutant then

increased to a similar level seen in the control after 2 hours incubation. The association of Rif1 in this mutant was higher at *PAC2* than in the controls, at several time-points (**Figure 6.2B**).

These results supported the previous conclusion that in strains in which Rif1 is not highly phosphorylated, it is more highly associated with the chromosome.

A



B

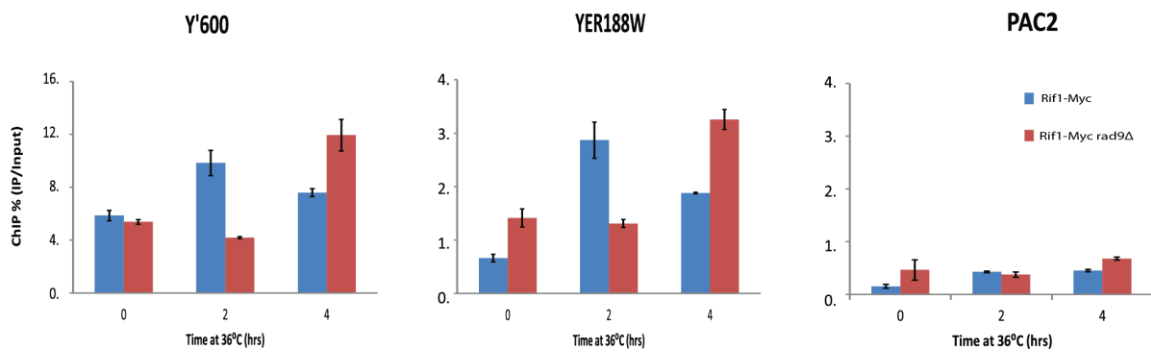


Figure 5.2.1 Chromatin Immunoprecipitation of Myc-tagged Rif1 in *cdc13-1* cells undergoing Telomere Uncapping.

ChIP of Rif1 from cells grown overnight at 20°C to low cell concentration (2×10^7 cells/mL) and shifted to 36°C for 4 hours, with samples taken every 2hrs. Samples were taken from *cdc13-1* strains. qPCR measurements made from three loci; *Y'600* (0.6kbp from telomere), *YER188W* (8kb from telomere) and *PAC2* (300kb from telomeres). Error bars show Standard Deviation of three individual measurements from qPCR. (A) *cdc13-1 RIF1-MYC*, *cdc13-1 dun1*Δ *RIF1-MYC*, *cdc13-1 mec1*Δ *RIF1-MYC*. (B) *cdc13-1 RIF1-MYC* and *cdc13-1 rad9*Δ *RIF1-MYC*. After each cell harvest those strains containing deletions of the checkpoint pathway were diluted 1:1 with fresh pre-warmed YPD to maintain cell concentration.

6.3 Discussion

This chapter aimed to address a key question about the phosphorylation of Rif1; what is the role of this modification on the role of Rif1 at a molecular level? To answer this question, I have shown the results of experiments using ChIP data to assess the chromatin binding of Rif1 during telomere damage in strains that do not contain phosphorylated Rif1, and in mutants in which I have shown Rif1 does not become phosphorylated during telomere damage.

To interpret this, it was important to both understand the binding of the Rif1 protein in *cdc13-1* cells, as well as how this association was affected in strains in which Rif1 phosphorylation has been removed or lowered. It is interesting to note that unlike in previous published data I observed a rising and falling pattern of Rif1-chromatin association across the 6-hour time-course (Xue *et al.*, 2011). This held in multiple experiments. This may imply that the phosphorylation of Rif1 may act as a negative regulatory mechanism on chromatin association. This is supported by the data I obtain from ChIP using deletions of the genes *RAD9*, and *MEC1*. In both strains Rif1 does not become phosphorylated, and association does not rapidly fall after 4 hours. However, in *cdc13-1 dun1Δ* strains I can see that the pattern of Rif1-chromatin association across 4 hours closely resembles that of the control.

An alternative explanation for the rising and declining chromatin association of Rif1 in uncapped telomeres might be that Rif1 is simply moving with the ss/dsDNA junction, and that the spike seen after 2 hours is as the junction travels through the region studied. Whilst this explanation may have some merit, I do not believe it to be the case. If this were true then I would not expect to see a peak of Rif1 association at loci telomere proximal, such as *Y'600*, after telomere uncapping has been initiated for a prolonged time as the junction would have long moved through this site. I certainly would not expect to see a binding spike which correlates across multiple sites after 2hrs, as the junction would not be expected to be passing through all sites at this time point. These results do suggest a genome-wide effect on Rif1 association, which would make a modification to the protein itself a more convincing explanation as to the pattern of binding observed.

It is known that in the absence of checkpoint kinases, such as Mec1 or Rad9, there are wide-ranging effects; from loss of cell viability, to increases in ssDNA during telomere uncapping (Jia *et al.*, 2004). However, data from mutants further verifies that increased binding is at least partially due to loss of Rif1 phosphorylation.

Furthermore, the previous chapters found that the phosphorylation events occurring within Rif1 in these arrests were also eliminated by the substitution of S57 and S110. These mutations have been shown here to lead to increased association of Rif1 with sites of ssDNA during telomere damage. This strongly supports the hypothesis that the phosphorylation of Rif1 has a negative regulatory effect on its binding with DNA damage, and its anti-checkpoint role. Furthermore, these mutants do not contain the side-effects known to occur from the deletion of checkpoint pathway genes, such as changes to DNA resection, or the absence of a G2/M arrest.

Chapter VII Investigating the Effect of Mimicking Rif1 Phosphorylation

7.1 Investigating the Phosphorylation of Phosphomimetic *RIF1* Mutations

When examining the behaviour of phosphorylated proteins via mutations, as well as producing protein variants that have the sites of phosphorylation removed it is also possible to create proteins with residues that are phosphomimetic. This means that at sites of phosphorylation the residue is substituted with an alternative amino acid that resembles size and charge of the phosphorylated form of the original residue. For serine residues, these are commonly changed to glutamic acid or aspartic acid. If successful, this would mimic the presence of constitutively phosphorylated Rif1. The mutagenesis Gibson assembly procedure used previously in **Chapter 3** was used again to substitute amino acid residue S57 and S110 with glutamic acid.

In the first experiment shown the Rif1 protein containing phosphomimetic residues was examined during telomere damage. For this, three strains were grown overnight at 20°C: a control strain *cdc13-1 RIF1-C Δ -MYC*, a mutant containing a substitution at both residues *cdc13-1 RIF1-S57E-S110E-C Δ -MYC*, and a mutant containing only one substitution *cdc13-1 RIF1-S57E-C Δ -MYC*. They were then incubated at 36°C for 4 hours.

The control samples Rif1 showed a clear shift in protein migration after incubation at 36°C. This was matched by a shift in Rad53 protein, indicating that both proteins had become phosphorylated as expected.

However, when examining the mutant Rif1 strains the results were unexpected. At T0 the migration of both mutated forms of Rif1 was identical to that of the control, despite the modifications to mimic phosphorylation. Furthermore, after 4 hours both proteins underwent shifts in migration. A *RIF1-S57E-S110E-C Δ* mutant appeared to show some phosphorylation of the protein, although not to the same level as in the control. A mutant of residue S57E alone appeared to be further phosphorylated than the strain containing substitutions at both this site and S110 (**Figure 7.1A**).

These results were somewhat unexpected. Not only do they indicate that the Rif1-S57E-S110E strain may be phosphorylated, this slower migrating band appears at 36°C indicating it is induced during telomere damage.

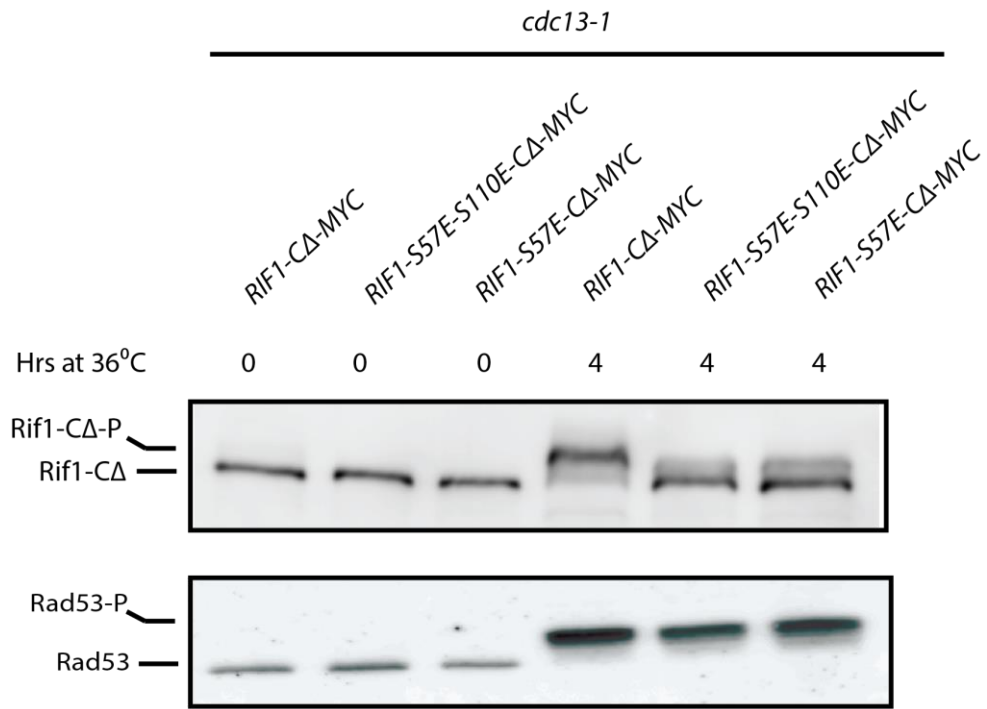
To validate these protein shifts were the result of phosphorylation, the previous experiment was repeated to gather fresh samples. Samples taken after four hours incubation at 36°C underwent treatment with alkaline phosphatase, or a mock treatment.

In the control *cdc13-1 RIF1-CΔ-MYC* T0 sample there was a single non-phosphorylated protein form of both Rif1 and Rad53. In T4 samples from this culture a slower migrating form was seen for Rif1, and several slower migrating protein forms for Rad53 in the mock treated samples. However, in those samples treated with alkaline phosphatase these slower migrating forms were eliminated and restored both Rif1 and Rad53 to single, faster migrating protein bands.

In the strain containing *RIF1-S57E-CΔ-MYC* it was also seen that the slower migrating form of Rif1 protein seen in the mock treated samples was eliminated by treatment with alkaline phosphatase. Similarly, this was also seen in *RIF1-S57E-S110E-CΔ-MYC* samples. Elimination of Rad53 phosphorylation was also seen, verifying activity of the alkaline phosphatase (**Figure 7.1B**).

These results confirm that the slower migrating Rif1 protein in *RIF1-S57E-S110E* and *RIF1-S57E* strains is a phosphorylated form of the protein. This would suggest that despite these mutations the protein can still become phosphorylated during telomere damage. The phosphorylation seen has likely moved to different residues which may have become exposed in this mutation.

A



B

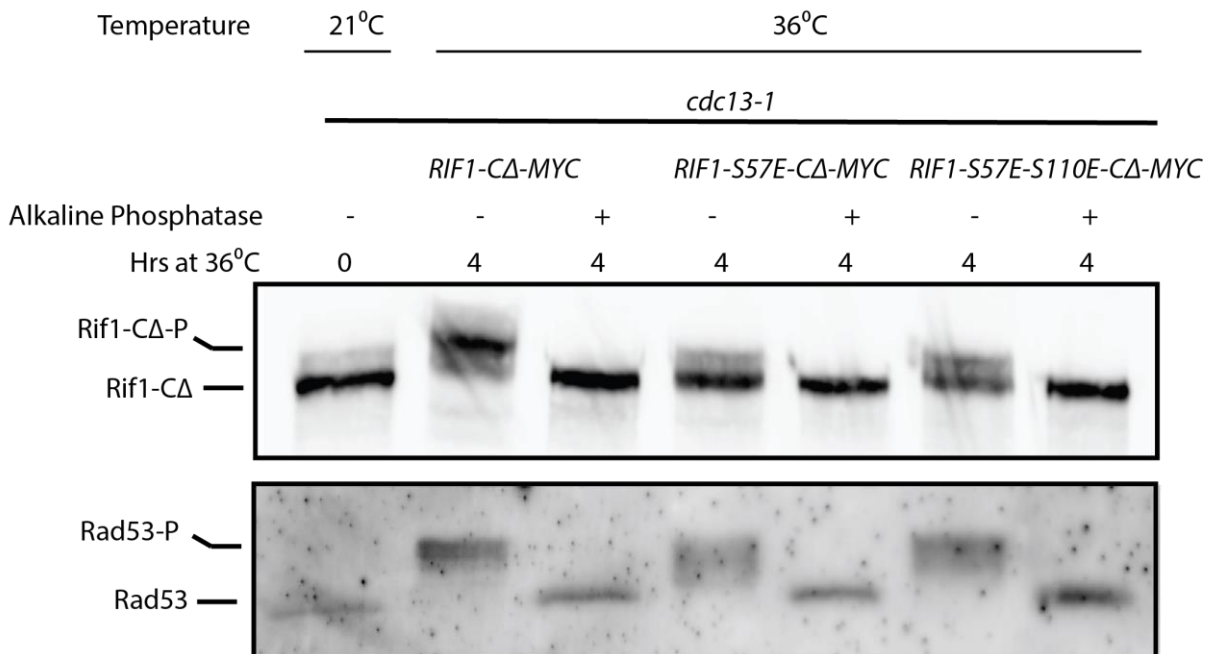


Figure 7.1 Rif1-S57E-S110E Becomes Phosphorylated During Telomere Damage

(A) Western blot analysis of Rif1 and Rad53 protein taken from cells incubated overnight at 20°C (T0) and shifted incubation temperature to 36°C for 4 hrs. Cells used were *cdc13-1 RIF1-S57E-S110E-CΔ-MYC*, *cdc13-1 RIF1-S57E-CΔ-MYC*. **(B)** Samples taken from strains above after 4hrs at 36°C were treated with alkaline phosphatase or underwent mock treatment. Rad53 samples were used as a positive control.

7.2 Examining the growth of phosphomimetic *RIF1* mutants

RIF1 variants containing phosphomimetic substitutions were shown to gain further phosphorylation in Rif1 during telomere damage that did not simply correlate with the addition of phosphomimetic residues. I therefore studied whether these strains would exacerbate or alleviate the sickness of *cdc13-1* cells grown at high temperature. Serial dilutions were carried out to determine the effect of phosphor-mimetic mutations on the temperature sensitivity of *cdc13-1*.

The controls strains in this experiment were *cdc13-1* **RIF1* studied in **chapter 5**, these acted as expected, demonstrating a slight increase in temperature sensitivity. The mutants containing phosphomimetic residues behaved interestingly in this experiment, as they also appeared to decrease the temperature sensitivity of *cdc13-1*. The *RIF1-S57E-S110E* and the *RIF1-S57E* saw the largest increase in growth at 26°C and 27°C. Whilst the mutant *RIF1-S110E* did not see as substantial an increase, it did however still see an improvement over the control strain. This is true for both *RIF1* and *RIF1-CΔ* cells (**Figure 7.2**).

These results may suggest phosphomimetic mutants may also reduce sickness of *cdc13-1* strains.

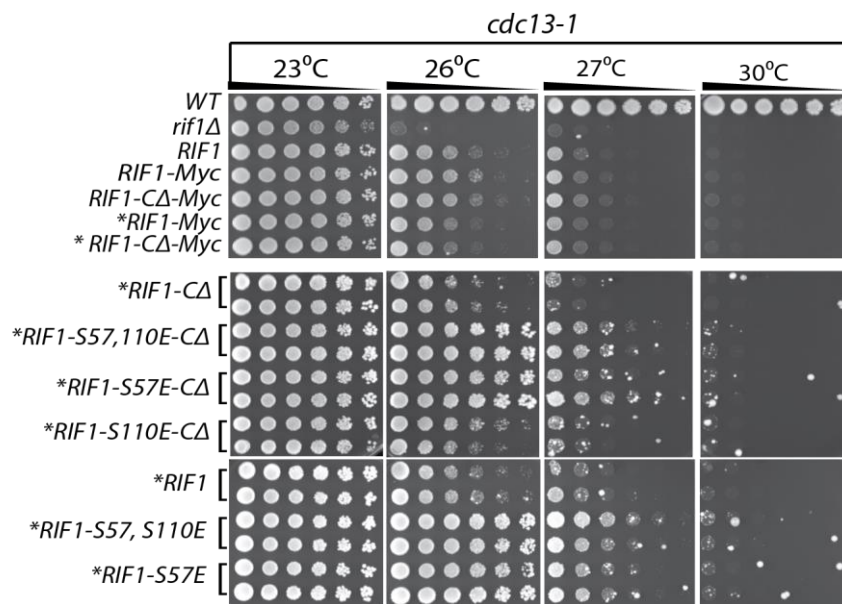


Figure 7.2 Phosphomimetic substitutions of Rif1 reduce the sickness of *cdc13-1* cells

Serial dilutions of cells across YPD plates, and then incubated at indicated temperatures for 3 days before being photographed. Comparison of *cdc13-1* strains containing *RIF1* with mutations to generate phosphomimetic substitutions at S57/S110 against the control strain containing the *HIS3* marker, indicated by *, but no substitutions within *RIF1*. Phosphomimetic substitutions switched alanine residues to glutamic acid residues.

7.3 Discussion

Unfortunately, the results presented in this chapter would suggest that the integration of phosphomimetic residues into Rif1 was not successful in accurately mimicking the structure or activity of a permanently phosphorylated Rif1. This is not unexpected as phosphomimetic residues are not perfect replications of the structural/charge changes introduced by phosphoryl groups, nor can it reflect the dynamic nature of phosphorylation.

The data gathered suggests that the integration of glutamic acid at sites of phosphorylation does not accurately mimic phosphorylation, as growth in spot tests resembles that of strains with alanine substitutions, nor does it eliminate phosphorylation. Interestingly, this may suggest that there are further potential phosphorylation sites in Rif1, which for some reason are not used in Rif1-S57A-S110A. This may indicate that these sites are only exposed once the protein has become phosphorylated. However, these sites do not affect growth and so are not sufficient to mimic the role played by phosphorylation of S57 and S110. It may be of interest to determine in future whether these sites are also exposed and phosphorylated following the phosphorylation of S57 and S110 during telomere uncapping. It is possible these sites may play a role that is dependent on the phosphorylation of S57 and S110.

Chapter VIII: Final Discussion

8.1 Rif1 Phosphorylation in *cdc13-1* cells

At the outset of this study, we hypothesised that the phosphorylation of Rif1 played a role in the regulation of function. Post-translational modifications are known to play major roles in the regulation of protein function, Rif1 is seen to undergo several modifications which mediate activity. Palmitoylation of Rif1 by Pfa4 was first shown to anchor it to the inner nuclear membrane, to control its influence on *HM* silencing (Park *et al.*, 2011). This was recently developed further to show that S-acylation of Rif1 at C466 and C473 may help to promote NHEJ in budding yeast (Fontana *et al.*, 2019). Interestingly, post-translational modifications of Rif1 are also seen to influence repair pathway choice in mammalian cells; Rif1 ubiquitination and SUMOylation are required to promote 53BP1-Rif1 dissociation from the DSB, and DSB repair by HR (Zhang *et al.*, 2016; Kumar and Cheok, 2017). Furthermore, there have been a number of potential phosphorylation sites previously identified in budding yeast Rif1, and phosphorylation by Cdk and DDK was shown as the mechanism controlling Rif1 function in the suppression of late firing origins of replication (Swaney *et al.*, 2013; Davé *et al.*, 2014). Previous studies have also suggested phosphorylation of Rif1 in the *yku70Δ* model of telomere damage. This study, using mass spectrometry, showed less phosphorylation at S110 during telomere uncapping at restrictive temperatures, and increased phosphorylation at residue S181 (Wang *et al.*, 2018). Both of these residues were studied here in *cdc13-1*, with different results. This may be due to the differences in the damage occurring at telomeres in *yku70Δ* cells compared to *cdc13-1* cells.

I have shown that phosphorylation of Rif1 occurs during telomere uncapping in *cdc13-1* cells at the N-terminal region, specifically residues S57 and S110. This appears to confirm the starting hypothesis that phosphorylation acts to regulate Rif1 anti-checkpoint function as I also demonstrated that phosphorylation acts to inhibit the association of Rif1 with DNA, and decreases the viability of *cdc13-1* cells. Further to this, I have shown that Cdc28 lies upstream of Rif1 phosphorylation.

The data presented here can be integrated into the model previously developed in Xue *et al.* (2011). This model showed Rif1 binds to regions of ssDNA in order to shield it from recognition by the DNA damage checkpoint proteins, when damage becomes extensive then Rif1 is not capable of shielding larger regions and a checkpoint response is triggered (Xue *et al.*, 2011). Through the integration of my phosphorylation data we propose that the phosphorylation of Rif1 acts as a negative regulator of this shielding, promoting Rif1

dissociation from the chromosome and leaving resected regions vulnerable. A checkpoint response from extensive damage leads through Rad53 and arrests the cell cycle. The G2/M arrest brings about an increase in Cdc28 activity, eventually leading to the targeted phosphorylation of Rif1 by Cdc28. This promotes dissociation of remaining Rif1 from the chromosome and leaves larger regions vulnerable to recognition, or accessible to DNA repair factors. This phosphorylation aids in the previously proposed function of Rif1 to set the threshold of tolerable DNA damage before the cell cycle is initiated. In strains without Rif1 capable of effectively binding damaged regions, such as *cdc13-1 rif1-Δ* cells, lower viability is seen as this threshold is lower (**Figure 8.1**).

Interestingly, Cdc28 is known to promote homologous recombination during S and G2 phases of the cell cycle in yeast and in mammals. In mammalian cells RIF1 is also known to repress homologous recombination during G1 through an interaction with 53BP1, and is removed from DSBs by BRCA1 during S and G2 phase. BRCA1 interacts with the phosphorylated form of the protein CtIP, a phosphorylation dependent upon CDK1 activity. Whilst the interaction of Rif1 with DSBs in yeast currently has conflicting evidence, recent evidence from Mattarocci et al (2017) suggested that Rif1 also acted to attenuate end resection and promote NHEJ in yeast. If this is true then phosphorylation of Rif1 by Cdc28 may be another method of promoting resection alongside the activation of exonuclease factors (Zimmermann *et al.*, 2013; Tomimatsu *et al.*, 2014; Mattarocci *et al.*, 2017).

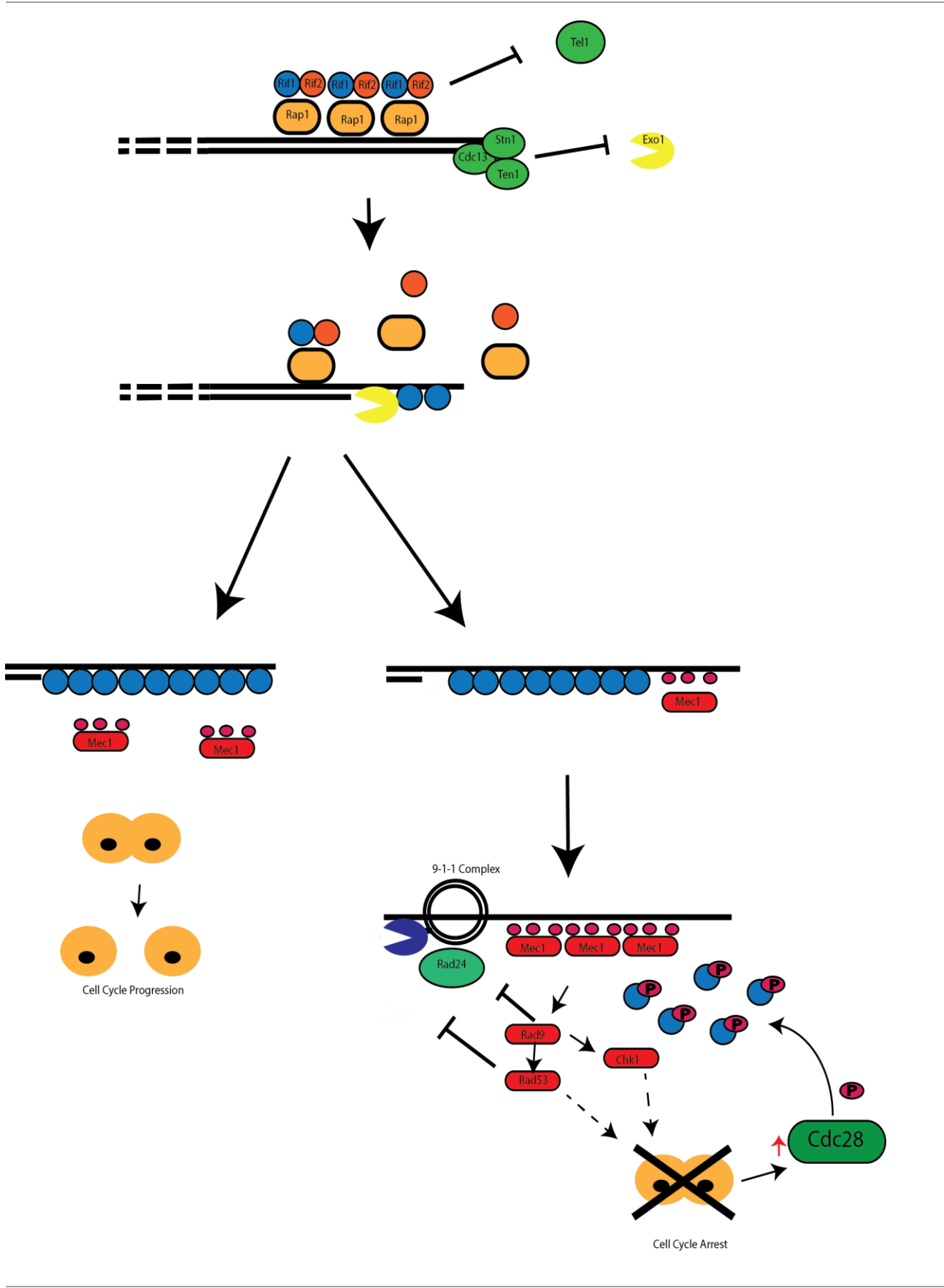


Figure 8.1 Rif1 phosphorylation by Cdc28 leads to dissociation from damaged DNA regions

Under normal growth conditions Rif1 is found at telomeres in complex with Rap1 and Rif2. In a *cdc13-1* strain at restrictive temperatures the CST complex is compromised leading to 5' telomeric resection, freeing telomere-bound Rif1. As damage becomes more extensive Rif1 becomes incapable of shielding role with sufficient efficiency and regions of ssDNA are vulnerable to recognition by checkpoint proteins (Model adapted from Xue *et al.* (2011)). The recognition of damage by checkpoint proteins causes an arrest of the cell cycle, ultimately leading to a prolonged period of increased Cdc28 activity. Cdc28 in-turn acts to phosphorylate Rif1. Phosphorylation of Rif1 causes it to increasingly dissociate from the damaged DNA to allow access of checkpoint machinery and repair factors.

8.2 The location and function of Rif1 phosphorylation

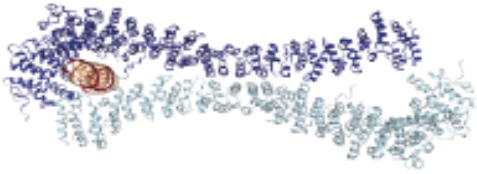
Previous studies demonstrated the C-terminus of Rif1 was dispensable for the anti-checkpoint role observed, this project supplemented this with the observation that the phosphorylation of Rif1 during telomere damage was not affected by this truncation (Xue *et al.*, 2011). To determine the role of phosphorylation, I demonstrated that the modification itself could be isolated to within 2 residues in the N-terminal region of Rif1. A number of phosphorylation sites have previously been identified in Rif1 from large-scale screens, the two sites identified here were amongst those sites (Swaney *et al.*, 2013b). A study carried out by Wang *et al.*, (2018) had previously shown increased phosphorylation of S181, and decreased phosphorylation of S110 during telomere damage in *yku70Δ* cells grown at restrictive temperatures (Wang *et al.*, 2018). The results of my analysis of these sites has several differences in *cdc13-1* cells. I demonstrated that the mutation of S181/Y183 did not lead to any noticeable effects on the phosphorylation of the Rif1 protein during telomere uncapping. Furthermore, my data suggests that the mutation of this site leads to an overall reduction in phosphorylation of Rif1 in *cdc13-1* cells. My study has not examined the *RIF1* mutations in *yku70Δ* mutants, and these may be worthy of further study in the future.

This study used mutants generated to directly demonstrate the role played by phosphorylation. ChIP data in checkpoint deficient cells demonstrated that Rif1 binding was affected by loss of phosphorylation, however the numerous side-effects including the loss of a G2/M checkpoint means these different binding patterns during telomere damage could have been caused by a multitude of factors. The ChIP data directly comparing Rif1 and Rif1-S57A-S110A however, offers a much clearer picture. We had previously seen that in *rif1-NΔ* mutants that the association of Rif1 and the chromosome was negligible. However, it appears that this was due to the large regional loss of the protein, as opposed to the elimination of Rif1 phosphorylation. In *RIF1-S57A-S110A* cells we saw that the loss of phosphorylation led to an increase in the association of the Rif1 with the chromosome. This can be seen in both protein abundance on the chromatin, even after the protein has begun to dissociate these levels are higher in the mutant cells. The overall dissociation however may suggest that the association is not guided by phosphorylation of Rif1 alone.

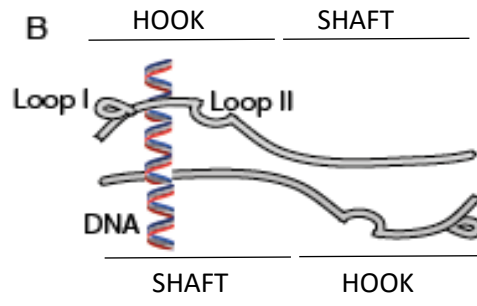
As this phosphorylation appears to play such a strong role in the regulation of Rif1 activity, it would be interesting to determine the mechanism by which phosphorylation promotes the removal of Rif1 from the chromosome. My prediction of the role utilises the crystal structure of Rif1 previously determined in Mattarocci *et al.*, (2017). Their work found that in the

presence of short tracts of DNA containing ssDNA-dsDNA junctions, Rif1 formed dimers to bind to these structures *in vitro*. Individual Rif1 proteins formed what they termed a “HOOK and SHAFT” structure, with the HOOK region of one dimer-mate forming a channel with the SHAFT region of the second dimer-mate, in a head-to-tail dimer configuration. These HOOK regions contain two loops of high electrostatic potential and it was hypothesised that the channels created in these dimers were suitable for DNA binding (**Figure 8.2A-B**). The residues I have determined to be the location of the DNA binding sites were not part of the protein structure examined in this study, and so would fall more proximal to the N-terminus than, although likely close to, the DNA channels in these dimers. We propose that this region may form a clasp on these dimers *in vivo* that acts to promote the secure binding of Rif1 dimers to damaged regions that we refer to as the Phospho-Gate Domain (PGD). This suggests an explanation for how the *rif1-NΔ* mutant sees increased sickness and poor chromosome association, despite the loss of phosphorylation. Without this PGD it may be that the dimer structure is less secure and more easily removed from the chromosome (**Figure 8.2C-D**). Further to this I suggest that the phosphorylation occurring within this region acts as a key to unlock this clasp and further promote dissociation. The model by which this takes place is shown below. We also propose that mate-dimers may act together to allow the interaction of two PGDs to form a plier-like structure around the DNA, creating a more secure binding that is dependent on the PGD. (**Figure 8.2E-F**).

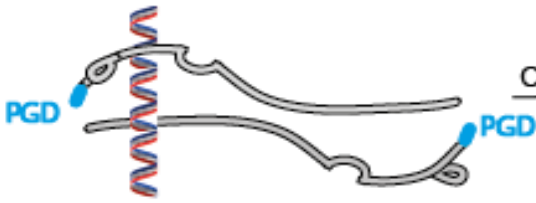
A



B



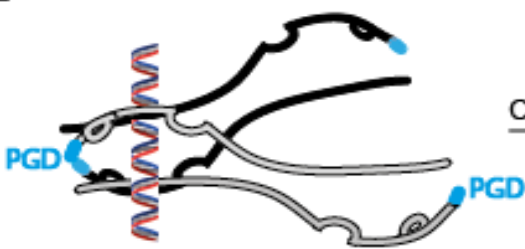
C



D



E



F

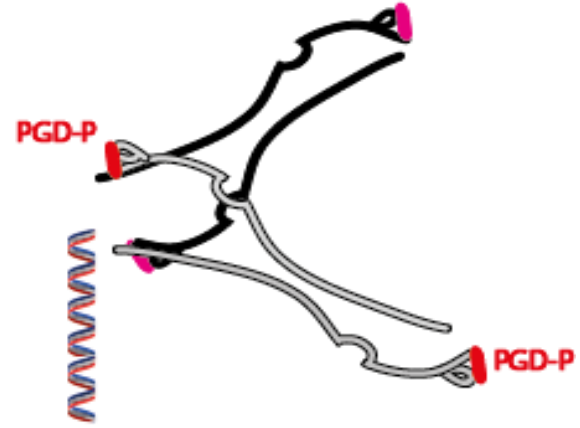


Figure 8.2 The Phospho-Gate-Domain: The Rif1 N-terminal cooperates to create a clasp to unlock the dimer structure.

(A) Crystal structures of the Rif1 dimers forming around DNA. Figure from Mattarocci *et al.* (2017) (B) The concave face of the HOOK domain creates a binding interface for DNA through positively charged residues contained in the Loop I and Loop II structures. The binding channels are sealed by the 'lid' created by the SHAFT domain of the dimer-mate. (C-D) The region immediately adjacent to the N-terminal of Rif1 creates the phospho-gate domain (PGD). In non-phosphorylated Rif1 this region may act as a clasp between the two dimers, securing it on the chromosome and closing the loop-encasement of the DNA. After phosphorylation the conformation of the region changes so as to open the gate. This leads to a less secure association of the dimer to the chromosome, and possibly may promote dimer dissociation, ultimately leading to Rif1 being removed from DNA. Protein structure informing these figures was taken from Mattarocci *et al.* (2017) (E-F) The study by Mattarocci *et al.* (2017), proposed that multiple Rif1 dimers may interact for secure binding to the DNA, we propose that the PGD may be one mechanism that promotes the secure binding of multiple dimers to the DNA, as well as rapid dissociation upon phosphorylation.

8.3 Phosphorylation of Rif1 outside of S57 and S110

The number of potential phosphorylation sites raised by previous studies raises a further question as to why they have not been observed for phosphorylation in this study. The data collected in *RIF1* mutants containing phosphomimetic residue substitutions of S57 and S110 may combine with our proposed model to potentially answer this question. One answer to this may be that the phosphorylation of S57 and S110 act as a first step to further phosphorylation of Rif1 protein. In Rif1-S57E-S110E mutants we see that mutation of these sites alone is not sufficient to alter the migration of the protein, therefore further migration changes must be due to phosphorylation at alternative sites. As these alternative sites are present on Rif1-S57A-S110A but are not used, this suggests that these sites are exposed by the integration of the phosphomimetic residue. This suggests that the phosphorylation of Rif1 at S57 and S110 may expose further residues for targeting by kinases. Furthermore, the phosphorylation seen in Rif1-S57E-S110E does not produce as large a change in protein migration as in WT structure Rif1 as the phosphomimetic residues only partially mimic the structure of phosphorylated Rif1. However, it must be noted that whether these alternative sites are usually phosphorylated in telomere damage or not, the data shown here suggests that the phosphorylation of these residues alone does not have a noticeable effect on phenotype.

8.4 Rif1 Phosphorylation Outside of *cdc13-1*

The model proposed explains how Rif1 may act in *cdc13-1* cells, as well as how the anti-checkpoint function is regulated. However, the phosphorylation I have seen in this study suggests a role for Rif1 in arrest resulting from other reagents. However, serial dilutions of mutants did not help to elucidate a role for Rif1 in these conditions. Substitution of S57 or S110 did not appear to affect the growth of cells exposed to UV radiation, or HU-supplemented media. This raises the question of what the function of phosphorylation is in cells in these conditions. This may be an intriguing question for future study.

Recent studies have further developed the idea that Rif1 may play a role at DSBs in yeast, despite previous evidence from our lab contrary to this (Xue, *et al.*, 2019). A number of the reagents tested do induce DSBs in the chromosome, it may be seen with further study that the phosphorylation of Rif1 in these cells may play the same role as Rif1 in *cdc13-1* and promote dissociation from the DSB in order for repair factors to better access the site. Recent studies have also shown potential roles for Rif1 in protecting stalled replication forks from resection of synthesised DNA in mammalian cells. Phosphorylation after exposure to

HU could also suggest a role for Rif1 in protecting stalled replication forks in budding yeast that may also be regulated by phosphorylation of the N-terminal (Garzón *et al.*, 2019).

The phosphorylation of Rif1 in nocodazole is a more perplexing modification that will require further study to determine the role that is played by Rif1 after impediments to spindle formation. Whilst I have shown that this phosphorylation was the result of Cdc28 activity, a molecular role for Rif1 or the function of phosphorylation during spindle damage is unknown. As well as the survival of *rif1*Δ cells exposed to spindle damaging agents, it may also be worthwhile to examine the abundance of Rif1 at kinetochores in cells exposed to a factor such as nocodazole. A presence here may suggest a role for Rif1 in regulating the spindle checkpoint proteins. Furthermore, it is known that the protein Glc7, which Rif1 interacts with during origin suppression, is also involved in regulation of the spindle checkpoint. This interaction may be relevant for this role.

8.5 Rif1 in Budding Yeast and Humans

The final key question left from this study is; how applicable is the Rif1 anti-checkpoint function outside of budding yeast? Whilst RIF1 has been demonstrated to be involved in the DSB repair pathway choice in mammalian cells, it is unclear whether this functions similarly to the anti-checkpoint function observed in budding yeast. Recent studies have suggested that the highly conserved N-terminus domain of RIF1 is also capable of DNA-binding in murine models, however this corresponds to the HOOK domain identified by Mattarocci *et al.*, which does not start immediately at the N-terminal in budding yeast, instead this domain is named for a region beginning ~180 residues from the N-terminal (Mattarocci *et al.*, 2017; Moriyama *et al.*, 2018). This 180 amino acid region is instead likely found in the C-terminal of higher eukaryotes, as it has been shown that the RVxF-SILK domains contained in this region have been translocated during the evolution of higher eukaryotes (Sreesankar *et al.*, 2012). However, if this shared binding domain does correspond to a shared function, then it is not unfeasible that alternative phosphorylation sites have been chosen over the course of evolution in order to serve this regulatory function.

A

Score	Expect	Method	Identities	Positives	Gaps
17.3 bits(33)	2.0	Compositional matrix adjust.	20/61(33%)	29/61(47%)	6/61(9%)
Query 14	DRIDQHILRRSQHDNYSNGSSPVMKTNLPPSPQAHMHIQSD---			LSPTPKRRKLASSSD	70
Sbjct 2217	D ID+ R S ++S+ SSP K+ P+ Q+ + S			LSP + K SS	
Query 71	C 71			LSPGSRSPKFKSSKK	2273
Sbjct 2274	C 2274				

B

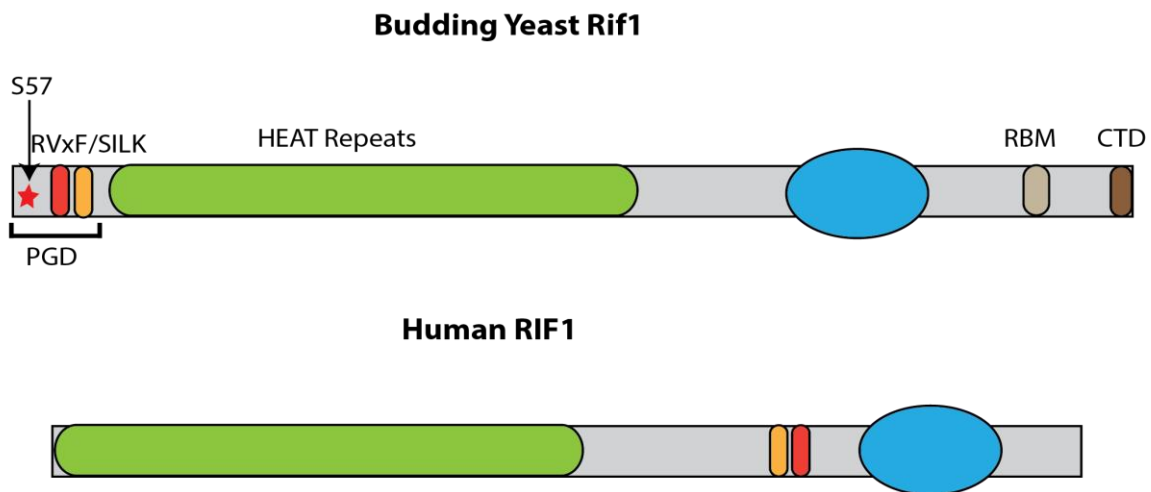


Figure 8.5 Human RIF1 is unlikely to phosphorylated at a conserved serine residue for any anti-checkpoint roles.

(A) pBLAST output using the protein sequence of human RIF1 to search for alignment with the first 185 residues of scRif1. The residue 57 key to Rif1 phosphorylation, and conserved adjacent residues, in budding yeast are highlighted. (B) Structural diagrams of budding yeast Rif1 and human Rif1. The location of S57 residue is notated, alongside the RVxF-SILK domains (translocated to the C-terminal of the protein in humans), the Phospho-Gate Domain (PGD), the RBM, the CTD, and the DNA-binding domain found in humans, and seen to be conserved. Models adapted from Mattarocci *et al.*, (2016).

I analysed a section of the N-terminal region corresponding to the first 180 amino acid residues of yeast Rif1 and used pBlast analysis to search for sequence homology with hRIF1. As previous studies suggest, portions of this this mapped to a region close to the C-terminal of hRIF1, however, results suggested substantial deviation in the protein sequence has occurred over the course of evolution. The most homologous sequence identified was a region stretching from aa14-71 in yeast Rif1 and 2217-2186 in hRIF1. This region had 33% matches in residue sequencing, and 47% overall positive similarity. However, a region this short still provided a relatively high e-score that was not registered as significant. Interestingly, residues S56-58 did precisely map onto a short section within this homologous section (**Figure 8.5A**). However, it must also be considered the role we propose that the phosphorylation of Rif1 plays in yeast, and how this is related to the structure of the protein. If our model is correct, this implies that the phosphorylation of Rif1 acts to mediate the interaction of an adjacent region to the DNA, as well as the HEAT repeats. If this site of phosphorylation was translocated to the C-terminal region of hRIF1 then it is unlikely to have maintained this role in mammalian cells without large changes to the 3D structure of the protein allowing modifications close to the C-terminal to interrupt protein interactions close to the N-terminal (**Figure 8.5B**). It is more likely that alternate residues in the N-terminal region of hRIF1 would have be utilised. Interestingly, there are only 8 instances of the core “SP” CDK1 target sequence within the 1000 residues of hRIF1 protein.

Bibliography

Abreu, C. M., Kumar, R., Hamilton, D., Dawdy, A. W., Creavin, K., Eivers, S., Finn, K., Balsbaugh, J. L., O'Connor, R., Kiely, P. A., Shabanowitz, J., Hunt, D. F., Grenon, M. and Lowndes, N. F. (2013) 'Site-specific phosphorylation of the DNA damage response mediator rad9 by cyclin-dependent kinases regulates activation of checkpoint kinase 1', *PLoS genet*, 9(4), pp. e1003310-e1003310.

Adams, I. R. and McLaren, A. (2004) 'Identification and characterisation of mRif1: a mouse telomere-associated protein highly expressed in germ cells and embryo-derived pluripotent stem cells', *Dev Dyn*, 229(4), pp. 733-44.

Al-Moghrabi, N. M., Al-Sharif, I. S. and Aboussekhra, A. (2001) 'The *Saccharomyces cerevisiae* RAD9 cell cycle checkpoint gene is required for optimal repair of UV-induced pyrimidine dimers in both G(1) and G(2)/M phases of the cell cycle', *Nucleic acids res*, 29(10), pp. 2020-2025.

Albuquerque, C. P., Smolka, M. B., Payne, S. H., Bafna, V., Eng, J. and Zhou, H. (2008) 'A multidimensional chromatography technology for in-depth phosphoproteome analysis', *Mol Cell Prot: MCP*, 7(7), pp. 1389-1396.

Anbalagan, S., Bonetti, D., Lucchini, G. and Longhese, M. P. (2011) 'Rif1 supports the function of the CST complex in yeast telomere capping', *PLoS Genet*, 7(3), p. e1002024.

Andrade, M. A. and Bork, P. (1995) 'HEAT repeats in the Huntington's disease protein', *Nat Genet*, 11(2), pp. 115-6.

Andrade, M. A., Petosa, C., O'Donoghue, S. I., Muller, C. W. and Bork, P. (2001) 'Comparison of ARM and HEAT protein repeats', *J Mol Biol*, 309(1), pp. 1-18.

Aylon, Y., Liefshitz, B. and Kupiec, M. (2004) 'The CDK regulates repair of double-strand breaks by homologous recombination during the cell cycle', *EMBO j*, 23(24), pp. 4868-4875.

Barlow, J. H. and Rothstein, R. (2009) 'Rad52 recruitment is DNA replication independent and regulated by Cdc28 and the Mec1 kinase', *EMBO j*, 28(8), pp. 1121-30.

Barnes, G. and Rio, D. (1997) 'DNA double-strand-break sensitivity, DNA replication, and cell cycle arrest phenotypes of Ku-deficient *Saccharomyces cerevisiae*', *Proc Natl Acad Sci*, 94(3), p. 867.

Bertuch, A. A. and Lundblad, V. (2004) 'EXO1 contributes to telomere maintenance in both telomerase-proficient and telomerase-deficient *Saccharomyces cerevisiae*', *Genetics*, 166(4), pp. 1651-1659.

Bianchi, A., Negrini, S. and Shore, D. (2004) 'Delivery of Yeast Telomerase to a DNA Break Depends on the Recruitment Functions of Cdc13 and Est1', *Mol Cell*, 16(1), pp. 139-146.

Bishop, A. C., Ubersax, J. A., Petsch, D. T., Matheos, D. P., Gray, N. S., Blethrow, J., Shimizu, E., Tsien, J. Z., Schultz, P. G., Rose, M. D., Wood, J. L., Morgan, D. O. and Shokat, K. M. (2000) 'A chemical switch for inhibitor-sensitive alleles of any protein kinase', *Nature*, 407(6802), pp. 395-401.

- Blankley, R. T. and Lydall, D. (2004) 'A domain of Rad9 specifically required for activation of Chk1 in budding yeast', *J Cell Sci*, 117(Pt 4), pp. 601-8.
- Booth, C., Griffith, E., Brady, G. and Lydall, D. (2001) 'Quantitative amplification of single-stranded DNA (QAOS) demonstrates that cdc13-1 mutants generate ssDNA in a telomere to centromere direction', *Nucleic Acids Res*, 29(21), pp. 4414-22.
- Boulton, S. J. and Jackson, S. P. (1996) 'Saccharomyces cerevisiae Ku70 potentiates illegitimate DNA double-strand break repair and serves as a barrier to error-prone DNA repair pathways', *EMBO j*, 15(18), pp. 5093-5103.
- Boulton, S. J. and Jackson, S. P. (1998) 'Components of the Ku-dependent non-homologous end-joining pathway are involved in telomeric length maintenance and telomeric silencing', *EMBO j*, 17(6), pp. 1819-28.
- Breitkreutz, A., Choi, H., Sharom, J. R., Boucher, L., Neduva, V., Larsen, B., Lin, Z. Y., Breitkreutz, B. J., Stark, C., Liu, G., Ahn, J., Dewar-Darch, D., Reguly, T., Tang, X., Almeida, R., Qin, Z. S., Pawson, T., Gingras, A. C., Nesvizhskii, A. I. and Tyers, M. (2010) 'A global protein kinase and phosphatase interaction network in yeast', *Science*, 328(5981), pp. 1043-6.
- Buonomo, S. B. C., Wu, Y., Ferguson, D. and de Lange, T. (2009) 'Mammalian Rif1 contributes to replication stress survival and homology-directed repair', *J Cell Biol*, 187(3), p. 385.
- Burton, J. L. and Solomon, M. J. (2007) 'Mad3p, a pseudosubstrate inhibitor of APCCdc20 in the spindle assembly checkpoint', *Genes Dev*, 21(6), pp. 655-67.
- Capra, J. A., Paeschke, K., Singh, M. and Zakian, V. A. (2010) 'G-quadruplex DNA sequences are evolutionarily conserved and associated with distinct genomic features in Saccharomyces cerevisiae', *PLoS Comput Biol*, 6(7), p. e1000861.
- Chan, A., Boulé, J.-B. and Zakian, V. A. (2008) 'Two pathways recruit telomerase to Saccharomyces cerevisiae telomeres', *PLoS Genet*, 4(10), pp. e1000236-e1000236.
- Chan, C. S. and Tye, B. K. (1983) 'Organization of DNA sequences and replication origins at yeast telomeres', *Cell*, 33(2), pp. 563-73.
- Chang, F. and Herskowitz, I. (1990) 'Identification of a gene necessary for cell cycle arrest by a negative growth factor of yeast: FAR1 is an inhibitor of a G1 cyclin, CLN2', *Cell*, 63(5), pp. 999-1011.
- Chapman, J. R., Barral, P., Vannier, J. B., Borel, V., Steger, M., Tomas-Loba, A., Sartori, A. A., Adams, I. R., Batista, F. D. and Boulton, S. J. (2013) 'RIF1 is essential for 53BP1-dependent nonhomologous end joining and suppression of DNA double-strand break resection', *Mol Cell*, 49(5), pp. 858-71.
- Chappidi, N., De Gregorio, G. and Ferrari, S. (2019) 'Replication stress-induced Exo1 phosphorylation is mediated by Rad53/Pph3 and Exo1 nuclear localization is controlled by 14-3-3 proteins', *Cell division*, 14, pp. 1-1.

- Chen, H., Donnianni, R. A., Handa, N., Deng, S. K., Oh, J., Timashev, L. A., Kowalczykowski, S. C. and Symington, L. S. (2015) 'Sae2 promotes DNA damage resistance by removing the Mre11-Rad50-Xrs2 complex from DNA and attenuating Rad53 signaling', *Proc Natl Acad Sci U S A*, 112(15), pp. E1880-7.
- Chen, L., Trujillo, K., Ramos, W., Sung, P. and Tomkinson, A. E. (2001a) 'Promotion of Dnl4-Catalyzed DNA End-Joining by the Rad50/Mre11/Xrs2 and Hdf1/Hdf2 Complexes', *Mol Cell*, 8(5), pp. 1105-1115.
- Chen, L. Y., Majerska, J. and Lingner, J. (2013) 'Molecular basis of telomere syndrome caused by CTC1 mutations', *Genes Dev*, 27(19), pp. 2099-108.
- Chen, Q., Ijma, A. and Greider, C. W. (2001b) 'Two survivor pathways that allow growth in the absence of telomerase are generated by distinct telomere recombination events', *Mol Cell Biol*, 21(5), pp. 1819-1827.
- Chen, Z., Odstrcil, E. A., Tu, B. P. and McKnight, S. L. (2007) 'Restriction of DNA replication to the reductive phase of the metabolic cycle protects genome integrity', *Science*, 316(5833), pp. 1916-9.
- Cheng, L., Hunke, L. and Hardy, C. F. (1998) 'Cell cycle regulation of the *Saccharomyces cerevisiae* polo-like kinase cdc5p', *Mol Cell Biol*, 18(12), pp. 7360-7370.
- Choudhary, C., Kumar, C., Gnad, F., Nielsen, M. L., Rehman, M., Walther, T. C., Olsen, J. V. and Mann, M. (2009) 'Lysine acetylation targets protein complexes and co-regulates major cellular functions', *Science*, 325(5942), pp. 834-40.
- Ciosk, R., Zachariae, W., Michaelis, C., Shevchenko, A., Mann, M. and Nasmyth, K. (1998) 'An ESP1/PDS1 complex regulates loss of sister chromatid cohesion at the metaphase to anaphase transition in yeast', *Cell*, 93(6), pp. 1067-76.
- Clemenson, C. and Marsolier-Kergoat, M. C. (2006) 'The spindle assembly checkpoint regulates the phosphorylation state of a subset of DNA checkpoint proteins in *Saccharomyces cerevisiae*', *Mol Cell Biol*, 26(24), pp. 9149-61.
- Clerici, M., Mantiero, D., Lucchini, G. and Longhese, M. P. (2006) 'The *Saccharomyces cerevisiae* Sae2 protein negatively regulates DNA damage checkpoint signalling', *EMBO rep*, 7(2), pp. 212-218.
- Clikeman, J. A., Khalsa, G. J., Barton, S. L. and Nickoloff, J. A. (2001) 'Homologous recombinational repair of double-strand breaks in yeast is enhanced by MAT heterozygosity through yKU-dependent and -independent mechanisms', *Genetics*, 157(2), pp. 579-589.
- Conrad, M. N., Wright, J. H., Wolf, A. J. and Zakian, V. A. (1990) 'RAP1 protein interacts with yeast telomeres in vivo: Overproduction alters telomere structure and decreases chromosome stability', *Cell*, 63(4), pp. 739-750.
- Cornacchia, D., Dileep, V., Quivy, J. P., Foti, R., Tili, F., Santarella-Mellwig, R., Antony, C., Almouzni, G., Gilbert, D. M. and Buonomo, S. B. (2012) 'Mouse Rif1 is a key regulator of the replication-timing programme in mammalian cells', *EMBO j*, 31(18), pp. 3678-90.

- Costanzo, M., Nishikawa, J. L., Tang, X., Millman, J. S., Schub, O., Breitzkreuz, K., Dewar, D., Rupes, I., Andrews, B. and Tyers, M. (2004) 'CDK activity antagonizes Whi5, an inhibitor of G1/S transcription in yeast', *Cell*, 117(7), pp. 899-913.
- Crasta, K., Lim, H. H., Zhang, T., Nirantar, S. and Surana, U. (2008) 'Consorting kinases, end of destruction and birth of a spindle', *Cell Cycle*, 7(19), pp. 2960-6.
- Dahmann, C., Diffley, J. F. and Nasmyth, K. A. (1995) 'S-phase-promoting cyclin-dependent kinases prevent re-replication by inhibiting the transition of replication origins to a pre-replicative state', *Curr Biol*, 5(11), pp. 1257-69.
- Dan, J., Liu, Y., Liu, N., Chiourea, M., Okuka, M., Wu, T., Ye, X., Mou, C., Wang, L., Wang, L., Yin, Y., Yuan, J., Zuo, B., Wang, F., Li, Z., Pan, X., Yin, Z., Chen, L., Keefe, David L., Gagos, S., Xiao, A. and Liu, L. (2014) 'Rif1 Maintains Telomere Length Homeostasis of ESCs by Mediating Heterochromatin Silencing', *Dev Cell*, 29(1), pp. 7-19.
- Davé, A., Cooley, C., Garg, M. and Bianchi, A. (2014) 'Protein phosphatase 1 recruitment by Rif1 regulates DNA replication origin firing by counteracting DDK activity', *Cell Rep*, 7(1), pp. 53-61.
- Di Virgilio, M., Callen, E., Yamane, A., Zhang, W., Jankovic, M., Gitlin, A. D., Feldhahn, N., Resch, W., Oliveira, T. Y., Chait, B. T., Nussenzweig, A., Casellas, R., Robbiani, D. F. and Nussenzweig, M. C. (2013) 'Rif1 prevents resection of DNA breaks and promotes immunoglobulin class switching', *Science*, 339(6120), pp. 711-5.
- Diani, L., Colombelli, C., Nachimuthu, B. T., Donnianni, R., Plevani, P., Muzi-Falconi, M. and Pellicoli, A. (2009a) 'Saccharomyces CDK1 phosphorylates Rad53 kinase in metaphase, influencing cellular morphogenesis', *J Biol Chem*, 284(47), pp. 32627-34.
- Donaldson, A. D. (2005) 'Shaping time: chromatin structure and the DNA replication programme', *Trends in Genetics*, 21(8), pp. 444-449.
- Egloff, M. P., Cohen, P. T., Reinemer, P. and Barford, D. (1995) 'Crystal structure of the catalytic subunit of human protein phosphatase 1 and its complex with tungstate', *J Mol Biol*, 254(5), pp. 942-59.
- Ellison, V. and Stillman, B. (2003) 'Biochemical characterization of DNA damage checkpoint complexes: clamp loader and clamp complexes with specificity for 5' recessed DNA', *PLoS Biol*, 1(2), pp. E33-E33.
- Emili, A. (1998) 'MEC1 Dependent Phosphorylation of Rad9p in Response to DNA Damage', *Mol Cell*, 2(2), pp. 183-189.
- Enserink, J. M., Hombauer, H., Huang, M.-E. and Kolodner, R. D. (2009) 'Cdc28/Cdk1 positively and negatively affects genome stability in *S. cerevisiae*', *J Cell Biol*, 185(3), p. 423.
- Enserink, J. M. and Kolodner, R. D. (2010) 'An overview of Cdk1-controlled targets and processes', *Cell division*, 5, pp. 11-11.

- Escribano-Diaz, C., Orthwein, A., Fradet-Turcotte, A., Xing, M., Young, J. T., Tkac, J., Cook, M. A., Rosebrock, A. P., Munro, M., Canny, M. D., Xu, D. and Durocher, D. (2013) 'A cell cycle-dependent regulatory circuit composed of 53BP1-RIF1 and BRCA1-CtIP controls DNA repair pathway choice', *Mol Cell*, 49(5), pp. 872-83.
- Evans, S. K. and Lundblad, V. (1999) 'Est1 and Cdc13 as comediators of telomerase access', *Science*, 286(5437), pp. 117-20.
- Eytan, E., Wang, K., Miniowitz-Shemtov, S., Sitry-Shevah, D., Kaisari, S., Yen, T. J., Liu, S. T. and Hershko, A. (2014) 'Disassembly of mitotic checkpoint complexes by the joint action of the AAA-ATPase TRIP13 and p31(comet)', *Proc Natl Acad Sci U S A*, 111(33), pp. 12019-24.
- Faure, V., Coulon, S., Hardy, J. and Géli, V. (2010) 'Cdc13 and Telomerase Bind through Different Mechanisms at the Lagging- and Leading-Strand Telomeres', *Mol Cell*, 38(6), pp. 842-852.
- Feldmann, H. and Winnacker, E. L. (1993) 'A putative homologue of the human autoantigen Ku from *Saccharomyces cerevisiae*', *J Biol Chem*, 268(17), pp. 12895-900.
- Fisher, T. S., Taggart, A. K. and Zakian, V. A. (2004) 'Cell cycle-dependent regulation of yeast telomerase by Ku', *Nat Struct Mol Biol*, 11(12), pp. 1198-205.
- Fisher, T. S. and Zakian, V. A. (2005) 'Ku: A multifunctional protein involved in telomere maintenance', *DNA Repair*, 4(11), pp. 1215-1226.
- Fontana, G. A., Hess, D., Reinert, J. K., Mattarocci, S., Falquet, B., Klein, D., Shore, D., Thomä, N. H. and Rass, U. (2019) 'Rif1 S-acylation mediates DNA double-strand break repair at the inner nuclear membrane', *Nat Comms*, 10(1), p. 2535.
- Foster, S. S., Zubko, M. K., Guillard, S. and Lydall, D. (2006) 'MRX protects telomeric DNA at uncapped telomeres of budding yeast cdc13-1 mutants', *DNA Repair (Amst)*, 5(7), pp. 840-51.
- Frank, C. J., Hyde, M. and Greider, C. W. (2006) 'Regulation of Telomere Elongation by the Cyclin-Dependent Kinase CDK1', *Mol Cell*, 24(3), pp. 423-432.
- Friedman, K. L. and Cech, T. R. (1999) 'Essential functions of amino-terminal domains in the yeast telomerase catalytic subunit revealed by selection for viable mutants', *Genes Dev*, 13(21), pp. 2863-2874.
- Galgoczy, D. J. and Toczyski, D. P. (2001) 'Checkpoint adaptation precedes spontaneous and damage-induced genomic instability in yeast', *Mol Cell Biol*, 21(5), pp. 1710-8.
- Gao, H., Cervantes, R. B., Mandell, E. K., Otero, J. H. and Lundblad, V. (2007) 'RPA-like proteins mediate yeast telomere function', *Nat Struct Mol Biol*, 14, p. 208.
- Gardner, R., Putnam, C. W. and Weinert, T. (1999) 'RAD53, DUN1 and PDS1 define two parallel G2/M checkpoint pathways in budding yeast', *EMBO j*, 18(11), pp. 3173-3185.

- Gartner, A., Jovanovic, A., Jeoung, D. I., Bourlat, S., Cross, F. R. and Ammerer, G. (1998) 'Pheromone-dependent G1 cell cycle arrest requires Far1 phosphorylation, but may not involve inhibition of Cdc28-Cln2 kinase, in vivo', *Mol Cell Biol*, 18(7), pp. 3681-91.
- Garvik, B., Carson, M. and Hartwell, L. (1995) 'Single-stranded DNA arising at telomeres in cdc13 mutants may constitute a specific signal for the RAD9 checkpoint', *Mol Cell Biol*, 15(11), pp. 6128-6138.
- Garzón, J., Ursich, S., Lopes, M., Hiraga, S.-i. and Donaldson, A. D. (2019) 'Human RIF1-Protein Phosphatase 1 Prevents Degradation and Breakage of Nascent DNA on Replication Stalling', *Cell Rep*, 27(9), pp. 2558-2566.e4.
- Gelinas, A. D., Paschini, M., Reyes, F. E., Héroux, A., Batey, R. T., Lundblad, V. and Wuttke, D. S. (2009) 'Telomere capping proteins are structurally related to RPA with an additional telomere-specific domain', *Proc Natl Acad Sci U S A*, 106(46), pp. 19298-19303.
- Geserick, C. and Blasco, M. A. (2006) 'Novel roles for telomerase in aging', *Mechanisms of Ageing and Development*, 127(6), pp. 579-583.
- Geymonat, M., Spanos, A., Wells, G. P., Smerdon, S. J. and Sedgwick, S. G. (2004) 'Cib6/Cdc28 and Cdc14 regulate phosphorylation status and cellular localization of Swi6', *Mol Cell Biol*, 24(6), pp. 2277-85.
- Gilson, E., Roberge, M., Giraldo, R., Rhodes, D. and Gasser, S. M. (1993) 'Distortion of the DNA Double Helix by RAP1 at Silencers and Multiple Telomeric Binding Sites', *J Mol Biol*, 231(2), pp. 293-310.
- Grandin, N., Damon, C. and Charbonneau, M. (2000) 'Cdc13 cooperates with the yeast Ku proteins and Stn1 to regulate telomerase recruitment', *Mol Cell Biol*, 20(22), pp. 8397-8408.
- Grandin, N., Damon, C. and Charbonneau, M. (2001) 'Cdc13 prevents telomere uncapping and Rad50-dependent homologous recombination', *EMBO j*, 20(21), pp. 6127-6139.
- Grandin, N., Reed, S. I. and Charbonneau, M. (1997) 'Stn1, a new *Saccharomyces cerevisiae* protein, is implicated in telomere size regulation in association with Cdc13', *Genes Dev*, 11(4), pp. 512-27.
- Gravel, S., Larrivee, M., Labrecque, P. and Wellinger, R. J. (1998) 'Yeast Ku as a regulator of chromosomal DNA end structure', *Science*, 280(5364), pp. 741-4.
- Gravel, S. and Wellinger, R. J. (2002) 'Maintenance of double-stranded telomeric repeats as the critical determinant for cell viability in yeast cells lacking Ku', *Mol Cell Biol*, 22(7), pp. 2182-93.
- Greider, C. W. and Blackburn, E. H. (1987) 'The telomere terminal transferase of tetrahymena is a ribonucleoprotein enzyme with two kinds of primer specificity', *Cell*, 51(6), pp. 887-898.
- Griffith, J. D., Comeau, L., Rosenfield, S., Stansel, R. M., Bianchi, A., Moss, H. and de Lange, T. (1999) 'Mammalian Telomeres End in a Large Duplex Loop', *Cell*, 97(4), pp. 503-514.
- Grossi, S., Puglisi, A., Dmitriev, P. V., Lopes, M. and Shore, D. (2004) 'Pol12, the B subunit of DNA polymerase alpha, functions in both telomere capping and length regulation', *Genes Dev*, 18(9), pp. 992-1006.

- Guillemain, G., Ma, E., Mauger, S., Miron, S., Thai, R., Guerois, R., Ochsenbein, F. and Marsolier-Kergoat, M. C. (2007) 'Mechanisms of checkpoint kinase Rad53 inactivation after a double-strand break in *Saccharomyces cerevisiae*', *Mol Cell Biol*, 27(9), pp. 3378-89.
- Gurden, M. D., Anderhub, S. J., Faisal, A. and Linardopoulos, S. (2018) 'Aurora B prevents premature removal of spindle assembly checkpoint proteins from the kinetochore: A key role for Aurora B in mitosis', *Oncotarget*, 9(28), pp. 19525-19542.
- Haase, S. B. and Reed, S. I. (1999) 'Evidence that a free-running oscillator drives G1 events in the budding yeast cell cycle', *Nature*, 401(6751), pp. 394-7.
- Hafner, L., Lezaja, A., Zhang, X., Lemmens, L., Shyian, M., Albert, B., Follonier, C., Nunes, J. M., Lopes, M., Shore, D. and Mattarocci, S. (2018) 'Rif1 Binding and Control of Chromosome-Internal DNA Replication Origins Is Limited by Telomere Sequestration', *Cell Rep*, 23(4), pp. 983-992.
- Hardy, C. F., Sussel, L. and Shore, D. (1992) 'A RAP1-interacting protein involved in transcriptional silencing and telomere length regulation', *Genes Dev*, 6(5), pp. 801-14.
- Harrison, J. C. and Haber, J. E. (2006) 'Surviving the Breakup: The DNA Damage Checkpoint', *Annual Review of Genetics*, 40(1), pp. 209-235.
- Hayano, M., Kanoh, Y., Matsumoto, S., Renard-Guillet, C., Shirahige, K. and Masai, H. (2012) 'Rif1 is a global regulator of timing of replication origin firing in fission yeast', *Genes Dev*, 26(2), pp. 137-50.
- Hecht, A., Laroche, T., Strahl-Bolsinger, S., Gasser, S. M. and Grunstein, M. (1995) 'Histone H3 and H4 N-termini interact with SIR3 and SIR4 proteins: A molecular model for the formation of heterochromatin in yeast', *Cell*, 80(4), pp. 583-592.
- Heller, R. C., Kang, S., Lam, W. M., Chen, S., Chan, C. S. and Bell, S. P. (2011) 'Eukaryotic origin-dependent DNA replication in vitro reveals sequential action of DDK and S-CDK kinases', *Cell*, 146(1), pp. 80-91.
- Hendrickx, A., Beullens, M., Ceulemans, H., Den Abt, T., Van Eynde, A., Nicolaescu, E., Lesage, B. and Bollen, M. (2009) 'Docking motif-guided mapping of the interactome of protein phosphatase-1', *Chem Biol*, 16(4), pp. 365-71.
- Henson, J. D., Neumann, A. A., Yeager, T. R. and Reddel, R. R. (2002) 'Alternative lengthening of telomeres in mammalian cells', *Oncogene*, 21(4), pp. 598-610.
- Herskowitz, I. (1995) 'MAP kinase pathways in yeast: For mating and more', *Cell*, 80(2), pp. 187-197.
- Hiraga, S., Alvino, G. M., Chang, F., Lian, H. Y., Sridhar, A., Kubota, T., Brewer, B. J., Weinreich, M., Raghuraman, M. K. and Donaldson, A. D. (2014) 'Rif1 controls DNA replication by directing Protein Phosphatase 1 to reverse Cdc7-mediated phosphorylation of the MCM complex', *Genes Dev*, 28(4), pp. 372-83.
- Hiraga, S. I., Ly, T., Garzon, J., Horejsi, Z., Ohkubo, Y. N., Endo, A., Obuse, C., Boulton, S. J., Lamond, A. I. and Donaldson, A. D. (2017) 'Human RIF1 and protein phosphatase 1 stimulate DNA replication origin licensing but suppress origin activation', *EMBO Rep*, 18(3), pp. 403-419.

- Hiraga, S. I., Monerawela, C., Katou, Y., Shaw, S., Clark, K. R., Shirahige, K. and Donaldson, A. D. (2018) 'Budding yeast Rif1 binds to replication origins and protects DNA at blocked replication forks', *EMBO Rep*, 19(9), p. e46222.
- Hirano, Y., Fukunaga, K. and Sugimoto, K. (2009) 'Rif1 and rif2 inhibit localization of tel1 to DNA ends', *Mol Cell*, 33(3), pp. 312-22.
- Holt, L., Tuch, B. B., Villén, J., Johnson, A. D., Gygi, S. P. and Morgan, D. O. (2009a) 'Global analysis of Cdk1 substrate phosphorylation sites provides insights into evolution', *Science (New York, N.Y.)*, 325(5948), pp. 1682-1686.
- dk1 substrate phosphorylation sites provides insights into evolution', *Science*, 325(5948), pp. 1682-6.
- Horowitz, H., Thorburn, P. and Haber, J. E. (1984) 'Rearrangements of highly polymorphic regions near telomeres of *Saccharomyces cerevisiae*', *Mol Cell Biol*, 4(11), pp. 2509-2517.
- Hoyt, M. A., He, L., Loo, K. K. and Saunders, W. S. (1992) 'Two *Saccharomyces cerevisiae* kinesin-related gene products required for mitotic spindle assembly', *J Cell Biol*, 118(1), pp. 109-20.
- Hu, F., Wang, Y., Liu, D., Li, Y., Qin, J. and Elledge, S. J. (2001) 'Regulation of the Bub2/Bfa1 GAP Complex by Cdc5 and Cell Cycle Checkpoints', *Cell*, 107(5), pp. 655-665.
- Huang, D., Friesen, H. and Andrews, B. (2007) 'Pho85, a multifunctional cyclin-dependent protein kinase in budding yeast', *Mol Microbiol*, 66(2), pp. 303-14.
- Huertas, P., Cortes-Ledesma, F., Sartori, A. A., Aguilera, A. and Jackson, S. P. (2008) 'CDK targets Sae2 to control DNA-end resection and homologous recombination', *Nature*, 455(7213), pp. 689-92.
- Hughes, T. R., Weilbaecher, R. G., Walterscheid, M. and Lundblad, V. (2000) 'Identification of the single-strand telomeric DNA binding domain of the *Saccharomyces cerevisiae* Cdc13 protein', *Proc Natl Acad Sci*, 97(12), p. 6457.
- Hwang, L. H., Lau, L. F., Smith, D. L., Mistrot, C. A., Hardwick, K. G., Hwang, E. S., Amon, A. and Murray, A. W. (1998) 'Budding yeast Cdc20: a target of the spindle checkpoint', *Science*, 279(5353), pp. 1041-4.
- Ijpm, A. S. and Greider, C. W. (2003) 'Short telomeres induce a DNA damage response in *Saccharomyces cerevisiae*', *Mol Biol Cell*, 14(3), pp. 987-1001.
- Ira, G., Pelliccioli, A., Balijja, A., Wang, X., Fiorani, S., Carotenuto, W., Liberi, G., Bressan, D., Wan, L., Hollingsworth, N. M., Haber, J. E. and Foiani, M. (2004) 'DNA end resection, homologous recombination and DNA damage checkpoint activation require CDK1', *Nature*, 431(7011), pp. 1011-1017.
- Jaspersen, S. L. and Morgan, D. O. (2000) 'Cdc14 activates cdc15 to promote mitotic exit in budding yeast', *Curr Biol*, 10(10), pp. 615-8.
- Jia, X., Weinert, T. and Lydall, D. (2004) 'Mec1 and Rad53 inhibit formation of single-stranded DNA at telomeres of *Saccharomyces cerevisiae* cdc13-1 mutants', *Genetics*, 166(2), pp. 753-64.

- Kaizer, H., Connelly, C. J., Bettridge, K., Viggiani, C. and Greider, C. W. (2015) 'Regulation of Telomere Length Requires a Conserved N-Terminal Domain of Rif2 in *Saccharomyces cerevisiae*', *Genetics*, 201(2), pp. 573-586.
- Kalsbeek, D. and Golsteyn, R. M. (2017) 'G2/M-Phase Checkpoint Adaptation and Micronuclei Formation as Mechanisms That Contribute to Genomic Instability in Human Cells', *Int J Mol Sci*, 18(11).
- Kanoh, J. and Ishikawa, F. (2001) 'spRap1 and spRif1, recruited to telomeres by Taz1, are essential for telomere function in fission yeast', *Curr Biol*, 11(20), pp. 1624-1630.
- Kanoh, Y., Matsumoto, S., Fukatsu, R., Kakusho, N., Kono, N., Renard-Guillet, C., Masuda, K., Iida, K., Nagasawa, K., Shirahige, K. and Masai, H. (2015) 'Rif1 binds to G quadruplexes and suppresses replication over long distances', *Nat Struct Mol Biol*, 22(11), pp. 889-97.
- Kaye, J. A., Melo, J. A., Cheung, S. K., Vaze, M. B., Haber, J. E. and Toczyski, D. P. (2004) 'DNA breaks promote genomic instability by impeding proper chromosome segregation', *Curr Biol*, 14(23), pp. 2096-106.
- Keaton, M. A. and Lew, D. J. (2006) 'Eavesdropping on the cytoskeleton: progress and controversy in the yeast morphogenesis checkpoint', *Curr Opin Microbiol*, 9(6), pp. 540-6.
- Kedziora, S., Gali, V. K., Wilson, R. H. C., Clark, K. R. M., Nieduszynski, C. A., Hiraga, S. I. and Donaldson, A. D. (2018) 'Rif1 acts through Protein Phosphatase 1 but independent of replication timing to suppress telomere extension in budding yeast', *Nucleic Acids Res*, 46(8), pp. 3993-4003.
- Kobayashi, S., Fukatsu, R., Kanoh, Y., Kakusho, N., Matsumoto, S., Chaen, S. and Masai, H. (2019) 'Both a Unique Motif at the C Terminus and an N-Terminal HEAT Repeat Contribute to G-Quadruplex Binding and Origin Regulation by the Rif1 Protein', *Mol Cell Biol*, 39(4).
- König, P., Giraldo, R., Chapman, L. and Rhodes, D. (1996) 'The Crystal Structure of the DNA-Binding Domain of Yeast RAP1 in Complex with Telomeric DNA', *Cell*, 85(1), pp. 125-136.
- Krejci, L., Van Komen, S., Li, Y., Villemain, J., Reddy, M. S., Klein, H., Ellenberger, T. and Sung, P. (2003) 'DNA helicase Srs2 disrupts the Rad51 presynaptic filament', *Nature*, 423(6937), pp. 305-9.
- Kumar, R. and Cheek, C. F. (2017) 'Dynamics of RIF1 SUMOylation is regulated by PIAS4 in the maintenance of Genomic Stability', *Scientific Reports*, 7(1), p. 17367.
- Kyrion, G., Boakye, K. A. and Lustig, A. J. (1992) 'C-terminal truncation of RAP1 results in the deregulation of telomere size, stability, and function in *Saccharomyces cerevisiae*', *Mol Cell Biol*, 12(11), pp. 5159-73.
- Labib, K. and Gambus, A. (2007) 'A key role for the GINS complex at DNA replication forks', *Trends Cell Biol*, 17(6), pp. 271-8.
- Lans, H., Martejijn, J. A. and Vermeulen, W. (2012) 'ATP-dependent chromatin remodeling in the DNA-damage response', *Epigenetics & Chromatin*, 5(1), p. 4.

- Lara-Gonzalez, P., Westhorpe, Frederick G. and Taylor, Stephen S. (2012) 'The Spindle Assembly Checkpoint', *Curr Biology*, 22(22), pp. R966-R980.
- Laroche, T., Martin, S. G., Gotta, M., Gorham, H. C., Pryde, F. E., Louis, E. J. and Gasser, S. M. (1998) 'Mutation of yeast Ku genes disrupts the subnuclear organization of telomeres', *Curr Biol*, 8(11), pp. 653-6.
- Larrivee, M. and Wellinger, R. J. (2006) 'Telomerase- and capping-independent yeast survivors with alternate telomere states', *Nat Cell Biol*, 8(7), pp. 741-7.
- Lee, J. M. and Greenleaf, A. L. (1991) 'CTD kinase large subunit is encoded by CTK1, a gene required for normal growth of *Saccharomyces cerevisiae*', *Gene Expr*, 1(2), pp. 149-67.
- Lee, S. E., Frenz, L. M., Wells, N. J., Johnson, A. L. and Johnston, L. H. (2001) 'Order of function of the budding-yeast mitotic exit-network proteins Tem1, Cdc15, Mob1, Dbf2, and Cdc5', *Curr Biol*, 11(10), pp. 784-788.
- Lee, S. E., Moore, J. K., Holmes, A., Umezū, K., Kolodner, R. D. and Haber, J. E. (1998) 'Saccharomyces Ku70, mre11/rad50 and RPA proteins regulate adaptation to G2/M arrest after DNA damage', *Cell*, 94(3), pp. 399-409.
- Lee, S. E., Pelliccioli, A., Vaze, M. B., Sugawara, N., Malkova, A., Foiani, M. and Haber, J. E. (2003) 'Yeast Rad52 and Rad51 recombination proteins define a second pathway of DNA damage assessment in response to a single double-strand break', *Mol Cell Biol*, 23(23), pp. 8913-8923.
- Lemon, L. D., Morris, D. K. and Bertuch, A. A. (2019) 'Loss of Ku's DNA end binding activity affects telomere length via destabilizing telomere-bound Est1 rather than altering TLC1 homeostasis', *Scientific Rep*, 9(1), p. 10607.
- Leroy, C., Lee, S. E., Vaze, M. B., Ochsenbein, F., Guerois, R., Haber, J. E. and Marsolier-Kergoat, M. C. (2003) 'PP2C phosphatases Ptc2 and Ptc3 are required for DNA checkpoint inactivation after a double-strand break', *Mol Cell*, 11(3), pp. 827-35.
- Levy, D. L. and Blackburn, E. H. (2004) 'Counting of Rif1p and Rif2p on *Saccharomyces cerevisiae* telomeres regulates telomere length', *Mol Cell Biol*, 24(24), pp. 10857-10867.
- Lew, D. J. and Reed, S. I. (1993) 'Morphogenesis in the yeast cell cycle: regulation by Cdc28 and cyclins', *J Cell Biol*, 120(6), pp. 1305-20.
- Li, B. and de Lange, T. (2003) 'Rap1 affects the length and heterogeneity of human telomeres', *Mol Biol Cell*, 14(12), pp. 5060-5068.
- Li, R. and Murray, A. W. (1991) 'Feedback control of mitosis in budding yeast', *Cell*, 66(3), pp. 519-31.
- Li, S., Makovets, S., Matsuguchi, T., Blethrow, J. D., Shokat, K. M. and Blackburn, E. H. (2009) 'Cdk1-dependent phosphorylation of Cdc13 coordinates telomere elongation during cell-cycle progression', *Cell*, 136(1), pp. 50-61.

- Lian, H. Y., Robertson, E. D., Hiraga, S., Alvino, G. M., Collingwood, D., McCune, H. J., Sridhar, A., Brewer, B. J., Raghuraman, M. K. and Donaldson, A. D. (2011) 'The effect of Ku on telomere replication time is mediated by telomere length but is independent of histone tail acetylation', *Mol Biol Cell*, 22(10), pp. 1753-65.
- Liang, F. and Wang, Y. (2007) 'DNA Damage Checkpoints Inhibit Mitotic Exit by Two Different Mechanisms', *Mol Cell Biol*, 27(14), p. 5067.
- Liberi, G., Chiolo, I., Pelliccioli, A., Lopes, M., Plevani, P., Muzi-Falconi, M. and Foiani, M. (2000) 'Srs2 DNA helicase is involved in checkpoint response and its regulation requires a functional Mec1-dependent pathway and Cdk1 activity', *EMBO j*, 19(18), pp. 5027-38.
- Lieb, J. D., Liu, X., Botstein, D. and Brown, P. O. (2001) 'Promoter-specific binding of Rap1 revealed by genome-wide maps of protein-DNA association', *Nat Genet*, 28(4), pp. 327-334.
- Lin, J. J. and Zakian, V. A. (1996) 'The *Saccharomyces* CDC13 protein is a single-strand TG1-3 telomeric DNA-binding protein in vitro that affects telomere behavior in vivo', *Proc Natl Acad Sci U S A*, 93(24), pp. 13760-13765.
- Lingner, J., Cech, T. R., Hughes, T. R. and Lundblad, V. (1997) 'Three Ever Shorter Telomere (EST) genes are dispensable for in vitro yeast telomerase activity', *Proc Natl Acad Sci U S A*, 94(21), pp. 11190-11195.
- Liu, J. and Kipreos, E. T. (2000) 'Evolution of cyclin-dependent kinases (CDKs) and CDK-activating kinases (CAKs): differential conservation of CAKs in yeast and metazoa', *Mol Biol Evol*, 17(7), pp. 1061-74.
- Longtine, M. S., Wilson, N. M., Petracek, M. E. and Berman, J. (1989) 'A yeast telomere binding activity binds to two related telomere sequence motifs and is indistinguishable from RAP1', *Curr Genet*, 16(4), pp. 225-39.
- Lopez, C. R., Ribes-Zamora, A., Indiviglio, S. M., Williams, C. L., Haricharan, S. and Bertuch, A. A. (2011) 'Ku must load directly onto the chromosome end in order to mediate its telomeric functions', *PLoS Genet*, 7(8), p. e1002233.
- Louis, E. J. and Haber, J. E. (1992) 'The structure and evolution of subtelomeric Y' repeats in *Saccharomyces cerevisiae*', *Genetics*, 131(3), pp. 559-574.
- Lue, N. F., Chan, J., Wright, W. E. and Hurwitz, J. (2014) 'The CDC13-STN1-TEN1 complex stimulates Pol α activity by promoting RNA priming and primase-to-polymerase switch', *Nat Comms*, 5, pp. 5762-5762.
- Lundblad, V. and Blackburn, E. H. (1993) 'An alternative pathway for yeast telomere maintenance rescues est1- senescence', *Cell*, 73(2), pp. 347-60.
- Lundblad, V. and Szostak, J. W. (1989) 'A mutant with a defect in telomere elongation leads to senescence in yeast', *Cell*, 57(4), pp. 633-43.
- Luo, K., Vega-Palas, M. A. and Grunstein, M. (2002) 'Rap1-Sir4 binding independent of other Sir, yKu, or histone interactions initiates the assembly of telomeric heterochromatin in yeast', *Genes Dev*, 16(12), pp. 1528-1539.

- Lupardus, P. J. and Cimprich, K. A. (2004) 'Checkpoint adaptation; molecular mechanisms uncovered', *Cell*, 117(5), pp. 555-6.
- MacGilvray, M. E., Shishkova, E., Chasman, D., Place, M., Gitter, A., Coon, J. J. and Gasch, A. P. (2018) 'Network inference reveals novel connections in pathways regulating growth and defense in the yeast salt response', *PLoS Comput Biol*, 13(5), p. e1006088.
- Mah, A. S., Jang, J. and Deshaies, R. J. (2001) 'Protein kinase Cdc15 activates the Dbf2-Mob1 kinase complex', *Proc Natl Acad Sci U S A*, 98(13), pp. 7325-30.
- Majka, J., Niedziela-Majka, A. and Burgers, P. M. J. (2006) 'The checkpoint clamp activates Mec1 kinase during initiation of the DNA damage checkpoint', *Mol Cell*, 24(6), pp. 891-901.
- Makarov, V. L., Hirose, Y. and Langmore, J. P. (1997) 'Long G Tails at Both Ends of Human Chromosomes Suggest a C Strand Degradation Mechanism for Telomere Shortening', *Cell*, 88(5), pp. 657-666.
- Mantiero, D., Mackenzie, A., Donaldson, A. and Zegerman, P. (2011) 'Limiting replication initiation factors execute the temporal programme of origin firing in budding yeast', *Embo j*, 30(23), pp. 4805-14.
- Marcand, S., Gilson, E. and Shore, D. (1997) 'A protein-counting mechanism for telomere length regulation in yeast', *Science*, 275(5302), pp. 986-90.
- Marcand, S., Pardo, B., Gratias, A., Cahun, S. and Callebaut, I. (2008) 'Multiple pathways inhibit NHEJ at telomeres', *Genes Dev*, 22(9), pp. 1153-1158.
- Maringele, L. and Lydall, D. (2002) 'EXO1-dependent single-stranded DNA at telomeres activates subsets of DNA damage and spindle checkpoint pathways in budding yeast yku70Delta mutants', *Genes Dev*, 16(15), pp. 1919-33.
- Maringele, L. and Lydall, D. (2004a) 'Telomerase- and recombination-independent immortalization of budding yeast', *Genes Dev*, 18(21), pp. 2663-75.
- Maringele, L. and Lydall, D. (2004b) 'Telomerase- and recombination-independent immortalization of budding yeast', *Genes Dev*, 18(21), pp. 2663-2675.
- Martina, M., Bonetti, D., Villa, M., Lucchini, G. and Longhese, M. P. (2014) 'Saccharomyces cerevisiae Rif1 cooperates with MRX-Sae2 in promoting DNA-end resection', *EMBO Rep*, 15(6), pp. 695-704.
- Masumoto, H., Sugino, A. and Araki, H. (2000) 'Dpb11 controls the association between DNA polymerases alpha and epsilon and the autonomously replicating sequence region of budding yeast', *Mol Cell Biol*, 20(8), pp. 2809-17.
- Mattarocci, S., Hafner, L., Lezaja, A., Shyian, M. and Shore, D. (2016) 'Rif1: A Conserved Regulator of DNA Replication and Repair Hijacked by Telomeres in Yeasts', *Front Genet*, 7, p. 45.

- Mattarocci, S., Reinert, J. K., Bunker, R. D., Fontana, G. A., Shi, T., Klein, D., Cavadini, S., Faty, M., Shyian, M., Hafner, L., Shore, D., Thoma, N. H. and Rass, U. (2017) 'Rif1 maintains telomeres and mediates DNA repair by encasing DNA ends', *Nat Struct Mol Biol*, 24(7), pp. 588-595.
- Mattarocci, S., Shyian, M., Lemmens, L., Damay, P., Altintas, D. M., Shi, T., Bartholomew, C. R., Thoma, N. H., Hardy, C. F. and Shore, D. (2014) 'Rif1 controls DNA replication timing in yeast through the PP1 phosphatase Glc7', *Cell Rep*, 7(1), pp. 62-9.
- McCusker, D., Royou, A., Velours, C. and Kellogg, D. (2012) 'Cdk1-dependent control of membrane-trafficking dynamics', *Mol Biol Cell*, 23(17), pp. 3336-47.
- McElligott, R. and Wellinger, R. J. (1997) 'The terminal DNA structure of mammalian chromosomes', *EMBO j*, 16(12), pp. 3705-3714.
- McGee, J. S., Phillips, J. A., Chan, A., Sabourin, M., Paeschke, K. and Zakian, V. A. (2010) 'Reduced Rif2 and lack of Mec1 target short telomeres for elongation rather than double-strand break repair', *Nat Struct Mol Biol*, 17(12), pp. 1438-1445.
- Melo, J. A., Cohen, J. and Toczyski, D. P. (2001) 'Two checkpoint complexes are independently recruited to sites of DNA damage in vivo', *Genes Dev*, 15(21), pp. 2809-2821.
- Mendenhall, M. D. (1993) 'An inhibitor of p34CDC28 protein kinase activity from *Saccharomyces cerevisiae*', *Science*, 259(5092), pp. 216-9.
- Mendenhall, M. D. and Hodge, A. E. (1998) 'Regulation of Cdc28 cyclin-dependent protein kinase activity during the cell cycle of the yeast *Saccharomyces cerevisiae*', *Microbiol Mol Biol Rev*, 62(4), pp. 1191-243.
- Michelson, R. J., Rosenstein, S. and Weinert, T. (2005) 'A telomeric repeat sequence adjacent to a DNA double-stranded break produces an antieckpoint', *Genes Dev*, 19(21), pp. 2546-59.
- Mimitou, E. P. and Symington, L. S. (2008) 'Sae2, Exo1 and Sgs1 collaborate in DNA double-strand break processing', *Nature*, 455(7214), pp. 770-774.
- Mishra, K. and Shore, D. (1999) 'Yeast Ku protein plays a direct role in telomeric silencing and counteracts inhibition by Rif proteins', *Curr Biol*, 9(19), pp. S1-S2.
- Miyake, Y., Nakamura, M., Nabetani, A., Shimamura, S., Tamura, M., Yonehara, S., Saito, M. and Ishikawa, F. (2009) 'RPA-like Mammalian Ctc1-Stn1-Ten1 Complex Binds to Single-Stranded DNA and Protects Telomeres Independently of the Pot1 Pathway', *Mol Cell*, 36(2), pp. 193-206.
- Mohl, D. A., Huddleston, M. J., Collingwood, T. S., Annan, R. S. and Deshaies, R. J. (2009) 'Dbf2-Mob1 drives relocalization of protein phosphatase Cdc14 to the cytoplasm during exit from mitosis', *J Cell Biol* 184(4), p. 527.
- Moorhead, G. B. G., Trinkle-Mulcahy, L., Nimick, M., De Wever, V., Campbell, D. G., Gourlay, R., Lam, Y. W. and Lamond, A. I. (2008) 'Displacement affinity chromatography of protein phosphatase one (PP1) complexes', *BMC Biochemistry*, 9(1), p. 28.

- Moretti, P., Freeman, K., Coodly, L. and Shore, D. (1994) 'Evidence that a complex of SIR proteins interacts with the silencer and telomere-binding protein RAP1', *Genes Dev*, 8(19), pp. 2257-69.
- Moriyama, K., Yoshizawa-Sugata, N. and Masai, H. (2018) 'Oligomer formation and G-quadruplex binding by purified murine Rif1 protein, a key organizer of higher-order chromatin architecture', *J Biol Chem*, 293(10), pp. 3607-3624.
- Morrow, C. J., Tighe, A., Johnson, V. L., Scott, M. I., Ditchfield, C. and Taylor, S. S. (2005) 'Bub1 and aurora B cooperate to maintain BubR1-mediated inhibition of APC/CCdc20', *J Cell Sci*, 118(Pt 16), pp. 3639-52.
- Munden, A., Rong, Z., Sun, A., Gangula, R., Mallal, S. and Nordman, J. T. (2018) 'Rif1 inhibits replication fork progression and controls DNA copy number in *Drosophila*', *eLife*, 7, p. e39140.
- Nern, A. and Arkowitz, R. A. (2000) 'Nucleocytoplasmic Shuttling of the Cdc42p Exchange Factor Cdc24p', *J Cell Biol*, 148(6), p. 1115.
- Ngo, G. H., Balakrishnan, L., Dubarry, M., Campbell, J. L. and Lydall, D. (2014) 'The 9-1-1 checkpoint clamp stimulates DNA resection by Dna2-Sgs1 and Exo1', *Nucleic Acids Res*, 42(16), pp. 10516-28.
- Ngo, G. H. and Lydall, D. (2015) 'The 9-1-1 checkpoint clamp coordinates resection at DNA double strand breaks', *Nucleic Acids Res*, 43(10), pp. 5017-32.
- Ngo, H. P. and Lydall, D. (2010) 'Survival and growth of yeast without telomere capping by Cdc13 in the absence of Sgs1, Exo1, and Rad9', *PLoS Genet*, 6(8), p. e1001072.
- Nguyen, V. Q., Co, C. and Li, J. J. (2001) 'Cyclin-dependent kinases prevent DNA re-replication through multiple mechanisms', *Nature*, 411(6841), pp. 1068-73.
- Nigg, E. A. (1993) 'Cellular substrates of p34(cdc2) and its companion cyclin-dependent kinases', *Trends Cell Biol*, 3(9), pp. 296-301.
- Nugent, C. I., Hughes, T. R., Lue, N. F. and Lundblad, V. (1996) 'Cdc13p: a single-strand telomeric DNA-binding protein with a dual role in yeast telomere maintenance', *Science*, 274(5285), pp. 249-52.
- Oehlen, L. J., McKinney, J. D. and Cross, F. R. (1996) 'Ste12 and Mcm1 regulate cell cycle-dependent transcription of FAR1', *Mol Cell Biol*, 16(6), pp. 2830-7.
- Orlando, D. A., Lin, C. Y., Bernard, A., Wang, J. Y., Socolar, J. E. S., Iversen, E. S., Hartemink, A. J. and Haase, S. B. (2008) 'Global control of cell-cycle transcription by coupled CDK and network oscillators', *Nature*, 453(7197), pp. 944-947.
- Parenteau, J. and Wellinger, R. J. (2002) 'Differential processing of leading- and lagging-strand ends at *Saccharomyces cerevisiae* telomeres revealed by the absence of Rad27p nuclease', *Genetics*, 162(4), pp. 1583-1594.

- Park, S., Patterson, E. E., Cobb, J., Audhya, A., Gartenberg, M. R. and Fox, C. A. (2011) 'Palmitoylation controls the dynamics of budding-yeast heterochromatin via the telomere-binding protein Rif1', *Proc Natl Acad Sci U S A*, 108(35), pp. 14572-7.
- Pelliccioli, A. and Foiani, M. (2005) 'Signal transduction: how rad53 kinase is activated', *Curr Biol*, 15(18), pp. R769-71.
- Pelliccioli, A., Lee, S. E., Lucca, C., Foiani, M. and Haber, J. E. (2001) 'Regulation of Saccharomyces Rad53 checkpoint kinase during adaptation from DNA damage-induced G2/M arrest', *Mol Cell*, 7(2), pp. 293-300.
- Peters, J. M. (2006) 'The anaphase promoting complex/cyclosome: a machine designed to destroy', *Nat Rev Mol Cell Biol*, 7(9), pp. 644-56.
- Petreaca, R. C., Chiu, H. C., Eckelhoefer, H. A., Chuang, C., Xu, L. and Nugent, C. I. (2006) 'Chromosome end protection plasticity revealed by Stn1p and Ten1p bypass of Cdc13p', *Nat Cell Biol*, 8(7), pp. 748-55.
- Piya, G., Mueller, E. N., Haas, H. K., Ghospurkar, P. L., Wilson, T. M., Jensen, J. L., Colbert, C. L. and Haring, S. J. (2015) 'Characterization of the Interaction between Rfa1 and Rad24 in Saccharomyces cerevisiae', *PLOS ONE*, 10(2), p. e0116512.
- Polotnianka, R. M., Li, J. and Lustig, A. J. (1998) 'The yeast Ku heterodimer is essential for protection of the telomere against nucleolytic and recombinational activities', *Curr Biology*, 8(14), pp. 831-835.
- Pramila, T., Wu, W., Miles, S., Noble, W. S. and Breeden, L. L. (2006) 'The Forkhead transcription factor Hcm1 regulates chromosome segregation genes and fills the S-phase gap in the transcriptional circuitry of the cell cycle', *Genes Dev*, 20(16), pp. 2266-78.
- Qi, H. and Zakian, V. A. (2000) 'The Saccharomyces telomere-binding protein Cdc13p interacts with both the catalytic subunit of DNA polymerase alpha and the telomerase-associated est1 protein', *Genes Dev*, 14(14), pp. 1777-1788.
- Randell, J. C., Bowers, J. L., Rodriguez, H. K. and Bell, S. P. (2006) 'Sequential ATP hydrolysis by Cdc6 and ORC directs loading of the Mcm2-7 helicase', *Mol Cell*, 21(1), pp. 29-39.
- Reynard, G. J., Reynolds, W., Verma, R. and Deshaies, R. J. (2000) 'Cks1 is required for G(1) cyclin-cyclin-dependent kinase activity in budding yeast', *Mol Cell Biol*, 20(16), pp. 5858-64.
- Ribeyre, C. and Shore, D. (2012) 'Anticheckpoint pathways at telomeres in yeast', *Nat Struct Mol Biol*, 19(3), pp. 307-13.
- Rice, C. and Skordalakes, E. (2016) 'Structure and function of the telomeric CST complex', *Computational and structural biotechnology journal*, 14, pp. 161-167.
- Richardson, H., Lew, D. J., Henze, M., Sugimoto, K. and Reed, S. I. (1992) 'Cyclin-B homologs in Saccharomyces cerevisiae function in S phase and in G2', *Genes Dev*, 6(11), pp. 2021-34.

- Rodriguez-Rodriguez, J. A., Moyano, Y., Jativa, S. and Queralt, E. (2016) 'Mitotic Exit Function of Polo-like Kinase Cdc5 Is Dependent on Sequential Activation by Cdk1', *Cell Rep*, 15(9), pp. 2050-62.
- Roy, R., Meier, B., McAinsh, A. D., Feldmann, H. M. and Jackson, S. P. (2004) 'Separation-of-function mutants of yeast Ku80 reveal a Yku80p-Sir4p interaction involved in telomeric silencing', *J Biol Chem*, 279(1), pp. 86-94.
- Rudner, A. D. and Murray, A. W. (2000) 'Phosphorylation by Cdc28 activates the Cdc20-dependent activity of the anaphase-promoting complex', *J Cell Biol*, 149(7), pp. 1377-90.
- Russell, P., Moreno, S. and Reed, S. I. (1989) 'Conservation of mitotic controls in fission and budding yeasts', *Cell*, 57(2), pp. 295-303.
- Samassekou, O., Gadji, M., Drouin, R. and Yan, J. (2010) 'Sizing the ends: Normal length of human telomeres', *Annals of Anatomy - Anatomischer Anzeiger*, 192(5), pp. 284-291.
- Sanchez, Y., Bachant, J., Wang, H., Hu, F., Liu, D., Tetzlaff, M. and Elledge, S. J. (1999) 'Control of the DNA damage checkpoint by chk1 and rad53 protein kinases through distinct mechanisms', *Science*, 286(5442), pp. 1166-71.
- Sandell, L. L. and Zakian, V. A. (1993) 'Loss of a yeast telomere: arrest, recovery, and chromosome loss', *Cell*, 75(4), pp. 729-39.
- Santos-Rosa, H., Leung, J., Grimsey, N., Peak-Chew, S. and Siniosoglou, S. (2005) 'The yeast lipin Smp2 couples phospholipid biosynthesis to nuclear membrane growth', *EMBO j*, 24(11), pp. 1931-41.
- Schleker, T., Shimada, K., Sack, R., Pike, B. L. and Gasser, S. M. (2010) 'Cell cycle-dependent phosphorylation of Rad53 kinase by Cdc5 and Cdc28 modulates checkpoint adaptation', *Cell Cycle*, 9(2), pp. 350-63.
- Schneider, B. L., Yang, Q. H. and Futcher, A. B. (1996) 'Linkage of replication to start by the Cdk inhibitor Sic1', *Science*, 272(5261), pp. 560-2.
- Schwob, E. and Nasmyth, K. (1993) 'CLB5 and CLB6, a new pair of B cyclins involved in DNA replication in *Saccharomyces cerevisiae*', *Genes Dev*, 7(7a), pp. 1160-75.
- Seto, A. G., Zaug, A. J., Sobel, S. G., Wolin, S. L. and Cech, T. R. (1999) '*Saccharomyces cerevisiae* telomerase is an Sm small nuclear ribonucleoprotein particle', *Nature*, 401(6749), pp. 177-180.
- Sheu, Y.-J. and Stillman, B. (2006) 'Cdc7-Dbf4 phosphorylates MCM proteins via a docking site-mediated mechanism to promote S phase progression', *Mol cell*, 24(1), pp. 101-113.
- Shi, T., Bunker, Richard D., Mattarocci, S., Ribeyre, C., Faty, M., Gut, H., Scrima, A., Rass, U., Rubin, Seth M., Shore, D. and Thomä, Nicolas H. (2013) 'Rif1 and Rif2 Shape Telomere Function and Architecture through Multivalent Rap1 Interactions', *Cell*, 153(6), pp. 1340-1353.

- Shirayama, M., Toth, A., Galova, M. and Nasmyth, K. (1999) 'APC(Cdc20) promotes exit from mitosis by destroying the anaphase inhibitor Pds1 and cyclin Clb5', *Nature*, 402(6758), pp. 203-7.
- Shore, D. and Nasmyth, K. (1987) 'Purification and cloning of a DNA binding protein from yeast that binds to both silencer and activator elements', *Cell*, 51(5), pp. 721-732.
- Shyian, M., Mattarocci, S., Albert, B., Hafner, L., Lezaja, A., Costanzo, M., Boone, C. and Shore, D. (2016) 'Budding Yeast Rif1 Controls Genome Integrity by Inhibiting rDNA Replication', *PLoS Genet*, 12(11), p. e1006414.
- Sia, R. A., Bardes, E. S. and Lew, D. J. (1998) 'Control of Swe1p degradation by the morphogenesis checkpoint', *EMBO j*, 17(22), pp. 6678-88.
- Silverman, J., Takai, H., Buonomo, S. B. C., Eisenhaber, F. and de Lange, T. (2004) 'Human Rif1, ortholog of a yeast telomeric protein, is regulated by ATM and 53BP1 and functions in the S-phase checkpoint', *Genes Dev*, 18(17), pp. 2108-2119.
- Simon, M., Seraphin, B. and Faye, G. (1986) 'KIN28, a yeast split gene coding for a putative protein kinase homologous to CDC28', *Embo j*, 5(10), pp. 2697-701.
- Singer, M. S. and Gottschling, D. E. (1994) 'TLC1: template RNA component of *Saccharomyces cerevisiae* telomerase', *Science*, 266(5184), pp. 404-9.
- Sopko, R., Huang, D., Smith, J. C., Figeys, D. and Andrews, B. J. (2007) 'Activation of the Cdc42p GTPase by cyclin-dependent protein kinases in budding yeast', *EMBO j*, 26(21), pp. 4487-500.
- Spellman, P. T., Sherlock, G., Zhang, M. Q., Iyer, V. R., Anders, K., Eisen, M. B., Brown, P. O., Botstein, D. and Futcher, B. (1998) 'Comprehensive identification of cell cycle-regulated genes of the yeast *Saccharomyces cerevisiae* by microarray hybridization', *Mol Biol Cell*, 9(12), pp. 3273-97.
- Sreesankar, E., Senthilkumar, R., Bharathi, V., Mishra, R. K. and Mishra, K. (2012) 'Functional diversification of yeast telomere associated protein, Rif1, in higher eukaryotes', *BMC genomics*, 13, pp. 255-255.
- Stewart, J. A., Chaiken, M. F., Wang, F. and Price, C. M. (2012) 'Maintaining the end: roles of telomere proteins in end-protection, telomere replication and length regulation', *Mutation research*, 730(1-2), pp. 12-19.
- Strathern, J. N., Shafer, B. K. and McGill, C. B. (1995) 'DNA synthesis errors associated with double-strand-break repair', *Genetics*, 140(3), pp. 965-972.
- Sudakin, V., Chan, G. K. and Yen, T. J. (2001) 'Checkpoint inhibition of the APC/C in HeLa cells is mediated by a complex of BUBR1, BUB3, CDC20, and MAD2', *J Cell Biol*, 154(5), pp. 925-36.
- Sugawara, N., Wang, X. and Haber, J. E. (2003) 'In Vivo Roles of Rad52, Rad54, and Rad55 Proteins in Rad51-Mediated Recombination', *Mol Cell*, 12(1), pp. 209-219.

- Sukackaite, R., Cornacchia, D., Jensen, Malene R., Mas, P. J., Blackledge, M., Enverald, E., Duan, G., Auchynnika, T., Köhn, M., Hart, D. J. and Buonomo, S. B. C. (2017) 'Mouse Rif1 is a regulatory subunit of protein phosphatase 1 (PP1)', *Scientific Rep*, 7(1), p. 2119.
- Sullivan, M. and Morgan, D. O. (2007) 'Finishing mitosis, one step at a time', *Nat Rev Mol Cell Biol*, 8(11), pp. 894-903.
- Sun, J., Yu, E. Y., Yang, Y., Confer, L. A., Sun, S. H., Wan, K., Lue, N. F. and Lei, M. (2009) 'Stn1-Ten1 is an Rpa2-Rpa3-like complex at telomeres', *Genes Dev*, 23(24), pp. 2900-14.
- Surovtseva, Y. V., Churikov, D., Boltz, K. A., Song, X., Lamb, J. C., Warrington, R., Leehy, K., Heacock, M., Price, C. M. and Shippen, D. E. (2009) 'Conserved telomere maintenance component 1 interacts with STN1 and maintains chromosome ends in higher eukaryotes', *Mol Cell*, 36(2), pp. 207-218.
- Swaney, D., Beltrao, P., Starita, L., Guo, A., Rush, J., Fields, S., Krogan, N. J. and Villén, J. (2013a) 'Global analysis of phosphorylation and ubiquitylation cross-talk in protein degradation', *Nat Methods*, 10(7), pp. 676-682.
- Syljuasen, R. G. (2007) 'Checkpoint adaptation in human cells', *Oncogene*, 26(40), pp. 5833-9.
- Syljuasen, R. G., Jensen, S., Bartek, J. and Lukas, J. (2006) 'Adaptation to the ionizing radiation-induced G2 checkpoint occurs in human cells and depends on checkpoint kinase 1 and Polo-like kinase 1 kinases', *Cancer Res*, 66(21), pp. 10253-7.
- Taggart, A. K., Teng, S. C. and Zakian, V. A. (2002) 'Est1p as a cell cycle-regulated activator of telomere-bound telomerase', *Science*, 297(5583), pp. 1023-6.
- Tanaka, S. and Araki, H. (2011) 'Multiple regulatory mechanisms to inhibit untimely initiation of DNA replication are important for stable genome maintenance', *PLoS Genet*, 7(6), p. e1002136.
- Taylor, S. S., Scott, M. I. and Holland, A. J. (2004) 'The spindle checkpoint: a quality control mechanism which ensures accurate chromosome segregation', *Chromosome Res*, 12(6), pp. 599-616.
- Teng, S.-C., Chang, J., McCowan, B. and Zakian, V. A. (2000) 'Telomerase-Independent Lengthening of Yeast Telomeres Occurs by an Abrupt Rad50p-Dependent, Rif-Inhibited Recombinational Process', *Mol Cell*, 6(4), pp. 947-952.
- Teng, S. C. and Zakian, V. A. (1999) 'Telomere-telomere recombination is an efficient bypass pathway for telomere maintenance in *Saccharomyces cerevisiae*', *Mol Cell Biol*, 19(12), pp. 8083-93.
- Teo, S. H. and Jackson, S. P. (2001) 'Telomerase subunit overexpression suppresses telomere-specific checkpoint activation in the yeast yku80 mutant', *EMBO Rep*, 2(3), pp. 197-202.
- Toczyski, D. P., Galgoczy, D. J. and Hartwell, L. H. (1997) 'CDC5 and CKII control adaptation to the yeast DNA damage checkpoint', *Cell*, 90(6), pp. 1097-106.

- Toh-e, A., Tanaka, K., Uesono, Y. and Wickner, R. B. (1988) 'PHO85, a negative regulator of the PHO system, is a homolog of the protein kinase gene, CDC28, of *Saccharomyces cerevisiae*', *Mol Gen Genet*, 214(1), pp. 162-4.
- Toh, G. W. L., O'Shaughnessy, A. M., Jimeno, S., Dobbie, I. M., Grenon, M., Maffini, S., O'Rourke, A. and Lowndes, N. F. (2006) 'Histone H2A phosphorylation and H3 methylation are required for a novel Rad9 DSB repair function following checkpoint activation', *DNA Repair*, 5(6), pp. 693-703.
- Tomimatsu, N., Mukherjee, B., Catherine Hardebeck, M., Ilcheva, M., Vanessa Camacho, C., Louise Harris, J., Porteus, M., Llorente, B., Khanna, K. K. and Burma, S. (2014) 'Phosphorylation of EXO1 by CDKs 1 and 2 regulates DNA end resection and repair pathway choice', *Nat Comms*, 5, pp. 3561-3561.
- Tseng, S.-F., Lin, J.-J. and Teng, S.-C. (2006) 'The telomerase-recruitment domain of the telomere binding protein Cdc13 is regulated by Mec1p/Tel1p-dependent phosphorylation', *Nucleic Acids Res*, 34(21), pp. 6327-6336.
- Tsukamoto, Y., Kato, J. and Ikeda, H. (1997) 'Silencing factors participate in DNA repair and recombination in *Saccharomyces cerevisiae*', *Nature*, 388(6645), pp. 900-3.
- Tuteja, R. and Tuteja, N. (2000) 'Ku autoantigen: a multifunctional DNA-binding protein', *Crit Rev Biochem Mol Biol*, 35(1), pp. 1-33.
- Tuzon, C. T., Wu, Y., Chan, A. and Zakian, V. A. (2011) 'The *Saccharomyces cerevisiae* telomerase subunit Est3 binds telomeres in a cell cycle- and Est1-dependent manner and interacts directly with Est1 in vitro', *PLoS Genet*, 7(5), pp. e1002060-e1002060.
- Tyers, M., Tokiwa, G. and Futcher, B. (1993) 'Comparison of the *Saccharomyces cerevisiae* G1 cyclins: Cln3 may be an upstream activator of Cln1, Cln2 and other cyclins', *EMBO j*, 12(5), pp. 1955-68.
- Tyers, M., Tokiwa, G., Nash, R. and Futcher, B. (1992) 'The Cln3-Cdc28 kinase complex of *S. cerevisiae* is regulated by proteolysis and phosphorylation', *EMBO j*, 11(5), pp. 1773-1784.
- Uzunova, K., Dye, B. T., Schutz, H., Ladurner, R., Petzold, G., Toyoda, Y., Jarvis, M. A., Brown, N. G., Poser, I., Novatchkova, M., Mechtler, K., Hyman, A. A., Stark, H., Schulman, B. A. and Peters, J. M. (2012) 'APC15 mediates CDC20 autoubiquitylation by APC/C(MCC) and disassembly of the mitotic checkpoint complex', *Nat Struct Mol Biol*, 19(11), pp. 1116-23.
- Valerio-Santiago, M., de Los Santos-Velazquez, A. I. and Monje-Casas, F. (2013) 'Inhibition of the mitotic exit network in response to damaged telomeres', *PLoS Genet*, 9(10), p. e1003859.
- Vaze, M. B., Pelliccioli, A., Lee, S. E., Ira, G., Liberi, G., Arbel-Eden, A., Foiani, M. and Haber, J. E. (2002) 'Recovery from checkpoint-mediated arrest after repair of a double-strand break requires Srs2 helicase', *Mol Cell*, 10(2), pp. 373-85.
- Veaute, X., Jeusset, J., Soustelle, C., Kowalczykowski, S. C., Le Cam, E. and Fabre, F. (2003) 'The Srs2 helicase prevents recombination by disrupting Rad51 nucleoprotein filaments', *Nature*, 423(6937), pp. 309-12.

- Venta, R., Valk, E., Koivomagi, M. and Loog, M. (2012) 'Double-negative feedback between S-phase cyclin-CDK and CKI generates abruptness in the G1/S switch', *Front Physiol*, 3, p. 459.
- Verdoodt, B., Decordier, I., Geleyns, K., Cunha, M., Cundari, E. and Kirsch-Volders, M. (1999) 'Induction of polyploidy and apoptosis after exposure to high concentrations of the spindle poison nocodazole', *Mutagenesis*, 14(5), pp. 513-520.
- Vidanes, G. M., Sweeney, F. D., Galicia, S., Cheung, S., Doyle, J. P., Durocher, D. and Toczyski, D. P. (2010) 'CDC5 Inhibits the Hyperphosphorylation of the Checkpoint Kinase Rad53, Leading to Checkpoint Adaptation', *PLOS Biol*, 8(1), p. e1000286.
- Viscardi, V., Bonetti, D., Cartagena-Lirola, H., Lucchini, G. and Longhese, M. P. (2007) 'MRX-dependent DNA damage response to short telomeres', *Mol Biol Cell*, 18(8), pp. 3047-3058.
- Visintin, C., Tomson, B. N., Rahal, R., Paulson, J., Cohen, M., Taunton, J., Amon, A. and Visintin, R. (2008) 'APC/C-Cdh1-mediated degradation of the Polo kinase Cdc5 promotes the return of Cdc14 into the nucleolus', *Genes Dev*, 22(1), pp. 79-90.
- Visintin, R., Craig, K., Hwang, E. S., Prinz, S., Tyers, M. and Amon, A. (1998) 'The phosphatase Cdc14 triggers mitotic exit by reversal of Cdk-dependent phosphorylation', *Mol Cell*, 2(6), pp. 709-18.
- Visintin, R., Prinz, S. and Amon, A. (1997) 'CDC20 and CDH1: a family of substrate-specific activators of APC-dependent proteolysis', *Science*, 278(5337), pp. 460-3.
- Vodenicharov, M. D. and Wellinger, R. J. (2006) 'DNA Degradation at Unprotected Telomeres in Yeast Is Regulated by the CDK1 (Cdc28/Clb) Cell-Cycle Kinase', *Mol Cell*, 24(1), pp. 127-137.
- Wang, H., Liu, D., Wang, Y., Qin, J. and Elledge, S. J. (2001) 'Pds1 phosphorylation in response to DNA damage is essential for its DNA damage checkpoint function', *Genes Dev*, 15(11), pp. 1361-72.
- Wang, H., Zhao, A., Chen, L., Zhong, X., Liao, J., Gao, M., Cai, M., Lee, D. H., Li, J., Chowdhury, D., Yang, Y. G., Pfeifer, G. P., Yen, Y. and Xu, X. (2009) 'Human RIF1 encodes an anti-apoptotic factor required for DNA repair', *Carcinogenesis*, 30(8), pp. 1314-9.
- Wang, J., Zhang, H., Al Shibar, M., Willard, B., Ray, A. and Runge, K. W. (2018) 'Rif1 phosphorylation site analysis in telomere length regulation and the response to damaged telomeres', *DNA Repair (Amst)*, 65, pp. 26-33.
- Wang, L., Xiao, H., Zhang, X., Wang, C. and Huang, H. (2014) 'The role of telomeres and telomerase in hematologic malignancies and hematopoietic stem cell transplantation', *Journal of hematology & oncology*, 7, pp. 61-61.
- Wang, Y. and Ng, T.-Y. (2006) 'Phosphatase 2A negatively regulates mitotic exit in *Saccharomyces cerevisiae*', *Mol Biol Cell*, 17(1), pp. 80-89.
- Wasch, R. and Cross, F. R. (2002) 'APC-dependent proteolysis of the mitotic cyclin Clb2 is essential for mitotic exit', *Nature*, 418(6897), pp. 556-62.

- Weinert, T. A. and Hartwell, L. H. (1993) 'Cell cycle arrest of cdc mutants and specificity of the RAD9 checkpoint', *Genetics*, 134(1), pp. 63-80.
- Wellinger, R. J., Wolf, A. J. and Zakian, V. A. (1993) 'Saccharomyces telomeres acquire single-strand TG-tails late in S phase', *Cell*, 72(1), pp. 51-60.
- Wellinger, R. J. and Zakian, V. A. (2012) 'Everything you ever wanted to know about Saccharomyces cerevisiae telomeres: beginning to end', *Genetics*, 191(4), pp. 1073-1105.
- Winters, M. J., Lamson, R. E., Nakanishi, H., Neiman, A. M. and Pryciak, P. M. (2005) 'A Membrane Binding Domain in the Ste5 Scaffold Synergizes with G β γ Binding to Control Localization and Signaling in Pheromone Response', *Mol Cell*, 20(1), pp. 21-32.
- Wood, J. S. and Hartwell, L. H. (1982) 'A dependent pathway of gene functions leading to chromosome segregation in Saccharomyces cerevisiae', *J Cell Biol*, 94(3), pp. 718-26.
- Wotton, D. and Shore, D. (1997) 'A novel Rap1p-interacting factor, Rif2p, cooperates with Rif1p to regulate telomere length in Saccharomyces cerevisiae', *Genes Dev*, 11(6), pp. 748-60.
- Wright, W. E., Tesmer, V. M., Huffman, K. E., Levene, S. D. and Shay, J. W. (1997) 'Normal human chromosomes have long G-rich telomeric overhangs at one end', *Genes Dev*, 11(21), pp. 2801-2809.
- Wu, C., Whiteway, M., Thomas, D. Y. and Leberer, E. (1995) 'Molecular characterization of Ste20p, a potential mitogen-activated protein or extracellular signal-regulated kinase kinase (MEK) kinase kinase from Saccharomyces cerevisiae', *J Biol Chem*, 270(27), pp. 15984-92.
- Xu, D., Muniandy, P., Leo, E., Yin, J., Thangavel, S., Shen, X., Li, M., Agama, K., Guo, R., Fox, D., 3rd, Meetei, A. R., Wilson, L., Nguyen, H., Weng, N. P., Brill, S. J., Li, L., Vindigni, A., Pommier, Y., Seidman, M. and Wang, W. (2010) 'Rif1 provides a new DNA-binding interface for the Bloom syndrome complex to maintain normal replication', *EMBO j*, 29(18), pp. 3140-55.
- Xu, L. and Blackburn, E. H. (2004) 'Human Rif1 protein binds aberrant telomeres and aligns along anaphase midzone microtubules', *J Cell Biol*, 167(5), pp. 819-830.
- Xue, Y., Marvin, M. E., Ivanova, I. G., Lydall, D., Louis, E. J. and Maringele, L. (2016) 'Rif1 and Exo1 regulate the genomic instability following telomere losses', *Aging Cell*, 15(3), pp. 553-62.
- Xue, Y., Rushton, M. D. and Maringele, L. (2011) 'A novel checkpoint and RPA inhibitory pathway regulated by Rif1', *PLoS Genet*, 7(12), p. e1002417.
- Yamazaki, S., Ishii, A., Kanoh, Y., Oda, M., Nishito, Y. and Masai, H. (2012) 'Rif1 regulates the replication timing domains on the human genome', *EMBO j*, 31(18), pp. 3667-77.
- Yao, S., Neiman, A. and Prelich, G. (2000) 'BUR1 and BUR2 encode a divergent cyclin-dependent kinase-cyclin complex important for transcription in vivo', *Mol Cell Biol*, 20(19), pp. 7080-7.

- Yoo, H. Y., Kumagai, A., Shevchenko, A., Shevchenko, A. and Dunphy, W. G. (2004) 'Adaptation of a DNA replication checkpoint response depends upon inactivation of Claspin by the Polo-like kinase', *Cell*, 117(5), pp. 575-88.
- Yu, L., Qi, M., Sheff, M. A. and Elion, E. A. (2008) 'Counteractive control of polarized morphogenesis during mating by mitogen-activated protein kinase Fus3 and G1 cyclin-dependent kinase', *Mol Biol Cell*, 19(4), pp. 1739-52.
- Zakian, V. A., Blanton, H. M. and Wetzell, L. (1986) 'Distribution of telomere-associated sequences in yeast', *Basic Life Sci*, 40, pp. 493-8.
- Zappulla, D. C., Goodrich, K. and Cech, T. R. (2005) 'A miniature yeast telomerase RNA functions in vivo and reconstitutes activity in vitro', *Nat Struct Mol Biol*, 12(12), pp. 1072-7.
- Zegerman, P. and Diffley, J. F. (2007) 'Phosphorylation of Sld2 and Sld3 by cyclin-dependent kinases promotes DNA replication in budding yeast', *Nature*, 445(7125), pp. 281-5.
- Zhang, H., Liu, H., Chen, Y., Yang, X., Wang, P., Liu, T., Deng, M., Qin, B., Correia, C., Lee, S., Kim, J., Sparks, M., Nair, A. A., Evans, D. L., Kalari, K. R., Zhang, P., Wang, L., You, Z., Kaufmann, S. H., Lou, Z. and Pei, H. (2016) 'A cell cycle-dependent BRCA1-UHRF1 cascade regulates DNA double-strand break repair pathway choice', *Nat Comms*, 7(1), p. 10201.
- Zhang, W. and Durocher, D. (2010) 'De novo telomere formation is suppressed by the Mec1-dependent inhibition of Cdc13 accumulation at DNA breaks', *Genes Dev*, 24(5), pp. 502-515.
- Zhu, Z., Chung, W.-H., Shim, E. Y., Lee, S. E. and Ira, G. (2008) 'Sgs1 helicase and two nucleases Dna2 and Exo1 resect DNA double-strand break ends', *Cell*, 134(6), pp. 981-994.
- Zimmermann, M., Lottersberger, F., Buonomo, S. B., Sfeir, A. and de Lange, T. (2013) '53BP1 regulates DSB repair using Rif1 to control 5' end resection', *Science*, 339(6120), pp. 700-4.
- Zofall, M., Smith, D. R., Mizuguchi, T., Dhakshnamoorthy, J. and Grewal, S. I. S. (2016) 'Taz1-Shelterin Promotes Facultative Heterochromatin Assembly at Chromosome-Internal Sites Containing Late Replication Origins', *Mol Cell*, 62(6), pp. 862-874.
- Zou, L. and Stillman, B. (1998) 'Formation of a preinitiation complex by S-phase cyclin CDK-dependent loading of Cdc45p onto chromatin', *Science*, 280(5363), pp. 593-6.
- Zou, L. and Stillman, B. (2000) 'Assembly of a complex containing Cdc45p, replication protein A, and Mcm2p at replication origins controlled by S-phase cyclin-dependent kinases and Cdc7p-Dbf4p kinase', *Mol Cell Biol*, 20(9), pp. 3086-96.
- Zubko, M. K., Guillard, S. and Lydall, D. (2004) 'Exo1 and Rad24 differentially regulate generation of ssDNA at telomeres of *Saccharomyces cerevisiae* cdc13-1 mutants', *Genetics*, 168(1), pp. 103-15.